

Université du Québec
Institut national de la recherche scientifique
Centre Armand-Frappier Santé Biotechnologie

Synthesis, characterization and anticancer/antifungal evaluation of ruthenium complexes bearing an enzyme inhibitor

Par
Golara Golbaghi

Thèse présentée pour l'obtention du grade
de Philosophiae Doctor (Ph.D.)
en Biologie

Jury d'évaluation

| | |
|---|---|
| Président du jury et examineur interne | Prof. Charles Gautier INRS - Centre Armand-Frappier Santé Biotechnologie |
| Examineur externe | Prof. Alfredo Angeles-Boza University of Connecticut |
| Examineur externe | Prof. Scott Bohle McGill University |
| Directeur de recherche | Prof. Annie Castonguay INRS - Centre Armand-Frappier Santé Biotechnologie |

ACKNOWLEDGEMENTS

My sincere gratitude would be dedicated to my PhD supervisor **Prof. Annie Castonguay** for her dedicated support and guidance. She continuously provided encouragements and was always enthusiastic to assist me in any way she could throughout this journey.

I would like to take this opportunity to thank professors **Kessen Patten, Nicolas Doucet, Thomas Sanderson** and **Eric Déziel** for the constructive collaborations and for sharing their lab, instruments and research knowledge with us.

I would also like to thank the members of my Ph.D. evaluation committee, professors **Scott Bohle, Alfredo Angeles-Boza** and **Charles Gauthier** for their constructive comments as well as **Armand-Frappier Foundation** and **INRS university** and for their financial support.

I would like to thank all the past and present members of the **Castonguay research group** and scientists at INRS, especially **Myriam Létourneau, Dr. Yossef Lopez de Los Santos** and **Marie-Christine Groleau** for their technical, scientific and moral contribution during the time course of my PhD.

This PhD dissertation is dedicated to:

my husband, for his continuous support and love;

my mother, for always believing in me;

my father, for his understanding and self-devotion;

and **my brother**, for sending his positive vibes;

without whom I would never have enjoyed so many opportunities in my life.

RÉSUMÉ

Plusieurs personnes à travers le monde et approximativement 50% des Canadiens seront atteints du cancer au cours de leur vie, et il est attendu qu'un quart de tous les Canadiens succombera à cette maladie. Plus spécifiquement, une Canadienne sur quatre recevra un diagnostic de cancer du sein durant sa vie. Malgré les nombreux problèmes y étant associés, la chimiothérapie est de loin l'une des méthodes les plus efficaces pour le traitement de différents cancers. À comparer aux composés purement organiques, les complexes inorganiques possèdent des propriétés uniques, et peuvent offrir d'intéressantes opportunités au champ de la chimiothérapie. Un exemple de drogue très connue et utilisée en chimiothérapie est le cisplatine, un complexe à base d'un métal de transition qui est administré aux patients cancéreux pour le traitement d'une variété de cancers incluant celui du sein. Comme la cible des drogues à base de platine est principalement l'ADN, ces composés ne sont pas seulement toxiques pour les cellules cancéreuses, mais le sont aussi pour les cellules saines. Étant donné ce manque de sélectivité, les patients souffrent de plusieurs effets secondaires importants tels que la toxicité neurologique et/ou rénale ou bien la suppression de la moelle osseuse. En parallèle, les cellules cancéreuses développent une certaine résistance aux drogues à base de platine, limitant ainsi leur usage clinique. Malgré les importants problèmes lui étant associés, le cisplatine et ses dérivés sont toujours largement utilisés aujourd'hui. Le développement de nouveaux traitements alternatifs est donc requis, incluant le design de drogues inorganiques ayant une activité et sélectivité accrues.

Les complexes à base de ruthénium attirent présentement beaucoup l'attention, comme ils sont très prometteurs en vue de remplacer les drogues à base de platine en tant que traitement de première ligne: par exemple, certains *i)* démontrent une activité considérable contre les lignées cellulaires résistantes au cisplatine, *ii)* induisent une incidence d'effets secondaires moins élevée à comparer aux agents thérapeutiques à base de platine, et *iii)* donnent lieu à activité antiproliférative selon différents mécanismes. Certains complexes à base de ruthénium comme RAPTA-C, NAMI-A, TLD-1433 et KP1090 ont été l'objet d'études précliniques et cliniques. Une stratégie intéressante pouvant potentiellement augmenter la probabilité de survie de patients atteints du cancer est de créer des drogues multitâches, capable de promouvoir la mort de cellules cancéreuses par divers mécanismes, simultanément. Les complexes de ruthénium comportant des ligands ayant une activité biologique connue émergent comme étant des candidats prometteurs pour différentes raisons: *i)* cette stratégie peut mener à des complexes de ruthénium multitâches pour lesquels le métal et les ligands sont mutuellement responsables pour

leur activité anticancéreuse, permettant ainsi de réduire l'incidence de mécanismes de résistance, et *ii*) les effets synergiques potentiels résultant de l'usage combiné de plusieurs drogues peut mener à des traitements à plus court terme.

Le projet de recherche présenté ici a pour but la création de nouvelles drogues à base de ruthénium comportant des inhibiteurs de croissance cellulaire (anastrozole et letrozole) qui sont largement utilisés pour le traitement des cancers à récepteurs d'oestrogène positifs (ER+). L'aromatase (CYP19) est une enzyme responsable de catalyser la réaction de production d'oestrogène chez les femmes ménopausées. Il a été rapporté que l'anastrozole et le letrozole se lient au fer de l'enzyme aromatase via la coordination d'un azote de leur cycle triazole, résultant en l'inhibition de l'activité catalytique de l'enzyme et la déprivation des cellules cancéreuses ER+ de leur oestrogène. Les principaux objectifs de cette thèse de doctorat sont les suivants: *i*) synthétiser, purifier et caractériser différents complexes de ruthénium comportant des ligands pouvant inhiber la croissance des cellules cancéreuses (anastrozole et letrozole); *ii*) évaluer *in vitro* l'activité antiproliférative ainsi que les propriétés inhibitrices de l'aromatase de ces complexes de ruthénium dans des lignées cellulaires de cancer du sein, et évaluer leur toxicité *in vivo*; *iii*) apporter des modifications structurales aux complexes de ruthénium, et évaluer leur influence sur leur activité, sélectivité et toxicité.

Au cours de ce projet, plusieurs complexes de Ru(II) et Ru(III) ayant des structures différentes et comportant des inhibiteurs de l'aromatase ont été synthétisés en utilisant des techniques d'atmosphère inerte telles que des systèmes de lignes à Schlenk, de boîte-à-gants et de purification de solvants. Les espèces ont ensuite été caractérisées en utilisant diverses techniques telles que la spectroscopie RMN, l'analyse élémentaire, la spectrométrie de masse et l'analyse structurale par diffraction des rayons-X. La solubilité et la stabilité des composés ont été testées préalablement à l'étude de leur activité en milieu biologique. Une série de complexes Ru(II)-benzene comportant un ligand anastrozole ont été synthétisés et leur potentiel anticancéreux évalué contre des cellules de cancer du sein ER+. Bien que les complexes ont démontré une considérable cytotoxicité *in vitro* contre les cellules de cancer du sein, seulement un de ces composés s'est avéré assez stable en milieu de culture cellulaire et a démontré s'accumuler de façon accrue dans les cellules cancéreuses. Alors que l'anastrozole seul n'a pas démontré de cytotoxicité *in vitro* contre les cellules cancéreuses, ce complexe de ruthénium a quant à lui démontré une considérable cytotoxicité ainsi qu'une certaine activité inhibitrice de l'enzyme aromatase, ce qui fut démontré de façons expérimentale et théorique. De plus, contrairement au cisplatine, les embryons de poisson zèbre ayant été exposés à certains de ces

complexes de ruthénium (à 12.5 μM) ont suivi un développement normal, indiquant une faible toxicité pour ce type de composés. Les résultats de cette étude ont été publiés dans *Organometallics* 2019, 38, 702-711.

Suite à cette étude initiale, nous avons été intéressés à évaluer à quel niveau la nature du type de structure des complexes de ruthénium peut affecter leurs propriétés chimiques et biologiques. En fait, contrairement aux complexes Ru(II)-benzène qui ont presque exclusivement été étudiés pour leurs applications contre le cancer, d'autres types de complexes de Ru(II) n'ont pas été étudiés en profondeur à cette fin. De plus, les complexes de Ru(III) ont été rapportés pour leurs propriétés antimétastatiques potentielles, faisant d'eux des candidats prometteurs pour l'inhibition de métastases chez les patients ayant reçu un diagnostic de cancer de sein métastatique. Lors de cette deuxième partie de l'étude, des espèces de ruthénium (II) (Ru(II)-cyclopentadiényle and Ru(II)-cyclooctadiène) et de Ru(III) comportant un inhibiteur de l'aromatase ont alors été synthétisées puis caractérisées. Dans le cas de la préparation du complexe Ru(II)-cyclooctadiène, une réaction assistée par un réacteur à micro-ondes fut développée puis optimisée afin d'améliorer le rendement et minimiser la durée de l'expérience. Plusieurs méthodes chromatographiques en phase normale ont aussi été développées afin de purifier certains des composés rapportés dans cette étude. Tandis que la plupart des complexes préparés pour cette étude se sont avérés instables en conditions biologiques, le complexe Ru(II)-cyclopentadiényle, la seule espèce de la série pour laquelle le ligand anastrozole est coordonné au ruthénium par une fonction nitrile (et non via l'azote de son cycle triazole), s'est avéré très stable en conditions biologiques, indiquant l'important effet du type de complexe de ruthénium et du mode de coordination de leurs ligands sur leur stabilité. Même si la cytotoxicité *in vitro* et la toxicité *in vivo* (modèle de poisson zèbre) de ce type de complexe a confirmé leur haut potentiel pour la thérapie du cancer du sein chez les cancers ER+ et les cancers agressifs triple négatif du sein (TNBC), nos études expérimentales et théoriques suggèrent que leur activité inhibitrice pour l'aromatase n'est pas plausible pour ce système étant donné l'encombrement stérique des groupes PPh_3 , prévenant ainsi l'interaction entre le complexe et l'enzyme cible. Les résultats de cette étude ont été publiés dans *European Journal of Medicinal Chemistry* 2020, 112030.

Le potentiel élevé de composés à base de métaux de transition pour des applications antifongiques et le fait que le mode d'action de certaines des drogues antifongiques (comme le fluconazole) soient connues pour impliquer une interaction entre un cycle azole et une enzyme fongique (CYP51), un mode d'action réminiscent de l'enzyme aromatase (CYP19) et certains de ses inhibiteurs, nous a motivé à évaluer l'activité antifongique du complexe de ruthénium

préalablement investigué (qui comprend un cycle triazole libre dans sa structure) ainsi que quelques espèces structurellement rapprochées. CYP51 est connu pour catalyser la biosynthèse de l'ergostérole, la composante majeure de la membrane cellulaire fongique, jouant un rôle essentiel de biorégulation de la fluidité et l'intégrité de la membrane fongique. Nous avons mis l'emphase sur les infections de type candidose étant donné qu'elles sont une des majeures causes de morbidité et de mortalité, et ont une incidence croissante. Étant donné les profils variables de résistance antifongique rapportés pour différentes espèces de *Candida*, il est de grande importance d'étudier de nouvelles alternatives aux drogues présentement utilisées. Parmi les trois complexes de ruthénium cyclopentadiényles investigués, seulement les deux espèces cationiques (indépendamment de la présence d'un cycle triazole libre dans leur structure) ont démontré une activité inhibitrice significative contre certaines espèces de *Candida*, de façon importante contre les espèces ne répondant pas au traitement au fluconazole, indiquant l'importance de la nature du type de complexe de ruthénium sur leurs propriétés antifongiques. Il a été démontré que l'activité antifongique de ces complexes est reliée à leur niveau d'internalisation cellulaire de même qu'à leur abileté à générer des espèces réactives de l'oxygène (ROS). De plus, il a été démontré théoriquement (simulation docking) qu'une interaction entre le complexe comportant l'anastrozole et l'enzyme fongique CYP51 est énergiquement favorisée (à un niveau même plus important que celle avec fluconazole), suggérant un mode d'action plausible additionnel pour ce composé. Les résultats de cette étude ont été acceptés pour publication dans *ChemBioChem – special issue metals in medicine 2020*.

Les résultats découlant de ce projet de recherche procurent de l'information importante quant au développement de nouveaux complexes de ruthénium pour le traitement du cancer du sein et pavent une nouvelle avenue pour le design de complexes antifongiques à base de ruthénium pour le traitement de la candidose.

Mots-clés : métallo-drogue, complexe de ruthénium, cancer du sein, résistance aux médicaments, anticancéreux, antifongique, candidose, inhibiteur de l'aromatase.

ABSTRACT

Many people all over the world and roughly 50% of Canadians will struggle with cancer in their lifetime, and a quarter of all Canadians are expected to die of this disease. More specifically, one out of four Canadian women will be diagnosed with breast cancer during their lifetime. Despite its numerous drawbacks, chemotherapy is so far one of the most effective methods to treat different cancers. Compared to purely organic compounds, inorganic complexes have unique properties, and can offer great opportunities to the field of chemotherapy. A well-known example of chemotherapy drugs is cisplatin, a transition metal-based complex that has been administered to cancer patients for the treatment of various cancers including breast cancer. As the target of platinum drugs is DNA, they are not only toxic to cancer cells, but to healthy cells as well. Due to their lack of selectivity, patients suffer from many side effects such as neuro- and/or renal-toxicity or bone marrow-suppression. Besides, cancer cells develop a resistance to platinum drugs, which limits their clinical use. Despite their important drawbacks, cisplatin and its derivatives are still widely used today. More development is then needed for the design of alternative inorganic drugs that are highly active and selective.

Ruthenium-based complexes currently attract great attention as they hold promise to replace platinum-based drugs as first line cancer treatment: for instance, they were found *i)* to exhibit considerable activity against cisplatin resistant cell lines, *ii)* to induce a lower occurrence of side effects in comparison to platinum-based therapeutics, and *iii)* to display their antiproliferative activity via different mechanisms. Some ruthenium-based compounds such as RAPTA-C, NAMI-A, TLD-1433 and KP1090 have successfully entered preclinical and clinical trials.

An appealing strategy to increase the survival probability of cancer patients is to create ruthenium multitasking drugs, able to promote cancer cell death by various mechanisms, simultaneously. Ruthenium complexes bearing ligands with known biological activity emerge as highly promising candidates due to different reasons: *i)* this strategy may lead to multi-targeting ruthenium complexes in which both the metal center and ligand are mutually responsible for the anticancer activity of the drug which might contribute to circumvent resistance mechanisms, and *ii)* potential synergistic effects resulting from the combined use of two drugs may lead to shorter-term treatments.

The research project presented here aims at creating novel ruthenium drugs bearing cancer cell growth inhibitors (anastrozole or letrozole) that are widely used aromatase inhibitors for the treatment of estrogen receptor positive (ER+) breast cancers. Aromatase (CYP19) is an enzyme responsible to catalyze the estrogen production reaction in postmenopausal women. It has been reported that anastrozole and letrozole bind to the heme iron of the aromatase enzyme through the coordination of one nitrogen of their triazole ring, resulting in the inhibition of the catalytic activity of the enzyme and the deprivation of ER+ breast cancer cells from estrogen. Herein, the main objectives of this PhD thesis were the following: *i)* to synthesize, purify and characterize various ruthenium complexes bearing cancer cell growth inhibitor ligand(s) (anastrozole or letrozole); *ii)* to investigate the *in vitro* antiproliferative activity and aromatase inhibition property of these ruthenium complexes against breast cancer cell lines, and assess their *in vivo* toxicity; *iii)* to bring structural modifications to ruthenium complexes, and to evaluate their influence on their activity, selectivity and toxicity.

In the course of this project, several structurally different Ru(II) and Ru(III) complexes bearing an aromatase inhibitor have been synthesized performing inert atmosphere techniques by using Schlenk line, glovebox and solvent purification systems. The species were characterized using various techniques such as NMR spectroscopy, elemental analysis, mass spectrometry and single crystal X-ray analysis. The stability and solubility of the compounds were tested prior to biological experiments. Accordingly, a series of Ru(II)-benzene complexes bearing anastrozole have been synthesized and their anticancer potential investigated against ER+ breast cancers. Whereas all these complexes showed considerable *in vitro* cytotoxicity in breast cancer cells, only one of them was found to be highly stable in cell culture media and to induce the most considerable cellular uptake in human breast cancer cells. Whereas anastrozole alone did not induce any *in vitro* cytotoxicity in the cancer cells, this ruthenium complex showed a considerable cytotoxicity and an aromatase enzyme inhibitory activity, which was studied experimentally and theoretically. Moreover, in contrast to cisplatin, zebrafish embryos exposed to the ruthenium complexes (at 12.5 μM) underwent a normal development, an indication of the lack of toxicity of this type of compounds. Results from this study were published in *Organometallics* 2019, 38, 702-711.

Following this initial study, we have been interested to evaluate to what extent the backbone of these ruthenium complexes can affect their chemical and biological properties. Ruthenium (II) (Ru(II)-cyclopentadienyl and Ru(II)-cyclooctadiene) and Ru(III) species bearing an aromatase inhibitor were then synthesized and characterized. In the case of the Ru(II)-cyclooctadiene

complex bearing anastrozole, a microwave-assisted reaction was developed and optimized to improve the reaction yield and minimize the duration of the experiment. Several normal-phase column chromatography methods were also developed to purify some of the species investigated in this study. In fact, in contrast to Ru(II)-benzene complexes which have been exclusively studied for anticancer applications, other types of Ru(II) species have been overlooked for this purpose. Moreover, Ru(III) complexes have been reported for their potential antimetastatic properties, making them promising candidates for the inhibition of metastasis in patients diagnosed with metastatic breast cancers. Whereas most of the complexes prepared for this study were found unstable under biological relevant conditions, a Ru(II)-cyclopentadienyl complex, the only species in this series for which anastrozole is coordinated ruthenium through the nitrile moiety (and not via the nitrogen of the triazole ring), was found to be highly stable under biologically relevant conditions, indicating the important effect of the ruthenium backbone on the stability and coordination mode of the complexes. Even though *in vitro* cytotoxicity and *in vivo* toxicity investigations (zebrafish model) of this complex confirmed its high potential for breast cancer therapy in both ER+ and aggressive triple negative breast cancer (TNBC), our experimental and theoretical studies suggested that its aromatase inhibitory activity is not likely to take place in this system due to the bulkiness of the PPh₃ moieties, preventing the interaction between the complex with the targeted enzyme. Results from this study were published in *European Journal of Medicinal Chemistry* 2020, 112030.

The high potential of metal-based compounds for antifungal applications and the fact that the mode of action of some currently used antifungal drugs (such as fluconazole) is known to involve an interaction between an azole ring and a fungal enzyme (CYP51), mode of action reminiscent of the aromatase enzyme (CYP19) and some of its inhibitors, prompted us to evaluate the antifungal activity of the ruthenium cyclopentadienyl complex we previously investigated (including a metal-uncoordinated triazole moiety in its structure) along with two closely related species. CYP51 is known to catalyze the biosynthesis of ergosterol, the major component of the fungal cell membrane, playing an essential role as a bioregulator of fungal membrane fluidity and integrity. We specifically focused on Candidiasis infections that are one of the most major causes of morbidity and mortality, and their increasing incidence ^{[1][1][1]}. Because of the variable antifungal resistance profiles reported for different *Candida* species, it is of high importance to study new possibilities that could be used as alternatives to the currently used antifungal drugs. Among the three ruthenium cyclopentadienyl complexes investigated, only the two cationic species (regardless of the presence of a free triazole in their structures) showed significant growth inhibitory activity in *Candida* species, more importantly in species that did not respond to a

fluconazole treatment, indicating the importance of the nature of the ruthenium complex backbone on its antifungal properties. The antifungal activity of these complexes was found to be related to the amount of ruthenium cellular uptaken and the intracellular reactive oxygen species (ROS) generated. Furthermore, we could theoretically demonstrate (docking simulation) that an interaction between the complex bearing anastrozole and the fungal CYP51 enzyme is energetically favorable (to an even greater extent than with fluconazole), suggesting a plausible additional mode of action for this compound. Results from this study were accepted for publication in *ChemBioChem – special issue metals in medicine 2020*.

Our research findings provide important information on the development of novel ruthenium complexes for the treatment of breast cancer and open a new door to the design of ruthenium-based drugs as anti-*Candida* species.

Keywords : metal-based drug, ruthenium complex, breast cancer, drug resistance, anticancer, antifungal, *Candida* infection, aromatase inhibitor.

TABLE OF CONTENTS

| | |
|--|------------|
| ACKNOWLEDGEMENTS | I |
| RÉSUMÉ | II |
| ABSTRACT | VI |
| TABLE OF CONTENTS | X |
| LIST OF FIGURES | XI |
| LIST OF TABLES | XI |
| LIST OF ABBREVIATIONS | XII |
| 1 INTRODUCTION | 1 |
| 1.1 Metals in medicine..... | 1 |
| 1.1.1 Ruthenium complexes for cancer therapy..... | 2 |
| 1.1.2 Ruthenium complexes for multitargeting approaches in cancer therapy..... | 4 |
| 1.2 Aromatase inhibitors for breast cancer therapy..... | 5 |
| 1.3 Rationally designed ruthenium complexes for breast cancer therapy (a review article: publication 1)..... | 8 |
| 1.4 Ruthenium complexes for antifungal applications..... | 35 |
| 1.5 Hypotheses and objectives..... | 39 |
| 2 PUBLICATION 2 | 40 |
| 2.1 Résumé | 42 |
| 2.2 Article (Ruthenium (II) complexes bearing an aromatase inhibitor: synthesis, characterization, in vitro biological activity and in vivo toxicity in zebrafish embryo)..... | 43 |
| 3 PUBLICATION 3 | 53 |
| 3.1 Résumé..... | 55 |
| 3.2 Article (Synthesis and biological assessment of a ruthenium(II) cyclopentadienyl complex in breast cancer cells and on the development of zebrafish embryos)..... | 56 |
| 4 PUBLICATION 4 | 67 |
| 4.1 Résumé..... | 68 |
| 4.2 Article (Ruthenium(II) cyclopentadienyl complexes with antifungal activity in several <i>Candida</i> species)..... | 69 |
| 5 CONCLUSION | 78 |
| 6 PERSPECTIVES | 80 |

| | | |
|---|---|----|
| 7 | REFERENCES..... | 83 |
| 8 | APPENDIX (SUPPLEMENTARY INFORMATION OF PUBLICATIONS 1-4)..... | 86 |

LIST OF FIGURES

| | | |
|-----------|---|----|
| Figure 1: | Metal ions are important in diagnosis and therapy for different human pathologies..... | 1 |
| Figure 2: | Ruthenium complexes that entered preclinical or/and clinical studies..... | 4 |
| Figure 3: | Examples of ruthenium complexes bearing biologically active ligands with potential multitargeting properties..... | 5 |
| Figure 4: | Chemical structures of third-generation aromatase inhibitors..... | 6 |
| Figure 5: | Schiff base-type ligands bearing a triazole ring..... | 80 |
| Figure 6: | Synthetic routes to complexes 1-4..... | 81 |
| Figure 7: | <i>In vitro</i> cytotoxicity of ligands and complexes at 50 μ M on ER+ breast cancer cells MCF7 and T47D after 48 h incubation using SRB assay..... | 82 |

LIST OF TABLES

| | | |
|----------|---|----|
| Table 1: | Anticandidal activity of previously reported ruthenium complexes..... | 37 |
|----------|---|----|

LIST OF ABBREVIATIONS

| | |
|-------|------------------------------------|
| HIV | Human immunodeficiency virus |
| AIDS | Acquired immunodeficiency syndrome |
| DNA | Deoxyribonucleic acid |
| NSLC | Non-small-cell lung carcinoma |
| PS | Photosensitizer |
| NMIBC | Non-muscle invasive bladder cancer |
| PDT | Photodynamic therapy |
| EGFR | Epidermal growth factor receptor |
| ER+ | Estrogen receptor positive |
| SAR | Structure activity relationship |
| COD | Cyclooctadienyl |
| Cp | Cyclopentadienyl |
| TNBC | Triple negative breast cancer |
| ROS | Reactive oxygen species |
| CYP | Cytochrome P450 |

1 INTRODUCTION

1.1 Metals in medicine

Inorganic compounds have wide spreading applications in catalysts, pigments, coatings, surfactants, fuels and medicine. Metal complexes can exhibit chemical reactivities that are different than either the metal or organic ligands alone. This reactivity can be refined by bringing small modifications to their structure and electronic properties, or by varying the metal center and its oxidation state [1]. Whereas carbon, the most significant element in drug design, can provide inert covalent bonds with connectivities of two to four, resulting in bonding geometries around the atom that range from linear to trigonal planar to tetrahedral, a wide range of coordination numbers and geometries with different possible redox states and thermodynamic and kinetic properties can be generated by metal ions. These features provide a versatile platform to construct molecules with a variety of potential medicinal properties that are not accessible for carbon-based compounds [2].

Metal ions do not only play an important role as essential nutrients, but are also becoming prevalent components of diagnostic or therapeutic agents for different diseases [3]. There are several examples of metal-based agents being used in medicine for different applications and selected examples are showed in Figure 1.

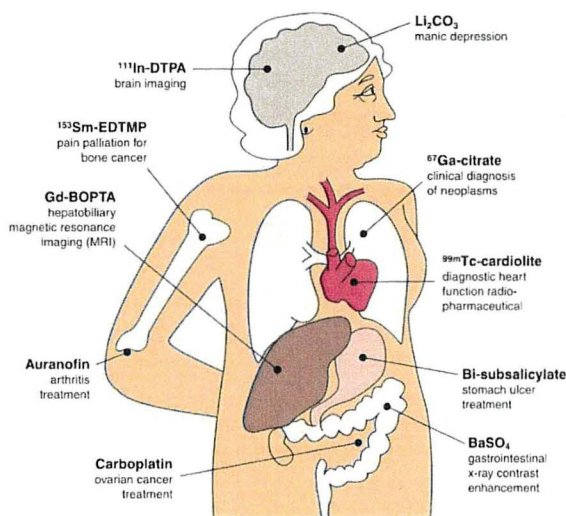


Figure 1. Metal ions are important in diagnosis and therapy of a host of different human pathologies. Gd, ^{111}In , and $^{99\text{m}}\text{Tc}$ are used in medical imaging, ^{153}Sm and Au relieve pain in bone cancer and arthritis, respectively, Bi soothes upset stomach and Li calms bipolar psychosis. ^{67}Ga -citrate is used in clinical diagnosis of neoplasms and Pt is used for cancer treatment. (from Thompson *et al* 2003)^[3].

For instance, bismuth and lithium salts have been in use for many years as antacids and as medications for mental disorders such as manic depression, respectively [4-5]. Barium sulfate is used as a contrast agent in diagnostic x-ray procedures (e.g. imaging of the gastrointestinal tract), given its proper mass attenuation coefficient [6]. Auranofin is a gold-based compound that is widely used for the treatment of rheumatoid arthritis but is also being investigated for potential therapeutic applications in other diseases such as cancer, neurodegenerative disorders, HIV/AIDS, parasitic and bacterial infections [7]. The targeted bone-seeking radioisotope ¹⁵³samarium ethylene-diamine-tetramethylene-phosphonic acid (¹⁵³Sm-EDTMP) has shown effective bone pain palliation in patients diagnosed with malignant bone tumors and recent evidence also suggests some cytotoxic activity for this drug [8]. Furthermore, one of the most well-known inorganic compounds for cancer therapy are platinum-based drugs such as cisplatin and carboplatin, which have been widely used for the treatment of different types of cancers [9]. Despite their great therapeutic success against solid tumors, severe side effects limit their clinical use. Although all the mechanistic details involved in the anticancer mode of action of Pt-based drugs remain unknown, these complexes are believed to act by intercalating into the DNA helix through covalent bonding at guanine residues and supplementary hydrogen bonding. Because this interaction is not only limited to cancer cells, the transcription and DNA replication of normal cells can also be altered, which may explain the numerous side effects induced by these agents [3, 10-11]. Another limiting factor for the clinical use of these agents is the emergence of drug resistance as a consequence of changes in cellular uptake, drug efflux, increased detoxification, inhibition of apoptosis or increased DNA repair [12].

1.1.1 Ruthenium complexes for cancer therapy

As alternatives to platinum-based anticancer drugs, in recent years, most efforts have been devoted to the design of compounds based on ruthenium because of their unique biochemical properties. For instance, some ruthenium complexes can potentially bind to serum transferrin and albumin by mimicking iron, resulting in the solubilization and transport of the species in plasma and in their enhanced accumulation in tumor masses [13-14]. Another characteristic of ruthenium compounds is believed to be their ability to undergo an “activation by reduction” process, suggesting a selective accumulation of active species at the tumor site [15]. This hypothesis is based on the assumption that some Ru(III) species that are relatively inert may remain intact in the blood until they reach the tumor tissue, where due to the more reducing environment, can be

reduced to Ru(II) species which are more labile and reactive. Moreover, similarly to platinum drugs, the ligand exchange kinetics of several ruthenium complexes is relatively slow, preventing spontaneous structural alterations prior to reaching the target ^[16-17]. Despite that both platinum and ruthenium compounds can bind to DNA, ruthenium antitumor complexes, either Ru(II) or Ru(III)), probably function in a manner different from that of cisplatin, owing to their octahedral structure as opposed to the square-planar geometry of platinum(II) compounds. However, the extent of DNA binding that is responsible for their mechanism of action still remains to be elucidated ^[18-19]. Interestingly, some ruthenium complexes induce fewer side effects than platinum-based complexes, and some have been reported to also be active against platinum resistant cancers, most probably because of their different modes of action in comparison with classical platinum anticancer drugs ^[20-22].

Ruthenium complexes then hold promise as several ones have entered preclinical or/and clinical trials (Figure 2). For instance, NAMI-A, a Ru(III) coordination compound was the first ruthenium anticancer compound to be studied on human beings that entered a phase I clinical trial in 1999. It was also the first ruthenium complex that reached the phase II stage to be tested in patients with non-small cell lung cancer (NSCLC) after first-line therapy ^[21]. Despite elegant antimetastatic properties of NAMI-A with a variety of mechanisms of action in the preclinic, its clinical study has been recently terminated due to the toxicity profile and the lack of convincing preliminary efficacy results. Nevertheless, additional trials in larger populations might be needed to be able to draw definitive conclusions ^[23]. KP1019 was the second ruthenium complex that entered a phase I study for cancer treatment. This compound did not cause serious side effects in the clinical study and importantly, stabilized the diseases in five out of six patients (diagnosed with different cancers) for up to ten weeks, making it a promising candidate for further clinical investigations ^[24]. A Ru(II) complex, RAPTA-C, showed significant growth inhibitory activity of primary tumors in preclinical models for ovarian and colorectal carcinomas, making Ru(II)-arene complexes other promising candidates for further pharmaceutical investigations ^[25]. Very recently, another Ru(II)-based anticancer drug, TLD-1433, entered a phase II clinical trial. TLD-1433 is a photosensitizer (PS) investigated for the treatment of nonmuscle-invasive bladder cancer (NMIBC) using photodynamic therapy (PDT). Results from the phase I study were promising, as 67% of the patients treated with the compound fully responded to the treatment: no presence, recurrence, nor progression of their bladder cancer was noted for 18 months following a single PDT treatment with TLD-1433 ^[26].

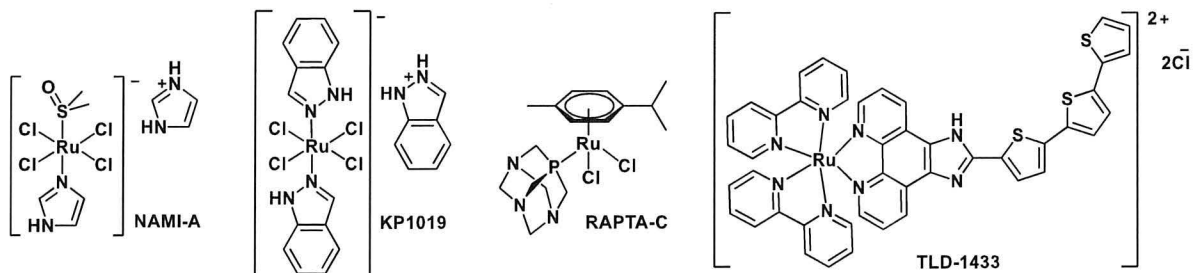


Figure 2. Ruthenium complexes that entered preclinical or/and clinical studies.

1.1.2 Ruthenium complexes for multitargeting approaches in cancer therapy

Of high interest are ruthenium complexes that can simultaneously act on more than one target, known as “multitargeting” complexes, potentially leading to enhanced efficacy and lower potential to induce drug resistance [27]. To date, “cocktail” therapy, such as drug combinations (multiple tablets of different agents) and multi-component drugs (one tablet comprising multiple agents), is used to enhance the efficacy of cancer treatment. However, factors such as poor patient compliance, unpredictable high cost, side effects, and variable rates of drug metabolism in different patients limit the clinical use of the cocktail strategy [27-29].

Alternatively, multitargeting therapy can be achieved by combining multiple drugs in a single molecule that can act on multiple targets simultaneously. This strategy may offer multiple advantages over the cocktail strategy such as a simplified drug metabolism, a lower risk of drug interactions, an improvement in the solubility and delivery mechanisms of the molecule, and potential diversity of the mode of action of the components [27].

In order to develop ruthenium drug candidates following this multitargeting approach for cancer therapy, several ruthenium complexes bearing biologically active ligands were synthesized, and their anticancer potential investigated. For this class of ruthenium complexes, both the metal and the ligands are mutually responsible for their biological activity. For instance, Hartinger et al (2012) reported Ru(II)arene-flavonoid complexes (Figure 3) with a considerable activity in different cancer cell lines, consisting of a DNA-binding metal centre and a biologically active ligand, capable to inhibit topoisomerase II α . In this study, a more significant enzyme inhibitory activity was observed for the metal complexes compared to their corresponding free ligands, indicating the impact of this combination on the efficacy of the original drugs [30]. In another study, Wang et al (2014) reported NAMI-A type Ru(III) complex derivatives tethering 4-anilinoquinazoline, an epidermal growth factor receptor (EGFR) inhibitor (Figure 3). EGFR plays an important role in cell division and growth, and is overexpressed in many types of tumor cells, making it a promising

target for cancer therapy. The species investigated in this study could represent a novel class of multitargeting anticancer agents involving both the blockage of EGFR signalling and the induction of early-stage apoptosis cascades ^[31]. As another example, Dyson et al (2014) reported RAPTA-type complexes bearing curcumin derivatives (Figure 3), previously reported to possess anticancer properties. Given that curcumin is insoluble and unstable in water, it is interesting to note that these Ru(II) complexes of curcumin were highly soluble and stable in aqueous medium, and induced a more significant cytotoxicity than curcumin ^[32]. These data confirm that the combination of two species in a single molecule can not only improve the chemical and physical properties of the original compounds but can also enhance their biological activity.

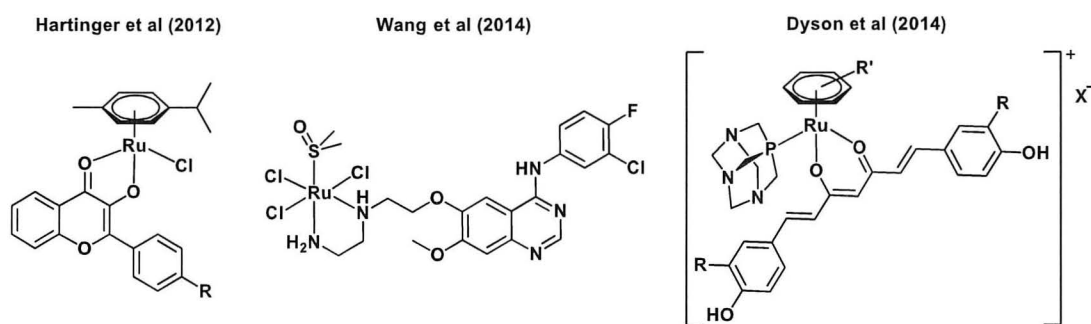


Figure 3. Examples of ruthenium complexes bearing biologically active ligands with potential multitargeting properties.

1.2 Aromatase inhibitors for breast cancer therapy

Enzyme inhibitors are substances which alter the catalytic activity of enzymes by slowing down, or in some cases stop, the catalysis process. The growth and the functions of cancer cells are often very dependant on the activity of enzymes, making them promising cellular targets for cancer treatment ^[33-35]. In the course of this study, we mainly focused on the design of potential multitargeting ruthenium complexes for breast cancer therapy, as this type of cancer is the most commonly diagnosed cancer in women, accounting for 1 in 4 (25%) of new cases worldwide ^[36]. To develop multitargeting ruthenium complexes for breast cancer treatment, we have selected aromatase inhibitors to act as ligands in the structures of the complexes.

Estrogen deprivation has long been an effective treatment for breast cancer, and the introduction of the antiestrogen tamoxifen produced marked improvements in breast cancer survival ^[37]. The

mode of action of tamoxifen involves blocking estrogen receptors, whose signalling represents a critical growth and survival pathway in breast tumours [38]. Unlike tamoxifen, aromatase inhibitors do not directly interact with estrogen receptors, but instead inhibit the conversion of androgens to estrogen in postmenopausal women [39]. It is believed that higher levels of estrogen result in a faster growth of breast cancer cells, specifically in the case of estrogen receptor positive (ER+) breast cancers. Aromatase inhibitors interact with the aromatase enzyme which catalyzes the key step of the estrogen biosynthesis, leading to estrogen deprivation and potentially breast cancer cell growth inhibition [40]. It is noteworthy that aromatase inhibitors can only efficiently deprive cells from estrogen in postmenopausal women for whom the estrogen production is no longer governed by ovaries and is only produced from the catalytic activity of aromatase [41].

Among aromatase inhibitors, the third-generation series (last generation), consisting of both nonsteroidal inhibitors, anastrozole and letrozole, and the steroidal inhibitor exemestane, has become one of the most commonly used drugs for treating ER+ breast cancers (Figure 4) [42]. Anastrozole and letrozole can bind to the heme iron of the aromatase through the coordination of one nitrogen of their triazole ring, and accordingly block the active site of the enzyme preventing the estrogen biosynthesis [43].

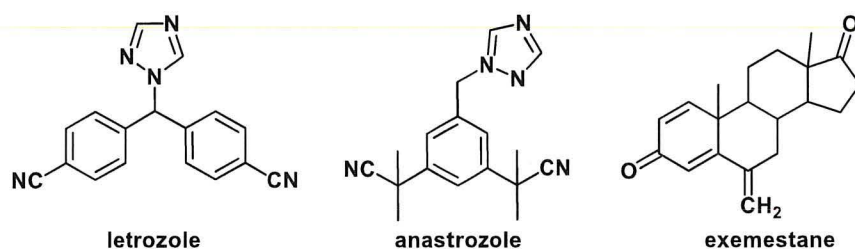


Figure 4. Chemical structures of third-generation aromatase inhibitors.

On the other hand, steroidal aromatase inhibitors such as exemestane compete with the endogenous ligands androstenedione and testosterone for the active site of the enzyme, where they are metabolized to intermediates that bind irreversibly to the active site, causing enzyme inhibition [44]. Among the third-generation aromatase inhibitors, the presence of a triazole ring in the structure of anastrozole and letrozole makes them appropriate candidates to act as ligands in the coordination sphere of ruthenium complexes, which could potentially provide multitargeting properties to the complexes for breast cancer therapy.

In the following chapter, a review on the importance of the development of new anticancer drugs for breast cancer therapy, using a multitargeting approach, as well as several examples of rationally designed ruthenium complexes for breast cancer therapy, organized by subtype of breast cancer, are presented.

1.3 Rationally designed ruthenium complexes for breast cancer therapy (a review article: publication 1)

Complexes de ruthénium rationnellement conçus pour le traitement du cancer du sein

Authors: Golara Golbaghi, Annie Castonguay*

INRS-Centre Armand-Frappier Santé Biotechnologie, Université du Québec, Laval, Canada

This article was published in *Molecules-Special Issue Metal Anticancer Complexes*, selected to be featured on the front cover 2020, 25(2), 265.

<https://doi.org/10.3390/molecules25020265>

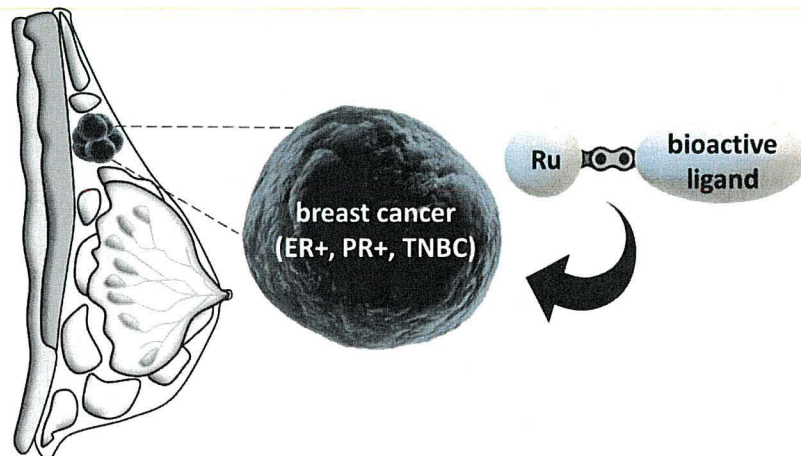
Author contributions:

Golara Golbaghi participated in conceptualization, writing the original draft and editing the manuscript.

Prof. Annie Castonguay supervised this project and participated in conceptualization, reviewing and editing the final version.


RÉSUMÉ:

Dans le monde, le cancer du sein est la forme la plus fréquente chez la femme. Depuis la découverte du potentiel anticancéreux des complexes de ruthénium, plusieurs se sont avérés prometteurs pour le traitement de ce type de cancer. Parmi ces derniers, les complexes comportant un ligand bioactif s'avèrent particulièrement intéressants puisqu'ils peuvent permettre l'identification de molécules thérapeutiques ayant une large gamme de modes d'action cellulaires. Cette revue de la littérature vise à fournir un aperçu des complexes à base de ruthénium comportant un ligand bioactif ayant démontré une efficacité intéressante contre les cancers du sein hormonaux dépendants aux œstrogènes (ER+) ou bien à la progestérone (PR+). De plus, cette revue met en lumière plusieurs exemples particulièrement importants de leur activité thérapeutique pour le traitement du cancer du sein triple négatif (TNBC), une forme de cancer parmi les plus agressifs.



Review

Rationally Designed Ruthenium Complexes for Breast Cancer Therapy

Golara Golbaghi and Annie Castonguay * 

Organometallic Chemistry Laboratory for the Design of Catalysts and Therapeutics,
INRS-Centre Armand-Frappier Santé Biotechnologie, Université du Québec, Laval, QC H7V 1B7, Canada;
golara.golbaghi@iaf.inrs.ca

* Correspondence: annie.castonguay@inrs.ca

Academic Editor: Kogularamanan Suntharalingam

Received: 1 November 2019; Accepted: 1 January 2020; Published: 9 January 2020



Abstract: Since the discovery of the anticancer potential of ruthenium-based complexes, several species were reported as promising candidates for the treatment of breast cancer, which accounts for the greatest number of new cases in women every year worldwide. Among these ruthenium complexes, species containing bioactive ligand(s) have attracted increasing attention due to their potential multitargeting properties, leading to anticancer drug candidates with a broader range of cellular targets/modes of action. This review of the literature aims at providing an overview of the rationally designed ruthenium-based complexes that have been reported to date for which ligands were carefully selected for the treatment of hormone receptor positive breast cancers (estrogen receptor (ER+) or progesterone receptor (PR+)). In addition, this brief survey highlights some of the most successful examples of ruthenium complexes reported for the treatment of triple negative breast cancer (TNBC), a highly aggressive type of cancer, regardless of if their ligands are known to have the ability to achieve a specific biological function.

Keywords: ruthenium; breast cancer; multitargeted therapy; metallodrug; hormone positive breast cancer; triple negative breast cancer (TNBC); enzyme inhibition

1. Introduction

Cancer is a major public health issue worldwide [1,2]. More specifically, breast cancer is the most common cause of cancer death in women in developing countries and the second most common cause of cancer death in developed countries [3]. Although death rates for breast cancer dropped by 40% from 1989 to 2016 [1], specific types of breast cancer are still incurable [4]. Estrogen and progesterone receptors play a crucial role in the development of the most common breast cancer subtypes, and their expression is very highly predictive of their response to endocrine therapy. Different subtypes of breast cancer include estrogen receptor alpha (ER α), overexpressed in approximately 70% of invasive breast cancers, and progesterone receptor (PR), overexpressed in over two-thirds of estrogen receptor positive (ER+) breast cancers [5,6]. Another common biomarker in breast cancer is the epidermal growth factor 2 (HER2), overexpressed in approximately 20% of breast cancers [4]. Cancer patients who test positive for that protein can benefit from HER2-targeted therapy [7]. Finally, triple-negative breast cancer (TNBC), which represents 10–20% of all breast carcinomas [8], is characterized by the absence of ER, PR, and HER2 biomarkers [8,9]. Because of the ineffectiveness of endocrine therapy or therapies targeted to HER2 for TNBC, this type of cancer requires the development of different treatment approaches [8,10]. It is noteworthy that approximately 10–30% of patients with breast cancer, regardless of their hormone receptor status, develop metastases to the lymph nodes or/and distant organs, making the design of an efficient treatment for this heterogeneous type of breast cancer a challenging task [11,12]. Despite the associated short- and long-term risks, chemotherapy frequently remains an essential treatment for

breast cancer, more particularly for late stage, metastatic, or triple-negative breast cancer [4]. Although patients with ER+ and/or PR+ breast cancer can benefit from endocrine therapy [4], alternative types of treatment including chemotherapy are often envisaged due to the side effects [13–15] and the high risk of post-therapy recurrence [16,17]. Besides, it was also reported that the combination of chemotherapy and endocrine therapy can significantly increase the survival rate of patients diagnosed with ER+ breast cancer [17].

Because of the wide range of coordination numbers and geometries, accessible redox states, and the thermodynamic/kinetic properties and nature of the coordinating ligands, inorganic compounds can exploit the unique properties of metal ions for the design of new anticancer drugs [18,19]. A well-known chemotherapeutic agent, cisplatin, is one of the most commonly used drugs to treat malignant breast cancers, either as a single agent or in combination with other drugs [20–22]. Although the success of cisplatin and its derivatives in breast cancer treatment is undeniable, these compounds usually display a range of severe side effects due to their lack of selectivity for cancerous over normal tissues [23]. The poor selectivity of cisplatin can be explained by its primary mode of action, which includes its interference with transcription and/or DNA replication mechanisms, not only limited to cancer cells but also to normal cells [23–25]. It has been reported that breast cancer cells can develop resistance to platinum-based drugs through different pathways, making it a major clinical obstacle to the development of successful treatments [26,27]. As an alternative to platinum-based chemotherapeutic agents, most efforts were devoted to the design of compounds based on ruthenium, as many were reported to display fewer side effects due to their different modes of action [28,29]. In many cases, ruthenium complexes were found to display a high cytotoxicity against platinum-resistant cancer cell lines, making them promising candidates for further investigation [30,31]. Also importantly, ruthenium species have demonstrated some promising activities in different types of breast cancer, opening the door to the design of novel metal-based chemotherapeutic agents. It is worth mentioning that several ruthenium complexes such as RAPTA-C [32], NAMI-A, and KP1019 [33] have successfully entered preclinical or clinical trials for the treatment of different cancers. Some ruthenium species also have the potential to act as photosensitizers (PS) in photodynamic therapy (PDT), which relies on the combination of a PS, light, and molecular oxygen. Upon light-activation, the excited state of the PS interacts with the ground state of molecular oxygen ($^3\text{O}_2$) to generate reactive oxygen species and notably singlet oxygen ($^1\text{O}_2$), which can interact with a wide range of biomolecules [34]. TLD-1433 is the first ruthenium(II)-based PS for PDT to enter a human clinical trial for the treatment of non-muscle invasive bladder cancer [35].

In recent years, the development of agents with enhanced anticancer properties via the coordination of biologically active molecules to metals, more specifically ruthenium, has attracted increasing attention [36–38]. Because ruthenium complexes are widely studied for their ability to induce cancer cell death, the introduction of biologically active ligands in their structure can be a promising approach for the development of drug candidates with a broader range of anticancer activities compared to ruthenium complexes or ligands alone [39,40]. This approach can potentially result in the creation of multitargeting drug candidates that could limit the emergence of cancer cell resistance mechanisms by leaving biological systems unable to compensate for the simultaneous action of two or more drugs [41]. The promising potential of this class of compounds was demonstrated by several rationally designed ruthenium complexes bearing biologically active ligands for the treatment of hormone receptor positive and hormone receptor negative breast cancers. For the former group of breast cancers, anticancer drugs including P450 inhibitors or steroid receptor-targeting molecules were included within the structure of the complexes whereas for the latter group, due to the lack of expression of hormone receptors, anticancer drugs with other modes of action (such as nonsteroidal anti-inflammatory drugs) were used as ligands. It is noteworthy that no ruthenium complex was specifically reported for the treatment of HER2+ breast cancer, so that reports of ruthenium complexes for hormone receptor negative breast cancer therapy are limited to TNBC therapy.

In this review, an overview of the rationally designed ruthenium-based complexes that were reported to date for breast cancer therapy is presented, with a special emphasis on species that include ligands that were carefully selected for the treatment of hormone receptor positive cancers, either estrogen receptor positive and/or progesterone receptor positive. In addition, this brief survey highlights some of the most successful examples of ruthenium complexes reported for the treatment of triple negative breast cancer, a highly aggressive type of cancer, regardless of if their ligands are known to have the ability to achieve a specific biological function. The information presented in this review is summarized in Table S1 (Supplementary Materials).

2. Ruthenium Complexes for the Treatment of Hormone Receptor Positive Breast Cancer

Anticancer drugs that are known to deprive cancer cells of the hormones they need for their growth, such as estrogen and progesterone, are promising ligand candidates for the design of multitargeting ruthenium complexes for the treatment of HR+ breast cancer. P450 enzyme inhibitors and steroid hormone receptor targeting moieties are examples of anticancer agents that are discussed in this section. Some successful examples of ruthenium complexes bearing other bioactive ligands such as nonsteroidal anti-inflammatory drugs (NSAIDs), epidermal growth factor receptor (EGFR) inhibitor, and glutathione S-transferase (GST) inhibitor are also presented.

2.1. Ruthenium Complexes Bearing P450 Enzyme Inhibitors

The combination of ruthenium with a P450 enzyme inhibitor in a single agent could potentially be beneficial for hormone receptor positive breast cancer therapy. P450 enzymes catalyze reactions that are involved in the biosynthesis and the metabolism of various important molecules [42,43]. For instance, the P450 enzyme aromatase (CYP19A1) plays a crucial role in steroid synthesis and thus in the growth of ER+ breast cancer [44]. Notably, it catalyzes the conversion of androgens to estrogens, a process known to provide the primary source of estrogens in postmenopausal women (for whom the production of estrogens is no longer governed by their ovaries) [45]. The mode of action of third-generation aromatase inhibitors is believed to take place via the N-interaction of their triazole ring with the iron of the enzyme's cofactor, thus preventing the catalytic activity of the enzyme [46]. Furthermore, the inhibition of aromatase in breast tissues can also sensitize cells to chemotherapeutic agents [47,48]. Maysinger et al. (2012) reported the preliminary *in vitro* anticancer potential assessment of a series of ruthenium(II) arene complexes of the aromatase inhibitor letrozole in breast cancer cells, a clinically used third-generation aromatase inhibitor [49]. Among the ruthenium arene complexes reported in this study, complex (1) (Figure 1) showed the most promising cytotoxicity in the ER+ breast cancer cell line MCF7. Notably, the cytotoxicity of this compound was found to be significantly higher than that of the control complex $[\text{Ru}(\eta^6\text{-C}_6\text{H}_6)\text{Cl}_2(\text{PPh}_3)]$ (with no aromatase inhibitor), suggesting a contribution of the letrozole ligand on the activity of the compound [49]. However, the aromatase enzyme inhibitory potential of these complexes was overlooked. More recently, Castonguay et al. (2019) reported a series of ruthenium(II) arene complexes bearing a slightly different third-generation aromatase inhibitor, namely anastrozole [40]. In this study, the stability, *in vitro* cytotoxicity, *in vitro* aromatase inhibitory activity, and the *in vivo* toxicity of the complexes on the development of zebrafish embryos were investigated. Cationic complexes with a more lipophilic counterion (BPh_4 vs BF_4) showed a higher *in vitro* cytotoxicity, which could potentially be associated with greater levels of ruthenium cellular uptake, as measured by ICP-MS. Among all the synthesized species, the highest *in vitro* cytotoxicity was observed for complex (2) (Figure 1), which also displayed a high stability in cell growth media. An IC_{50} value of 4 μM was noted in both MCF7 and T47D breast cell lines, an activity significantly higher than that of the clinically-relevant drug cisplatin ($\text{IC}_{50} > 150 \mu\text{M}$, T47D; $37.0 \pm 2.4 \mu\text{M}$, MCF7). More importantly, the aromatase inhibitory activity of (2) was studied theoretically (by performing a docking simulation) and experimentally (using the tritiated water assay), which both showed a possible enzyme inhibitory activity for this compound, despite the involvement of the nitrogen atom of its triazole ring in the ruthenium coordination sphere. Also interestingly, no apparent *in vivo* toxicity (at 12.5 μM) was

observed for this complex on the development of zebrafish embryos, which has become a prominent model for drug discovery and toxicity assessment [50]. Notably, more than 50% of zebrafish embryos treated with cisplatin under the same conditions could not hatch after 96 h, a clear indication of the toxicity of this chemotherapeutic agent [40]. Importantly, Castonguay et al. (2020) recently developed a novel ruthenium(II) cyclopentadiene (Cp) complex of anastrozole (3) (Figure 1) with a high in vitro cytotoxicity not only in ER+ breast cancer cells ($IC_{50} = 0.50 \pm 0.09 \mu\text{M}$, MCF7; $0.32 \pm 0.03 \mu\text{M}$, T47D) but also in a TNBC cell line, MDA-MB-231 ($IC_{50} = 0.39 \pm 0.09 \mu\text{M}$) [51]. Although this species was also cytotoxic in a non-cancerous breast cell line, MCF-12A ($IC_{50} = 0.58 \pm 0.02 \mu\text{M}$), no apparent in vivo toxicity was observed on the development of zebrafish embryos at concentrations around its IC_{50} values. It is worth mentioning that both experimental and theoretical studies suggested that the interaction between this species and the aromatase enzyme is not likely to occur, most probably because of the bulkiness of the PPh_3 moieties, preventing the compound from reaching the active site of the enzyme. Overall, the significant cytotoxicity of (3) against cancer cells, combined with its low toxicity on the development of zebrafish embryos, makes it an interesting candidate for further investigations. Some other P450 enzymes, such as CYP1B1, are also known to play a role in cancer initiation, progression, and drug resistance [52,53]. For instance, Glazer et al. (2017) reported an interesting study involving ruthenium(II) complexes bearing the P450 enzyme inhibitor etomidate, (4) (Figure 1), with dual enzyme inhibitory and DNA damaging activities upon light activation [54]. Although the drug candidate was not specifically designed nor tested for its activity in breast cancer, we reasoned that mentioning that study could be of interest to the reader as etomidate can also inhibit the activity of the aromatase enzyme [55–57]. Despite the interesting dual activity observed for this complex, its in vitro cytotoxicity was not studied [54].

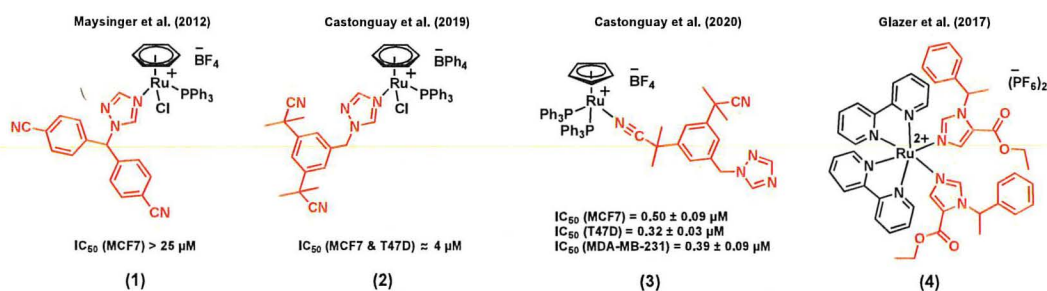


Figure 1. Ruthenium complexes bearing P450 enzyme inhibitors.

2.2. Ruthenium Complexes Bearing Steroid Hormone Receptor Targeting Moieties

Steroid hormones play a major role in regulating the expression of specific gene networks, and their biological effects on target tissues is mediated by specific receptors [58]. Several reports have shown that targeting hormone receptors in breast cancers can prevent their interaction with hormones and, as a result, block their function and lead to cancer cell death [59]. Thus, linking steroid hormone receptor-targeting moieties to metal-based drug candidates appears to be a promising avenue for the design of therapeutic agents [60].

Accordingly, Jaouen et al. (2005) reported a series of ruthenocene-substituted tamoxifen derivatives, (5) (Figure 2), including alkyl chains of various lengths ($n = 2-5$) and investigated their in vitro cytotoxicity in both ER+ and TNBC cell lines [61]. Tamoxifen is known to compete with estrogens for the specific binding of estrogen receptors and, as a result, induce programmed cell death [62]. Notably, a slight activity was observed at $1 \mu\text{M}$ (% proteins/control ≈ 80) for the shortest alkyl chain complex ($n = 2$) in the ER+ cell line MCF7, an activity similar to that of the corresponding free ligand, whereas a slightly better cytotoxicity (% proteins/control $\approx 60-70$) was noted for the derivatives with a longer alkyl chain ($n = 3-5$). No apparent cytotoxicity was observed when the TNBC cell line MDA-MB-231 was exposed to these ruthenium(II) complexes. Importantly, a much higher (>2 times) ER α relative binding

affinity (RBA) was observed for the ruthenium complex bearing the shortest alkyl chain derivative ($n = 2$) when compared to that of its corresponding free ligand, demonstrating the receptor targeting potential of the ruthenium backbone [61]. Peng et al. (2018) reported an estrogen receptor-targeting ruthenium(II) polypyridyl photosensitizer, (6) (Figure 2), for the photodynamic therapy (PDT) of ER+ breast cancers [63], also bearing a tamoxifen derivative. The ruthenium polypyridyl backbone of the complex can serve as both a two-photon excited singlet oxygen-generating photosensitizer and a two-photon fluorescence probe for tracking the cellular uptake and localization of the drug candidate. On the other hand, the tamoxifen ligand linked to the ruthenium polypyridyl backbone through a triazole linker can provide efficient estrogen receptor targeting of ER+ breast cancer cells. Importantly, compound (6) displayed a significantly higher phototoxicity in ER+ breast cancer cells (MCF7) than in a triple negative cell line (MDA-MB-231), suggesting a non-negligible effect from tamoxifen on the internalization of the complex through its interaction with the multiple estrogen receptors found in MCF7 cells. The mode of action of this complex is believed to be associated with the generation of $^1\text{O}_2$, causing damage to lysosomes, resulting in cell death. It is noteworthy that the phototoxicity of (6) was found to be significantly higher than that of a control compound (with no tamoxifen in its structure), but also higher than that of a mixture of the same control complex with tamoxifen (1:1 ratio), indicating a possible synergistic effect arising from the ruthenium and tamoxifen combination within a complex [63].

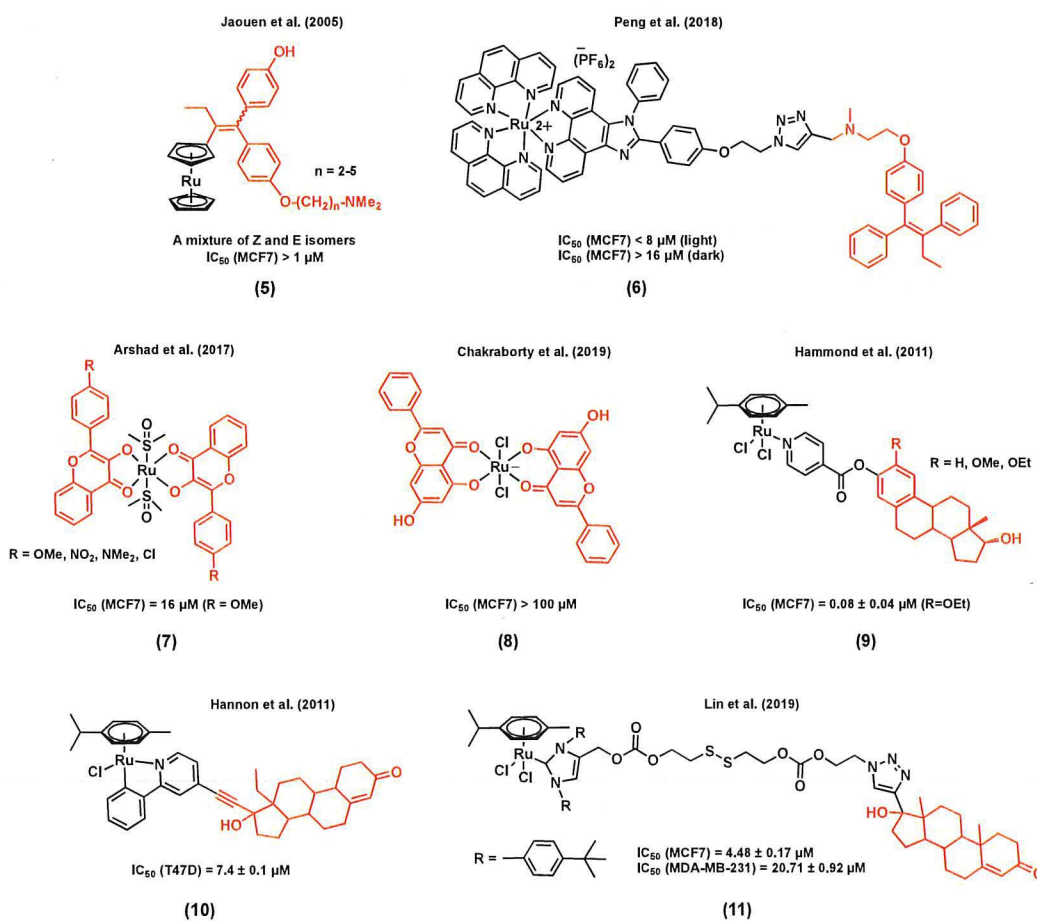


Figure 2. Ruthenium complexes bearing hormone receptor targeting moieties.

Other examples of estrogen receptor-targeting ruthenium species include complexes with substituted flavones as ligands, (7) (Figure 2), which were studied by Arshad et al. (2017) [64]. Flavones belong to a class of compounds called flavonoids, known to display different biological functions, including some antiestrogenic activity, due to their ability to bind estrogen receptors [65,66]. All the ruthenium-flavone complexes reported in this study displayed almost equal or slightly lower IC_{50} values in MCF7 breast cells compared to the corresponding flavones alone, suggesting a retained activity from the flavones upon coordination. It is also interesting to note that the lowest IC_{50} value in MCF7 cells (16 μ M) was observed for a ruthenium complex that includes a flavone ligand bearing a methoxy substituent, known to inhibit DNA synthesis [64]. In another study, the potential modes of action of a ruthenium(III)-flavone (chrysin), complex (8) (Figure 2), was studied by Chakraborty et al. (2019). Results have demonstrated the ability of this compound to arrest the cell cycle and to induce apoptosis, following the upregulation of p53 and Bax and the downregulation of Bcl2, VEGF, and mTOR. The in vivo toxicity of (8) was also assessed by exposing rats to 250 to 1000 mg/kg doses of the complex. On Day 20, treatment-related mortality and body weight loss were observed when a 1000 mg/kg dose of (8) was used [67]. It is worth mentioning that none of the above publications on ruthenium-flavone complexes reported the potential interaction of the complexes with estrogen receptors.

It has been reported that the coordination of estrogens or androgens to an organometallic backbone can mediate hormone receptor targeting, facilitating the cellular uptake of the corresponding complexes [68,69]. For instance, a series of ruthenium(II) complexes with *N*-coordinated estradiol isonicotinates were reported by Hammond et al. (2011) (9) [70]. Their in vitro cytotoxicity in MCF7 cells was found to be considerable (IC_{50} values < 20 μ M) with the highest activity being observed for the R = OEt derivative ($IC_{50} = 0.08 \pm 0.04 \mu$ M). Despite the promising cytotoxicity of these complexes, none of them showed any affinity for the estrogen receptor ER α . However, most of them were found to display a significant affinity, although to a lesser extent than their respective parent steroid, with the sex hormone binding globulin that transports steroid hormones in the blood and facilitates their cellular uptake by allowing their accumulation on the plasma membrane [70–72]. A steroid-conjugated (levonorgestrel) ruthenium(II) arene complex, (10) (Figure 2) [73], was reported by Hannon et al. (2011) to be 8-fold more active than cisplatin in T47D human breast cancer cells. The antiproliferative activities of free levonorgestrel and a control complex containing no steroid, Ru(η^6 -*p*-cymene)(ppy)Cl, were found to be much lower than the ruthenium bioconjugate complex. Theoretical DFT calculations on complex (10) showed that the metal center is distant enough from the lipophilic steroidal moiety to allow a possible interaction between the ruthenium and biomolecules such as N-nucleophiles, more specifically 9-ethylguanine (9-EtG), following the replacement of the chloride ligand with the nucleophile. Finally, ESI-MS analysis data also showed experimental evidence for the possible formation of a 9-EtG monoadduct, resulting from the incubation of 9-ethylguanine with (10). In another study, Lin et al. (2019) reported a ruthenium(II) N-heterocyclic carbene complex (Ru-NHC) conjugated to a 17 α -ethynyl testosterone (Te structure very similar to progesterone) through a disulfide linkage to generate a new complex, Ru-NHC-S-S-Te, (11) (Figure 2) [74]. The cytotoxicity of (11) was studied in MCF7 (PR+) and MDA-MB-231 (PR-) cell lines, and was also compared with that of the original Ru-NHC complex as a control (with no steroid conjugated moiety). The IC_{50} value of (11) ($4.48 \pm 0.17 \mu$ M) was found to be about twice as low as that of Ru-NHC ($10.54 \pm 0.34 \mu$ M) in MCF7 cells. However, when MDA-MB-231 cells were treated with the complexes, an opposite trend was observed as a lower IC_{50} value was noted for Ru-NHC ($14.18 \pm 1.01 \mu$ M) when compared with that of (11) ($20.71 \pm 0.92 \mu$ M). The mode of action of (11) is associated with blocking the cell cycle progression and inducing cell apoptosis. Moreover, compound (11) showed a lower cytotoxicity in normal breast cells, Hs578Bst ($IC_{50} = 37.36 \pm 1.89 \mu$ M), compared with that of Ru-NHC in the same cell line ($IC_{50} = 11.42 \pm 1.12 \mu$ M). An ICP-MS analysis showed significantly higher ruthenium cellular levels in MCF7 cells treated with (10) compared to those treated with Ru-NHC. However, the ruthenium accumulation in the MDA-MB-231 cell line was found to be only slightly different between the two compounds. Taken together, cytotoxicity and cellular uptake studies suggest that the steroid moiety

acts as a targeting unit to PR+ tumor cells. The in vivo antitumor activity of (11) and Ru-NHC was also assessed in a nude mice MCF7 xenograft model. Both compounds were successful at suppressing tumor growth but notably, a slight decrease in the tumor volume of mice treated with (11) was also noted. Moreover, mice treated with (11) survived for a longer time than mice from the control group, whereas mice treated with Ru-NHC died prior to the ones from the control group, demonstrating the effect of the ligand on the toxicity of ruthenium complexes [74].

2.3. Other Ruthenium Complexes for the Treatment of Hormone Receptor Positive Breast Cancers

Whereas examples of ruthenium complexes bearing ligands that have a specific target in hormone receptor positive breast cancers are limited, several complexes bearing other types of bioactive ligands with different targets were also found to display a considerable activity for hormone receptor positive cancers. For example, several reports have demonstrated that nonsteroidal anti-inflammatory drugs (NSAIDs) have promising anticancer properties, making them suitable ligands for the design of multifunctional anticancer ruthenium complexes [75–77]. The main mode of action of NSAIDs in different cancer types, including breast cancer, is believed to be associated with the inhibition of the cyclooxygenase (COX) enzyme [75,78]. The most obvious consequence of the overexpression of COX enzymes, more specifically COX-2, is the increased production of inflammatory prostaglandins (PG), mediators that may contribute to carcinogenesis, stimulate cancer cell proliferation, and mediate immune system suppression [79]. Furthermore, several studies suggest that COX-2 inhibitors such as NSAIDs might not only play a role in the treatment of breast cancer, but also in its prevention [80]. For instance, the in vitro cytotoxicity of two cationic ruthenium(II) dppm (diphenylphosphinomethane) complexes (12), respectively bearing diclofenac (Ru-Dicl) and ibuprofen (Ru-Ibp) (Figure 3) in MCF7 breast cancer cells, was reported by Von Poelhsitz et al. (2015) and compared with that of a ruthenium complex control (with no bioactive ligand), *cis*-[RuCl₂(dppm)₂], and cisplatin [81]. Both ruthenium complexes displayed a higher cytotoxicity (IC₅₀ = 47 ± 6 μM for Ru-Dicl, MCF7; IC₅₀ = 9 ± 3 μM for Ru-Ibp, MCF7) than that of the ruthenium complex control (IC₅₀ = 191 ± 13 μM, MCF7), highlighting the importance of the NSAID ligand on the anticancer activity of the compounds. Moreover, the IC₅₀ value of Ru-Ibp was found to be significantly lower than that of cisplatin (IC₅₀ = 34 ± 4 μM, MCF7) [81]. It is worth mentioning that the potential COX inhibition activity of the compounds discussed above was not studied. More recently, Mukhopadhyay et al. (2018) reported a series of ruthenium(II) cymene complexes bearing different NSAID ligands, (13) (Figure 3), including diclofenac and ibuprofen, but also naproxen (Npx) and aspirin (Asp) [82]. Except for the Ru-Asp complex, which was found inactive against MCF7 cells, all complexes displayed a lower IC₅₀ value (<0.1 μM) than their corresponding free NSAID (>80 μM) in this cell line. Furthermore, the COX inhibitory activity of the complexes was investigated, and all complexes showed higher in vitro COX inhibition than that of their corresponding free NSAID. Notably, the Ru-Ibp and Ru-Asp complexes could inhibit the activity of the enzyme more significantly than the Ru-Npx and Ru-Dicl species. The COX inhibition by Ru-Npx and Ru-Dicl and their corresponding NSAID was further investigated by a docking simulation. Both complexes exhibited significantly higher binding affinities than the corresponding free ligands naproxen and diclofenac towards COX-2, which could be due to the higher affinity and to the more extensive different non-bonding interactions of the ruthenium species with proximal amino acid residues of proteins, H-bonding interactions, and other non-bonding interactions such as halogen and pi–pi stacking interactions. Although this study suggests a potential for metal-NSAID complexes to target COX enzymes, the lack of stability of the reported complexes in DMSO and DMSO/water mixtures [82] prevents one from drawing conclusions about their potential multitargeting properties.

Another interesting example of a type of ruthenium(II) complex bearing an enzyme inhibitor was reported by Bhattacharyya et al. (2011), discussing a bifunctional ruthenium species of ethacrynic acid, a glutathione S-transferase (GST) inhibitor, (14) (Figure 3), and its in vitro cytotoxicity in MCF7 cancer cells [83]. Complex (14) is an analogue of the ruthenium arene complex RAPTA, which was previously reported for its promising anticancer potential in different cancer cell lines and its notable activity with

regard to reducing the number and weight of solid metastases *in vivo* [32,84]. GSTs have multiple biological functions such as cell protection against oxidative stress and several toxic molecules. Because cancer cells overexpress GSTs, they can develop multifactorial drug resistance, making GST an efficient target for cancer therapy [85]. Among the members of the GST family, GSTP1-1, which catalyzes the conjugation of reduced glutathione (GSH) with a broad range of substrates including chemotherapeutic agents, has been linked to drug resistance and is frequently overexpressed in drug-resistant cell lines [86]. Exposure of MCF7 breast cancer cells to 20 μM of (14) led to a 10% reduction in cell viability after 24 h, whereas a more considerable reduction of 30% was noted after 72 h. Since reactive oxygen species (ROS) generation is one of the known modes of action of ethacrynic acid, ROS levels in cancer cells treated with (14) were also measured after 24 h and 72 h, resulting in significantly higher levels of ROS after 72 h. Due to its delayed cytotoxicity and ROS generation, compound (14) is believed to first interact with GSTP1-1, disrupting the apoptosis inhibition elicited by this enzyme, followed by the release of the metal fragment and the induction of cytotoxicity via a multiple mechanism pathway [83].

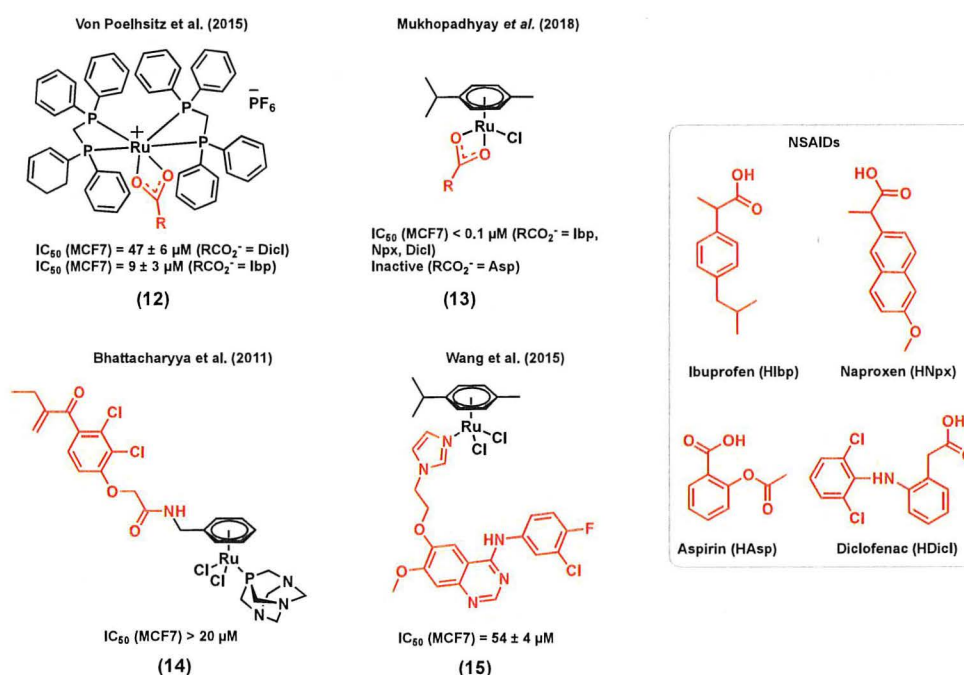


Figure 3. Ruthenium complexes bearing bioactive ligands.

The epidermal growth factor receptor (EGFR) is also a coveted target for cancer therapeutics. Part of the receptor tyrosine kinase (RTK) family, EGFR is overexpressed in a broad range of human cancer cells, including breast cancer cells, making it a potential target for the development of new anticancer agents for breast cancer therapy [87]. The extracellular ligand-binding region of the EGFR or the intracellular tyrosine kinase region can be targeted by specific anticancer agents, which may interfere with the signaling pathways that modulate mitogenic and other cancer-promoting responses such as cell motility, cell adhesion, invasion, and angiogenesis [88]. 4-anilinoquinazoline derivatives are examples of antitumor agents for which the mode of action is to inhibit the tyrosine kinase activity of EGFR via competitive binding at the ATP site of the enzyme, resulting in cancer cell growth inhibition [89]. Wang *et al.* (2015) reported a series of ruthenium(II) cymene complexes of 4-anilinoquinazoline derivatives that showed dual-targeting properties, including a significant inhibitory activity of EGFR and a high affinity with DNA via a minor groove binding mode of interaction in different types of cancers including breast cancer [90]. In this series of complexes, the most notable results were obtained for (15) (Figure 3) for which the EGFR inhibitory activity ($\text{IC}_{50} = 66.1 \pm 11 \text{ nM}$) was very close to that

of the corresponding 4-anilinoquinazoline ligand ($IC_{50} = 60.2$ nM) and higher than that of gefitinib, a well-known EGFR inhibitor ($IC_{50} = 94.0$ nM). The EGFR inhibitory activity of this complex was also supported by results obtained from a docking simulation. However, this study was performed for the aqua version of (15), as it was found to readily undergo hydrolysis in aqueous solutions. This result suggests that the introduction of ruthenium does not eradicate the activity of the 4-anilinoquinazoline ligand towards the EGFR. The presence of the chloride ligand in this class of complexes was found to be important for maintaining an EGFR inhibitory activity, which was found to be correlated to the hydrolysis potential of the compound, often considered as an essential step to activate metal-based complexes towards biomolecules [90]. The cytotoxicity of (15) was assessed in cancer cells, including human MCF7 breast cancer cells, either in the presence or in the absence of EGF (100 ng/mL), in order to evaluate the effect of blocking the signal transduction of the EGF on the inhibitory potency of the tested complexes. Complex (15) displayed a moderate cytotoxicity towards MCF7 cells ($IC_{50} = 54 \pm 4$ μ M) in the absence of EGF but was found to be inactive when exogenous EGF was added ($IC_{50} > 100$ μ M). This result indicates that EGFR inhibition may not be the only mechanism of action for this complex, and other modes of action such as DNA interaction are likely to occur, which, however, may not be efficient enough to compensate for the effect of added EGF.

3. Ruthenium Complexes for the Treatment of Triple Negative Breast Cancer (TNBC)

Since triple negative breast cancers do not respond to hormonal therapy, the commonly used anticancer drugs for hormone receptor positive breast cancers, such as P450 enzyme inhibitors or estrogen receptor targeting molecules, are not appropriate candidates to act as ligands in the structure of the ruthenium complexes for the treatment of this cancer. However, other types of anticancer agents could allow the preparation of ruthenium complexes with different cellular targets and thus improve their anticancer activity in TNBC or/and prevent the development of cancer cell resistance. In this section, several ruthenium complexes with remarkable anticancer activities in TNBC are discussed. Although the focus of this section is on multitargeting approaches, due to the importance of finding novel efficient drugs for the treatment of aggressive TNBC, other successful examples of ruthenium complex drug candidates are briefly presented, regardless of if their ligands are biologically active.

3.1. Ruthenium Complexes Bearing Nonsteroidal Anti-Inflammatory Drugs (NSAIDs)

It is noteworthy that NSAIDs may not only induce an anticancer activity in hormone receptor positive breast cancers, but also in TNBC, making them versatile moieties for the design of ruthenium species for breast cancer treatment. de Oliveira Silva et al. (2017) reported diruthenium(II,III) metallodrugs, (16) (Figure 4), of ibuprofen (Ru-Ibp) and naproxen (Ru-Npx) encapsulated into intravenously injectable solid-polymer-lipid nanoparticles (Ru-NSAID-SPLNs), which were prepared from a combination of two lipids (myristic acid and ethyl arachidate ester) [77]. The *in vitro* cytotoxicity of both dimeric metallodrugs was first studied in a triple negative breast cancer cell line, MDA-MB-231, and compared with that of ibuprofen and naproxen alone, and that of a ruthenium complex used as a control (which does not contain any bioactive ligand, $[Ru_2(O_2CCH_3)_4Cl]$). Although all observed IC_{50} values were found to be very high (>200 μ M), the cytotoxicities of both dimeric metallodrugs, Ru-Ibp and Ru-Npx, were found to be higher than that of their corresponding parent drug, ibuprofen and naproxen, and that of the control ruthenium complex, suggesting that neither the diruthenium core nor the NSAID ligand alone is responsible for the observed anticancer activities. The encapsulation of the metallodrugs or the NSAIDs with SPLNs resulted in a significant enhancement of their anticancer activity. A higher cytotoxicity was observed for the Ru-NSAID-SPLNs compared to the NSAID-SPLNs, suggesting a contribution from the metal in both cases. Notably, a higher cytotoxicity was noted for Ru-Ibp-SPLNs in MDA-MB-231 cells ($IC_{50} = 70.3 \pm 8.1$ μ M) than for Ru-Npx-SPLNs ($IC_{50} = 101.8 \pm 6.7$ μ M) in the same cell line. It was postulated that the reported SPLN formulation can promote the cellular uptake of metallodrugs and, as a result, improve their anticancer potential [77].

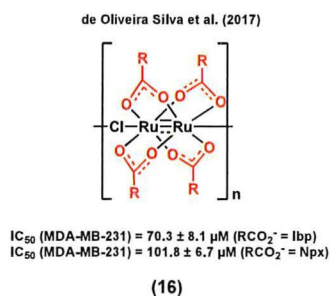


Figure 4. Ruthenium complexes bearing nonsteroidal anti-inflammatory drugs (NSAIDs), encapsulated into solid-polymer-lipid nanoparticles (SPLNs).

3.2. Ruthenium Complexes Bearing a PARP Inhibitor

Poly (ADP-ribose) polymerase (PARP) is a 17-member protein superfamily that has a well-established role in the DNA repair processes. The polymerization of ADP-ribose moieties to target proteins is catalyzed by PARPs using NAD^+ as a substrate for which nicotinamide is a by-product of the process [91]. It is of interest that nicotinamide and its analogues were found to be a weak PARP inhibitor by acting as competitive inhibitors of the PARP substrate NAD^+ . Because PARP inhibitors interrupt the DNA repair processes and sensitize cells to DNA damaging agents, they are considered as promising anticancer candidates either as single agents or in combination with other anticancer drugs [91]. It is worth mentioning that PARP inhibitors are emerging as some of the most promising targeted therapeutics to treat TNBC [92], making them suitable candidates for the design of multitargeting ruthenium complexes for the treatment of this type of breast cancer. Notably, Zhu et al. (2014) developed ruthenium(II) arene anticancer complexes based on the PARP-1 inhibitor [93]. Interestingly, the coordination of this PARP inhibitor to ruthenium led to a more water-soluble species (solubility = 0.49 mM for (17) vs 0.12 mM for the free ligand) [93]. The resulting complex showed a higher in vitro cytotoxicity than its corresponding free PARP-1 inhibitor in different human cancer cell lines. Importantly, complex (17) (Figure 5) was found to be more cytotoxic in triple negative breast cancer Hcc1937 cells ($IC_{50} = 93.3 \pm 11.4 \mu\text{M}$) than in noncancerous MRC-5 cells ($IC_{50} = 143.0 \pm 6.3 \mu\text{M}$). It worth noting that RAPTA-C, a complex used as a control (with no PARP-1 inhibitor), did not induce any change in the viability of Hcc1937 cells, even at high concentrations ($IC_{50} > 500 \mu\text{M}$), highlighting the important contribution from the inhibitor in the observed activity of complex (17). The Ru-PARP inhibitor complex showed slightly better PARP inhibitory properties compared to the corresponding free inhibitor (IC_{50} of PARP-1 inhibition (μM): 0.32 for (17) vs 0.41 for the free ligand), and DNA-binding was also reported to be involved in its mode of action, suggesting that complex (17) would have multitargeting properties.

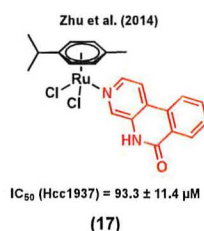


Figure 5. A ruthenium complex bearing Poly (ADP-ribose) polymerase (PARP) inhibitor.

3.3. Ruthenium Complexes Bearing an Aerobic Glycolysis Inhibitor

Unlike healthy tissues, tumors undergo aerobic glycolysis, a well-known metabolic reprogramming of cancer cells to sustain cell proliferation [94]. It has been reported that dichloroacetate (DCA) can inhibit this process, which is essential for cancer cells to produce energy in order to survive in the

hypoxic environment of rapidly growing malignant tumors [95–98]. Brabec et al. (2018) reported a ruthenium(II) arene complex of DCA, (18) (Figure 6), with considerable cytotoxicity and antimetastatic properties in MDA-MB-231 cells [99]. The IC_{50} value of (18) in the MDA-MB-231 cell line was found to be $0.86 \pm 0.01 \mu\text{M}$ (vs $56.0 \pm 5.0 \mu\text{M}$ for cisplatin), whereas higher IC_{50} values were obtained when noncancerous cells HEK-293 ($9.4 \pm 0.5 \mu\text{M}$) and primary skin fibroblasts ($>50 \mu\text{M}$) were treated with the complex. Compound (18) could reduce migration, invasion, and re-adhesion of TNBC cells, indicative of potential antimetastatic properties for this species. The antimetastatic properties of (18) were found to be associated with the ability of the compound to suppress matrix-metalloproteinase (MMP-9) activity and/or production, which is an important factor involved in the migration and adhesion processes [99,100]. Furthermore, compound (18) could slightly inhibit glycolysis in MDA-MB-231 cells, whereas cisplatin could not significantly impact glycolysis in this cell line. However, it is worth mentioning that osmium analogues of (18) showed more promising anticancer properties, such as a higher glycolysis inhibitory activity [99].

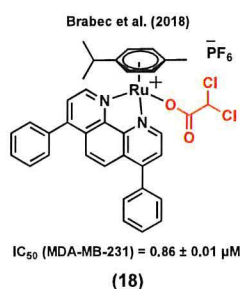


Figure 6. A ruthenium complex bearing dichloroacetato (DCA).

3.4. Ruthenium Complexes Bearing Gallic Acid

Gallic acid can induce cell death by activating several signaling pathways in different cancer types such as breast, prostate, and lung [101]. Cell cycle arrest, and as a result, apoptosis, are possible mechanisms responsible for the anticancer activity of this compound [101,102]. A ruthenium(II) complex of gallic acid (GA), (19) (Figure 7), was synthesized by Cominetti et al. (2019) and its anticancer potential evaluated in triple negative breast MDA-MB-231 and MDA-MB-468 cancer cells, and in breast MCF-10A noncancerous cells [103]. Complex (19) exhibited a higher cytotoxicity in the two triple-negative cancer cell lines ($IC_{50} = 0.81 \pm 0.08 \mu\text{M}$, MDA-MB-231; $IC_{50} = 1.00 \pm 0.10 \mu\text{M}$, MDA-MB-468) than in MCF-10A noncancerous cells ($IC_{50} = 5.82 \pm 0.33 \mu\text{M}$). The coordination of GA to ruthenium did not only lead to an improvement of the water solubility of its parent molecule, *cis*-[RuCl₂(dppe)₂] (which could not be tested due to its poor solubility in cell growth medium), but also led to a compound with a significantly increased cytotoxicity compared to that of GA ($IC_{50} > 150 \mu\text{M}$ in both cancer cell lines). It is worth mentioning that the transferrin protein was found to play an important role in the internalization and cytotoxicity of (19). It was previously reported that some ruthenium species might have the ability to mimic iron to enter cancer cells via transferrin receptors, which are usually overexpressed in cancer cells compared to normal cells [103,104]. Accordingly, when concentrations of apo-transferrin were increased, while maintaining the (19) concentration constant, a significant drop in cancer cell viability was observed. However, under the same conditions, the viability of MCF-10A cells was not significantly altered, suggesting that ruthenium species are possibly more selective towards cancerous cells because of their higher levels of transferrin receptors [103].

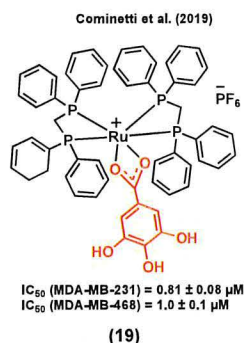


Figure 7. A ruthenium complex bearing gallic acid (GA).

3.5. Ruthenium Complexes Bearing Lapachol

Lapachol is a naturally occurring 1,4-naphthoquinone with known cytotoxicity and antimetastatic properties [105]. Its anticancer mode of action is known to mainly be due to its capacity to interact with topoisomerases and to generate reactive oxygen species (ROS) within cancer cells [106]. Batista et al. (2017) reported ruthenium(II) complexes of lapachol, (20) (Figure 8) and investigated their in vitro cytotoxicity in TNBC MDA-MB-231 cells [107]. Results showed a notable improvement in the anticancer activity of lapachol upon complexation to ruthenium ($IC_{50} = 0.20 \pm 0.01 \mu\text{M}$ for (20) vs $IC_{50} > 100 \mu\text{M}$ for lapachol). Besides, it was suggested that the main mode of action of this complex would most likely not involve DNA binding, as only very weak DNA interactions were observed for (20) [107].

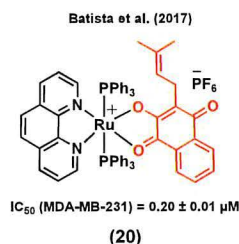


Figure 8. A ruthenium complex bearing lapachol.

3.6. Ruthenium Complexes Bearing Biotin

Vitamin–drug conjugates have attracted increased attention for cancer therapy in the last years as they can lead to an enhancement in the cancer cell uptake of some drugs due to the overexpression of vitamin receptors at their surface [108,109]. For instance, biotin (vitamin B7) is a promising candidate for exploiting this strategy due to its potential cancer cell selectivity resulting from its receptor-mediated uptake [110]. Notably, a sodium-dependent multivitamin transporter (SMVT) is overexpressed in different cancer cell lines, including breast cancer, making it an appropriate target for the selective treatment of this disease [111]. Accordingly, Valente et al. (2019) reported a ruthenium(II) cyclopentadiene complex bearing biotin, (21) ($R = \text{biotin}$), with a considerable in vitro cytotoxicity in MDA-MB-231 breast cancer cells ($IC_{50} = 11.6 \pm 1.5 \mu\text{M}$) [112] (Figure 9). The study showed that (21) ($R = \text{biotin}$) could block the activity of the ABC transporter, P-glycoprotein (P-gp), which is known to play an important role at inducing multidrug resistance (MDR) in several cancer cells [113]. It is worth noting that the inhibition of P-gp was not observed for a biotin-free analogue of the complex ($R = \text{H}$), demonstrating the importance of this conjugation to biotin [112]. An overall toxicity assessment of (21) ($R = \text{biotin}$) on the embryonic development of zebrafish revealed a tolerance up to 1.17 mg/L for this complex, with morphologic lesions such as curved spine/tail malformation, yolk sac and pericardial sac edema, cranial malformation, and underdeveloped eyes being observed when embryos were exposed to a concentration of 2.18 mg/L or higher [112]. In another publication, Valente et al. (2019) also

reported analogous biotinylated ruthenium(II) cyclopentadiene complexes for breast cancer therapy, bearing a substituted triphenylphosphine [111]. Among these species, complexes (22) (Figure 9) were found to be generally more cytotoxic to MDA-MB-231 cells than MCF7 cells, with a more considerable activity being observed for the species bearing an electron donating substituent on the phosphine aryl groups ($IC_{50} = 7.7 \pm 0.3 \mu M$, $R' = OCH_3$) than for the analogous version of the complex bearing an electron withdrawing substituent ($IC_{50} = 14.2 \pm 0.7 \mu M$, $R' = F$). To evaluate the ability of the complexes to interact with SMVT, the interaction of the species with avidin, a tetrameric glycoprotein with high specificity and affinity to biotin, was studied [114]. Importantly, the biotinylated complexes showed a significant affinity to avidin, although to a lesser extent than that of biotin alone, whereas nonbiotinylated analogues of these compounds did not interact with this protein, indicating that the complexes bearing the vitamin can potentially target SMVT. The in vivo toxicity evaluation of some of the complexes on the development of zebrafish embryos revealed that the biotinylated species (22) caused less severe toxic effects (major lesions were yolk sac and pericardial sac edemas) compared to the nonbiotinylated complexes (necrosis/cell lysis), suggesting that the targeting approach could lead to an increased in vivo tolerability. Moreover, these complexes were reported to be mainly retained within the membrane of cancer cells (>90% for MDA-MB-231) and to be able to inhibit the formation of colonies (loss of adhesive interactions), an indication of the antimetastatic behavior potential of these species [111].

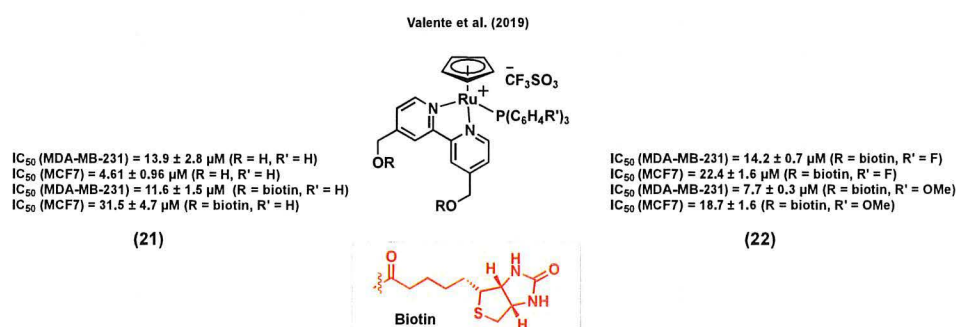


Figure 9. Ruthenium complexes bearing biotin.

3.7. Other Ruthenium Complexes for the Treatment of TNBC

Several ruthenium complexes bearing ligands that were not previously reported to display a biological activity were found to be highly active in vitro and/or in vivo against aggressive TNBC. For instance, Garcia et al. (2012) reported a ruthenium(II) cyclopentadiene species (23) (Figure 10), TM90, for which the in vitro cytotoxicity was found to be particularly high ($IC_{50} = 0.03 \pm 0.01 \mu M$) in MDA-MB-231 cells, and considerably higher than that of cisplatin ($IC_{50} = 39.0 \pm 5.0 \mu M$) in the same cell line [115]. The important stability of this complex in a cell growth medium containing 2% DMSO (used as a vehicle) was reported a few years later by Garcia et al. (2017) [116]. Interestingly, it was found that (23) could form an adduct with human serum albumin (HSA). The coincubation of the complex with different concentrations of HSA showed no significant change in the observed cytotoxicity, suggesting that the interaction of (23) with HSA does not inactivate the complex and could likely facilitate its distribution and delivery to cancer cells [116]. Moreover, MDA-MB-231 cells exposed to (23) showed a major population of necrotic cells and a smaller population of apoptotic cells, indicating that necrosis could be the main cell death mechanism caused by this species. An investigation of the in vivo antitumor activity of (23) on an MDA-MB-231 tumor in female athymic nude mice demonstrated the superior ability of this complex to suppress tumor growth, but also to inhibit the development of metastases. Furthermore, mice treated with (23) showed a significantly increased lifetime after surgical removal of the tumor compared to those that were not treated. Unlike cisplatin, which induced

significant body weight loss, no apparent change was observed between mice treated with (23) and the control group over time, showing that this compound did not affect the well-being of the animals.

In another study, Contel et al. (2014) reported a series of ruthenium(II) arene complexes of nontoxic iminophosphorane (IM) ligands with a promising in vitro and in vivo anticancer potential in TNBC [117]. Metal complexes of IM displayed a high in vitro cytotoxicity in a variety of human cancer cell lines with different degrees of selectivity and pathways other than DNA interaction, such as mitochondrial production of ROS and inhibition of PARP-1 proteins [118–120]. Compound (24) (Figure 10) was found to be highly water-soluble and to display a considerable cytotoxicity against several cisplatin resistant cell lines. Notably, the cytotoxicity of (24) in MDA-MB-231 was found to be much higher ($IC_{50} = 2.61 \pm 1.2 \mu\text{M}$) than that of cisplatin ($IC_{50} = 131.2 \pm 18 \mu\text{M}$) in this cell line. However, this complex was not found to be selective towards cancer cells, as it was found to also be highly cytotoxic in a noncancerous cell line, HEK-293T ($IC_{50} = 2.8 \pm 0.2 \mu\text{M}$). The mode of action of this complex was reported to take place through canonical- or caspase-dependent apoptosis, whereas DNA interaction and protease cathepsin B inhibition were not found to be likely to take place. Moreover, NOD.CB17-Prkdc scid/J mice were used as an in vivo model in which MDA-MB-231 tumor cells were injected. A significant decrease in tumor volume (56%) was reported after a 28 day-treatment (14 doses of 5 mg/kg of (24) every other day) with low systemic toxicity and preferential accumulation in the breast tumor tissues compared to other organs such as kidney and liver, suggesting the high in vivo efficacy of this complex [117].

It has been reported that ruthenium-based agents can be promising anticancer candidates to treat BRCA1-mutant breast cancers, frequently associated with TNBC [121,122]. The BRCA1 gene responds to DNA damage by being involved in cellular pathways for DNA repair, mRNA transcription, cell cycle regulation, and protein ubiquitination [123,124]. The role of BRCA1 is also to regulate chemotherapy-induced DNA damage [124]. Ratanaphan et al. (2014) reported ruthenium(II) complexes that showed a promising cytotoxicity in a BRCA1 defective TNBC cell line, HCC1937 [121]. Importantly, complex (25) (Figure 10) induced significantly more cytotoxicity in BRCA1 defective-HCC1937 cells ($IC_{50} = 1.8 \pm 0.1 \mu\text{M}$) than in the BRCA1 wild-type cell lines MDA-MB-231 ($IC_{50} = 13.2 \pm 0.3 \mu\text{M}$) and MCF7 ($IC_{50} = 8.2 \pm 0.1 \mu\text{M}$), suggesting that the higher sensitivity of the BRCA1 defective breast cancer cells to (25) might be due to the inability of the dysfunctional BRCA1 to repair ruthenium-induced DNA damage. Besides, cell exposure to (25) demonstrated a higher degree of cytotoxicity than cisplatin against all three cell lines. Upon internalization in HCC1937 cells, (25) was found to be mainly located in the nuclear fraction after 12–48 h. Moreover, a significant inhibition in the G2/M phase of the cell cycle, an increased induction of apoptotic cells, an upregulation of p53 mRNA and a downregulation of BRCA1 mRNA were observed in breast cancer cells treated with (25) [121].

In another example of ruthenium complexes for the treatment of TNBC, Chen et al. (2015) identified a ruthenium(II) complex, (26) (Figure 10), that could act as a potent antimetastatic agent and metal-based chemosensitizer towards MDA-MB-231 cells [125]. Complex (26) induced a higher cytotoxicity in TNBC cell lines ($IC_{50} = 14.6 \pm 3.1 \mu\text{M}$, MDA-MB-231; $78.0 \pm 19.8 \mu\text{M}$, MDA-MB-468) than in human normal kidney cells ($IC_{50} = 143.9 \pm 10.2 \mu\text{M}$, HK-2), and its cytotoxicity is believed to be associated with transferrin-mediated endocytosis. A low-dose (1–2 μM) and short-term treatment of (26) inhibited the migration and invasion of MDA-MB-231 cells in a cytotoxicity-independent manner. Regulating the expression levels of metastatic regulatory proteins and inhibiting the secretion of vascular endothelial growth factor (VEGF) were suggested to be associated with the anticancer activity of (26) in MDA-MB-231 cells. A co-treatment of MDA-MB-231 cells with (26) and tumor necrosis factor-related apoptosis-inducing ligand (TRAIL) suggested that the ruthenium complex could potentiate TRAIL-induced apoptosis through intrinsic and extrinsic apoptotic pathways, indicating that this combined treatment could be a novel strategy to inhibit the growth and the metastatic potential of tumor cells and synergistically enhance TRAIL-induced apoptotic cell death [125].

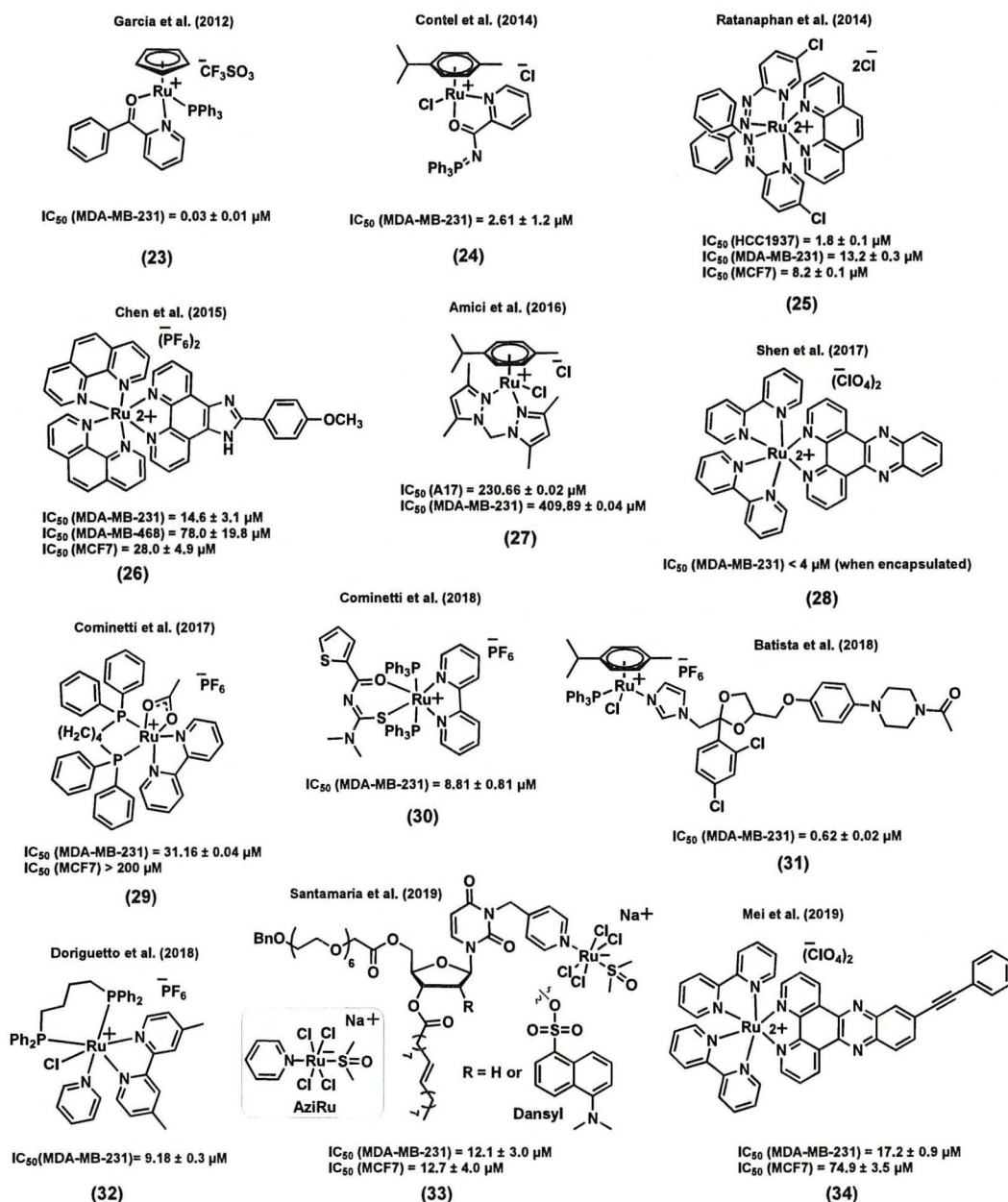


Figure 10. Other ruthenium complexes for triple negative breast cancer (TNBC) treatment.

Amici et al. (2016) reported a water soluble ruthenium(II) complex, (27) (Figure 10), with potent *in vivo* antitumor activity against TNBC [126], even though it displayed a very poor *in vitro* activity in TNBC cell lines (IC_{50} = $230.66 \pm 0.02 \mu\text{M}$, A17; $409.89 \pm 0.04 \mu\text{M}$, MDA-MB-231). As a reference, it is interesting to note that the complex was found to be much less cytotoxic than cisplatin (IC_{50} = $6.93 \pm 0.14 \mu\text{M}$, A17; $38.70 \pm 0.03 \mu\text{M}$, MDA-MB-231) but nevertheless more cytotoxic than NAMI-A (IC_{50} = $485.58 \pm 0.02 \mu\text{M}$, A17; $840.21 \pm 0.03 \mu\text{M}$, MDA-MB-231) in the same cell lines. Interestingly, only (27) resulted in the induction of cancer cell death by the activation of the apoptotic caspase-3 when compared to NAMI-A or cisplatin treatments. A female FVB/NCr1 mice model with A17 cells was then used to study the *in vivo* antitumor activity of (27). An intraperitoneal injection of (27) (52.5 mg/kg/day) or cisplatin (3 mg/kg/day), repeated 4 times at 3-day intervals, resulted in

a suppression of tumor growth, whereas the same treatment with NAMI-A (52.5 mg/kg/day) was found to be less effective. NAMI-A and cisplatin treatments were associated with weight loss, whereas the body weight of the mice treated with (27) was not found to be significantly different than that of untreated mice, suggesting a low toxicity for this complex at the selected dose. The antitumor activity of (27) is believed to be associated with reduced regulatory T cells (T_{reg}) infiltration and increased dendritic cells/macrophage recruitment into the tumor microenvironment [126].

Shen et al. (2017) reported a liposome-based nanodelivery system as a strategy to improve the anticancer potential of a ruthenium(II) complex of dipyrrophenazine (dppz), (28) (Figure 10), against TNBC [127]. This liposome encapsulation strategy did not only improve the biodistribution and pharmacokinetics of the ruthenium complex, but could also provide a hydrophobic environment, helping the ruthenium species emit fluorescence light and, as a result, leading to nanoparticle tracking inside the body. The cell viability of MDA-MB-231 cells was studied upon exposure to liposomes alone, compound (28), and encapsulated-(28). The two former molecules did not notably change the viability of cancer cells; however, the encapsulated complex could significantly inhibit the cell viability ($IC_{50} < 4 \mu M$). Cell uptake studies demonstrated considerably higher ruthenium cellular uptake for the encapsulated complex (about 15-fold higher) than the complex itself. An athymic nude mice inoculated with MDA-MB-231 tumor cells was used to further study the *in vivo* anticancer potential of the species. A considerable suppression of tumor growth was observed for the mice treated with the encapsulated complex which was not the case for those treated with the ruthenium complex, indicating that the liposome encapsulation is not only enhancing the *in vitro* cytotoxicity of the ruthenium complex but also its *in vivo* activity. It is worth mentioning that no apparent morphological changes were observed in tumor free mice treated with the encapsulated complex, suggesting potential selectivity for this system. DNA damage, cell cycle arrest, and apoptosis were reported to be possible modes of action of the liposome-encapsulated ruthenium complex (28) [127].

Cominetti et al. (2017) reported a series of biphosphine bipyridine ruthenium(II) complexes with considerable cytotoxicity and antimetastatic potential in TNBC [128]. From this series, compound (29) (Figure 10) showed the most significant anticancer activity. This complex could reduce the viability of MDA-MB-231 cells ($IC_{50} = 31.16 \pm 0.04 \mu M$) to a greater extent than that of the ER+ breast cell line MCF7 ($IC_{50} > 200 \mu M$) and the noncancerous breast cell line MCF-10A ($IC_{50} = 48.89 \pm 0.09 \mu M$), suggesting a possible selectivity towards triple negative cancers. Although this complex did not induce a high cytotoxicity at low concentration (20 μM), it could notably inhibit migration, adhesion, and invasion of MDA-MB-231 cells, likely due to the inhibition of the MMP-9 enzyme and the alteration of the cytoskeleton proteins responsible for the provision of the basic infrastructure for the maintenance of cell adhesion and motility [128].

Cominetti et al. (2018) also reported a ruthenium(II) complex of acylthiourea, (30) (Figure 10), which was also found to be active against TNBC tumor cells [129]. The inhibition of proliferation, migration, invasion, and adhesion was observed for cancer cells exposed to (30). The *in vitro* cytotoxicity of this compound in MDA-MB-231 cancer cells ($IC_{50} = 8.81 \pm 0.81 \mu M$) was found to be higher than that in the noncancerous breast cell line MCF-10A ($IC_{50} = 14.82 \pm 2.50 \mu M$). Furthermore, a change in morphology, induced apoptosis, DNA damage, and nuclear fragmentation were reported as possible modes of action for this complex. The *in vivo* toxicity of (30) was assessed using a mice model. At the doses administered intraperitoneally (50 and 300 mg/kg), this compound did not lead to a change in the weight of the animal compared to the control groups, which is indicative of a low toxicity [129].

Since azole compounds usually show a broad range of biological activities such as antifungal and anticancer properties because of their affinity to bind to biomolecules [130,131], Batista et al. (2018) reported a series of ruthenium(II) arene complexes tethering azole-containing ligands and studied their *in vitro* cytotoxicity and antimigration activity [132]. Although the azole-containing drugs used in this study are known as antifungal species, promising cytotoxicities against the TNBC cell line MDA-MB-231 were observed, more particularly for compounds for which ketoconazole was

coordinated to the metal center, (31) ($IC_{50} = 0.62 \pm 0.02 \mu M$) (Figure 10). Furthermore, human serum albumin (HSA) binding was reported as one of the possible modes of action for these compounds [132].

Doriguetto et al. (2018) reported a new series of ruthenium(II) diimine/phosphine complexes and tested their in vitro cytotoxicity in various cell lines [133]. For instance, complex (32) (Figure 10) showed a high cytotoxicity in the MDA-MB-231 cell line ($IC_{50} = 9.18 \pm 0.30 \mu M$) compared to that in fibroblasts derived from normal skin ($IC_{50} = 24.19 \pm 3.02 \mu M$), indicating a potential selectivity for this species. Complex (32) induced morphological changes and inhibited the size and number of colonies, suggesting an anti-clonogenic activity against MDA-MB-231 cells. Moreover, apoptosis was induced by (32) in MDA-MB-231 tumor cells in a concentration-dependent manner [133].

Some nucleolipidic ruthenium(III) complexes incorporated into a nanosystem have also been developed as a potential strategy for cancer therapy and have shown some promising anticancer potential in both ER+ breast and TNBC cancer cell lines [134,135]. For instance, Santamaria et al. (2019) reported nanosystems designed to improve the efficacy of nucleolipidic anticancer ruthenium(III) complexes for biomedical applications, and to deliver AziRu (Figure 10), a ruthenium(III) complex structurally inspired by the well-known drug candidate NAMI-A [135]. The ruthenium(III) complex, (33) (R = H) (Figure 10), was incorporated into a 1,2-dioleoyl-3-trimethylammoniumpropane chloride (DOTAP) nanocarrier and its cytotoxicity in breast cancer cells (ER+ and TNBC) was compared with that of AziRu (Figure 10) and cisplatin. Notably, in the TNBC cell line MDA-MB-231, the (33)/DOTAP (R = H) nanosystem proved to be more effective ($IC_{50} = 12.1 \pm 3 \mu M$, corresponding to the effective metal concentration carried by the nanoaggregate, 15% mol/mol,) than cisplatin ($IC_{50} = 19 \pm 4 \mu M$), in contrast to AziRu, which was found to be inactive. Importantly, (33)/DOTAP (R = H) did not induce a high cytotoxicity in non-cancerous MCF-10A cells ($IC_{50} > 100 \mu M$). A fluorescently-tagged analogue of complex (33) (R = dansyl) (Figure 10) was developed to further study the cellular uptake and accumulation of the compound. Although it was previously reported that a large extent of AziRu (about 80%) remained in the culture medium after incubation, large intracellular amounts of ruthenium (about 85% of the administered quantity) were found (mainly at the nuclear level) after treatment with (33)/DOTAP (R = dansyl). Furthermore, Bcl-2 down-regulation and autophagy were suggested to be involved in the mechanism(s) of action of this complex. An in vivo assessment of the antitumor potential of (33) (R = H) was also performed using athymic nude mice bearing human BCC xenografts (although only using MCF7 cells inoculated into the nude mice). The administration of (33)/DOTAP (R = H) at a 15 mg/kg (i.p.) dose, once a week for 28 days resulted in a suppression of tumor growth. Also importantly, the treatment was well-tolerated in mice since no sign of toxicity was observed [135].

Finally, Mei et al. (2019) reported a class of ruthenium(II) phenazine derivatives (DPPZ) with interesting anticancer properties against TNBC cells [136]. The most promising results were obtained for compound (34) (Figure 10), which displayed a notable inhibitory activity against the proliferation ($IC_{50} = 17.2 \pm 0.9 \mu M$), migration, and invasion of MDA-MB-231 cells. A structure-activity relationship analysis showed that the increased number of aromatic planar rings in the ligands can effectively enhance the antitumor activity of this series of complexes. Compound (34) was found to enter breast cancer cells and localize into the nucleus, which is indicative that the complex might induce DNA damage to cause cell apoptosis. Furthermore, an in vivo anticancer evaluation of (34) in the xenograft model of human MDA-MB-231 in zebrafish showed that the number of cancer cells was notably reduced compared with the control group, suggesting that (34) can effectively inhibit the proliferation of TNBC cells in zebrafish. Moreover, a scarce number of MDA-MB-231 cells were found in the blood vessels of zebrafish, suggesting that (34) might inhibit the metastasis of the cancer cells in vivo [136].

4. Conclusions

In this review, we briefly report rationally designed ruthenium complexes bearing bioactive ligand(s) as potential candidates for the treatment of hormone receptor positive breast cancers and TNBCs. The bioactive ligands included in these complexes are known to have a broad range of molecular targets such as enzymes, hormone receptors, growth factors, etc. Some of these complexes

could undergo multiple anticancer mechanisms or/and illustrate a synergistic effect. Cytotoxicities and antimetastatic activities can both be induced in breast cancer cells using these types of ruthenium complexes. As expected, the most promising cytotoxicities reported were noted for ruthenium (II) complexes, which is in line with the inert nature of ruthenium (III) species. Notably, ruthenium (II) arene and ruthenium (II) cyclopentadienyl complexes were found to display particularly interesting activities, with IC₅₀ values lower than 1 µM in some cases. The information presented in this review also revealed low IC₅₀ values for several ruthenium species in TNBCs, which normally do not respond to currently used drugs, making these compounds attractive candidates for further investigation. Despite the fact that several publications have presented the in vitro activity of ruthenium complexes in breast cancer cells, fewer reports have presented results regarding the solubility, stability, and in vivo anticancer activity of these species. Moreover, the studies reported so far were not always performed under the same conditions (stock solution preparation, type of in vitro assay/in vivo model, duration of treatment, etc.), preventing a direct comparison of their overall bioactivity. We believe that this review can contribute to open new doors for the development of novel Ru-based complexes for the treatment of the most frequently diagnosed cancer among women.

Supplementary Materials: The following are available online, Table S1: Summary of the activity of the ruthenium complexes reviewed in this study.

Author Contributions: Conceptualization, A.C. and G.G.; Writing—original draft preparation, G.G.; Writing—review and editing, A.C. and G.G.; Supervision, A.C. All authors have read and agreed to the published version of the manuscript.

Funding: This work was supported by INRS University, the Fonds de Recherche du Québec Santé (Établissement de Jeunes Chercheurs 32622) and the Armand-Frappier Foundation (Banque Nationale scholarship to G.G.).

Acknowledgments: We would like to thank Isabelle Plante and Yves St-Pierre for their assistance at editing the final draft of this manuscript.

Conflicts of Interest: The authors declare no conflict of interest.

References

1. Siegel, R.L.; Miller, K.D.; Jemal, A. Cancer statistics, 2019. *CA-Cancer J. Clin.* **2019**, *69*, 7–34. [[CrossRef](#)] [[PubMed](#)]
2. Bray, F.; Ferlay, J.; Soerjomataram, I.; Siegel, R.L.; Torre, L.A.; Jemal, A. Global cancer statistics 2018: GLOBOCAN estimates of incidence and mortality worldwide for 36 cancers in 185 countries. *CA-Cancer J. Clin.* **2018**, *68*, 394–424. [[CrossRef](#)] [[PubMed](#)]
3. Kumar, A.; Singla, A. Epidemiology of Breast Cancer: Current Figures and Trends. In *Preventive Oncology for the Gynecologist*; Mehta, S., Singla, A., Eds.; Springer: Singapore, 2019; pp. 335–339. [[CrossRef](#)]
4. Waks, A.G.; Winer, E.P. Breast Cancer Treatment: A review. *JAMA* **2019**, *321*, 316. [[CrossRef](#)]
5. Joshi, H.; Press, M.F. 22-Molecular Oncology of Breast Cancer. In *The Breast*, 5th ed.; Bland, K.I., Copeland, E.M., Klimberg, V.S., Gradishar, W.J., Eds.; Elsevier: Amsterdam, The Netherlands, 2018; pp. 282–307. [[CrossRef](#)]
6. Lim, E.; Palmieri, C.; Tilley, W.D. Renewed interest in the progesterone receptor in breast cancer. *Br. J. Cancer* **2016**, *115*, 909–911. [[CrossRef](#)] [[PubMed](#)]
7. Piccart-Gebhart, M.J.; Procter, M.; Leyland-Jones, B.; Goldhirsch, A.; Untch, M.; Smith, I.; Gianni, L.; Baselga, J.; Bell, R.; Jackisch, C.; et al. Trastuzumab after Adjuvant Chemotherapy in HER2-Positive Breast Cancer. *N. Engl. J. Med.* **2005**, *353*, 1659–1672. [[CrossRef](#)] [[PubMed](#)]
8. Al-Mahmood, S.; Sapiezynski, J.; Garbuzenko, O.B.; Minko, T. Metastatic and triple-negative breast cancer: Challenges and treatment options. *Drug Deliv. Transl. Res.* **2018**, *8*, 1483–1507. [[CrossRef](#)]
9. Bianchini, G.; Balko, J.M.; Mayer, I.A.; Sanders, M.E.; Gianni, L. Triple-negative breast cancer: Challenges and opportunities of a heterogeneous disease. *Nat. Rev. Clin. Oncol.* **2016**, *13*, 674–690. [[CrossRef](#)]
10. Pareja, F.; Geyer, F.C.; Marchiò, C.; Burke, K.A.; Weigelt, B.; Reis-Filho, J.S. Triple-negative breast cancer: The importance of molecular and histologic subtyping, and recognition of low-grade variants. *NPJ Breast Cancer* **2016**, *2*, 16036. [[CrossRef](#)]
11. Weigelt, B.; Peterse, J.L.; van't Veer, L.J. Breast cancer metastasis: Markers and models. *Nat. Rev. Cancer* **2005**, *5*, 591–602. [[CrossRef](#)]

12. Reinert, T.; Barrios, C.H. Optimal management of hormone receptor positive metastatic breast cancer in 2016. *Ther. Adv. Med. Oncol.* **2015**, *7*, 304–320. [[CrossRef](#)]
13. Fisher, B.; Dignam, J.; Bryant, J.; DeCillis, A.; Wickerham, D.L.; Wolmark, N.; Costantino, J.; Redmond, C.; Fisher, E.R.; Bowman, D.M.; et al. Five Versus More Than Five Years of Tamoxifen Therapy for Breast Cancer Patients with Negative Lymph Nodes and Estrogen Receptor-Positive Tumors. *J. Natl. Cancer Inst.* **1996**, *88*, 1529–1542. [[CrossRef](#)] [[PubMed](#)]
14. Garreau, J.R.; DeLaMelena, T.; Walts, D.; Karamlou, K.; Johnson, N. Side effects of aromatase inhibitors versus tamoxifen: The patients' perspective. *Am. J. Surg.* **2006**, *192*, 496–498. [[CrossRef](#)] [[PubMed](#)]
15. Mouridsen, H.T. Incidence and management of side effects associated with aromatase inhibitors in the adjuvant treatment of breast cancer in postmenopausal women. *Curr. Med. Res. Opin.* **2006**, *22*, 1609–1621. [[CrossRef](#)] [[PubMed](#)]
16. Pan, H.; Gray, R.; Braybrooke, J.; Davies, C.; Taylor, C.; McGale, P.; Peto, R.; Pritchard, K.I.; Bergh, J.; Dowsett, M.; et al. 20-Year Risks of Breast-Cancer Recurrence after Stopping Endocrine Therapy at 5 Years. *N. Engl. J. Med.* **2017**, *377*, 1836–1846. [[CrossRef](#)] [[PubMed](#)]
17. Early Breast Cancer Trialists' Collaborative Group (EBCTCG). Effects of chemotherapy and hormonal therapy for early breast cancer on recurrence and 15-year survival: An overview of the randomised trials. *Lancet* **2005**, *365*, 1687–1717. [[CrossRef](#)]
18. Bruijninx, P.C.A.; Sadler, P.J. New trends for metal complexes with anticancer activity. *Curr. Opin. Chem. Biol.* **2008**, *12*, 197–206. [[CrossRef](#)]
19. Muhammad, N.; Guo, Z. Metal-based anticancer chemotherapeutic agents. *Curr. Opin. Chem. Biol.* **2014**, *19*, 144–153. [[CrossRef](#)]
20. Dasari, S.; Bernard Tchounwou, P. Cisplatin in cancer therapy: Molecular mechanisms of action. *Eur. J. Pharmacol.* **2014**, *740*, 364–378. [[CrossRef](#)]
21. Koshy, N.; Quispe, D.; Shi, R.; Mansour, R.; Burton, G.V. Cisplatin–gemcitabine therapy in metastatic breast cancer: Improved outcome in triple negative breast cancer patients compared to non-triple negative patients. *Breast J.* **2010**, *19*, 246–248. [[CrossRef](#)]
22. Byrski, T.; Dent, R.; Blecharz, P.; Foszczynska-Kloda, M.; Gronwald, J.; Huzarski, T.; Cybulski, C.; Marczyk, E.; Chrzan, R.; Eisen, A.; et al. Results of a phase II open-label, non-randomized trial of cisplatin chemotherapy in patients with BRCA1-positive metastatic breast cancer. *Breast Cancer Res.* **2012**, *14*, R110. [[CrossRef](#)]
23. Oun, R.; Moussa, Y.E.; Wheate, N.J. The side effects of platinum-based chemotherapy drugs: A review for chemists. *Dalton Trans.* **2018**, *47*, 6645–6653. [[CrossRef](#)] [[PubMed](#)]
24. Florea, A.-M.; Büsselberg, D. Cisplatin as an Anti-Tumor Drug: Cellular Mechanisms of Activity, Drug Resistance and Induced Side Effects. *Cancers* **2011**, *3*, 1351–1371. [[CrossRef](#)] [[PubMed](#)]
25. Manohar, S.; Leung, N. Cisplatin nephrotoxicity: A review of the literature. *J. Nephrol.* **2018**, *31*, 15–25. [[CrossRef](#)] [[PubMed](#)]
26. Kwok, J.M.-M.; Peck, B.; Monteiro, L.J.; Schwenen, H.D.C.; Millour, J.; Coombes, R.C.; Myatt, S.S.; Lam, E.W.-F. FOXM1 Confers Acquired Cisplatin Resistance in Breast Cancer Cells. *Mol. Cancer Res.* **2010**, *8*, 24–34. [[CrossRef](#)] [[PubMed](#)]
27. Pogribny, I.P.; Filkowski, J.N.; Tryndyak, V.P.; Golubov, A.; Shpyleva, S.I.; Kovalchuk, O. Alterations of microRNAs and their targets are associated with acquired resistance of MCF-7 breast cancer cells to cisplatin. *Int. J. Cancer* **2010**, *127*, 1785–1794. [[CrossRef](#)]
28. Bergamo, A.; Sava, G. Ruthenium anticancer compounds: Myths and realities of the emerging metal-based drugs. *Dalton Trans.* **2011**, *40*, 7817–7823. [[CrossRef](#)]
29. Trondl, R.; Heffeter, P.; Kowol, C.R.; Jakupec, M.A.; Berger, W.; Keppler, B.K. NKP-1339, the first ruthenium-based anticancer drug on the edge to clinical application. *Chem. Sci.* **2014**, *5*, 2925–2932. [[CrossRef](#)]
30. Alessio, E. Thirty Years of the Drug Candidate NAMI-A and the Myths in the Field of Ruthenium Anticancer Compounds: A Personal Perspective. *Eur. J. Inorg. Chem.* **2017**, *2017*, 1549–1560. [[CrossRef](#)]
31. Vock, C.A.; Ang, W.H.; Scolaro, C.; Phillips, A.D.; Lagopoulos, L.; Juillerat-Jeanneret, L.; Sava, G.; Scopelliti, R.; Dyson, P.J. Development of Ruthenium Antitumor Drugs that Overcome Multidrug Resistance Mechanisms. *J. Med. Chem.* **2007**, *50*, 2166–2175. [[CrossRef](#)]

32. Weiss, A.; Berndsen, R.H.; Dubois, M.; Müller, C.; Schibli, R.; Griffioen, A.W.; Dyson, P.J.; Nowak-Sliwinska, P. In vivo anti-tumor activity of the organometallic ruthenium(II)-arene complex [Ru(η^6 -p-cymene)Cl₂(pta)] (RAPTA-C) in human ovarian and colorectal carcinomas. *Chem. Sci.* **2014**, *5*, 4742–4748. [[CrossRef](#)]
33. Alessio, E.; Messori, L. NAMI-A and KP1019/1339, Two Iconic Ruthenium Anticancer Drug Candidates Face-to-Face: A Case Story in Medicinal Inorganic Chemistry. *Molecules* **2019**, *24*, 1995. [[CrossRef](#)] [[PubMed](#)]
34. Mari, C.; Pierroz, V.; Ferrari, S.; Gasser, G. Combination of Ruthenium(II) complexes and light: New frontiers in cancer therapy. *Chem. Sci.* **2015**, *6*, 2660–2686. [[CrossRef](#)] [[PubMed](#)]
35. Monro, S.; Colón, K.L.; Yin, H.; Roque, J.; Konda, P.; Gujar, S.; Thummel, R.P.; Lilge, L.; Cameron, C.G.; McFarland, S.A. Transition Metal Complexes and Photodynamic Therapy from a Tumor-Centered Approach: Challenges, Opportunities, and Highlights from the Development of TLD1433. *Chem. Rev.* **2019**, *119*, 797–828. [[CrossRef](#)] [[PubMed](#)]
36. Ma, D.-L.; Wu, C.; Cheng, S.-S.; Lee, F.-W.; Han, Q.-B.; Leung, C.-H. Development of Natural Product-Conjugated Metal Complexes as Cancer Therapies. *Int. J. Mol. Sci.* **2019**, *20*, 341. [[CrossRef](#)] [[PubMed](#)]
37. Vessières, A.; Top, S.; Beck, W.; Hillard, E.; Jaouen, G. Metal complex SERMs (selective oestrogen receptor modulators). The influence of different metal units on breast cancer cell antiproliferative effects. *Dalton Trans.* **2006**, *4*, 529–541. [[CrossRef](#)] [[PubMed](#)]
38. Štarha, P.; Trávníček, Z. Non-platinum complexes containing releasable biologically active ligands. *Coord. Chem. Rev.* **2019**, *395*, 130–145. [[CrossRef](#)]
39. Kilpin, K.J.; Dyson, P.J. Enzyme inhibition by metal complexes: Concepts, strategies and applications. *Chem. Sci.* **2013**, *4*, 1410–1419. [[CrossRef](#)]
40. Golbaghi, G.; Haghdost, M.M.; Yancu, D.; López de los Santos, Y.; Doucet, N.; Patten, S.A.; Sanderson, J.T.; Castonguay, A. Organoruthenium(II) Complexes Bearing an Aromatase Inhibitor: Synthesis, Characterization, in Vitro Biological Activity and in Vivo Toxicity in Zebrafish Embryos. *Organometallics* **2019**, *38*, 702–711. [[CrossRef](#)]
41. Zimmermann, G.R.; Lehár, J.; Keith, C.T. Multi-target therapeutics: When the whole is greater than the sum of the parts. *Drug Discov. Today* **2007**, *12*, 34–42. [[CrossRef](#)]
42. Werck-Reichhart, D.; Feyereisen, R. Cytochromes P450: A success story. *Genome Biol.* **2000**, *1*, reviews3003. [[CrossRef](#)]
43. Lewis, D.F. 57 varieties: The human cytochromes P450. *Pharm. J.* **2004**, *5*, 305–318. [[CrossRef](#)] [[PubMed](#)]
44. Bruno, R.D.; Njar, V.C.O. Targeting cytochrome P450 enzymes: A new approach in anti-cancer drug development. *Bioorg. Med. Chem.* **2007**, *15*, 5047–5060. [[CrossRef](#)] [[PubMed](#)]
45. Brueggemeier, R.W.; Hackett, J.C.; Diaz-Cruz, E.S. Aromatase Inhibitors in the Treatment of Breast Cancer. *Endocr. Rev.* **2005**, *26*, 331–345. [[CrossRef](#)] [[PubMed](#)]
46. Galeazzi, R.; Massaccesi, L. Insight into the binding interactions of CYP450 aromatase inhibitors with their target enzyme: A combined molecular docking and molecular dynamics study. *J. Mol. Model.* **2012**, *18*, 1153–1166. [[CrossRef](#)] [[PubMed](#)]
47. O'Neill, M.; Paulin, F.E.M.; Vendrell, J.; Ali, C.W.; Thompson, A.M. The aromatase inhibitor letrozole enhances the effect of doxorubicin and docetaxel in an MCF7 cell line model. *BioDiscovery* **2012**, *6*. [[CrossRef](#)]
48. Miranda, A.A.; Limon, J.; Medina, F.L.; Arce, C.; Zinser, J.W.; Rocha, E.B.; Villarreal-Garza, C.M. Combination treatment with aromatase inhibitor and capecitabine as first- or second-line treatment in metastatic breast cancer. *J. Clin. Oncol.* **2012**, *30*, e11016. [[CrossRef](#)]
49. Castonguay, A.; Doucet, C.; Juhas, M.; Maysinger, D. New Ruthenium(II)–Letrozole Complexes as Anticancer Therapeutics. *J. Med. Chem.* **2012**, *55*, 8799–8806. [[CrossRef](#)]
50. MacRae, C.A.; Peterson, R.T. Zebrafish as tools for drug discovery. *Nat. Rev. Drug Discov.* **2015**, *14*, 721. [[CrossRef](#)]
51. Golbaghi, G.; Pitard, I.; Lucas, M.; Haghdost, M.M.; López de los Santos, Y.; Doucet, N.; Patten, S.A.; Sanderson, J.T.; Castonguay, A. Synthesis and biological assessment of a ruthenium(II) cyclopentadienyl complex in breast cancer cells and on the development of zebrafish embryos. *Eur. J. Med. Chem.* **2020**. [[CrossRef](#)]
52. Li, Y.; Steppi, A.; Zhou, Y.; Mao, F.; Miller, P.C.; He, M.M.; Zhao, T.; Sun, Q.; Zhang, J. Tumoral expression of drug and xenobiotic metabolizing enzymes in breast cancer patients of different ethnicities with implications to personalized medicine. *Sci. Rep.* **2017**, *7*, 4747. [[CrossRef](#)]

53. Li, F.; Zhu, W.; Gonzalez, F.J. Potential role of CYP1B1 in the development and treatment of metabolic diseases. *Pharmacol. Ther.* **2017**, *178*, 18–30. [[CrossRef](#)] [[PubMed](#)]
54. Zamora, A.; Denning, C.A.; Heidary, D.K.; Wachter, E.; Nease, L.A.; Ruiz, J.; Glazer, E.C. Ruthenium-containing P450 inhibitors for dual enzyme inhibition and DNA damage. *Dalton Trans.* **2017**, *46*, 2165–2173. [[CrossRef](#)] [[PubMed](#)]
55. Kao, Y.-C.; Higashiyama, T.; Sun, X.; Okubo, T.; Yarborough, C.; Choi, I.; Osawa, Y.; Simmen, F.A.; Chen, S. Catalytic differences between porcine blastocyst and placental aromatase isozymes. *Eur. J. Biochem.* **2000**, *267*, 6134–6139. [[CrossRef](#)] [[PubMed](#)]
56. Henderson, D.; Habenicht, U.F.; Nishino, Y.; Kerb, U.; El Etreby, M.F. Aromatase inhibitors and benign prostatic hyperplasia. *J. Steroid Biochem.* **1986**, *25*, 867–876. [[CrossRef](#)]
57. Kometani, M.; Yoneda, T.; Demura, M.; Koide, H.; Nishimoto, K.; Mukai, K.; Gomez-Sanchez, C.E.; Akagi, T.; Yokota, T.; Horike, S.-I.; et al. Cortisol overproduction results from DNA methylation of CYP11B1 in hypercortisolemia. *Sci. Rep.* **2017**, *7*, 11205. [[CrossRef](#)] [[PubMed](#)]
58. Truong, T.H.; Lange, C.A. Deciphering Steroid Receptor Crosstalk in Hormone-Driven Cancers. *Endocrinology* **2018**, *159*, 3897–3907. [[CrossRef](#)]
59. Shao, W.; Brown, M. Advances in estrogen receptor biology: Prospects for improvements in targeted breast cancer therapy. *Breast Cancer Res.* **2003**, *6*, 39–52. [[CrossRef](#)]
60. Kennedy, B.J. Hormone therapy for advanced breast cancer. *Cancer* **1965**, *18*, 1551–1557. [[CrossRef](#)]
61. Pigeon, P.; Top, S.; Vessières, A.; Huché, M.; Hillard, E.A.; Salomon, E.; Jaouen, G. Selective Estrogen Receptor Modulators in the Ruthenocene Series. Synthesis and Biological Behavior. *J. Med. Chem.* **2005**, *48*, 2814–2821. [[CrossRef](#)]
62. Zhang, F.-L.; Song, M.-R.; Yuan, G.-K.; Ye, H.-N.; Tian, Y.; Huang, M.-D.; Xue, J.-P.; Zhang, Z.-H.; Liu, J.-Y. A Molecular Combination of Zinc(II) Phthalocyanine and Tamoxifen Derivative for Dual Targeting Photodynamic Therapy and Hormone Therapy. *J. Med. Chem.* **2017**, *60*, 6693–6703. [[CrossRef](#)]
63. Zhao, X.; Li, M.; Sun, W.; Fan, J.; Du, J.; Peng, X. An estrogen receptor targeted ruthenium complex as a two-photon photodynamic therapy agent for breast cancer cells. *Chem. Commun.* **2018**, *54*, 7038–7041. [[CrossRef](#)] [[PubMed](#)]
64. Singh, A.K.; Saxena, G.; Sahabjada; Arshad, M. Synthesis, characterization and biological evaluation of ruthenium flavanol complexes against breast cancer. *Spectrochim. Acta Mol. Biomol. Spectrosc.* **2017**, *180*, 97–104. [[CrossRef](#)] [[PubMed](#)]
65. Wang, Y.; Ho, C.T. Metabolism of Flavonoids. *Forum Nutr. Baselkarger* **2009**, *61*, 64–74. [[CrossRef](#)]
66. Pan, M.-H.; Ho, C.-T. Chemopreventive effects of natural dietary compounds on cancer development. *Chem. Soc. Rev.* **2008**, *37*, 2558–2574. [[CrossRef](#)] [[PubMed](#)]
67. Roy, S.; Sil, A.; Chakraborty, T. Potentiating apoptosis and modulation of p53, Bcl2, and Bax by a novel chrysin ruthenium complex for effective chemotherapeutic efficacy against breast cancer. *J. Cell. Physiol.* **2019**, *234*, 4888–4909. [[CrossRef](#)]
68. Hannon, M.J.; Green, P.S.; Fisher, D.M.; Derrick, P.J.; Beck, J.L.; Watt, S.J.; Ralph, S.F.; Sheil, M.M.; Barker, P.R.; Alcock, N.W.; et al. An Estrogen–Platinum Terpyridine Conjugate: DNA and Protein Binding and Cellular Delivery. *Chem. Eur. J.* **2006**, *12*, 8000–8013. [[CrossRef](#)]
69. Jackson, A.; Davis, J.; Pither, R.J.; Rodger, A.; Hannon, M.J. Estrogen-Derived Steroidal Metal Complexes: Agents for Cellular Delivery of Metal Centers to Estrogen Receptor-Positive Cells. *Inorg. Chem.* **2001**, *40*, 3964–3973. [[CrossRef](#)]
70. Schobert, R.; Seibt, S.; Effenberger-Neidnicht, K.; Underhill, C.; Biersack, B.; Hammond, G.L. (Arene)Cl₂Ruthenium(II) complexes with N-coordinated estrogen and androgen isonicotinates: Interaction with sex hormone binding globulin and anticancer activity. *Steroids* **2011**, *76*, 393–399. [[CrossRef](#)]
71. Kahn, S.M.; Hryb, D.J.; Nakhla, A.M.; Romas, N.A.; Rosner, W. Sex hormone-binding globulin is synthesized in target cells. *J. Endocrinol.* **2002**, *175*, 113–120. [[CrossRef](#)]
72. Krupenko, S.A.; Krupenko, N.I.; Danzo, B.J. Interaction of sex hormone-binding globulin with plasma membranes from the rat epididymis and other tissues. *J. Steroid Biochem. Mol. Biol.* **1994**, *51*, 115–124. [[CrossRef](#)]
73. Ruiz, J.; Rodríguez, V.; Cutillas, N.; Espinosa, A.; Hannon, M.J. A Potent Ruthenium(II) Antitumor Complex Bearing a Lipophilic Levonorgestrel Group. *Inorg. Chem.* **2011**, *50*, 9164–9171. [[CrossRef](#)] [[PubMed](#)]

74. Lv, G.; Qiu, L.; Li, K.; Liu, Q.; Li, X.; Peng, Y.; Wang, S.; Lin, J. Enhancement of therapeutic effect in breast cancer with a steroid-conjugated ruthenium complex. *New J. Chem.* **2019**, *43*, 3419–3427. [[CrossRef](#)]
75. Jänne, P.A.; Mayer, R.J. Chemoprevention of Colorectal Cancer. *N. Engl. J. Med.* **2000**, *342*, 1960–1968. [[CrossRef](#)] [[PubMed](#)]
76. Thun, M.J.; Henley, S.J.; Patrono, C. Nonsteroidal Anti-inflammatory Drugs as Anticancer Agents: Mechanistic, Pharmacologic, and Clinical Issues. *J. Natl. Cancer Inst.* **2002**, *94*, 252–266. [[CrossRef](#)]
77. Alves Rico, S.R.; Abbasi, A.Z.; Ribeiro, G.; Ahmed, T.; Wu, X.Y.; de Oliveira Silva, D. Diruthenium(ii,iii) metallodrugs of ibuprofen and naproxen encapsulated in intravenously injectable polymer–lipid nanoparticles exhibit enhanced activity against breast and prostate cancer cells. *Nanoscale* **2017**, *9*, 10701–10714. [[CrossRef](#)]
78. Harris, R.E.; Chlebowski, R.T.; Jackson, R.D.; Frid, D.J.; Ascenseo, J.L.; Anderson, G.; Loar, A.; Rodabough, R.J.; White, E.; McTiernan, A. Breast Cancer and Nonsteroidal Anti-Inflammatory Drugs: Prospective Results from the Women’s Health Initiative. *Cancer Res.* **2003**, *63*, 6096–6101.
79. Howe, L.R.; Subbaramaiah, K.; Brown, A.M.; Dannenberg, A.J. Cyclooxygenase-2: A target for the prevention and treatment of breast cancer. *Endocr. Relat. Cancer* **2001**, *8*, 97–114. [[CrossRef](#)]
80. Arun, B.; Goss, P. The role of COX-2 inhibition in breast cancer treatment and prevention. *Semin. Oncol.* **2004**, *31*, 22–29. [[CrossRef](#)]
81. Lopes, J.C.S.; Damasceno, J.L.; Oliveira, P.F.; Guedes, A.P.M.; Tavares, D.C.; Deflon, V.M.; Lopes, N.P.; Pivatto, M.; Batista, A.A.; Maia, P.I.S.; et al. Ruthenium(II) Complexes Containing Anti-Inflammatory Drugs as Ligands: Synthesis, Characterization and in vitro Cytotoxicity Activities on Cancer Cell Lines. *J. Braz. Chem. Soc.* **2015**, *26*, 1838–1847. [[CrossRef](#)]
82. Mandal, P.; Kundu, B.K.; Vyas, K.; Sabu, V.; Helen, A.; Dhankhar, S.S.; Nagaraja, C.M.; Bhattacharjee, D.; Bhabak, K.P.; Mukhopadhyay, S. Ruthenium(II) arene NSAID complexes: Inhibition of cyclooxygenase and antiproliferative activity against cancer cell lines. *Dalton Trans.* **2018**, *47*, 517–527. [[CrossRef](#)]
83. Chatterjee, S.; Biondi, I.; Dyson, P.J.; Bhattacharyya, A. A bifunctional organometallic ruthenium drug with multiple modes of inducing apoptosis. *J. Biol. Inorg. Chem.* **2011**, *16*, 715–724. [[CrossRef](#)] [[PubMed](#)]
84. Scolaro, C.; Bergamo, A.; Brescacin, L.; Delfino, R.; Cocchietto, M.; Laurenczy, G.; Geldbach, T.J.; Sava, G.; Dyson, P.J. In Vitro and in Vivo Evaluation of Ruthenium(II)–Arene PTA Complexes. *J. Med. Chem.* **2005**, *48*, 4161–4171. [[CrossRef](#)] [[PubMed](#)]
85. Allocati, N.; Masulli, M.; Di Ilio, C.; Federici, L. Glutathione transferases: Substrates, inhibitors and pro-drugs in cancer and neurodegenerative diseases. *Oncogenesis* **2018**, *7*, 8. [[CrossRef](#)] [[PubMed](#)]
86. Goto, S.; Iida, T.; Cho, S.; Oka, M.; Kohno, S.; Kondo, T. Overexpression of glutathione S-transferase π enhances the adduct formation of cisplatin with glutathione in human cancer cells. *Free Radic. Res.* **1999**, *31*, 549–558. [[CrossRef](#)] [[PubMed](#)]
87. Campiglio, M.; Locatelli, A.; Olgiati, C.; Normanno, N.; Somenzi, G.; Viganò, L.; Fumagalli, M.; Ménard, S.; Gianni, L. Inhibition of proliferation and induction of apoptosis in breast cancer cells by the epidermal growth factor receptor (EGFR) tyrosine kinase inhibitor ZD1839 (‘Iressa’) is independent of EGFR expression level. *J. Cell. Physiol.* **2004**, *198*, 259–268. [[CrossRef](#)] [[PubMed](#)]
88. Raymond, E.; Faivre, S.; Armand, J.P. Epidermal Growth Factor Receptor Tyrosine Kinase as a Target for Anticancer Therapy. *Drugs* **2000**, *60*, 15–23. [[CrossRef](#)] [[PubMed](#)]
89. Lee, J.Y.; Park, Y.K.; Seo, S.H.; So, I.-S.; Chung, H.-K.; Yang, B.-S.; Lee, S.J.; Park, H.; Lee, Y.S. 1,4-Dioxane-fused 4-anilinoquinazoline as inhibitors of epidermal growth factor receptor kinase. *Arch. Pharm.* **2001**, *334*, 357–360. [[CrossRef](#)]
90. Du, J.; Zhang, E.; Zhao, Y.; Zheng, W.; Zhang, Y.; Lin, Y.; Wang, Z.; Luo, Q.; Wu, K.; Wang, F. Discovery of a dual-targeting organometallic ruthenium complex with high activity inducing early stage apoptosis of cancer cells. *Metallomics* **2015**, *7*, 1573–1583. [[CrossRef](#)]
91. Lord, C.J.; Ashworth, A. Targeted therapy for cancer using PARP inhibitors. *Curr. Opin. Pharmacol.* **2008**, *8*, 363–369. [[CrossRef](#)]
92. Anders, C.K.; Winer, E.P.; Ford, J.M.; Dent, R.; Silver, D.P.; Sledge, G.W.; Carey, L.A. Poly(ADP-Ribose) Polymerase Inhibition: “Targeted” Therapy for Triple-Negative Breast Cancer. *Clin. Cancer Res.* **2010**, *16*, 4702–4710. [[CrossRef](#)]
93. Wang, Z.; Qian, H.; Yiu, S.-M.; Sun, J.; Zhu, G. Multi-targeted organometallic ruthenium(II)–arene anticancer complexes bearing inhibitors of poly(ADP-ribose) polymerase-1: A strategy to improve cytotoxicity. *J. Inorg. Biochem.* **2014**, *131*, 47–55. [[CrossRef](#)] [[PubMed](#)]

94. Lim, S.-O.; Li, C.-W.; Xia, W.; Lee, H.-H.; Chang, S.-S.; Shen, J.; Hsu, J.L.; Raftery, D.; Djukovic, D.; Gu, H.; et al. EGFR Signaling Enhances Aerobic Glycolysis in Triple-Negative Breast Cancer Cells to Promote Tumor Growth and Immune Escape. *Cancer Res.* **2016**, *76*, 1284–1296. [[CrossRef](#)] [[PubMed](#)]
95. Song, G.-Q.; Zhao, Y. Kisspeptin 10 inhibits the Warburg effect in breast cancer through the Smad signaling pathway: Both in vitro and in vivo. *Am. J. Transl. Res.* **2016**, *8*, 188–195. [[PubMed](#)]
96. Samudio, I.; Fiegl, M.; Andreeff, M. Mitochondrial Uncoupling and the Warburg Effect: Molecular Basis for the Reprogramming of Cancer Cell Metabolism. *Cancer Res.* **2009**, *69*, 2163–2166. [[CrossRef](#)]
97. Xie, J.; Wang, B.S.; Yu, D.H.; Lu, Q.; Ma, J.; Qi, H.; Fang, C.; Chen, H.Z. Dichloroacetate shifts the metabolism from glycolysis to glucose oxidation and exhibits synergistic growth inhibition with cisplatin in HeLa cells. *Int. J. Oncol.* **2010**, *38*, 409–417. [[CrossRef](#)]
98. Gatenby, R.A.; Gillies, R.J. Why do cancers have high aerobic glycolysis? *Nat. Rev. Cancer* **2004**, *4*, 891–899. [[CrossRef](#)]
99. Pracharova, J.; Novohradsky, V.; Kostřhunova, H.; Štarha, P.; Trávníček, Z.; Kasparkova, J.; Brabec, V. Half-sandwich Os(II) and Ruthenium(II) bathophenanthroline complexes: Anticancer drug candidates with unusual potency and a cellular activity profile in highly invasive triple-negative breast cancer cells. *Dalton Trans.* **2018**, *47*, 12197–12208. [[CrossRef](#)]
100. Sledge, G.W., Jr.; Qulali, M.; Goulet, R.; Bone, E.A.; Fife, R. Effect of Matrix Metalloproteinase Inhibitor Batimastat on Breast Cancer Regrowth and Metastasis in Athymic Mice. *J. Natl. Cancer Inst.* **1995**, *87*, 1546–1551. [[CrossRef](#)]
101. Verma, S.; Singh, A.; Mishra, A. Gallic acid: Molecular rival of cancer. *Environ. Toxicol. Pharmacol.* **2013**, *35*, 473–485. [[CrossRef](#)]
102. Lee, H.-L.; Lin, C.-S.; Kao, S.-H.; Chou, M.-C. Gallic acid induces G1 phase arrest and apoptosis of triple-negative breast cancer cell MDA-MB-231 via p38 mitogen-activated protein kinase/p21/p27 axis. *Anti-Cancer Drugs* **2017**, *28*, 1150–1156. [[CrossRef](#)]
103. Naves, M.A.; Graminha, A.E.; Vegas, L.C.; Luna-Dulcey, L.; Honorato, J.; Menezes, A.C.S.; Batista, A.A.; Cominetti, M.R. Transport of the Ruthenium Complex [Ru(GA)(dppf)₂]PF₆ into Triple-Negative Breast Cancer Cells Is Facilitated by Transferrin Receptors. *Mol. Pharm.* **2019**, *16*, 1167–1183. [[CrossRef](#)]
104. Mazuryk, O.; Kurpiewska, K.; Lewiński, K.; Stochel, G.; Brindell, M. Interaction of apo-transferrin with anticancer ruthenium complexes NAMI-A and its reduced form. *J. Inorg. Biochem.* **2012**, *116*, 11–18. [[CrossRef](#)] [[PubMed](#)]
105. Epifano, F.; Genovese, S.; Fiorito, S.; Mathieu, V.; Kiss, R. Lapachol and its congeners as anticancer agents: A review. *Phytochem. Rev.* **2014**, *13*, 37–49. [[CrossRef](#)]
106. Fiorito, S.; Epifano, F.; Bruyère, C.; Mathieu, V.; Kiss, R.; Genovese, S. Growth inhibitory activity for cancer cell lines of lapachol and its natural and semi-synthetic derivatives. *Bioorg. Med. Chem. Lett.* **2014**, *24*, 454–457. [[CrossRef](#)] [[PubMed](#)]
107. Oliveira, K.M.; Corrêa, R.S.; Barbosa, M.I.F.; Ellena, J.; Cominetti, M.R.; Batista, A.A. Ruthenium(II)/triphenylphosphine complexes: An effective way to improve the cytotoxicity of lapachol. *Polyhedron* **2017**, *130*, 108–114. [[CrossRef](#)]
108. Russell-Jones, G.; McTavish, K.; McEwan, J.; Rice, J.; Nowotnik, D. Vitamin-mediated targeting as a potential mechanism to increase drug uptake by tumours. *J. Inorg. Biochem.* **2004**, *98*, 1625–1633. [[CrossRef](#)] [[PubMed](#)]
109. Waibel, R.; Treichler, H.; Schaefer, N.G.; van Staveren, D.R.; Mundwiler, S.; Kunze, S.; Küenzi, M.; Alberto, R.; Nüesch, J.; Knuth, A.; et al. New Derivatives of Vitamin B12 Show Preferential Targeting of Tumors. *Cancer Res.* **2008**, *68*, 2904–2911. [[CrossRef](#)] [[PubMed](#)]
110. Chen, S.; Zhao, X.; Chen, J.; Chen, J.; Kuznetsova, L.; Wong, S.S.; Ojima, I. Mechanism-Based Tumor-Targeting Drug Delivery System. Validation of Efficient Vitamin Receptor-Mediated Endocytosis and Drug Release. *Bioconj. Chem.* **2010**, *21*, 979–987. [[CrossRef](#)]
111. Côte-Real, L.; Karas, B.; Brás, A.R.; Pilon, A.; Avecilla, F.; Marques, F.; Preto, A.; Buckley, B.T.; Cooper, K.R.; Doherty, C.; et al. Ruthenium–Cyclopentadienyl Bipyridine–Biotin Based Compounds: Synthesis and Biological Effect. *Inorg. Chem.* **2019**, *58*, 9135–9149. [[CrossRef](#)]
112. Côte-Real, L.; Karas, B.; Gírio, P.; Moreno, A.; Avecilla, F.; Marques, F.; Buckley, B.T.; Cooper, K.R.; Doherty, C.; Falson, P.; et al. Unprecedented inhibition of P-gp activity by a novel ruthenium-cyclopentadienyl compound bearing a bipyridine-biotin ligand. *Eur. J. Med. Chem.* **2019**, *163*, 853–863. [[CrossRef](#)]

113. Bellamy, W.T. P-Glycoproteins and Multidrug Resistance. *Ann. Rev. Pharmacol. Toxicol.* **1996**, *36*, 161–183. [[CrossRef](#)] [[PubMed](#)]
114. Jain, A.; Cheng, K. The principles and applications of avidin-based nanoparticles in drug delivery and diagnosis. *J. Control Release* **2017**, *245*, 27–40. [[CrossRef](#)] [[PubMed](#)]
115. Morais, T.S.; Silva, T.J.L.; Marques, F.; Robalo, M.P.; Avecilla, F.; Madeira, P.J.A.; Mendes, P.J.G.; Santos, I.; Garcia, M.H. Synthesis of organometallic ruthenium(II) complexes with strong activity against several human cancer cell lines. *J. Inorg. Biochem.* **2012**, *114*, 65–74. [[CrossRef](#)]
116. Mendes, N.; Tortosa, F.; Valente, A.; Marques, F.; Matos, A.; Morais, T.S.; Tomaz, A.I.; Gärtner, F.; Garcia, M.H. In Vivo Performance of a Ruthenium-cyclopentadienyl Compound in an Orthotopic Triple Negative Breast Cancer Model. *Anti-Cancer Agent Med. Chem.* **2017**, *17*, 126–136. [[CrossRef](#)]
117. Frik, M.; Martínez, A.; Elie, B.T.; Gonzalo, O.; Ramírez de Mingo, D.; Sanaú, M.; Sánchez-Delgado, R.; Sadhukha, T.; Prabha, S.; Ramos, J.W.; et al. In Vitro and in Vivo Evaluation of Water-Soluble Iminophosphorane Ruthenium(II) Compounds. A Potential Chemotherapeutic Agent for Triple Negative Breast Cancer. *J. Med. Chem.* **2014**, *57*, 9995–10012. [[CrossRef](#)] [[PubMed](#)]
118. Shaik, N.; Martínez, A.; Augustin, I.; Giovinazzo, H.; Varela-Ramírez, A.; Sanaú, M.; Aguilera, R.J.; Contel, M. Synthesis of Apoptosis-Inducing Iminophosphorane Organogold(III) Complexes and Study of Their Interactions with Biomolecular Targets. *Inorg. Chem.* **2009**, *48*, 1577–1587. [[CrossRef](#)] [[PubMed](#)]
119. Carreira, M.; Calvo-Sanjuán, R.; Sanaú, M.; Marzo, I.; Contel, M. Organometallic Palladium Complexes with a Water-Soluble Iminophosphorane Ligand as Potential Anticancer Agents. *Organometallics* **2012**, *31*, 5772–5781. [[CrossRef](#)] [[PubMed](#)]
120. Frik, M.; Jiménez, J.; Vasilevski, V.; Carreira, M.; de Almeida, A.; Gascón, E.; Benoit, F.; Sanaú, M.; Casini, A.; Contel, M. Luminescent iminophosphorane gold, palladium and platinum complexes as potential anticancer agents. *Inorg. Chem. Front.* **2014**, *1*, 231–241. [[CrossRef](#)]
121. Nhuikaw, T.; Temboot, P.; Hansongnern, K.; Ratanaphan, A. Cellular responses of BRCA1-defective and triple-negative breast cancer cells and in vitro BRCA1 interactions induced by metallo-intercalator ruthenium(II) complexes containing chloro-substituted phenylazopyridine. *BMC Cancer* **2014**, *14*, 73. [[CrossRef](#)]
122. Khwanjira, H.; Adisorn, R. BRCA1-Associated Triple-Negative Breast Cancer and Potential Treatment for Ruthenium-Based Compounds. *Curr. Cancer Drug Targets* **2016**, *16*, 606–617. [[CrossRef](#)]
123. Farmer, H.; McCabe, N.; Lord, C.J.; Tutt, A.N.J.; Johnson, D.A.; Richardson, T.B.; Santarosa, M.; Dillon, K.J.; Hickson, I.; Knights, C.; et al. Targeting the DNA repair defect in BRCA mutant cells as a therapeutic strategy. *Nature* **2005**, *434*, 917–921. [[CrossRef](#)]
124. Kennedy, R.D.; Quinn, J.E.; Mullan, P.B.; Johnston, P.G.; Harkin, D.P. The Role of BRCA1 in the Cellular Response to Chemotherapy. *J. Natl. Cancer Inst.* **2004**, *96*, 1659–1668. [[CrossRef](#)] [[PubMed](#)]
125. Cao, W.; Zheng, W.; Chen, T. Ruthenium polypyridyl complex inhibits growth and metastasis of breast cancer cells by suppressing FAK signaling with enhancement of TRAIL-induced apoptosis. *Sci. Rep.* **2015**, *5*, 9157. [[CrossRef](#)] [[PubMed](#)]
126. Montani, M.; Pazmay, G.V.B.; Hysi, A.; Lupidi, G.; Pettinari, R.; Gambini, V.; Tilio, M.; Marchetti, F.; Pettinari, C.; Ferraro, S.; et al. The water soluble ruthenium(II) organometallic compound [Ru(p-cymene)(bis(3,5 dimethylpyrazol-1-yl)methane)Cl]Cl suppresses triple negative breast cancer growth by inhibiting tumor infiltration of regulatory T cells. *Pharmacol. Res.* **2016**, *107*, 282–290. [[CrossRef](#)] [[PubMed](#)]
127. Shen, J.; Kim, H.-C.; Wolfram, J.; Mu, C.; Zhang, W.; Liu, H.; Xie, Y.; Mai, J.; Zhang, H.; Li, Z.; et al. A Liposome Encapsulated Ruthenium Polypyridine Complex as a Theranostic Platform for Triple-Negative Breast Cancer. *Nano Lett.* **2017**, *17*, 2913–2920. [[CrossRef](#)] [[PubMed](#)]
128. Popolin, C.P.; Reis, J.P.B.; Becceneri, A.B.; Graminha, A.E.; Almeida, M.A.P.; Corrêa, R.S.; Colina-Vegas, L.A.; Ellena, J.; Batista, A.A.; Cominetti, M.R. Cytotoxicity and anti-tumor effects of new ruthenium complexes on triple negative breast cancer cells. *PLoS ONE* **2017**, *12*, e0183275. [[CrossRef](#)] [[PubMed](#)]
129. Becceneri, A.B.; Popolin, C.P.; Plutin, A.M.; Maistro, E.L.; Castellano, E.E.; Batista, A.A.; Cominetti, M.R. The trans-[Ru(PPh₃)₂(N,N-dimethyl-N'-thiophenylthioureato-k₂O,S)(bipy)]PF₆ complex has pro-apoptotic effects on triple negative breast cancer cells and presents low toxicity in vivo. *J. Inorg. Biochem.* **2018**, *186*, 70–84. [[CrossRef](#)]
130. Zhan, T.; Lou, H. Synthesis ofazole nucleoside analogues of d-pinitol as potential antitumor agents. *Carbohydr. Res.* **2007**, *342*, 865–869. [[CrossRef](#)]

131. Han Ang, W.; Dyson, P.J. Classical and Non-Classical Ruthenium-Based Anticancer Drugs: Towards Targeted Chemotherapy. *Eur. J. Inorg. Chem.* **2006**, *2006*, 4003–4018. [[CrossRef](#)]
132. Colina-Vegas, L.; Oliveira, K.M.; Cunha, B.N.; Cominetti, M.R.; Navarro, M.; Batista, A.A. Anti-Proliferative and Anti-Migration Activity of Arene–Ruthenium(II) Complexes with Azole Therapeutic Agents. *Inorganics* **2018**, *6*, 132. [[CrossRef](#)]
133. Silva, H.V.R.; Dias, J.S.M.; Ferreira-Silva, G.Á.; Vegas, L.C.; Ionta, M.; Corrêa, C.C.; Batista, A.A.; Barbosa, M.I.F.; Doriguetto, A.C. Phosphine/diimine ruthenium complexes with Cl^- , CO, NO^+ , NO_2^- , NO_3^- and pyridine ligands: Pro-apoptotic activity on triple-negative breast cancer cells and DNA/HSA interactions. *Polyhedron* **2018**, *144*, 55–65. [[CrossRef](#)]
134. Irace, C.; Misso, G.; Capuozzo, A.; Piccolo, M.; Riccardi, C.; Luchini, A.; Caraglia, M.; Paduano, L.; Montesarchio, D.; Santamaria, R. Antiproliferative effects of ruthenium-based nucleolipidic nanoaggregates in human models of breast cancer in vitro: Insights into their mode of action. *Sci. Rep.* **2017**, *7*, 45236. [[CrossRef](#)] [[PubMed](#)]
135. Piccolo, M.; Misso, G.; Ferraro, M.G.; Riccardi, C.; Capuozzo, A.; Zarone, M.R.; Maione, F.; Trifuoggi, M.; Stiuso, P.; D’Errico, G.; et al. Exploring cellular uptake, accumulation and mechanism of action of a cationic Ru-based nanosystem in human preclinical models of breast cancer. *Sci. Rep.* **2019**, *9*, 7006. [[CrossRef](#)] [[PubMed](#)]
136. Zhao, X.; Li, L.; Yu, G.; Zhang, S.; Li, Y.; Wu, Q.; Huang, X.; Mei, W. Nucleus-enriched Ruthenium Polypyridine Complex Acts as a Potent Inhibitor to Suppress Triple-negative Breast Cancer Metastasis In vivo. *Comput. Struct. Biotechnol. J.* **2019**, *17*, 21–30. [[CrossRef](#)] [[PubMed](#)]



© 2020 by the authors. Licensee MDPI, Basel, Switzerland. This article is an open access article distributed under the terms and conditions of the Creative Commons Attribution (CC BY) license (<http://creativecommons.org/licenses/by/4.0/>).

1.4 RUTHENIUM COMPLEXES FOR ANTIFUNGAL APPLICATIONS

The incidence of major fungal infections has increased in the past few years and Candidiasis stands out as one of the most serious infectious diseases with an associated mortality exceeding 70% in the case of invasive Candidiasis ^[45-46]. Although more than fifteen distinct *Candida* species can infect humans, most infections are usually caused by six pathogens: *C. albicans*, *C. glabrata*, *C. tropicalis*, *C. parapsilosis*, *C. krusei* and *C. auris* ^[46]. Whereas *C. albicans* is the most common pathogen in clinical settings, non-*albicans Candida* species could collectively represent >50% of the bloodstream isolates ^[47-48]. A key challenge to the treatment of Candidiasis is antifungal resistance, an emerging problem worldwide, complicating the selection of an appropriate antifungal therapy ^[46, 49]. *Candida* species that do not respond to first-line antifungals (such as echinocandins and fluconazole) are increasingly being recognized, and their appearance usually correlates with high azole and/or echinocandin background usage ^[50]. Azole-containing antifungal drugs such as fluconazole are one of the largest classes of antifungal agents in clinical use, however, they have presented cases of resistance ^[51-52]. Thus, development of new antifungal agents for the treatment of Candidiasis is very urgent.

The unique characteristics of metal-based compounds could also be exploited in the field of antifungal therapy, potentially leading to alternatives to the traditionally used drugs ^[3]. A quick survey of the literature on metal-based agents reported for their pharmaceutical applications shows a high potential for these species as antifungal drugs. Promising antifungal activities were reported for different metal complexes based on copper, cobalt, silver, manganese etc ^[53-55]. Importantly, according to a quite recent review by Stoianoff *et al* (2018), several ruthenium complexes have showed a promising antifungal potential, including a few examples with anticandidal properties ^[56]. One of the very first studies on the antifungal activity of ruthenium species was reported by Sengupta *et al* (1987). In this study, several Ru(III) Schiff base complexes were synthesized and their antifungal activity tested against *Aspergillus niger*. All the complexes from this study showed a more notable antifungal activity than their corresponding Schiff base ligands (at 1000 ppm), indicating the importance of the complexation ^[57]. Since then, several Ru-based species have been studied to determine their antifungal potential, however, the anticandidal potential of these species was often overlooked. It has been reported that ruthenium complexes including various types of ligands in their structure such as aromatic, heteroaromatic, Schiff bases, thiosemicarbazones, chalcones, catecholamines, hydridotris(pyrazolyl)borate, organophosphorated and even in several kinds of structures including mononuclear, dinuclear,

trinuclear and polymeric species, can act as promising antifungal agents against different fungal infections. Almost all ruthenium complexes reported so far are more active than their corresponding free ligands. Structure activity relationship (SAR) studies have indicated that steric and lipophilic parameters are important factors affecting their antifungal potential, which was further confirmed by the high activity reported for ruthenium complexes bearing triphenylphosphine, triphenyl arsine, aromatic, or heteroaromatic lipophilic moieties ^[56].

There are several studies of ruthenium complexes (Ru(II) and Ru(III)) tested against *Candida* species, causing one of the most invasive fungal infections. *C. albicans* was often selected to evaluate the anticandidal activity of the ruthenium complexes, however, unlike other species such as *C. Krusei* and *C. glabrata*, this species is usually susceptible to the currently used drugs. Due to the differences between the *in vitro* experimental parameters reported in the several studies of the anticandidal activity of ruthenium complexes (such as time of incubation, type of antifungal assay, temperature and the way of representing the activity, etc), it is unfortunately not possible to directly compare their activity (table 1). However, many of these studies indicated a better antifungal activity for some ruthenium complexes compared to the currently used drugs ^[58-68]. Although oxidative stress and alterations in the cell wall have been suggested to be associated with the mode of action of some ruthenium complexes ^[66], further investigations are required to draw concrete conclusions about their anticandidal mechanism. Taken together, the numerous preliminary anticandidal activity reports for ruthenium complexes and the emergence of non-*albicans Candida* species that are not susceptible to available drugs, indicate that ruthenium complexes can provide a rich platform and suitable building blocks for the design of novel antifungal agents that are not only limited to *C. albicans*. In addition, the combination of ruthenium and biologically active ligands (such as azole containing moieties) and/or lipophilic molecules (such as triphenylphosphine) previously reported to enhance antifungal activity of ruthenium complexes ^[56] could potentially lead to antifungal agents with an enhanced activity.

Table 1. Anticandidal activity of previously reported ruthenium complexes.

| | Type of assay | Species | Anticandidal activity [d] |
|--|--|------------------------|-------------------------------|
| Ihm <i>et al</i> [1] | Disk diffusion ^[a] | <i>C. albicans</i> | 9-13% (at 0.5%) |
| Mobin <i>et al</i> [2] | | | 9-13 mm (at 100 ppm) |
| Liu <i>et al</i> [3] | | | 6-7 mm (at 100 ppm) |
| Jayabalakrishnan <i>et al</i> [4] | | | 11-15 mm (at 2%) |
| Jayabalakrishnan <i>et al</i> [5] | | | 12-17 mm (at 2%) |
| Ben hadda <i>et al</i> [6] | | | 22.5 mm (at 0.2 mg/mL) |
| Fekry <i>et al</i> [7] | | | ≈ 17 mm (at 50 ppm) |
| Anandaram <i>et al</i> [8] | Disk diffusion ^[b] | | 16.11-17.86 µg/mL |
| Radacki <i>et al</i> [9] | Turbidity (broth microdilution) ^[b] | | 6.77 nM |
| De Resende Stoianoff <i>et al</i> [10] | | <i>C. albicans</i> | 0.4-13.6 × 10 ⁻⁵ M |
| | | <i>C. krusei</i> | 1.70–7.3 × 10 ⁻⁵ M |
| | | <i>C. parapsilosis</i> | 0.8–4.1 × 10 ⁻⁵ M |
| | | <i>C. tropicalis</i> | 0.8–7.3 × 10 ⁻⁵ M |
| | | <i>C. glabrata</i> | 4.0–29.3 × 10 ⁻⁵ M |
| Güenal <i>et al</i> [11] | | <i>C. albicans</i> | 100 µg/mL |
| | <i>C. tropicalis</i> | 100 µg/mL | |
| Mansour [12] | <i>C. albicans</i> | | 24 nM |
| Radacki <i>et al</i> [13] | | | 24 nM |
| Alici <i>et al</i> [14] | | | 200 µg/mL |

| | | | |
|---|-------------------------------|-------------------------------|-----------------------|
| Vannier-Santos <i>et al</i> ^[15] | Cell counting ^[c] | <i>C. tropicalis</i> | 20.3 μ M |
| Shaikh <i>et al</i> ^[16] | Well diffusion ^[a] | <i>C. albicans</i> | 12-15 mm (at 1 mg/mL) |
| Natarajan <i>et al</i> ^[17] | Well diffusion ^[b] | | 50-100 μ g/mL |
| Prabhakaran <i>et al</i> ^[18] | | Well diffusion ^[b] | <i>C. albicans</i> |
| | <i>C. tropicalis</i> | | 15-20 μ M |

Antifungal activity reported as: ^[a] inhibition zone diameter; ^[b] minimum inhibitory concentration (MIC); ^[c] IC₅₀.

^[d] Please note that the incubation time (24-72h) and the temperature (26-37 °C) varied from one study to another.

1.5 HYPOTHESES AND OBJECTIVES

Hypotheses:

- Ruthenium complexes bearing biologically active ligands (such as azole containing drugs) are superior anticancer or/and antifungal agents than ruthenium complexes or the ligands alone;
- The anticancer/antifungal potential and the selectivity of the ruthenium complexes bearing biologically active ligands are much higher than that of the currently used anticancer (e.g. cisplatin) and antifungal (e.g. fluconazole) species.

General objective:

The research project presented here aims at creating novel ruthenium drugs with the potential to lead to multitargeting species for cancer treatment (more specifically breast cancer treatment), and antifungal applications (more specifically anticandidal applications). By creating new avenues for the development of superior pharmaceutical species able to overcome the issues related to current therapies including drug resistance, this project also aims at modifying established beliefs regarding metallic cancer therapeutics.

Specific aims:

- To synthesize, purify and characterize various ruthenium complexes bearing biologically active ligands, more specifically aromatase inhibitors (anastrozole and letrozole);
- To investigate the *in vitro* antiproliferative activity and aromatase inhibitory property of ruthenium complexes bearing aromatase inhibitors against specific cancer cell lines, as well as their *in vivo* toxicity;
- To investigate the *in vitro* antifungal activity and potential mode of action of the ruthenium complexes against different *Candida* species;
- To bring electronic and structural modifications to ruthenium complexes, and to evaluate their influence on their activity, selectivity and toxicity.

2 PUBLICATION 2

Organoruthenium(II) Complexes Bearing an Aromatase Inhibitor: Synthesis, Characterization, *in Vitro* Biological Activity and *in Vivo* Toxicity in Zebrafish Embryos

Complexes d'organoruthénium (II) portant un inhibiteur de l'aromatase: synthèse, caractérisation, activité biologique *in vitro* et toxicité *in vivo* dans les embryons de poisson zèbre

Authors: Golara Golbaghi, Mohammad Mehdi Haghdoost, Debbie Yancu, Yossef López de los Santos, Nicolas Doucet, Shunmoogum A. Patten, J. Thomas Sanderson and Annie Castonguay*

INRS - Institut Armand-Frappier, Université du Québec, 531 boul. des Prairies, Laval, Québec, H7V 1B7, Canada

This article was published in *Organometallics* (2019), 38(3), 702-711.

<https://doi.org/10.1021/acs.organomet.8b00897>

Contribution of authors:

Golara Golbaghi designed and performed the biology and chemistry experiments, the statistical analyses and wrote the original draft of the manuscript.

Dr. Mohammad Mehdi Haghdoost performed the Zebrafish experiments.

Debbie Yancu trained me to perform aromatase assay.

Dr. Yossef López de los Santos performed the Docking simulations.

Professors Nicolas Doucet, Shunmoogum A. Patten, and J. Thomas Sanderson were our collaborators who provided us with their knowledge, materials and facilities to perform theoretical studies, Zebrafish experiments and aromatase assay, respectively.

Prof. Annie Castonguay obtained the research funding, supervised the project and participated in conceptualization, writing and revising the manuscript.

RÉSUMÉ

Les inhibiteurs de l'aromatase de 3^e génération tels que l'anastrozole (ATZ) et le letrozole (LTZ) sont communément utilisés pour traiter les cancers du sein à récepteurs d'œstrogène positifs (ER+). La capacité de ces inhibiteurs à coordonner les métaux est considérée comme une piste intéressante à étudier, qui pourrait conduire à l'émergence d'une nouvelle catégorie de candidats de médicaments anticancéreux avec un large spectre d'activité pharmaceutique. Au cours de cette étude, une série de complexes de ruthenium(II) arene comportant un inhibiteur de l'aromatase, l'anastrozole, a été synthétisée et caractérisée. Parmi ces complexes, $[\text{Ru}(\eta^6\text{-C}_6\text{H}_6)(\text{PPh}_3)(\eta^1\text{-ATZ})\text{Cl}]\text{BPh}_4$ (3) s'est avéré être le plus stable dans le milieu de culture utilisé pour effectuer les tests d'activité biologique. De plus, ce complexe a démontré une accumulation accrue dans les cellules cancéreuses et l'induction d'une plus importante cytotoxicité *in vitro* chez les deux lignées cellulaires humaines cancéreuses (ER+) (MCF7 and T47D), à comparer aux autres complexes de la série. Ce dernier a également mené à une diminution de l'activité de l'aromatase dans les cellules H295R. Enfin, l'exposition d'embryons de poissons zèbres à ce complexe (12.5 μM) sur une période de 96 heures n'a pas mené à l'observation de signes de cytotoxicité significatifs. De ce fait, l'ensemble de ces résultats font de ce complexe le candidat le plus prometteur pour de potentiels études *in vivo*.

Reprinted with permission from (*Organometallics* 2019, 38, 702–711). Copyright (2019) American Chemical Society.

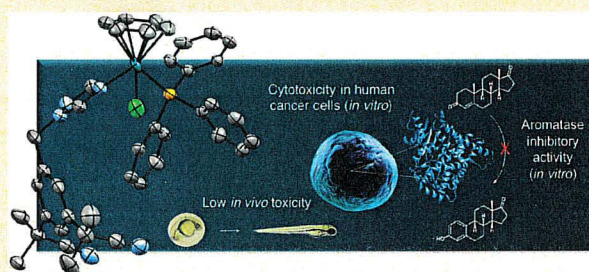
Organoruthenium(II) Complexes Bearing an Aromatase Inhibitor: Synthesis, Characterization, *in Vitro* Biological Activity and *in Vivo* Toxicity in Zebrafish Embryos

Golara Golbaghi, Mohammad Mehdi Haghdoost, Debbie Yancu, Yossef López de los Santos, Nicolas Doucet, Shunmoogum A. Patten, J. Thomas Sanderson, and Annie Castonguay*[✉]

INRS - Institut Armand-Frappier, Université du Québec, 531 boul. des Prairies, Laval, Quebec, H7V 1B7, Canada

Supporting Information

ABSTRACT: Third-generation aromatase inhibitors such as anastrozole (ATZ) and letrozole (LTZ) are widely used to treat estrogen receptor-positive (ER+) breast cancers in postmenopausal women. Investigating their ability to coordinate metals could lead to the emergence of a new category of anticancer drug candidates with a broader spectrum of pharmacological activities. In this study, a series of ruthenium(II) arene complexes bearing the aromatase inhibitor anastrozole was synthesized and characterized. Among these complexes, $[\text{Ru}(\eta^6\text{-C}_6\text{H}_6)(\text{PPh}_3)(\eta^1\text{-ATZ})\text{Cl}]\text{-BPh}_4$ (**3**) was found to be the most stable in cell culture media, to lead to the highest cellular uptake and *in vitro* cytotoxicity in two ER+ human breast cancer cell lines (MCF7 and T47D), and to induce a decrease in aromatase activity in H295R cells. Exposure of zebrafish embryos to complex **3** ($12.5 \mu\text{M}$) did not lead to noticeable signs of toxicity over 96 h, making it a suitable candidate for further *in vivo* investigations.



INTRODUCTION

The coordination of biologically active molecules to metals is a promising strategy for the development of agents with a broader range of anticancer properties. Because metal complexes are widely studied for their ability to reduce the viability of cancer cells, the introduction of biologically active ligands within their structure can result in multitargeting drug candidates that could limit the emergence of cancer cell resistance mechanisms.^{1–3} For instance, numerous enzyme inhibitors are used to treat and/or prevent several types of cancers,^{4–6} making them promising ligands for the design of metal-based therapeutics. In addition, metal complexation greatly increases the structural possibilities to form enzyme inhibitors relative to purely organic molecules. Because they can adopt geometries other than linear, trigonal, or tetrahedral, metals can allow organic ligands (or enzyme inhibitors) to occupy a specific position in the active site of enzymes.^{7,8} A number of anticancer metal complexes including an enzyme inhibitor in their structure have been reported previously.^{9–11} However, metal complexes bearing aromatase inhibitors have so far been overlooked. Aromatase is the enzyme that catalyzes the final, rate-limiting step in estrogen synthesis from androgens.¹² More than two-thirds of breast tumors are estrogen receptor positive (ER+),¹³ and estrogens play a key role in initiating and promoting this type of hormone-dependent cancer.^{14–17} Currently, third-generation aromatase inhibitors such as the nonsteroidal triazole derivatives anastrozole (Arimidex) and letrozole (Femara) are found to

inhibit the aromatase activity in breast tissues. They are widely used to treat ER+ breast cancer, particularly in postmenopausal women who no longer produce ovarian estrogens and derive their estrogens mainly from adrenal androgens in extra ovarian tissues that have aromatase activity such as (breast) adipose.¹⁸ However, in about one-third of patients with metastatic ER+ breast cancer, endocrine therapies that involve aromatase inhibitors (or tamoxifen, known to inhibit ER+ cancer growth by blocking estrogen receptors) lead to the emergence of tumor cells that grow even in the absence of estrogens, resulting in a treatment-resistant cancer that is often incurable.¹⁹ Depriving ER+ cells of estrogens was also previously shown to sensitize them to cytotoxic agents.^{20,21} Thus, investigating the anticancer properties arising from the coordination of aromatase inhibitors to metals could lead to the development of efficient drug/prodrug candidates that display more than one mode of action, which could potentially circumvent the emergence of drug resistance mechanisms, a common cause of mortality in ER+ breast cancer patients. It was recently reported that the coordination of hydroquinoline, aminoquinoline, and uracyl ligands to copper can lead to cytotoxic complexes with an aromatase inhibitory activity.^{22,23} To our knowledge, only a few investigations from other groups involved the preparation of letrozole (Cu, Co, and Ni)^{24,25} or anastrozole (Pt)²⁶ metal complexes, and none of these studies

Received: December 12, 2018

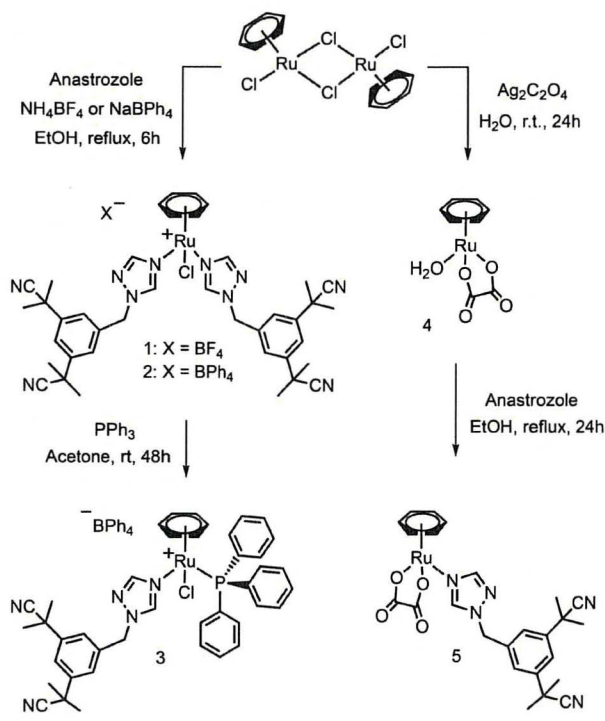
Published: January 31, 2019

reported an assessment of their aromatase inhibitory activity. Organoruthenium complexes are of particular interest for their activity against numerous types of cancer cells via multiple mechanisms and are often considered as interesting alternatives to currently used therapeutics.^{27–32} Maysinger et al. previously reported a preliminary account of the cytotoxicity of a series of ruthenium complexes bearing letrozole ligands.³³ Here, we report the synthesis, characterization, and biological activity of a similar class of ruthenium(II) complexes bearing the aromatase inhibitor anastrozole.

RESULTS AND DISCUSSION

Cationic complex **1** was obtained from a previously reported procedure³³ that led to its letrozole analogue $[\text{Ru}(\eta^6\text{-C}_6\text{H}_6)(\eta^1\text{-LTZ})_2\text{Cl}]\text{BF}_4$ (Ru-LTZ) by refluxing an ethanol solution of $[\text{Ru}(\eta^6\text{-C}_6\text{H}_6)_2\text{Cl}_2]$ and anastrozole (4 equiv) with an excess of NH_4BF_4 (68% yield) (Scheme 1). The same

Scheme 1. Synthetic Route to Complexes 1–5



synthetic strategy was used to prepare complex **2**, using NaBPh₄ (60% yield). As the ability of the triphenylphosphine ligand to enhance the cytotoxicity of complexes by improving their lipophilicity and by providing them with a mitochondrial targeting ability is well-precedented,^{34–37} the synthesis of compound **3** was undertaken by allowing an acetone solution of **2** to react with an excess of PPh₃ (74% yield). During the preparation of this 18-electron complex, only one of its anastrozole ligands underwent a substitution reaction, most likely via a dissociative mechanism. Complexes **1–3** are air-stable, soluble in acetone, in chlorinated solvents and DMSO, but poorly soluble in water. In alcohols, complex **1** is highly soluble whereas complexes **2** and **3** have a relatively lower solubility. In addition to obtaining the right balance between their lipophilicity and hydrophilicity, improving the poor water solubility of drug candidates remains an essential challenge in

drug design.³⁸ It was previously reported that oxalate ligands could significantly enhance the water solubility of ruthenium arene complexes when included in their coordination sphere.³⁹ Complex **5**, bearing both an oxalate and an anastrozole ligand, was therefore prepared by refluxing an ethanol solution of anastrozole and the ruthenium oxalate precursor **4** (52% yield). The identity of complexes **1–5** was confirmed by high-resolution electrospray ionization mass spectrometry (HR-ESI-MS), elemental analysis, and NMR spectroscopy. As expected, in the ¹H NMR spectrum of complexes **1–3** and **5**, resonances corresponding to the triazole protons of anastrozole are observed at downfield chemical shifts compared to the corresponding resonances in the spectrum of the free ligand. In the case of compound **3**, the presence of a singlet at 35 ppm (acetone-*d*₆) observed by ³¹P{¹H} NMR confirms the coordination of triphenylphosphine to the ruthenium.^{33,40–42}

Solid-state structures of complexes **2–5** were obtained from single-crystal X-ray diffraction analyses (Table S1 in the Supporting Information). ORTEP views of the complexes are shown in Figure 1. As expected, they revealed a piano-stool

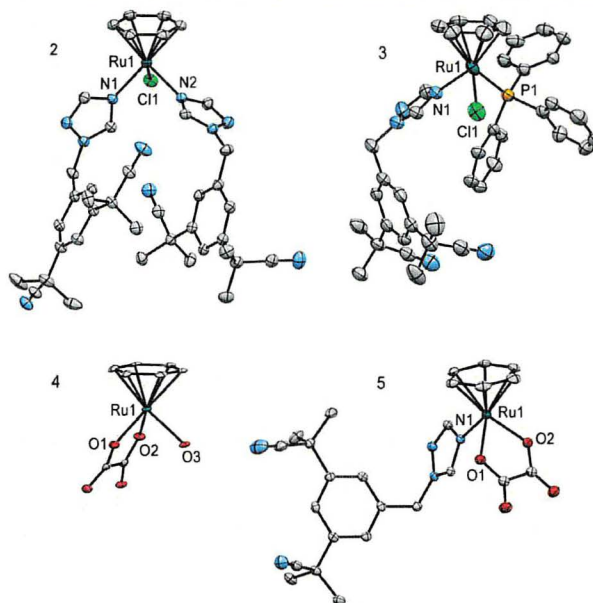


Figure 1. ORTEP diagrams (showing thermal ellipsoids at the 50% probability level) of complexes 2–5. Note that in the case of **3**, only one site is shown for the disordered benzene, Cl and CN. 2: Ru1–N1, 2.1024(12) Å; Ru1–N2, 2.1104(12) Å. 3: Ru1–N1, 2.114(4) Å; Ru1–N1', 2.091(5) Å. 5: Ru1–N1, 2.1130(15) Å.

configuration, characteristic of ruthenium arene complexes.⁴³ Notably, similar Ru–N (anastrozole) bond lengths were noted for complexes **2**, **3**, and **5**, reflecting their comparable bond strength (Figure 1 and Table S2).

As metal-based drug candidates often display a limited solubility in cell culture media, DMSO is commonly used for the preparation of metal complex stock solutions for biological screenings. However, their solubility once diluted in culture medium and the lability of their ligand(s) in the presence of DMSO are often overlooked.⁴⁴ All complexes reported here were found to be soluble in cell culture medium (0.5% DMSO) at concentrations typically used for cytotoxicity screenings, as assessed by ultraviolet–visible (UV–vis) absorbance measurements. Their stability was evaluated in

three different conditions relevant to the biological experiments performed in this study: (i) in DMSO- d_6 , (ii) in water (0.5% DMSO), and (iii) in DMEM-F12 medium (0.1% DMSO). ^1H NMR analysis of all complexes in DMSO- d_6 revealed a high stability for all the complexes for which less than 5% of anastrozole dissociation was observed, except for 5, for which a 15% anastrozole release was noted. Moreover, a limited anastrozole release (3–15%) was observed for all complexes when 150 μM aqueous solutions (0.5% DMSO) were separately incubated at 37 $^\circ\text{C}$ for 48 h (3 being the most stable) (Table S3), as assessed by ^1H NMR spectroscopy. The stability of each complex was also evaluated under conditions similar to that of the tritiated water-release assay. To this aim, a liquid/liquid extraction/HPLC-UV method was developed (Figure S1) to measure the amount of released anastrozole (or letrozole) when 10 μM solutions of complexes 1–3, 5, and Ru-LTZ (previously reported letrozole analogue of 1)³³ were incubated in DMEM/F-12 medium for 1.5 h (the duration of the tritiated water-release assay). The release of anastrozole (or letrozole) from most complexes was found to be considerable, except for complex 3, for which only 4% of its aromatase inhibitor ligand was released (Table S4).

Because all ruthenium complexes reported in this study (except 4) include at least one anastrozole ligand, their cytotoxicity was evaluated after 48 h in two ER+ human breast cancer cell lines, T47D and MCF7, using the sulforhodamine B (SRB) assay, and compared to clinically approved anticancer drugs *cis*-platin and anastrozole. As previously reported,³³ the cell growth inhibitor anastrozole did not display any noticeable cytotoxicity in MCF7 or T47D cells (results not shown). However, complexes 1–3 were each found to be active to various extents (Figure 2 and Table 1), whereas complexes 4 and 5 did not display any significant cytotoxicity (results not shown). It is noteworthy that because of the significant contribution of the tumor microenvironment to the implementation of the antitumor activity of similar types of Ru(II) species, the observed *in vitro* cytotoxicities of the complexes reported in this study are not necessarily indicative

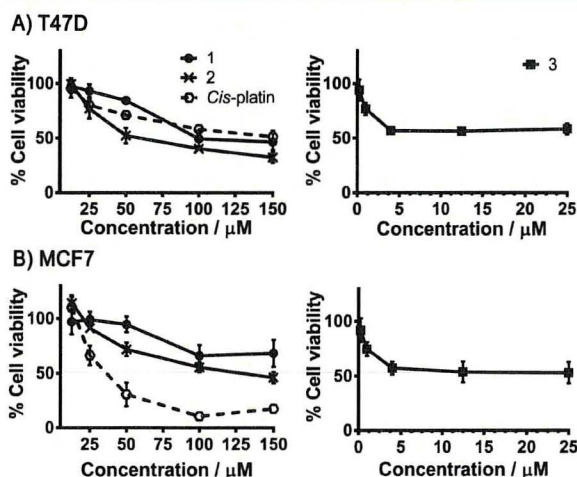


Figure 2. Cell viability determined by the SRB assay (48 h) in ER(+) breast cancer cells: T47D (A) and MCF7 (B), treated with 1, 2, and *cis*-platin (black dashed line) at the concentrations 12.5, 25, 50, 100, and 150 μM (left) and 3 at the concentrations 0.25, 1, 4, 12.5, and 25 μM (right). All values are expressed as means (from three independent experiments) \pm SD relative to the carrier.

Table 1. Estimated IC_{50} Values Illustrating the Effect of Complexes 1–3 and *cis*-Platin on the Viability of MCF7 and T47D Cancer Cells^a

| | IC_{50} (μM) ^b | |
|--------------------|---|--------------------|
| | MCF7 | T47D |
| 1 | >150 | >150 |
| 2 | 139.4 (± 14.3) | 53.5 (± 9.1) |
| 3 ^c | ≥ 4 | ≥ 4 |
| <i>cis</i> -platin | 37.0 (± 2.4) | >150 |

^aData extracted from Figure 2. ^bCytotoxicity was determined by exposure of cell lines to each complex for 48 h and expressed as the concentration required to inhibit cell viability by 50% (IC_{50}). Values in parentheses correspond to the standard deviation of three independent experiments. ^cAs seen in Figure 2, cell viability reached a plateau at concentrations above 4 μM .

of their potential *in vivo* antitumor activities.^{29,45} Although complexes 1 and 2 were less cytotoxic than *cis*-platin in MCF7 cancer cells, compounds 2 and 3 had a similar or even more effective cytotoxicity than that of the clinically approved drug in T47D cancer cells, which are known for their *cis*-platin resistance.⁴⁶ These results highlight the importance of developing such alternative complexes for breast cancer therapy. At concentrations below 12.5 μM , compound 3 was found to be the most cytotoxic of all complexes, reducing T47D and MCF7 cell viability by almost half at 4 μM . Cancer cells exposed to higher concentrations of the various complexes were especially susceptible to compound 2, more significantly in the case of T47D cells, where the cell viability was inhibited by almost half at 50 μM . Interestingly, a significant difference was observed between the cytotoxicity of complexes 1 and 2 on both cell lines, which differ only in the nature of their counterion (BF_4^- vs BPh_4^-) (Table 1). The higher cytotoxicity of complexes 2 and 3 is not likely due to the sole contribution of the BPh_4^- counterion as both complexes induced a significantly higher cytotoxicity than NaBPh_4 in T47D cells at 25 μM (Figure S2).

Cellular levels of ruthenium were measured by inductively coupled plasma mass spectrometry (ICP-MS) after MCF7 cells were exposed to 4 μM solutions of all complexes for 48 h (Figure 3A). Compared to nontreated cells (control), a significant amount of ruthenium was observed in cells treated with each complex. Cellular ruthenium levels of each complex appeared to depend on their respective lipophilicity, in agreement with previous reports demonstrating that more

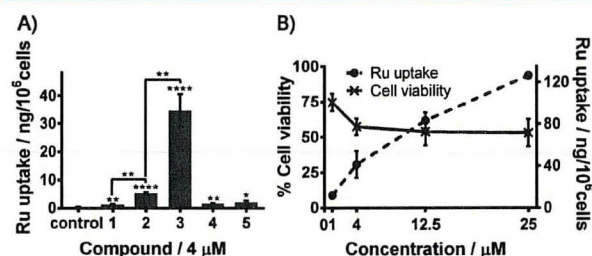


Figure 3. (A) Ruthenium cellular uptake (determined by ICP-MS) after exposure of MCF7 cells to 4 μM solutions of 1–5 (48 h); (B) ruthenium cellular uptake (determined by ICP-MS) and cell viability after exposure of MCF7 cells to 1, 4, 12.5, and 25 μM solutions of 3 (48 h). Error bars in the graph represent the standard deviation. Significant differences: * $p < 0.05$; ** $p < 0.01$; *** $p < 0.0001$.

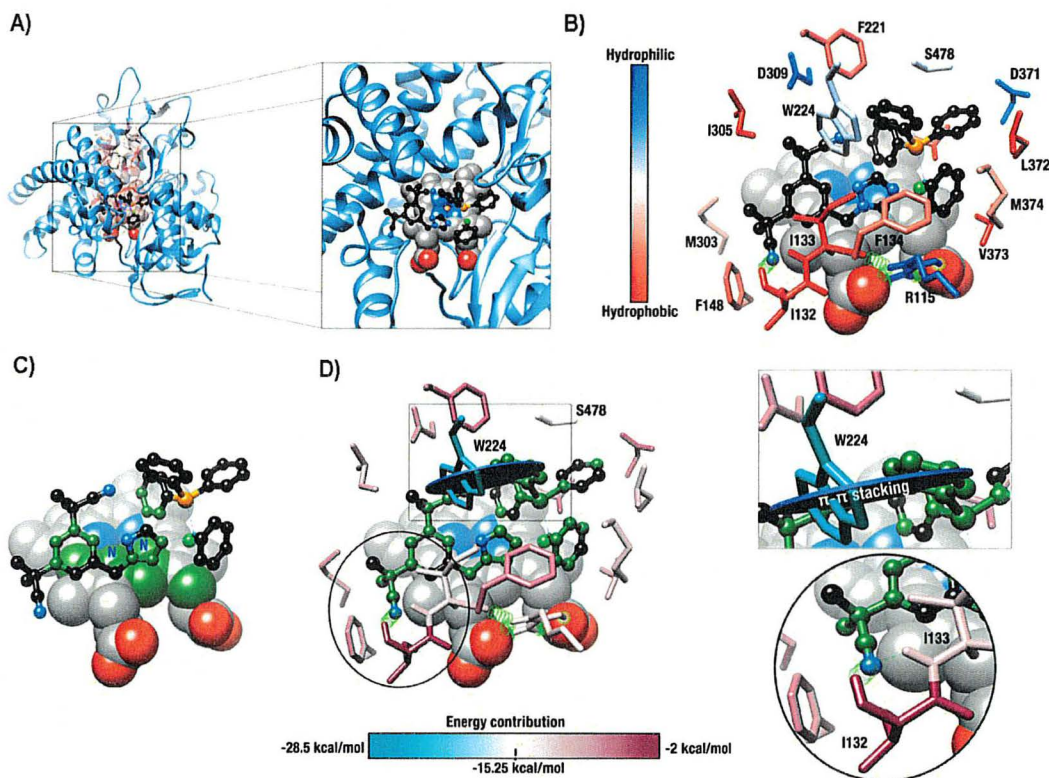


Figure 4. Ternary complex formation between compound 3, human aromatase, and a heme group as enzymatic cofactor. (A) Active-site pocket of aromatase⁶¹ highlighted by a red transparent surface with a zoomed view of the ligand interacting with the cofactor. (B) Ternary complex showing the most important stabilizing interactions between enzyme residues and the ruthenium complex. Amino acid (stick representation) identity is shown with single-letter code, and their hydrophobic profile is illustrated using the Kyte–Doolittle scale.⁶² Cofactor atoms (sphere representation) are color-coded as follows: carbon (gray), nitrogen (blue), iron (orange), and oxygen (red). Only hydrogen atoms participating in H-bonding interactions are shown (green strings and dotted lines). The ruthenium complex atoms (ball-and-stick representation) are shown using the same color coding, except for carbon (black) and phosphorus atoms (orange). The ruthenium and chlorine atoms are depicted in dark and light green, respectively. (C) Atomic interactions exhibiting higher energy values between the ruthenium-based ligand and cofactor in the ternary complex are highlighted in dark green. (D) Energy contributions for amino acids that stabilize the ternary complex are shown on a scale ranging from -2 to -28.5 kcal/mol. Trp224 is the most important energy contributor to this interaction, exhibiting a potential orthogonal π – π stacking energy value of -28.5 kcal/mol (black circle in the rectangle inset). Two alternative hydrogen bonding interactions were identified for Ile132 and Ile133 (circle inset). All panels show the same atomic orientation.

hydrophobic systems have a greater affinity for the cell membrane.⁴⁷ For instance, lipophilic counterion-containing compounds 2 and 3 (BPh_4^-) displayed the highest ruthenium cellular uptake ($3 > 2 > 1$, 4, 5). As previously suggested,⁴⁸ hydrophobic interactions between the arene ligands of organoruthenium cations and the phenyl groups of their BPh_4^- counterion might lead to strong ion-pairing, which might modulate drug uptake and consequently have an impact on their cytotoxicity. More specifically, complex 3 produced 7-fold higher cellular ruthenium levels than complex 2 (at $4 \mu\text{M}$), most likely because of the high lipophilicity of its PPh_3 ligand. Interestingly, we found that the steady cytotoxicity of complex 3 at concentrations greater than $1 \mu\text{M}$ was not a consequence of its limited cellular uptake at those concentrations (Figure 3B), as higher concentrations did result in higher ruthenium levels in MCF7 cells. A solubility assessment by UV–vis absorbance measurements also revealed that solutions of the complexes were not saturated at the tested concentrations. This suggests that complex 3 might act via a distinct mechanism of action. Whereas complex 3 was found to display the highest ruthenium cellular uptake, complexes 4 and 5 resulted in a very low ruthenium cellular uptake. It is

noteworthy that further studies revealed that 4 and 5 can inhibit the migration of MCF7 breast cancer cells (Figure S3), for which extracellular modes of action are often known to take place.⁴⁹

Because complex 3 showed negligible anastrozole ligand lability in DMSO and DMSO/media, we evaluated, theoretically and experimentally, the potential of this compound to act as an aromatase inhibitor. Docking simulations have been previously used to study the plausible interactions between transition-metal complexes and proteins or DNA.^{50–52} Here, we report a theoretical investigation of the potential interaction between a ruthenium complex (compound 3) and the aromatase enzyme using a docking simulation, based on the crystal structure of human placental aromatase cytochrome P450 (CYP19A1). Indeed, unlike suggested from previous docking studies for free anastrozole,^{53,54} the binding of anastrozole to the heme iron of CYP19 via its N1 triazole nitrogen atom (see Figure 1) is not possible in this system because of its involvement in the ruthenium coordination sphere. Nevertheless, results from this docking calculation (Figure 4) suggest that the interaction between the aromatase

protein and the inhibitor-containing ruthenium complex is energetically highly favorable.

The tritiated water-release assay was then selected to measure aromatase activity because it is a rapid and simple technique with high sensitivity and reproducibility.^{55,56} Given the low levels of aromatase in MCF7 cells,⁵⁷ human H295R adrenocortical carcinoma cells were selected for this study. Notably, H295R cells express numerous steroidogenic enzymes, including aromatase, making them very useful to examine compounds for their potential to interfere with the activity and/or expression of several key cytochrome P450 (CYP) enzymes involved in the biosynthesis of steroid hormones.^{58–60} Moreover, H295R cells were found to be less sensitive than MCF7 cells to the cytotoxicity of the ruthenium complexes we report here, allowing their use for this assay (Figure S4).

To determine the level of inhibition of the catalytic activity of aromatase in the presence of each complex (all complexes were studied for comparison purposes), H295R cells were coincubated with 1β -³H-androstenedione and each ruthenium complex for 1.5 h. Aromatase activity was assessed by quantifying the radioactivity of the tritium oxide produced from the aromatization reaction of the labeled androstenedione. Exposure of H295R cells to all complexes at concentrations greater than 1 nM resulted in a statistically significant, concentration-dependent reduction of aromatase activity (Figure 5), except for complex 4 (data not shown),

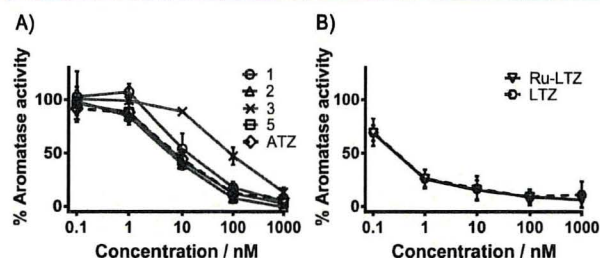


Figure 5. Effects of the exposure of H295R cells with (A) anastrozole (ATZ) (black dashed line), 1, 2, 3, and 5 and (B) letrozole (LTZ) (black dashed line) and Ru-LTZ on aromatase activity. Cells were treated for 1.5 h with the indicated concentrations of the compounds. Values represent the mean \pm SD. Significant differences for aromatase activity are reported relative to the controls. Significant differences ($p < 0.001$): $14 \pm 4\%$ for 1000 nM vs $34 \pm 7\%$ for ATZ at 40 nM; $47 \pm 3\%$ for 3 at 100 nM vs $74 \pm 3\%$ for ATZ at 4 nM (ATZ results obtained from interpolation).

confirming the crucial role of anastrozole in the structure of the ruthenium complex. The aromatase inhibitory activity observed for complexes 1, 2, 5, and Ru-LTZ was not significantly different from that of the corresponding aromatase inhibitor alone, an observation which is consistent with the considerable lability of the enzyme inhibitor ligands under these conditions (*vide supra*). Interestingly, complex 3 was found to be a less potent inhibitor of aromatase activity than anastrozole alone but to have a significantly higher activity than the free anastrozole levels expected from stability studies (Figure 5A). The observed activity for 3 suggests a supplementary contribution from the intact complex, as supported by docking studies (Figure 4), and/or an intracellular substitution of the anastrozole ligand. Notably, during this short period of incubation (1.5 h), a relatively high level of ruthenium in H295R cells treated with 3 was revealed by ICP-

MS (Figure S5), which confirms the internalization of the complex.

Over the past few years, the development of zebrafish embryos has become a prominent *in vivo* model for drug discovery and toxicity assessment because of their high degree of genetic conservation with humans, rapid embryogenesis, short reproductive cycle, high transparency, and low cost.^{63,64} Also, the zebrafish embryo assay has previously been reported to be a suitable phenotype-based screening method to assess the *in vivo* toxicity of ruthenium complexes.^{47,65–67} Because of their greater *in vitro* cytotoxicity in T47D cells compared to that of the currently used chemotherapeutic agent *cis*-platin, complexes 2 and 3 were selected for an *in vivo* toxicity assessment using the zebrafish embryo assay. Hatching rates, survival rates, and phenotype changes of the zebrafish embryos treated with $12.5 \mu\text{M}$ of each compound were determined at 24, 48, 72, and 96 h post fertilization (hpf) (Figure 6). Given

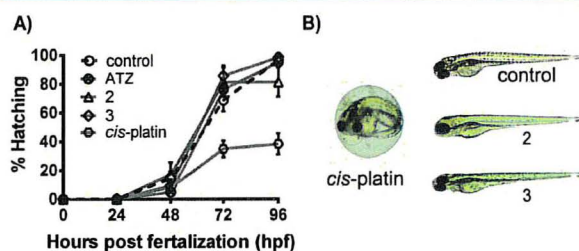


Figure 6. (A) Effect of 2, 3, anastrozole (ATZ), and *cis*-platin on the hatching rate of developing zebrafish embryos. Hatching rates were assessed at $12.5 \mu\text{M}$ over 4 days postfertilization (96 hpf). Control is shown as a black dashed line. (B) Gross morphological phenotypes in zebrafish embryos: untreated (control) and treated with $12.5 \mu\text{M}$ 2, 3, and *cis*-platin. Data are expressed as means \pm standard deviation from three independent experiments (a total of 60 embryos).

the poor solubility of the complexes in fish medium, concentrations higher than $12.5 \mu\text{M}$ were not tested. Specifically, *cis*-platin was more toxic to the embryos than the other compounds. Until 96 hpf, no significant mortality of zebrafish embryos was observed for any of the ruthenium complexes. However, a 72 h exposure to *cis*-platin dramatically decreased hatching rates, whereas no significant difference was observed between the hatching rate of embryos treated with complexes 2, 3, and anastrozole and that of nontreated embryos. Moreover, at 96 hpf, a significant number of phenotype abnormalities such as edema ($25\% \pm 5\%$) was detected in *cis*-platin treated embryos.

CONCLUSION

A series of ruthenium complexes bearing anastrozole ligands were prepared and characterized. Among these complexes, 3 was found to be the most stable in cell culture media and to lead to the highest cellular uptake in ER+ human breast cancer cells. In contrast to anastrozole alone, considerable *in vitro* cytotoxicity was observed in two ER+ human breast cancer cell lines (MCF7 and T47D) treated with 3. In addition, complex 3 was found to induce a decrease in aromatase activity in H295R cells. Exposure of zebrafish embryos to complex 3 ($12.5 \mu\text{M}$) did not lead to noticeable signs of toxicity over 96 h, making it a suitable candidate for further *in vivo* investigations. This study opens the door to the development of a novel class of anastrozole-containing organometallic

anticancer drug candidates with a broader spectrum of pharmacological activities.

EXPERIMENTAL SECTION

General Comments. All chemicals were obtained from commercial sources and were used as received. Anastrozole and letrozole were purchased from Triplebond and AK scientific, respectively. $\text{RuCl}_3 \cdot x\text{H}_2\text{O}$, ammonium tetrafluoroborate, sodium tetraphenylborate, triphenylphosphine, silver nitrate, hydrocortisone, and oxalic acid were purchased from Sigma-Aldrich. $[\text{Ru}(\eta^6\text{-C}_6\text{H}_6)_2\text{Cl}]_2$ dimer, silver oxalate, and Ru-LTZ were prepared from previously reported procedures.^{33,68,69} Experiments were performed under a nitrogen atmosphere, and solvents were dried using a solvent purification system (Pure Process Technology). All NMR spectra were recorded at room temperature on a 400 MHz (or 600 MHz) Varian spectrometer and were referenced to solvent resonances. Chemical shifts and coupling constants are reported in parts per million and Hertz, respectively. Mass spectral data was obtained from high-resolution and high accuracy mass analysis (HR-ESI-MS) using an Exactive Orbitrap spectrometer from ThermoFisher Scientific (Department of Chemistry, McGill University). A PerkinElmer Nexion 300X ICP mass spectrometer was used for the determination of ruthenium in biological samples (Department of Chemistry, Université de Montréal). The purity of all ruthenium complexes (>95%) was assessed by elemental analyses (Laboratoire d'Analyse Élémentaire, Department of Chemistry, Université de Montréal) and HPLC-MS, using a Waters 2795 separation module coupled to a Waters Micromass Quattro Premier XE tandem quadrupole mass spectrometer.

Complex Synthesis and Characterization. $[\text{Ru}(\eta^6\text{-C}_6\text{H}_6)(\eta^1\text{-ATZ})_2\text{Cl}]/\text{BF}_4$ **1**. Anastrozole (0.235 g, 0.80 mmol), $[\text{Ru}(\eta^6\text{-C}_6\text{H}_6)_2\text{Cl}]_2$ (0.100 g, 0.20 mmol), and NH_4BF_4 (0.104 g, 1.00 mmol) were dissolved in degassed ethanol (20 mL). The mixture was heated under reflux for 6 h, allowed to cool to room temperature, filtered, and the precipitate was washed with a minimum of ethanol. The filtrate was then collected and dried under vacuum. The residue was dissolved in dichloromethane (10 mL), filtered, and concentrated to a minimum. Compound **1** was precipitated with diethyl ether, washed with hexane, and dried under vacuum. The final product was obtained as a yellow powder (0.240 g, 68%). ^1H NMR (CDCl_3 , 400 MHz): δ 1.75 (d, $J = 4.9$ Hz, CH_3 , 24H), 5.40 (m, CH_2 , 4H), 5.9 (s, C_6H_6 , 6H), 7.43 (d, $J = 1.6$ Hz, ArH, 4H), 7.54 (t, $J = 1.5$ Hz, ArH, 2H), 8.27 (s, H_{triazole} , 2H), 9.35 (s, H_{triazole} , 2H). $^{13}\text{C}\{^1\text{H}\}$ NMR (CDCl_3 , 100 MHz): δ 28.8 (CH_3 , 8C), 37.3 (CCN, 4C), 54.2 (CH_2 , 2C), 85.5 (C_6H_6 , 6C), 122.3 (CHC_{Ar}, 2C), 124.0 (CN, 4C), 125.0 (CHC_{Ar}, 4C), 135.4 (C_{Ar}, 2C), 143.4 (C_{Ar}, 4C), 146.7 (C_{triazole}, 2C), 151.6 (C_{triazole}, 2C). Found (%): C, 54.65; H, 5.18; N, 16.05. $\text{C}_{40}\text{H}_{44}\text{B}_1\text{Cl}_1\text{F}_4\text{N}_{10}\text{Ru}_1 \cdot 1/16 \text{C}_6\text{H}_{14}$ requires C, 54.28; H, 5.06; N, 15.67. HR-ESI-MS m/z (+): found 801.25 M^+ ($[\text{Ru}(\eta^6\text{-C}_6\text{H}_6)(\eta^1\text{-ATZ})_2\text{Cl}]^+$) (calcd 801.25), 508.08 $[\text{M}^+ - \text{ATZ}]^+$ (calcd 508.08).

$[\text{Ru}(\eta^6\text{-C}_6\text{H}_6)(\eta^1\text{-ATZ})_2\text{Cl}]/\text{BPh}_4$ **2**. Degassed ethanol (20 mL) was added to anastrozole (0.235 g, 0.80 mmol), $[\text{Ru}(\eta^6\text{-C}_6\text{H}_6)_2\text{Cl}]_2$ (0.100 g, 0.20 mmol), and NaBPh_4 (0.342 g, 1.00 mmol). The mixture was heated under reflux for 6 h until a yellow precipitate appeared and was then cooled to room temperature and filtered. The precipitate was washed with a minimum amount of ethanol before being dissolved in acetone (5 mL). The resulting solution was filtered on a Celite pad, and the filtrate was concentrated under reduced pressure. Compound **2** was precipitated with diethyl ether, washed with hexane, and dried under vacuum. The final product was obtained as a yellow powder (0.270 g, 60%). ^1H NMR ($(\text{CD}_3)_2\text{CO}$, 400 MHz): δ 1.73 (s, CH_3 , 24H), 5.60 (m, CH_2 , 4H), 6.07 (s, C_6H_6 , 6H), 6.77 (t, $J = 7.2$ Hz, H_{BPh_4} , 4H), 6.91 (t, $J = 7.4$ Hz, H_{BPh_4} , 8H), 7.33 (m, H_{BPh_4} , 8H), 7.45 (d, $J = 1.7$ Hz, ArH, 4H), 7.67 (t, $J = 1.8$ Hz, ArH, 2H), 8.50 (s, H_{triazole} , 2H), 9.08 (s, H_{triazole} , 2H). $^{13}\text{C}\{^1\text{H}\}$ NMR ($(\text{CD}_3)_2\text{CO}$, 100 MHz): δ 28.1 (CH_3 , 8C), 37.2 (CCN, 4C), 53.6 (CH_2 , 2C), 85.3 (C_6H_6 , 6C), 121.3 (C_{BPh_4} , 4C), 122.0 (CHC_{Ar}, 2C), 123.8 (CN, 4C), 124.7 (CHC_{Ar}, 4C), 125.1 (C_{BPh_4} , 8C), 136.1 (C_{BPh_4} , 8C), 136.4 (C_{Ar}, 2C), 143.5 (C_{Ar}, 4C), 146.4 (C_{triazole}, 2C), 153.0

(C_{triazole}, 2C), 163.3 (C_{BPh4}, 4C). Found (%): C, 69.27; H, 6.13; N, 11.70. $\text{C}_{64}\text{H}_{64}\text{B}_1\text{Cl}_1\text{N}_{10}\text{Ru}_1 \cdot 1/2\text{C}_6\text{H}_{14}$ requires C, 69.16; H, 6.15; N, 12.03. HR-ESI-MS m/z (+): 801.25 M^+ ($[\text{Ru}(\eta^6\text{-C}_6\text{H}_6)(\eta^1\text{-ATZ})_2\text{Cl}]^+$) (calcd 801.25), 508.08 $[\text{M}^+ - \text{ATZ}]^+$ (calcd 508.08), 1922.66 $[2\text{M}^+ + \text{BPh}_4]^+$ (calcd 1922.66).

$[\text{Ru}(\eta^6\text{-C}_6\text{H}_6)(\eta^1\text{-ATZ})(\text{PPh}_3)\text{Cl}]/\text{BPh}_4$ **3**. Triphenylphosphine (0.032 g, 0.12 mmol) was added to a solution of **2** (0.112 g, 0.10 mmol) in acetone (8 mL), and the mixture was stirred at ambient temperature for 48 h. The solvent was then concentrated, and the product precipitated with diethyl ether. After the powder was washed with diethyl ether, compound **3** was collected as a yellow powder (0.081 g, 74%). ^1H NMR ($(\text{CD}_3)_2\text{CO}$, 400 MHz): δ 1.77 (s, CH_3 , 12H), 5.44 (m, CH_2 , 2H), 6.01 (s, C_6H_6 , 6H), 6.77 (t, $J = 7.2$ Hz, H_{BPh_4} , 4H), 6.91 (t, $J = 7.4$ Hz, H_{BPh_4} , 8H), 7.33 (m, H_{BPh_4} , 8H), 7.39–7.51 (m, H_{PPh_3} , 15H), 7.62 (d, $J = 1.8$ Hz, ArH, 2H), 7.75 (t, $J = 1.8$ Hz, ArH, 1H), 8.35 (s, H_{triazole} , 1H), 9.03 (s, H_{triazole} , 1H). $^{13}\text{C}\{^1\text{H}\}$ NMR ($(\text{CD}_3)_2\text{CO}$, 100 MHz): δ 28.2 (CH_3 , 4C), 37.2 (CCN, 2C), 53.5 (CH_2 , 1C), 90.7 (C_6H_6 , 6C), 121.3 (C_{BPh_4} , 4C), 122.3 (CHC_{Ar}, 1C), 123.9 (CN, 2C), 125.1 (C_{BPh_4} , 8C), 125.5 (CHC_{Ar}, 2C), 128.5 (C_{PPh3}), 128.6 (C_{PPh3}), 131.1 (C_{PPh3}), 133.7 (C_{PPh3}), 133.8 (C_{PPh3}), 135.9 (C_{Ar}, 1C), 136.1 (C_{BPh4}, 8C), 143.5 (C_{Ar}, 2C), 146.4 (C_{triazole}, 1C), 154.2 (C_{triazole}, 1C), 164.2 (C_{BPh4}, 4C). $^{31}\text{P}\{^1\text{H}\}$ NMR ($(\text{CD}_3)_2\text{CO}$, 200 MHz): δ 35.4. Found (%): C, 70.45; H, 5.45; N, 7.16. $\text{C}_{65}\text{H}_{60}\text{B}_1\text{Cl}_1\text{N}_3\text{P}_1\text{Ru}_1 \cdot \text{H}_2\text{O}$ requires C, 70.49; H, 5.64; N, 6.32. [Although the elemental analysis value of N is outside the range viewed as establishing analytical purity, it is provided to illustrate the best value obtained to date. NMR spectra are provided in the Supporting Information as evidence of bulk purity (Figures S6–S8).] HR-ESI-MS m/z (+): 770.17 M^+ ($[\text{Ru}(\eta^6\text{-C}_6\text{H}_6)(\eta^1\text{-ATZ})(\text{PPh}_3)\text{Cl}]^+$) (calcd 770.17).

$[\text{Ru}(\eta^6\text{-C}_6\text{H}_6)\text{oxalate}(\text{H}_2\text{O})]$ **4**. A mixture of silver oxalate (0.303 g, 1.00 mmol) and $[\text{Ru}(\eta^6\text{-C}_6\text{H}_6)_2\text{Cl}]_2$ (0.200 g, 0.40 mmol) was stirred in degassed water (60 mL) at ambient temperature for 24 h. The reaction mixture was filtered on a Celite pad and washed with water (30 mL), and the filtrate was dried under reduced pressure. After adding dichloromethane, the product precipitated as an orange powder (0.157 g, 65%). ^1H NMR (D_2O , 400 MHz): δ 5.75 (s, C_6H_6 , 6H). $^{13}\text{C}\{^1\text{H}\}$ NMR (D_2O , 100 MHz): δ 77.9 (C_6H_6 , 6C), 163.8 (C_{oxalate}, 2C). Found (%): C, 32.40; H, 2.58. $\text{C}_8\text{H}_8\text{O}_5\text{Ru}_1 \cdot 1/4\text{CH}_2\text{Cl}_2$ requires C, 32.34; H, 2.80. HR-ESI-MS m/z (-): 284.93 $[\text{M-H}]^-$ (calcd 284.93), 552.87 $[2\text{M-H}_2\text{O-H}]^-$ (calcd 552.86), 820.80 $[3\text{M}-2\text{H}_2\text{O-H}]^-$ (calcd 820.80).

$[\text{Ru}(\eta^6\text{-C}_6\text{H}_6)\text{oxalate}(\eta^1\text{-ATZ})]$ **5**. Silver oxalate (0.303 g, 1.00 mmol) was added to a solution of $[\text{Ru}(\eta^6\text{-C}_6\text{H}_6)_2\text{Cl}]_2$ (0.200 g, 0.40 mmol) in degassed water (60 mL), and the suspension was stirred at ambient temperature for 24 h. The reaction mixture was filtered on a Celite pad, washed with water (30 mL), and the filtrate was dried under reduced pressure. The resulting intermediate was dissolved in ethanol (60 mL), and anastrozole (0.469 g, 1.60 mmol) was added to the solution. The mixture was then heated under reflux for 24 h. The reaction mixture was concentrated under reduced pressure to dryness, and the product was purified by column chromatography (silica gel) using dichloromethane/methanol (7:1 v/v). Compound **5** was obtained as a light yellow powder (0.235 g, 52%). ^1H NMR (CD_3OD , 400 MHz): δ 1.71 (s, CH_3 , 12H), 5.54 (s, CH_2 , 2H), 5.88 (s, C_6H_6 , 6H), 7.44 (d, $J = 1.8$ Hz, ArH, 2H), 7.64 (t, $J = 1.8$ Hz, ArH, 1H), 8.21 (s, H_{triazole} , 1H), 8.88 (s, H_{triazole} , 1H). $^{13}\text{C}\{^1\text{H}\}$ NMR ($(\text{CD}_3)_2\text{CO}$, 100 MHz): δ 27.7 (CH_3 , 4C), 37.2 (CCN, 2C), 53.4 (CH_2 , 1C), 82.5 (C_6H_6 , 6C), 122.1 (CHC_{Ar}, 1C), 123.7 (CN, 2C), 124.3 (CHC_{Ar}, 2C), 136.2 (C_{Ar}, 1C), 143.5 (C_{Ar}, 2C), 145.2 (C_{triazole}, 1C), 151.7 (C_{triazole}, 1C), 165.7 (C_{oxalate}, 2C). Found (%): C, 52.76; H, 4.62; N, 12.16. $\text{C}_{25}\text{H}_{25}\text{N}_5\text{O}_5\text{Ru}_1 \cdot 1/8\text{CH}_2\text{Cl}_2$ requires C, 52.84; H, 4.46; N, 12.26. HR-ESI-MS m/z (+): 584.08 $[\text{M} + \text{Na}]^+$ (calcd 584.08), 852.01 $[2\text{M} - \text{ATZ} + \text{Na}]^+$ (calcd 852.01), 1145.18 $[2\text{M} + \text{Na}]^+$ (calcd 1145.18).

Solubility in DMSO/Media. UV–vis spectroscopy was used to evaluate the solubility of the ruthenium complexes. Accordingly, a 2 mL solution of each complex was prepared in full RMPI growth media (phenol red free) at the concentrations used for cellular proliferation studies (DMSO final concentration: 0.5%). After incubation for 48 h

at 37 °C, the solution was filtered on a Celite pad, and the absorbance was recorded using a Cary 300 Bio UV-vis spectrometer. The concentration of saturation of the complexes in growth media was assessed by determining the concentration at which a maximum intensity in UV absorbance (274–278 nm) was observed.

X-ray Diffraction. Four ruthenium(II) complexes were structurally characterized by single-crystal X-ray analysis. Suitable crystals were obtained by slow evaporation of the solutions of compounds 2, 3, 4, and 5 in ethanol/acetone, acetone/diethyl ether, water, and methanol, respectively. Data were collected at 100 K using a Bruker Smart APEX diffractometer. Structures were solved with the XT structure solution program and refined with the XL refinement package using least squares minimizations.^{70–72}

Cell Culture. Protocols used for biological studies were approved by the Institutional Research Ethics Committee of INRS - Institut Armand-Frappier. Estrogen receptor positive (ER+) breast cancer cells MCF7 and T47D were respectively provided by Prof. Chatenet and Prof. Plante (INRS). The H295R human adrenocortical carcinoma cell line that expresses CYP19 (aromatase)⁵⁹ were obtained from Prof. Sanderson's collection (INRS). Human MCF7 breast cancer cells were grown in RPMI 1640 containing fetal bovine serum (10%). The growth medium for T47D breast cancer cells was RPMI 1640 supplemented with HEPES (2.38 g/L), sodium pyruvate (0.11 g/L), glucose (2.5 g/L), insulin bovine (10 µg/mL), and fetal bovine serum (10%). H295R cells were cultured in DMEM/F-12 supplemented with Nu Serum (2.5%) and ITS (1%). All growth media were supplemented with penicillin/streptomycin. All cell culture products were obtained from commercial sources, including Gibco, Sigma-Aldrich, Corning, and Invitrogen.

Cytotoxicity. Cell viability was examined by slightly modified standard methods using the SRB colorimetric assay described by Vichai and Kirtikara.⁷³ Briefly, for all experiments, cells were seeded in 96-well plates (Sarstedt) at a density of 1×10^4 cells/well (MCF7 and T47D) or 3×10^4 cells/well (H295R) maintained at 37 °C, 5% CO₂ in a humidified atmosphere and were grown in serum-containing media for 24 h before treatment. Stock solutions of the compounds were prepared in DMSO, and the final concentration of DMSO was kept constant (nontoxic concentration) depending on the cell line: 0.5% for MCF-7 and T47D and 0.25% for H295R. To reach final concentrations of 1, 4, 12.5, 25, 50, 100, and 150 µM, 1 µL (or 0.5 µL) of each stock solution (200 or 400 times more concentrated than the corresponding final concentration) was added to each well containing 200 µL of fresh and complete growth medium. Also, cancer cells were exposed to complete growth medium alone, growth medium containing 0.5% or 0.25% DMSO (negative control), and growth medium containing 25% DMSO (positive control). After incubation for 48 h, without removing the cell culture supernatant, cells in each well were fixed with 100 µL of cold trichloroacetic acid (TCA) 10% w/v at 4 °C for 1 h. After fixation, TCA was discarded, and wells were washed four times with slow-running tap water and then air-dried. An SRB solution (0.057% w/v) was added to the wells, and plates were kept for 30 min at room temperature. Unbound SRB was removed by washing the wells four times with 1% acetic acid. Plates were air-dried. To dissolve the protein-bound dye, cells from each well were exposed to 200 µL of 10 mM Tris base solution (pH 10.5) for 30 min. Absorbance was measured at 510 nm using a microplate reader. The viability of the cancer cells versus different concentrations of each complex was reported. This assay was carried out in two or three independent sets of experiments, each experiment with four or five replicates per concentration level.

Stability in DMSO/Water. Stock solutions of the test compounds in DMSO (150 µL) were diluted with distilled water (40 mL) to give a final concentration of 150 µM (maximum DMSO content did not exceed 0.5%). After incubation of the samples for 48 h at 37 °C, solutions were dried by vacuum. An NMR sample of each compound was prepared in an appropriate deuterated solvent (the same solvents as the ones used for ¹H NMR characterizations) in which both the complex and the aromatase inhibitor were highly soluble. For each complex, the percentage of released aromatase inhibitor was calculated by comparing the signal intensity of one of the protons

of anastrozole or letrozole with that of corresponding signal in the ¹H NMR spectrum of their complex. This experiment was done in triplicate.

Stability in DMSO/Media. A HPLC-UV method was developed and consisted of a simple liquid/liquid extraction after incubation of the complexes in media. The method was found to be reproducible and linear over the range of concentrations used for the aromatase activity assessment. **Preparation of standards.** Solutions of anastrozole (or letrozole) in 20 mL of phenol red free DMEM/F-12 at 0.1, 1, 5, 10, and 15 µM (DMSO final concentration: 0.1%) were incubated at 37 °C for 1.5 h (conditions used for the tritiated water-release assay). After incubation, anastrozole or letrozole was retrieved from the media solution by liquid/liquid extraction using diethyl ether (3 × 10 mL), which has previously been reported as an adequate solvent to recover anastrozole from human plasma.⁷⁴ The diethyl ether solution was then dried under vacuum, and the residue was dissolved in 2 mL of acetone and loaded on a thin layer of silica. Acetone (20 mL) was used as a mobile phase to completely recover anastrozole (or letrozole) from silica and minimize the amount of media residue in the final HPLC samples. Final HPLC samples were prepared by evaporating the acetone solution to dryness and dissolving the residue in 1 mL of HPLC grade acetone containing 100 µM hydrocortisone as an external standard. Standard curves of anastrozole and letrozole are shown in Figure S1. **HPLC-UV method.** The chromatography was performed on an Agilent UHPLC system (1260 Infinity GPC/SEC). An Agilent Poroshell 120 EC-C18 column (4.6 × 100 mm, 2.7 µm) was used, and the column temperature was maintained at room temperature. Chromatographic separation was obtained through a 13 min gradient delivery of a mixture of acetonitrile and water at a flow rate of 2 mL/min: (a) 0–1 min, water, 100%; (b) 1–4 min, acetonitrile, 0–30%; (c) 4–10 min, acetonitrile, 30%; (d) 10–11 min, acetonitrile, 30%–100%; (e) 11–13 min, acetonitrile, 100%. UV absorbance at both 254 and 215 nm was recorded, but only the data acquired at 215 nm was used. **Sample preparation.** Stock solutions (10⁴ µM) of anastrozole, letrozole and all complexes (except 4, which has no aromatase inhibitor ligand) were prepared in DMSO. The 10 µM solutions of the compounds were prepared by adding 20 µL of a stock solution to 20 µL of DMEM/F12 (DMSO final concentration: 0.1%). Solutions were incubated at 37 °C for 1.5 h, and further steps were as described for the standards' preparation. The experiment was carried out in triplicate.

Antimigratory Activity. MCF7 cells were cultured in RPMI 1640 supplemented with 10% FBS and penicillin-streptomycin. 100 000 cells/well were seeded in 24 well plates (Sarstedt) and incubated at 37 °C and 5% CO₂ to reach confluency. Scratches were created using a pipet tip on the confluent monolayer and washed with full growth medium (1 × 500 µL) to remove cellular debris. The fresh medium (500 µL) supplemented with 0.5% FBS containing 10 µM of the synthesized complexes (except compound 3 which was cytotoxic at 10 µM) was individually added into each well and incubated for 48 h to allow the wound closure. The RPMI-1640 medium containing 0.5% FBS and 0.1% DMSO (vehicle) was used as a control. The migration of the treated and untreated cells (vehicle) into the wound area at incubation 0 and 48 h were compared by capturing the images with a Nikon Eclipse Ti microscope (equipped with a Nikon DS-Ri2 camera) at 10× magnification. Cell migration was analyzed using ImageJ software and the MRI wound healing tool plugin (NIH, Bethesda, MD) and computed into a percentage of control (means ± SEM; n = 8) using untreated wells at 100%.

Cellular Uptake. MCF7 cells were grown in 6-well plates (200 000 cells/well) and incubated for 24 h. Stock solutions (20 mM) of the complexes in DMSO were freshly prepared and diluted with cell culture medium to the desired concentration, for which no cytotoxicity was expected to maintain nearly complete cell survival (final complex concentration was 4 µM, except compound 3, which was tested at four concentrations: 1, 4, 12.5, and 25 µM). The cell culture medium of each well was replaced with 2 mL of the cell culture medium solutions containing the complexes, and the plates were incubated at 37 °C under 5% CO₂ for 48 h. The culture medium was removed, and the cell layer of each well was washed with 2 mL of

phosphate buffered saline (PBS). Then cells in each well were trypsinized (300 μL) and resuspended in 1700 μL of growth media. The number of cells in each well was counted, and cell pellets were isolated by centrifugation (3000g for 10 min at room temperature). Each pellet was digested for 3 days at room temperature in HNO_3 (70%, Sigma-Aldrich), and the resulting solutions were diluted to 25 mL using Milli-Q water (final concentration of 2.8% nitric acid). The amount of Ru cellular uptake was evaluated by ICP-MS. The experiment was carried out in triplicate.

Aromatase Inhibition. The H295R cell line was selected for this study because it expresses CYP19 enzyme, making it a suitable model for the study of aromatase activity.⁵⁸ Aromatase activity was measured using a tritiated water-release assay as described previously.^{59,75} Briefly, H295R cells were cultured in 24-well plates (100 000 cells/well) containing 1 mL of the appropriate culture medium. After 24 h, the medium was removed and cells were washed once with 500 μL PBS. Then, a volume of 250 μL of culture medium containing 54 nM $1\beta\text{-}^3\text{H}$ -androstenedione and different concentrations of anastrozole, letrozole, or each complex (0.1, 1, 10, 100, and 1000 nM) was added to each well, and cells were incubated for 1.5 h at 37°C (5% CO_2). Further steps were as described previously.⁵⁹ Tritiated water was counted in 24-well plates containing a liquid scintillation cocktail using a Microbeta Trilux (PerkinElmer, Waltham, MA). Incubations in the absence of cells (blanks) and in the presence of DMSO 0.1% (which was the concentration used to dissolve the complexes in the growth media for this study) were included as negative and positive controls, respectively.

Virtual Docking of Compound 3 with the Human Aromatase Enzyme. Formation of the ternary complex between human aromatase, compound 3, and the heme group was simulated using a ligand-imprinted docking procedure.¹² A Nelder–Mead simplex iteration was applied during the energy minimization steps, and the steric interactions, hydrogen bonding, and electrostatic forces were calculated by piecewise linear potentials and Coulomb potentials, respectively.¹³ The crystal structure of 3 was generated with the XT structure solution program and refined with the XL refinement package using least squares minimization against the crystallographically resolved aromatase template (PDB entry 5JI6).⁶¹ The MolDock scoring function was used in combination with a cavity prediction algorithm using the Molegro Virtual Docker 6.0 suite without the inclusion of water molecules.¹³ Twenty rounds of docking simulations were performed to maintain search robustness, with the best conformations emerging from a group of up to 4 000 000 combinations.

Zebrafish Embryo Assay. Wild-type zebrafish (*Danio rerio*) embryos were raised at 28.5 °C and staged as previously described.⁷⁶ Embryos at the 4-cell stage were separately exposed to 2, 3, anastrozole, and *cis*-platin solutions (12.5 μM), prepared by diluting the DMSO stock solution of each compound in the fish medium (DMSO final concentration = 0.1%). The medium (containing the compound to be tested) was refreshed after 48 h for each experiment. A no-treatment control was also included. Experiments were performed in triplicate, and a total of 60 embryos from the pooling of three different crosses have been used per each treatment. The mortality, gross morphology, and hatching rates of the embryos in each system were observed every 24 h for a period of 96 h under a stereo microscope (Leika S6E). Zebrafish experiments were performed following a protocol approved by the Canadian Council for Animal Care (CCAC) and our local animal care committee.

■ ASSOCIATED CONTENT

● Supporting Information

The Supporting Information is available free of charge on the ACS Publications website at DOI: 10.1021/acs.organo- met.8b00897.

(PDF)

■ Accession Codes

CCDC 1840870–1840873 contain the supplementary crystallographic data for this paper. These data can be obtained free of charge via www.ccdc.cam.ac.uk/data_request/cif, or by emailing data_request@ccdc.cam.ac.uk, or by contacting The Cambridge Crystallographic Data Centre, 12 Union Road, Cambridge CB2 1EZ, UK; fax: +44 1223 336033.

■ AUTHOR INFORMATION

ORCID

Annie Castonguay: 0000-0001-5705-6353

Notes

The authors declare no competing financial interest.

■ ACKNOWLEDGMENTS

This work was supported by the Institut National de la Recherche Scientifique (INRS), the Natural Sciences and Engineering Research Council of Canada (NSERC) (A.C., J.T.S., and N.D.), the Fonds de Recherche en Santé (FRQS) (A.C., S.A.P., and N.D.), the Canadian Institutes of Health Research (CIHR) (S.A.P.), the Canada Foundation for Innovation (CFI) (A.C., S.A.P., and N.D.), Mitacs (scholarship to Y.L.d.l.S.), the National Institutes of Health (NIH) (N.D.), and the Armand-Frappier Foundation (scholarships to G.G. and Y.L.d.l.S.). We would like to thank Prof. David Chatenet and Prof. Isabelle Plante for providing the human cancer cell lines used in this study. We would also like to thank Prof. Charles Ramassamy and Prof. Géraldine Delbès for providing access to some of their instruments.

■ REFERENCES

- (1) Vessières, A.; Top, S.; Beck, W.; Hillard, E.; Jaouen, G. Metal complex SERMs (selective oestrogen receptor modulators). The influence of different metal units on breast cancer cell antiproliferative effects. *Dalton Trans.* **2006**, *4*, 529–541.
- (2) Mandal, P.; Kundu, B. K.; Vyas, K.; Sabu, V.; Helen, A.; Dhankhar, S. S.; Nagaraja, C. M.; Bhattacharjee, D.; Bhabak, K. P.; Mukhopadhyay, S. Ruthenium(II) arene NSAID complexes: inhibition of cyclooxygenase and antiproliferative activity against cancer cell lines. *Dalton Trans.* **2018**, *47*, 517–527.
- (3) Li, P.; Su, W.; Lei, X.; Xiao, Q.; Huang, S. Synthesis, characterization and anticancer activity of a series of curcuminoids and their half-sandwich ruthenium(II) complexes. *Appl. Organomet. Chem.* **2017**, *31*, No. e3685.
- (4) Vasaitis, T. S.; Bruno, R. D.; Njar, V. C. O. CYP17 inhibitors for prostate cancer therapy. *J. Steroid Biochem. Mol. Biol.* **2011**, *125*, 23–31.
- (5) Carpenter, R.; Miller, W. R. Role of aromatase inhibitors in breast cancer. *Br. J. Cancer* **2005**, *93*, S1–S5.
- (6) Dikmen, Z. G.; Gellert, G. C.; Jackson, S.; Gryaznov, S.; Tressler, R.; Dogan, P.; Wright, W. E.; Shay, J. W. *In vivo* Inhibition of Lung Cancer by GRN163L: A Novel Human Telomerase Inhibitor. *Cancer Res.* **2005**, *65*, 7866–7873.
- (7) Meggers, E.; Atilla-Gokcumen, G. E.; Bregman, H.; Maksimoska, J.; Mulcahy, S. P.; Pagano, N.; Williams, D. S. Exploring Chemical Space with Organometallics: Ruthenium Complexes as Protein Kinase Inhibitors. *Synlett* **2007**, *2007* (8), 1177–1189.
- (8) Mulcahy, S. P.; Meggers, E. Organometallics as Structural Scaffolds for Enzyme Inhibitor Design. In *Medicinal Organometallic Chemistry*, 1st ed.; Jaouen, G., Metzler-Nolte, N., Eds.; Springer: Heidelberg, 2010; pp 141–153.
- (9) Kilpin, K. J.; Dyson, P. J. Enzyme inhibition by metal complexes: concepts, strategies and applications. *Chem. Sci.* **2013**, *4*, 1410–1419.
- (10) Anstaett, P.; Gasser, G. Organometallic Complexes as Enzyme Inhibitors: A Conceptual Overview. In *Bioorganometallic Chemistry*,

- 1st ed.; Jaouen, G., Salmain, M., Eds.; Wiley: Weinheim, 2014; pp 1–42.
- (11) Zamora, A.; Denning, C. A.; Heidary, D. K.; Wachter, E.; Nease, L. A.; Ruiz, J.; Glazer, E. C. Ruthenium-containing P450 inhibitors for dual enzyme inhibition and DNA damage. *Dalton Trans.* **2017**, *46*, 2165–2173.
- (12) Siiteri, P. K.; Thompson, E. A. Studies of human placental aromatase. *J. Steroid Biochem.* **1975**, *6*, 317–322.
- (13) Huang, W.-Y.; Newman, B.; Millikan, R. C.; Schell, M. J.; Hulka, B. S.; Moorman, P. G. Hormone-related Factors and Risk of Breast Cancer in Relation to Estrogen Receptor and Progesterone Receptor Status. *Am. J. Epidemiol.* **2000**, *151*, 703–714.
- (14) Osborne, C. K. Steroid hormone receptors in breast cancer management. *Breast Cancer Res. Treat.* **1998**, *51*, 227–238.
- (15) Simpson, E.; Rubin, G.; Clyne, C.; Robertson, K.; O'Donnell, L.; Jones, M.; Davis, S. The Role of Local Estrogen Biosynthesis in Males and Females. *Trends Endocrinol. Metab.* **2000**, *11*, 184–188.
- (16) Junko, Y.; Takara, Y.; Hiroji, O. Aromatization of androstenedione by normal and neoplastic endometrium of the uterus. *J. Steroid Biochem.* **1985**, *22*, 63–66.
- (17) Watanabe, K.; Sasano, H.; Harada, N.; Ozaki, M.; Niikura, H.; Sato, S.; Yajima, A. Aromatase in human endometrial carcinoma and hyperplasia. Immunohistochemical, in situ hybridization, and biochemical studies. *Am. J. Pathol.* **1995**, *146*, 491–500.
- (18) Brueggemeier, R. W.; Hackett, J. C.; Diaz-Cruz, E. S. Aromatase Inhibitors in the Treatment of Breast Cancer. *Endocr. Rev.* **2005**, *26*, 331–345.
- (19) Jeselsohn, R.; Bergholz, J. S.; Pun, M.; Cornwell, M.; Liu, W.; Nardone, A.; Xiao, T.; Li, W.; Qiu, X.; Buchwalter, G.; Feiglin, A.; Abell-Hart, K.; Fei, T.; Rao, P.; Long, H.; Kwiatkowski, N.; Zhang, T.; Gray, N.; Melchers, D.; Houtman, R.; Liu, X. S.; Cohen, O.; Wagle, N.; Winer, E. P.; Zhao, J.; Brown, M. Allele-Specific Chromatin Recruitment and Therapeutic Vulnerabilities of ESR1 Activating Mutations. *Cancer Cell* **2018**, *33*, 173–186.
- (20) O'Neill, M.; Paulin, F. E. M.; Vendrell, J.; Ali, C. W.; Thompson, A. M. The aromatase inhibitor letrozole enhances the effect of doxorubicin and docetaxel in an MCF7 cell line model. *BioDiscovery* **2012**, *6*, No. e8940.
- (21) Miranda, A. A.; Limon, J.; Medina, F. L.; Arce, C.; Zinser, J. W.; Rocha, E. B.; Villarreal-Garza, C. M. Combination treatment with aromatase inhibitor and capecitabine as first- or second-line treatment in metastatic breast cancer. *J. Clin. Oncol.* **2012**, *30*, No. e11016.
- (22) Prachayasittikul, V.; Pingaew, R.; Nantasenamat, C.; Prachayasittikul, S.; Ruchirawat, S.; Prachayasittikul, V. Investigation of aromatase inhibitory activity of metal complexes of 8-hydroxyquinoline and uracil derivatives. *Drug Des., Dev. Ther.* **2014**, *8*, 1089–1096.
- (23) Sinthupoom, N.; Prachayasittikul, V.; Pingaew, R.; Worachartcheewan, A.; Prachayasittikul, S.; Ruchirawat, S.; Prachayasittikul, V. Copper Complexes of 8-Aminoquinoline and Uracils as Novel Aromatase Inhibitors. *Letts. Drug Des. Discovery* **2017**, *14*, 880–884.
- (24) Yuan, R.-X.; Xiong, R.-G.; Abrahams, B. F.; Lee, G.-H.; Peng, S.-M.; Che, C.-M.; You, X.-Z. A Cu(I) coordination polymer employing a nonsteroidal aromatase inhibitor letrozole as a building block. *Dalton Trans.* **2001**, *14*, 2071–2073.
- (25) Tang, Y.-Z.; Zhou, M.; Huang, J.; Cao, Z.; Qi, T.-T.; Huang, G.-H.; Wen, H.-R. Synthesis, Crystal Structure, and Characterization of three New Letrozole Complexes. *Z. Anorg. Allg. Chem.* **2012**, *638*, 372–376.
- (26) Tran, M. T. Q.; Furger, E.; Alberto, R. Two-step activation prodrugs: transplatin mediated binding of chemotherapeutic agents to vitamin B12. *Org. Biomol. Chem.* **2013**, *11*, 3247–3254.
- (27) Aird, R. E.; Cummings, J.; Ritchie, A. A.; Muir, M.; Morris, R. E.; Chen, H.; Sadler, P. J.; Jodrell, D. I. *In vitro* and *in vivo* activity and cross resistance profiles of novel ruthenium (II) organometallic arene complexes in human ovarian cancer. *Br. J. Cancer* **2002**, *86*, 1652.
- (28) Guerriero, A.; Oberhauser, W.; Riedel, T.; Peruzzini, M.; Dyson, P. J.; Gonsalvi, L. New Class of Half-Sandwich Ruthenium(II) Arene Complexes Bearing the Water-Soluble CAP Ligand as an *In Vitro* Anticancer Agent. *Inorg. Chem.* **2017**, *56*, 5514–5518.
- (29) Scolaro, C.; Bergamo, A.; Brescacin, L.; Delfino, R.; Cocchietto, M.; Laurenczy, G.; Geldbach, T. J.; Sava, G.; Dyson, P. J. *In Vitro* and *In Vivo* Evaluation of Ruthenium(II)–Arene PTA Complexes. *J. Med. Chem.* **2005**, *48*, 4161–4171.
- (30) Gasser, G.; Ott, I.; Metzler-Nolte, N. Organometallic Anticancer Compounds. *J. Med. Chem.* **2011**, *54*, 3–25.
- (31) Zhang, P.; Sadler, P. J. Advances in the design of organometallic anticancer complexes. *J. Organomet. Chem.* **2017**, *839*, 5–14.
- (32) Gasser, G.; Metzler-Nolte, N. The potential of organometallic complexes in medicinal chemistry. *Curr. Opin. Chem. Biol.* **2012**, *16*, 84–91.
- (33) Castonguay, A.; Doucet, C.; Juhas, M.; Maysinger, D. New Ruthenium(II)–Letrozole Complexes as Anticancer Therapeutics. *J. Med. Chem.* **2012**, *55*, 8799–8806.
- (34) Zhou, W.; Wang, X.; Hu, M.; Zhu, C.; Guo, Z. A mitochondrion-targeting copper complex exhibits potent cytotoxicity against cisplatin-resistant tumor cells through multiple mechanisms of action. *Chem. Sci.* **2014**, *5*, 2761–2770.
- (35) Lee, M. H.; Han, J. H.; Lee, J.-H.; Choi, H. G.; Kang, C.; Kim, J. S. Mitochondrial Thioredoxin-Responding Off–On Fluorescent Probe. *J. Am. Chem. Soc.* **2012**, *134*, 17314–17319.
- (36) Han, M.; Vakili, M. R.; Soleymani Abyaneh, H.; Molavi, O.; Lai, R.; Lavasanifar, A. Mitochondrial Delivery of Doxorubicin via Triphenylphosphine Modification for Overcoming Drug Resistance in MDA-MB-435/DOX Cells. *Mol. Pharmaceutics* **2014**, *11*, 2640–2649.
- (37) Sáez, R.; Lorenzo, J.; Prieto, M. J.; Font-Bardia, M.; Calvet, T.; Omeñaca, N.; Vilaseca, M.; Moreno, V. Influence of PPh₃ moiety in the anticancer activity of new organometallic ruthenium complexes. *J. Inorg. Biochem.* **2014**, *136*, 1–12.
- (38) Di, L.; Fish, P. V.; Mano, T. Bridging solubility between drug discovery and development. *Drug Discovery Today* **2012**, *17*, 486–495.
- (39) Ang, W. H.; Daldini, E.; Scolaro, C.; Scopelliti, R.; Juillerat-Jeannerat, L.; Dyson, P. J. Development of Organometallic Ruthenium–Arene Anticancer Drugs That Resist Hydrolysis. *Inorg. Chem.* **2006**, *45*, 9006–9013.
- (40) Sengupta, P.; Ghosh, S.; Mak, T. C. W. A new route for the synthesis of bis(pyridine dicarboxylato)bis(triphenylphosphine) complexes of ruthenium(II) and X-ray structural characterisation of the biologically active trans-[Ru(PPh₃)₂(L¹H)₂] (L¹H₂=pyridine 2,3-dicarboxylic acid). *Polyhedron* **2001**, *20*, 975–980.
- (41) Bhalla, R.; Boxwell, C. J.; Duckett, S. B.; Dyson, P. J.; Humphrey, D. G.; Steed, J. W.; Suman, P. Chemical, Electrochemical, and Structural Aspects of the Ruthenium Complexes Ru(η⁶-arene)Cl₂(P) (Where Arene = Benzene, [2.2]Paracyclophane and P = Triphenylphosphine, rac-[2.2]Paracyclophanylphosphine). *Organometallics* **2002**, *21*, 924–928.
- (42) Dharmaraj, N.; Viswanathamurthi, P.; Natarajan, K. Ruthenium(II) complexes containing bidentate Schiff bases and their antifungal activity. *Transition Met. Chem.* **2001**, *26*, 105–109.
- (43) Habtemariam, A.; Melchart, M.; Fernández, R.; Parsons, S.; Oswald, I. D. H.; Parkin, A.; Fabbiani, F. P. A.; Davidson, J. E.; Dawson, A.; Aird, R. E.; Jodrell, D. I.; Sadler, P. J. Structure–Activity Relationships for Cytotoxic Ruthenium(II) Arene Complexes Containing N,N-, N,O-, and O,O-Chelating Ligands. *J. Med. Chem.* **2006**, *49*, 6858–6868.
- (44) Patra, M.; Joshi, T.; Pierroz, V.; Ingram, K.; Kaiser, M.; Ferrari, S.; Spingler, B.; Keiser, J.; Gasser, G. DMSO-Mediated Ligand Dissociation: Renaissance for Biological Activity of N-Heterocyclic-[Ru(η⁶-arene)Cl₂] Drug Candidates. *Chem. - Eur. J.* **2013**, *19*, 14768–14772.
- (45) Renfrew, A. K.; Phillips, A. D.; Egger, A. E.; Hartinger, C. G.; Bosquain, S. S.; Nazarov, A. A.; Keppler, B. K.; Gonsalvi, L.; Peruzzini, M.; Dyson, P. J. Influence of Structural Variation on the Anticancer Activity of RAPTA-Type Complexes: ptn versus pta. *Organometallics* **2009**, *28*, 1165–1172.

- (46) Ang, W. H.; Khalaila, I.; Allardyce, C. S.; Juillerat-Jeanneret, L.; Dyson, P. J. Rational Design of Platinum(IV) Compounds to Overcome Glutathione-S-Transferase Mediated Drug Resistance. *J. Am. Chem. Soc.* **2005**, *127*, 1382–1383.
- (47) Haghdoost, M.; Golbaghi, G.; Létourneau, M.; Patten, S. A.; Castonguay, A. Lipophilicity-antiproliferative activity relationship study leads to the preparation of a ruthenium(II) arene complex with considerable *in vitro* cytotoxicity against cancer cells and a lower *in vivo* toxicity in zebrafish embryos than clinically approved cis-platin. *Eur. J. Med. Chem.* **2017**, *132*, 282–293.
- (48) Loughrey, B. T.; Healy, P. C.; Parsons, P. G.; Williams, M. L. Selective Cytotoxic Ru(II) Arene Cp* Complex Salts [R-PhRuCp*]⁺X⁻ for X = BF₄⁻, PF₆⁻, and BPh₄⁻. *Inorg. Chem.* **2008**, *47*, 8589–8591.
- (49) Bergamo, A.; Sava, G. Linking the future of anticancer metal-complexes to the therapy of tumour metastases. *Chem. Soc. Rev.* **2015**, *44*, 8818–8835.
- (50) Zhao, J.; Zhang, D.; Hua, W.; Li, W.; Xu, G.; Gou, S. Anticancer Activity of Bifunctional Organometallic Ru(II) Arene Complexes Containing a 7-Hydroxycoumarin Group. *Organometallics* **2018**, *37*, 441–447.
- (51) Liu, Y.; Agrawal, N. J.; Radhakrishnan, R. A flexible-protein molecular docking study of the binding of ruthenium complex compounds to PIM1, GSK-3 β , and CDK2/Cyclin A protein kinases. *J. Mol. Model.* **2013**, *19*, 371–382.
- (52) Huang, H.-L.; Tang, B.; Yi, Q.-Y.; Wan, D.; Yang, L.-L.; Liu, Y.-J. Synthesis, DNA-binding, molecular docking and cytotoxic activity *in vitro* evaluation of ruthenium(II) complexes. *Transition Met. Chem.* **2018**, 1–14.
- (53) Hong, Y.; Li, H.; Yuan, Y.-C.; Chen, S. Molecular Characterization of Aromatase. *Ann. N. Y. Acad. Sci.* **2009**, *1155*, 112–120.
- (54) Maurelli, S.; Chiesa, M.; Giamello, E.; Di Nardo, G.; V. Ferrero, V. E.; Gilardi, G.; Van Doorslaer, S. Direct spectroscopic evidence for binding of anastrozole to the iron heme of human aromatase. Peering into the mechanism of aromatase inhibition. *Chem. Commun. (Cambridge, U. K.)* **2011**, *47*, 10737–10739.
- (55) Weisz, J. *In vitro* assays of aromatase and their role in studies of estrogen formation in target tissues. *Cancer Res.* **1982**, *42*, 3295s–3298s.
- (56) Lephart, E. D.; Simpson, E. R. Assay of aromatase activity. *Methods Enzymol.* **1991**, *206*, 477–483.
- (57) Sanderson, J. T.; Letcher, R. J.; Heneweer, M.; Giesy, J. P.; van den Berg, M. Effects of chloro-s-triazine herbicides and metabolites on aromatase activity in various human cell lines and on vitellogenin production in male carp hepatocytes. *Environ. Health Perspect.* **2001**, *109*, 1027–1031.
- (58) Caron-Beaudoin, E.; Denison, M. S.; Sanderson, J. T. Effects of Neonicotinoids on Promoter-Specific Expression and Activity of Aromatase (CYP19) in Human Adrenocortical Carcinoma (H295R) and Primary Umbilical Vein Endothelial (HUVEC) Cells. *Toxicol. Sci.* **2016**, *149*, 134–44.
- (59) Sanderson, J. T.; Seinen, W.; Giesy, J. P.; van den Berg, M. 2-Chloro-s-triazine herbicides induce aromatase (CYP19) activity in H295R human adrenocortical carcinoma cells: a novel mechanism for estrogenicity? *Toxicol. Sci.* **2000**, *54*, 121–7.
- (60) Sanderson, J. T.; Boerma, J.; Lansbergen, G. W. A.; van den Berg, M. Induction and Inhibition of Aromatase (CYP19) Activity by Various Classes of Pesticides in H295R Human Adrenocortical Carcinoma Cells. *Toxicol. Appl. Pharmacol.* **2002**, *182*, 44–54.
- (61) Ghosh, D.; Egbuta, C.; Lo, J. Testosterone complex and non-steroidal ligands of human aromatase. *J. Steroid Biochem. Mol. Biol.* **2018**, *181*, 11–19.
- (62) Kyte, J.; Doolittle, R. F. A simple method for displaying the hydropathic character of a protein. *J. Mol. Biol.* **1982**, *157*, 105–132.
- (63) Mandrekar, N.; Thakur, N. L. Significance of the zebrafish model in the discovery of bioactive molecules from nature. *Biotechnol. Lett.* **2009**, *31*, 171.
- (64) MacRae, C. A.; Peterson, R. T. Zebrafish as tools for drug discovery. *Nat. Rev. Drug Discovery* **2015**, *14*, 721.
- (65) Wu, Q.; Zheng, K.; Liao, S.; Ding, Y.; Li, Y.; Mei, W. Arene Ruthenium(II) Complexes as Low-Toxicity Inhibitor against the Proliferation, Migration, and Invasion of MDA-MB-231 Cells through Binding and Stabilizing c-myc G-Quadruplex DNA. *Organometallics* **2016**, *35*, 317–326.
- (66) Wang, Y.-H.; Cheng, C.-C.; Lee, W.-J.; Chiou, M.-L.; Pai, C.-W.; Wen, C.-C.; Chen, W.-L.; Chen, Y.-H. A novel phenotype-based approach for systematically screening antiproliferation metallodrugs. *Chem.-Biol. Interact.* **2009**, *182*, 84–91.
- (67) Lenis-Rojas, O. A.; Fernandes, A. R.; Roma-Rodrigues, C.; Baptista, P. V.; Marques, F.; Pérez-Fernández, D.; Guerra-Varela, J.; Sánchez, L.; Vázquez-García, D.; Torres, M. L.; Fernández, A.; Fernández, J. J. Heteroleptic mononuclear compounds of ruthenium(II): synthesis, structural analyses, *in vitro* antitumor activity and *in vivo* toxicity on zebrafish embryos. *Dalton Trans.* **2016**, *45*, 19127–19140.
- (68) Bennett, M. A.; Smith, A. K. Arene ruthenium(II) complexes formed by dehydrogenation of cyclohexadienes with ruthenium(III) trichloride. *J. Chem. Soc., Dalton Trans.* **1974**, 233–241.
- (69) Dong, Y.; Li, X.; Liu, S.; Zhu, Q.; Li, J.-G.; Sun, X. Facile synthesis of high silver content MOD ink by using silver oxalate precursor for inkjet printing applications. *Thin Solid Films* **2015**, *589*, 381–387.
- (70) Sheldrick, G. M. A short history of SHELX. *Acta Crystallogr., Sect. A: Found. Crystallogr.* **2008**, *64*, 112–22.
- (71) Dolomanov, O. V.; Bourhis, L. J.; Gildea, R. J.; Howard, J. A. K.; Puschmann, H. OLEX2: a complete structure solution, refinement and analysis program. *J. Appl. Crystallogr.* **2009**, *42*, 339–341.
- (72) Sheldrick, G. SHELXT - Integrated space-group and crystal-structure determination. *Acta Crystallogr., Sect. A: Found. Adv.* **2015**, *71*, 3–8.
- (73) Vichai, V.; Kirtikara, K. Sulforhodamine B colorimetric assay for cytotoxicity screening. *Nat. Protoc.* **2006**, *1*, 1112–1116.
- (74) Yu, J.; He, J.; Zhang, Y.; Qin, F.; Xiong, Z.; Li, F. An ultraperformance liquid chromatography–tandem mass spectrometry method for determination of anastrozole in human plasma and its application to a pharmacokinetic study. *Biomed. Chromatogr.* **2011**, *25*, 511–516.
- (75) Higley, E. B.; Newsted, J. L.; Zhang, X.; Giesy, J. P.; Hecker, M. Assessment of chemical effects on aromatase activity using the H295R cell line. *Environ. Sci. Pollut. Res.* **2010**, *17*, 1137–48.
- (76) Kimmel, C. B.; Ballard, W. W.; Kimmel, S. R.; Ullmann, B.; Schilling, T. F. Stages of embryonic development of the zebrafish. *Dev. Dyn.* **1995**, *203*, 253–310.

3 PUBLICATION 3

Synthesis and biological assessment of a ruthenium(II) cyclopentadienyl complex in breast cancer cells and on the development of zebrafish embryos

Synthèse et évaluation biologique d'un complexe cyclopentadiényle de ruthénium(II) dans des cellules de cancer du sein et sur le développement embryonnaire de poissons zèbres

Authors: Golara Golbaghi, Irène Pitard, Matthieu Lucas, Mohammad Mehdi Haghdoost, Yossef López de los Santos, Nicolas Doucet, Shunmoogum A. Patten, J. Thomas Sanderson, Annie Castonguay

INRS-Centre Armand-Frappier Santé Biotechnologie, Université du Québec, Laval, Canada

This article was published in European Journal of Medicinal Chemistry (2020), 188, 112030.

<https://doi.org/10.1016/j.ejmech.2019.112030>

Author contributions:

Golara Golbaghi designed and performed the biology and chemistry experiments, the statistical analyses and wrote the original draft of the manuscript.

Irène Pitard and Matthieu Lucas were summer trainee students who were involved in some chemistry experiments done for this project.

Dr. Mohammad Mehdi Haghdoost trained me to perform Zebrafish experiments.

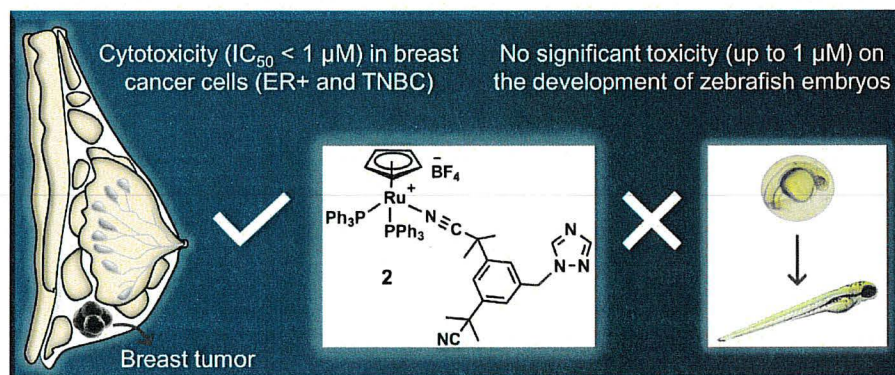
Dr. Yossef López de los Santos performed the Docking simulations.

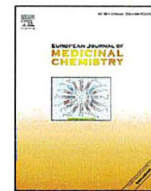
Professors Nicolas Doucet, Shunmoogum A. Patten, and J. Thomas Sanderson were our collaborators who provided us with their knowledge, materials and facilities to perform theoretical studies, Zebrafish experiments and aromatase assay, respectively.

Prof. Annie Castonguay obtained the research funding, supervised the project and participated in conceptualization, writing and revising the manuscript.

RÉSUMÉ :

Les complexes à base de ruthénium attirent actuellement beaucoup l'attention car ils ont le potentiel de remplacer les médicaments à base de platine en tant que traitement anticancéreux de première ligne. Alors que les complexes de ruthénium arène sont parmi les espèces les plus étudiées pour leurs propriétés anticancéreuses potentielles, d'autres types de complexes de ruthénium ont été négligés à cette fin. Dans cette étude, nous rapportons la synthèse et la caractérisation de complexes Ru(II) cyclopentadiényle (Cp), Ru(II) cyclooctadiényle (COD) et Ru(III) portant des ligands anastrozole ou létrozole, inhibiteurs d'aromatase de troisième génération actuellement utilisés pour le traitement du cancer du sein à récepteurs d'œstrogène positifs (ER+). Parmi ces complexes, Ru (II) Cp (2) était le seul à présenter une stabilité élevée dans le DMSO et dans les milieux de culture et, par conséquent, le seul complexe pour lequel l'activité biologique *in vitro* et *in vivo* fut étudiée. Contrairement à l'anastrozole seul, le complexe 2 était considérablement cytotoxique *in vitro* (valeurs $IC_{50} < 1 \mu M$) pour le cancer du sein ER+ humain (T47D et MCF7), le cancer du sein triple négatif (TNBC) (MBA-MB-231) et le carcinome corticosurrénalien (H295R). Des études théoriques (simulation « docking ») et expérimentales (activité catalytique de l'aromatase) ont suggéré qu'une interaction entre 2 et l'enzyme aromatase n'était pas susceptible de se produire et que l'encombrement des ligands PPh_3 pourrait être un facteur important empêchant le complexe d'atteindre le site actif de l'enzyme. L'exposition d'embryons de poissons zèbres au complexe 2, à des concentrations proches de sa valeur de cytotoxicité *in vitro* IC_{50} (0,1-1 μM), n'a pas conduit à des signes notables de toxicité sur une période de 96 h, ce qui en fait un candidat approprié pour d'éventuelles investigations *in vivo*. Cette étude confirme le potentiel des complexes Ru(II) Cp pour le traitement du cancer du sein, plus spécifiquement contre les TNBC qui ne répondent généralement pas aux agents de chimiothérapie actuellement utilisés.





Research paper

Synthesis and biological assessment of a ruthenium(II) cyclopentadienyl complex in breast cancer cells and on the development of zebrafish embryos

Golara Golbaghi, Irène Pitard, Matthieu Lucas, Mohammad Mehdi Haghdoost, Yossef López de los Santos, Nicolas Doucet, Shunmoogum A. Patten, J. Thomas Sanderson, Annie Castonguay*

Organometallic Chemistry Laboratory for the Design of Catalysts and Therapeutics, and Endocrine Toxicology Laboratory, INRS-Centre Armand-Frappier Santé Biotechnologie, Université du Québec, Laval, Canada



ARTICLE INFO

Article history:

Received 31 October 2019
Received in revised form
17 December 2019
Accepted 30 December 2019
Available online 3 January 2020

Keywords:

Ruthenium complex
Breast cancer therapy
Estrogen receptor positive breast cancer
Triple negative breast cancer
Aromatase inhibitor
Zebrafish

ABSTRACT

Ruthenium-based complexes currently attract great attention as they hold promise to replace platinum-based drugs as a first line cancer treatment. Whereas ruthenium arene complexes are some of the most studied species for their potential anticancer properties, other types of ruthenium complexes have been overlooked for this purpose. Here, we report the synthesis and characterization of Ru(II) cyclopentadienyl (Cp), Ru(II) cyclooctadienyl (COD) and Ru(III) complexes bearing anastrozole or letrozole ligands, third-generation aromatase inhibitors currently used for the treatment of estrogen receptor positive (ER+) breast cancer. Among these complexes, Ru(II)Cp **2** was the only one that displayed a high stability in DMSO and in cell culture media and consequently, the only complex for which the *in vitro* and *in vivo* biological activities were investigated. Unlike anastrozole alone, complex **2** was considerably cytotoxic *in vitro* (IC₅₀ values < 1 μM) in human ER+ breast cancer (T47D and MCF7), triple negative breast cancer (TNBC) (MBA-MB-231), and in adrenocortical carcinoma (H295R) cells. Theoretical (docking simulation) and experimental (aromatase catalytic activity) studies suggested that an interaction between **2** and the aromatase enzyme was not likely to occur and that the bulkiness of the PPh₃ ligands could be an important factor preventing the complex to reach the active site of the enzyme. Exposure of zebrafish embryos to complex **2** at concentrations around its *in vitro* cytotoxicity IC₅₀ value (0.1–1 μM) did not lead to noticeable signs of toxicity over 96 h, making it a suitable candidate for further *in vivo* investigations. This study confirms the potential of Ru(II)Cp complexes for breast cancer therapy, more specifically against TNBCs that are usually not responsive to currently used chemotherapeutic agents.

© 2020 Elsevier Masson SAS. All rights reserved.

1. Introduction

Metal complexes are a useful class of molecules with a broad spectrum of therapeutic applications. Despite the considerable success of platinum-based anticancer agents, which are administered to nearly 50% of patients undergoing chemotherapy, factors such as severe side effects and emergence of cancer cell resistance limit their clinical applications [1–4]. In the past years, ruthenium compounds have attracted increasing attention and are often

considered potential alternatives to platinum drugs given their selective bioactivity and their ability to overcome platinum-mediated cancer cell resistance. They are known for their cytotoxicity and/or their antimetastatic properties through distinct mechanisms of action, notably DNA or protein binding, reactive oxygen species (ROS) generation and cancer cell mobility inhibition [1,5–7]. Importantly, several ruthenium complexes have entered and/or are currently in various stages of clinical trials [8–15]. Of particular interest is the design of organoruthenium complexes bearing carefully selected biologically active ligands such as enzyme inhibitors involved in the treatment of cancer, allowing the development of efficient drug/prodrug candidates that can display multiple modes of action. This strategy can potentially circumvent

* Corresponding author.
E-mail address: annie.castonguay@inrs.ca (A. Castonguay).

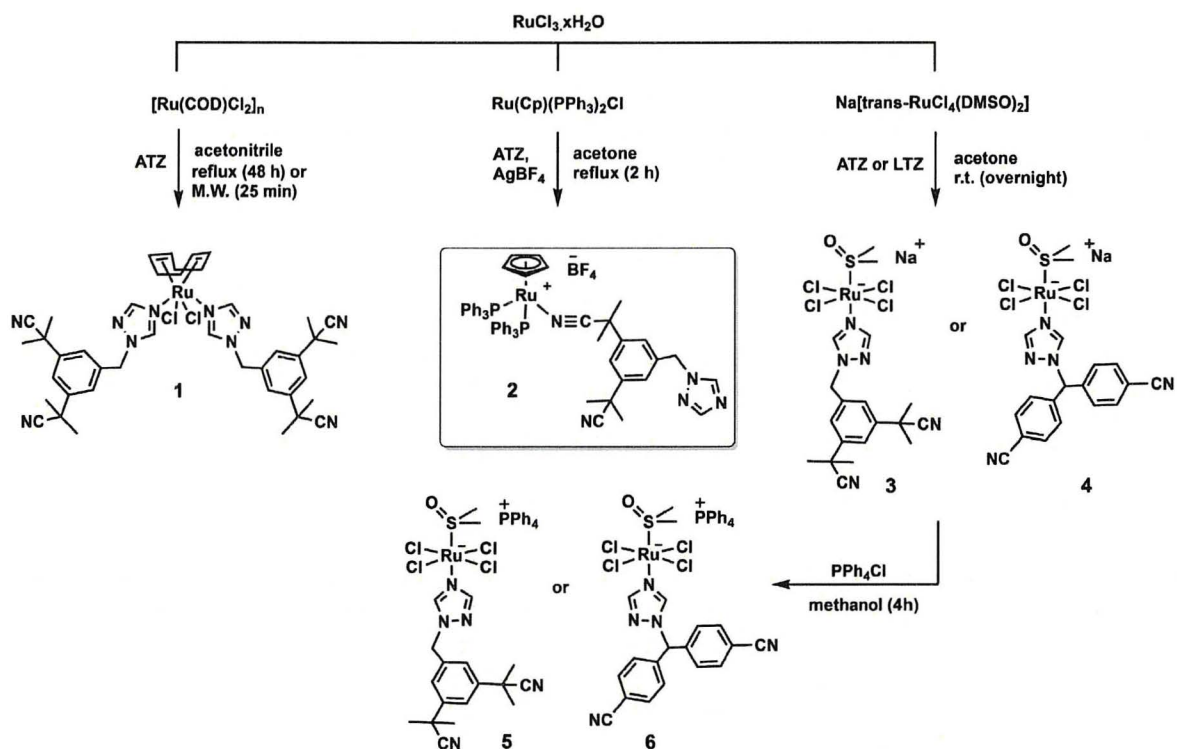
emerging drug resistance mechanisms, a common cause of mortality in cancer patients [16–19]. For instance, we reasoned that third-generation aromatase inhibitors such as the nonsteroidal triazole derivatives anastrozole (Arimidex®) and letrozole (Femara®) could be suitable candidates for this purpose, as they are widely used to treat estrogen receptor positive (ER+) breast cancer in postmenopausal women, and have the ability to coordinate ruthenium [20]. ER+ breast cancer cells proliferate under the influence of elevated estrogen levels, but are deprived of this hormone by aromatase inhibitors, which act by preventing the aromatase-catalyzed production of estrogens from androgens [21]. Despite the success of third generation aromatase inhibitors for the treatment of breast cancer, in approximately one third of patients diagnosed with metastatic ER+ breast cancer, therapies involving these drugs lead to the mutation of the ER gene, resulting in a treatment-resistant cancer that is often incurable [22,23]. Furthermore, estrogen deprivation was previously reported to sensitize ER+ breast cancer cells to cytotoxic agents [24,25].

We recently reported the biological activity of a series of half-sandwich ruthenium (II) arene complexes with anastrozole ligands [26]. This previous study followed a preliminary investigation by Maysinger et al. on the cytotoxicity of a series of ruthenium (II) arene complexes bearing letrozole ligands [16]. To get more insights into the potential effectiveness of ruthenium-anastrozole complexes in cancer therapy, we were interested in exploring the physical and biological properties of structurally and electronically diverse types of ruthenium complexes. Although half-sandwich ruthenium (II) arene complexes have been extensively investigated for their ability to induce cancer cell toxicity and, in some cases, with high selectivity toward cancer cells [27–29], there are far fewer studies of the anticancer potential of ruthenium (II) complexes based on cyclooctadiene (COD) or cyclopentadiene (Cp) ligands [30–41]. For instance, Sheldrick et al. reported a cationic Ru(II)COD complex with considerable cytotoxicity in Jurkat leukemia cells, for which the mode of action is believed to be associated with the generation of reactive oxygen species (ROS) [41]. Another report from Omondi revealed that a series of Ru(II)COD complexes with bidentate N,N-donor ligands had a high affinity with human serum albumin (HSA). However, the cytotoxicity of these complexes was not investigated [33]. Promising anticancer activities were also reported for some Ru(II)Cp complexes [34,42–47]. For instance, it was shown by Severin et al. that replacing the arene ligand in the structure of a RAPTA-type complex, $[(\eta^6\text{-arene})\text{RuCl}_2(\text{PTA})]$ (PTA = 1,3,5-triaza-7-phosphaadamantane), with a bulky cyclopentadienyl electron-donating ligand led to compounds with enhanced cytotoxicities [43,44]. This effect is believed to be associated with the improved ability of the complexes to cross cancer cell membranes [43]. Notably, Garcia et al. reported a new family of Ru(II)Cp complexes with N,O- and N,N'-heteroaromatic bidentate ligands that revealed an exceptional activity with IC₅₀ values in the nanomolar range against the MDA-MB-231 breast cancer cell line [45,47]. They also investigated the *in vivo* antitumor activity of a Ru(II)Cp (TM90, $[\text{Ru}(\eta^5\text{-C}_5\text{H}_5)(\text{PPh}_3)(\text{bopy})][\text{CF}_3\text{SO}_3]$ (bopy = 2-benzoylpyridine) on nude female mice bearing TNBC orthotopic tumors. Importantly, the study revealed the ability of the complex to suppress tumor growth and to inhibit the development of metastases, to increase the lifetime of mice after surgical removal of the tumor (compared to untreated mice) and to not negatively affect their behavior [42]. Fernandes et al. synthesized and characterized a series of Ru(II)Cp complexes bearing carbohydrates such as glucose and fructose with promising *in vitro* cytotoxicities against HeLa human cervical cancer and HCT116 human colon carcinoma cells [34,37]. The cytotoxicity of these complexes was found to be significantly influenced by the nature of the carbohydrate moiety and the metal center. Interestingly, iron

complexes of the same ligands induced less cytotoxicity in cancer cells compared to the corresponding ruthenium complexes, confirming the importance of the ruthenium metal for the anticancer activity of such metallodrugs [34]. Valente et al. reported Ru(II)Cp complexes with the ability to induce inhibition of proliferation and apoptosis, not only in an estrogen receptor positive (ER+) breast cancer cell line (MCF7), but also in an aggressive triple negative breast cancer (TNBC) cell line (MDA-MB-231). These compounds were found to interact with mitochondria and with cytoskeleton, and to reduce the colony formation potential of breast cancer cells [46]. It is of high importance that Ru(II)Cp complexes display promising activities for the treatment of TNBC which, in contrast to hormone receptor positive (HR+) breast cancers, does not respond to hormonal therapy approaches [48,49]. DNA interaction [30,35,39], cell-membrane transporter inhibition [40], human serum albumin (HSA) binding [36] and cell cycle disturbance [39] have been also reported as other possible modes of action for Ru(II)Cp complexes. Ru(III) complexes have also attracted interest due to their cytotoxicity or/and antimetastatic properties alongside their low systemic toxicity [7,15,50]. For instance, the ruthenium (III) complex KP1339 did not only show cytotoxicity in different *in vivo* tumor models (more specifically in colon cancer) in preclinical studies, but was also found to stabilize the disease in clinical studies involving cancer patients while only inducing mild side effects. Disruption of endoplasmic reticulum homeostasis and induction of immunogenic cell death have been reported as mechanisms of action for this complex [15]. In the present study, we report the synthesis, characterization and stability assessment of Ru(II)COD, Ru(II)Cp, and Ru(III) complexes bearing anastrozole (ATZ) or letrozole (LTZ). Results regarding the *in vitro* anticancer activity in several human cell lines and *in vivo* toxicity in a zebrafish model of the most promising candidate is also presented.

2. Results and discussion

The synthesis of complex **1**, RuCOD(ATZ)₂Cl₂, was first attempted by allowing $[\text{Ru}(\text{COD})\text{Cl}_2]_n$ to react with two equivalents of anastrozole in refluxing acetonitrile. No product could be detected after 18 h, and only a 13% conversion could be observed after 48 h. The yield could be increased up to 22% and the reaction time decreased to 25 min when the reaction was performed in a microwave reactor (15 psi, 200 W, 80 °C) (Scheme 1). It is noteworthy that using the microwave for longer periods of time under the above-mentioned conditions resulted in a significant decrease in the yield of the reaction, possibly due to some interactions of the final product with other molecules present in the reaction mixture. Only few examples of microwave-assisted syntheses of ruthenium complexes were previously reported [51–53]. The synthesis of cationic complex **2**, RuCp(PPh₃)₂(ATZ)BF₄, was performed by reacting RuCp(PPh₃)₂Cl and anastrozole in the presence of AgBF₄ in refluxing acetone for 2 h (36% yield, Scheme 1). Both Ru(II) complexes **1** and **2** are soluble in acetone, alcohols and dimethyl sulfoxide (DMSO) but poorly soluble in water. The anionic Ru(III) species **3**, Na[*trans*-RuCl₄ATZ(DMSO)]], was also prepared by allowing Na[*trans*-RuCl₄(DMSO)₂] to react with anastrozole in acetone overnight at room temperature (56% yield). Keeping in mind that the anticancer properties of metal complexes often vary with their lipophilicity [27,54], the sodium counterion in the structure of **3** was replaced with a more lipophilic cation. Complex **5**, PPh₄[*trans*-RuCl₄ATZ(DMSO)]], was then obtained (70% yield) by allowing a methanol solution of compound **3** to react with PPh₄Cl for 4 h at room temperature (Scheme 1). Although anastrozole and letrozole both belong to the third-generation class of aromatase inhibitors and have closely related structures, their efficacy has been reported to differ in some cases. For instance, letrozole was



Scheme 1. Synthetic route to complexes 1–6.

more effective at lowering estrogen levels than anastrozole in human breast cancer tissues [55,56]. For comparison purposes, letrozole derivatives of complexes **3** and **5**, **4** (66% yield) and **6** (39% yield), were also synthesized using the same reaction conditions (Scheme 1). All Ru(III) complexes were soluble in most organic solvents except **6** which had a poor solubility in most solvents. Due to the nature of the counterions, only complexes **3** and **4** were found to be soluble in water. The identity and purity of all complexes were confirmed by nuclear magnetic resonance (NMR) (only in the case of diamagnetic species **1** and **2**), high-resolution electrospray ionization mass spectrometry (HR-ESI-MS) and elemental analysis. In contrast to complex **1** and previously reported Ru(II) arene complexes bearing anastrozole or letrozole [16,26], signals corresponding to the protons and/or carbons of the anastrozole moiety in the ¹H NMR and ¹³C{¹H} NMR spectra of **2** were non-equivalent (phenyl, nitrile and methyl groups), suggesting a different coordination mode of this ligand in this complex. Compared to the downfield chemical shift of ¹H NMR signals assigned to the protons of the triazole ring of **1**, the corresponding signals in the spectrum of **2** were only slightly shifted in comparison with the ones observed for free anastrozole (Fig. 1), suggesting that anastrozole is coordinated to ruthenium via one of its nitrile moieties, which was further confirmed by X-ray crystallography analysis (Fig. 2, *vide infra*). This mode of coordination may be favored due to the steric hindrance of the two bulky triphenylphosphine ligands, preventing the triazole ring from reaching the metal site. As reported for other Ru(II)Cp and Ru(II)COD complexes [30,57], a singlet at 4.51 ppm was observed for the cyclopentadienyl moiety of **2**, whereas three signals at 2.06, 2.66, 4.09 ppm were observed for the non-equivalent protons in of the cyclooctadienyl moiety of **1** (endo CH₂, exo CH₂ and CH).

The solid-state structure of all compounds (except **3**) was also confirmed by single crystal X-ray diffraction (Fig. 2 and Table S1). The six-coordinate metal center in **1** exhibits a distorted octahedral

geometry. The Ru–C bond lengths are similar to those reported for other Ru(II)COD complexes [33,58,59]. The two chloride ligands *trans* to one another are directed away from the 1,5-COD ligand (the Cl1–Ru–Cl2 bond angle is 159.95 (2)°, a common distortion found for ligands axial to an equatorial plane containing 1,5-COD in ruthenium (II) complexes [33,58,59]). The two anastrozole ligands are *cis* to one another (N1–Ru–N2 89.87 (6)°) and *trans* to 1,5-COD. Compound **2** adopts a piano stool geometry, which is typical of cationic half-sandwich ruthenium complexes [34,39]. As previously stated, X-ray analysis data obtained for this complex confirmed the coordination of the anastrozole through one of its nitrile moieties. To the best of our knowledge, this is the first example of this coordination mode for a ruthenium complex bearing anastrozole. The Ru–N bond length in **2**, 2.048 (3) Å, is in the same range as bond lengths reported for other nitrile-coordinated Ru(II)Cp complexes (2.056 (3) Å [60] and 2.053 (2) Å [61]) and Ru(II)-arene complexes (2.066 (4) Å [62] and 2.050 (4) Å [63]), but as expected, significantly shorter than the ones noted for **1** (Ru–N1: 2.136 (1) Å and Ru–N2: 2.133 (1) Å) and for previously reported Ru(II)-arene complexes of triazole-coordinating anastrozole [26]. The crystallography data for **4–6** also revealed a disordered octahedral geometry, which is well documented and characteristic for this type of Ru(III) complexes [64–67]. All the synthesized Ru(III) species include four chloride ligands in the equatorial positions and a DMSO molecule bound via its sulfur atom *trans* to the triazole ring of anastrozole or letrozole in the axial position. The Ru–N bond lengths observed in the structure of all Ru(III) species are very similar to one another (Ru–N: **4**, 2.091 (2); **5**, 2.103 (2); **6**, 2.093 (3)) and to those reported for structurally similar complexes [67,68]. The bond lengths and angles are also similar to those found in other NAMI-A derivatives [65–68].

DMSO was selected to prepare stock solutions of the compounds to assess their biological activity. DMSO is commonly used as a solvent of choice for this purpose as it allows the biological

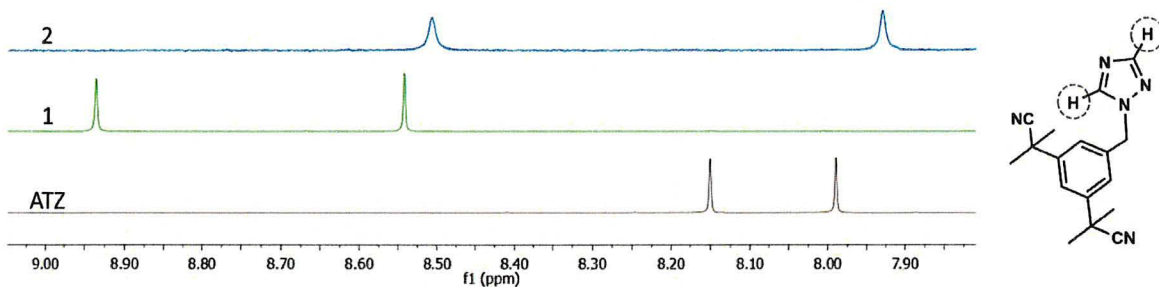


Fig. 1. Selected area of the ^1H NMR spectra of free anastrozole (red), complex **1** (green) and complex **2** (blue) in CDCl_3 , showing the resonances corresponding to their triazole protons. (For interpretation of the references to colour in this figure legend, the reader is referred to the Web version of this article.)

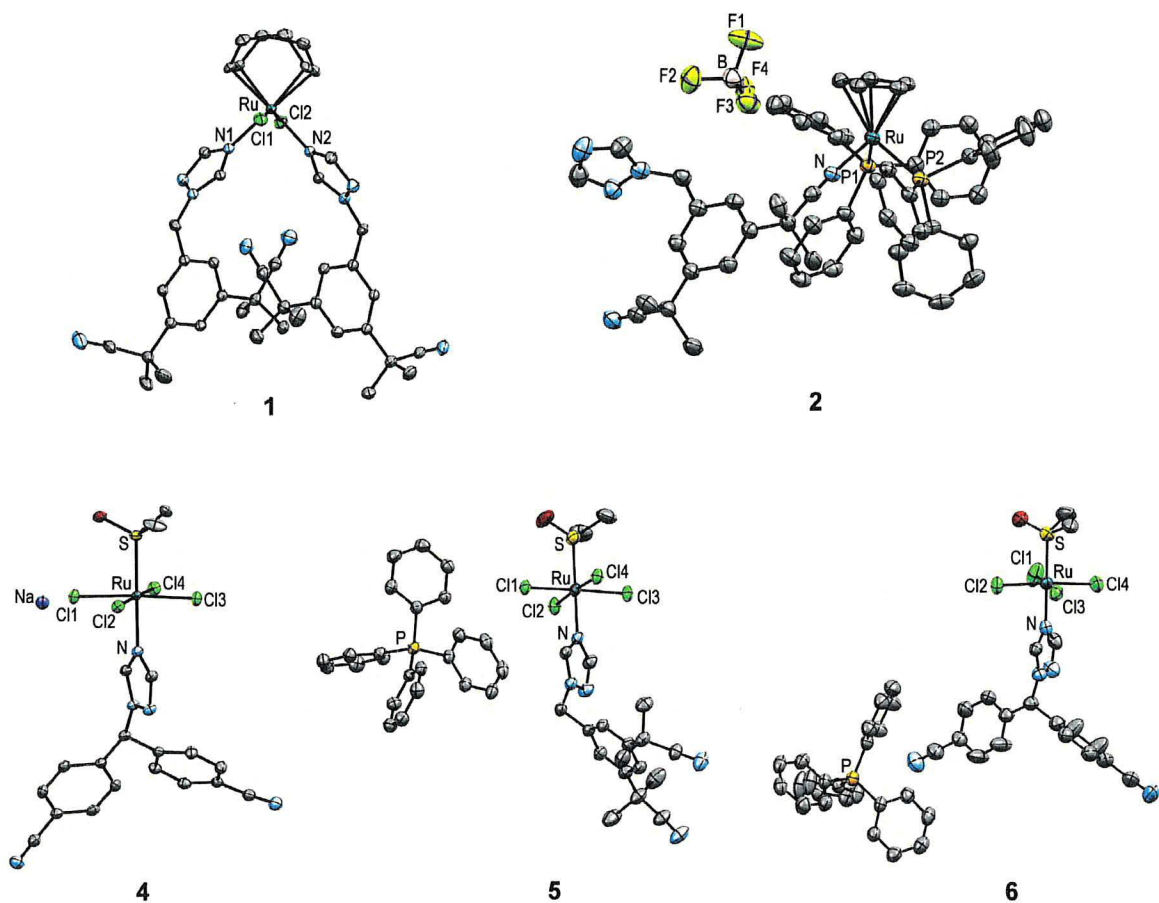


Fig. 2. ORTEP diagrams of **1**, **2** and **4–6** with thermal ellipsoids drawn at the 50% probability level. Note that only one site is shown for the disordered dimethyl sulfoxide molecule in the asymmetric unit of **6**, whereas two co-crystallized molecules of water in the asymmetric unit of **2** are omitted for clarity.

evaluation of compounds with poor aqueous solubility and does not induce noticeable *in vitro* or *in vivo* cytotoxicity at low concentrations. Prior to performing biological experiments, the solubility of the complexes in DMSO was estimated by measuring the UV–Vis absorbance of solutions of various concentrations after fine filtration. All complexes were found to be soluble in DMSO at concentrations as high as 20 mM, except complex **6** for which the biological activity was not assessed. The stability of the complexes in DMSO (2 mM, 15 min) was also evaluated by NMR spectroscopy (only for the diamagnetic species). Whereas the ^1H NMR spectrum of complex **2** revealed its high stability in DMSO (only 2% of free anastrozole was observed) (Fig. S1), the ^1H NMR spectrum of

compound **1** revealed a much lower stability in this solvent. Although the ^1H NMR spectrum of **1** (Fig. S1) indicated that **1** remained the major species in solution, the appearance of two new series of peaks corresponding to free anastrozole (25%) and a new complex bearing anastrozole discouraged us from pursuing the biological activity assessment of compound **1**. The stability of **2** in DMSO was further confirmed by UV–Vis spectrometry experiments. No apparent change was observed in the absorption spectrum of this compound over 1 h (Fig. S2).

To further investigate the stability of **2–5** under conditions similar to those of the tritiated water-release assay of aromatase activity, a previously established HPLC technique [26] was used,

allowing the measurement of the amount of released anastrozole or letrozole after a 1.5 h incubation of the complexes in full DMEM/F12 medium (with a maximum 0.1% DMSO) at 10 μM . Whereas all three Ru(III) complexes underwent transformation(s) in media, resulting in a significant release of their ligands (Table S2), compound **2** was found to be highly stable under the conditions tested (only 4% of released anastrozole was detected). Since complex **2** was the only species found to be stable under biologically relevant conditions, its solubility was verified by UV–Vis spectrometry under conditions similar to those used for the *in vitro* and *in vivo* experiments: *i*) in full DMEM/F12 medium (0.1% DMSO) and *ii*) in water (max 0.5% DMSO), respectively (Fig. S3). Compound **2** was found to be highly soluble at all tested concentrations (up to 15 μM in water and up to 20 μM in culture medium), confirming the suitability of this compound for biological experiments.

The cytotoxicity of complex **2** was evaluated at different concentrations using a sulforhodamine B (SRB) assay [69] in different human cell lines: MCF7 and T47D (ER + breast cancer), MDA-MB-231 (ER - breast cancer), H295R (adrenocortical carcinoma which expresses high levels of the aromatase enzyme) and MCF12A (non-cancerous breast) [70,71]. IC_{50} values were determined after a 48 h exposure of the cancer cells to the complex (Table 1).

In contrast to anastrozole alone ($\text{IC}_{50} > 100 \mu\text{M}$ in all cell lines, results not shown), compound **2** displayed a high cytotoxicity against all the cancer cell lines with IC_{50} values lower than 1 μM . Although complex **2** approximately equally affected the healthy cell line tested with a selectivity index of 1.16, it is important to keep in mind that *i*) the same *in vitro* lack of selectivity was also observed for the widely used chemotherapeutic drug cisplatin ($\text{SI} \ll 1$ in case of T47D and H295R cells) and that *ii*) although considered as an acceptable indicator, the *in vitro* cytotoxicity of a compound does not necessarily reflect its acute systemic toxicity and as a consequence, *in vivo* toxicities cannot be predicted from *in vitro* experiments with high confidence [72–74]. Importantly, complex **2** was more cytotoxic than cisplatin in all cancer cell lines used in this study, particularly in H295R and T47D cells (the latter being cisplatin resistant). Notably, compound **2** was not only found to be highly cytotoxic in ER + breast cancer cells ($\text{IC}_{50} = 0.50 \pm 0.09 \mu\text{M}$, MCF7; $0.32 \pm 0.03 \mu\text{M}$, T47D) but also in a triple negative breast cancer (TNBC) cell line ($\text{IC}_{50} = 0.39 \pm 0.09 \mu\text{M}$, MDA-MB-231), suggesting a mode of action that is independent of the estrogen receptor status of the cells. Indeed, it is of high importance to identify drug candidates for the treatment of aggressive hormone receptor negative (HR -, TNBC) breast cancers (about 10–20% of cases) for which endocrine therapies that target hormone receptors are ineffective [48,75]. The IC_{50} values observed for compound **2** are in the range expected for Ru(II)Cp complexes in both ER + breast cancer and TNBC cell lines (0.03–20 μM) [46,47,76–78], confirming the high potential of this class of ruthenium complexes for breast cancer treatment. Finally, compound **2** is a rare example of a ruthenium complex with significant cytotoxicity in H295R cells ($\text{IC}_{50} = 0.63 \pm 0.05 \mu\text{M}$), warranting further investigations on the design of ruthenium species for the treatment of aggressive adrenocortical carcinomas. Nevertheless, it is important to keep in mind that *in vitro* cytotoxicity is not necessarily representative of *in vivo* antitumor activity, due to the potential impact of the tumor microenvironment on the tumor growth and drug effectiveness [79,80].

The binding of third generation aromatase inhibitors to the catalytic centre of the cytochrome P450 enzyme aromatase (CYP19A1) (consisting of an iron porphyrin complex) via their triazole nitrogen atom is considered to be their main mode of action [81]. Therefore, considering the availability of the triazole ring in the structure of **2**, we performed a molecular modeling study to evaluate the potential occurrence of interactions between this

Table 1

IC_{50} values determined for **2** and cisplatin in human cancer MCF7, T47D, MDA-MB-231, H295R and non-cancerous MCF12A cell lines (and corresponding selectivity indexes).

| | IC_{50} (μM) ^a | | Selectivity index (SI) ^b | |
|------------|---|--------------------|-------------------------------------|-----------|
| | 2 | cisplatin | 2 | cisplatin |
| MCF7 | 0.50 (± 0.09) | 20.1 (± 3.5) | 1.16 | 2.12 |
| T47D | 0.32 (± 0.03) | >150 | 1.81 | <0.28 |
| MDA-MB-231 | 0.39 (± 0.09) | 32.4 (± 7.4) | 1.49 | 1.32 |
| H295R | 0.63 (± 0.05) | 86.5 (± 1.2) | 0.92 | 0.49 |
| MCF12A | 0.58 (± 0.02) | 42.7 (± 7.2) | – | – |

^a Inhibitory activity was determined by exposure of cell lines to each complex for 48 h and expressed as the concentration required to inhibit cell metabolic activity by 50% (IC_{50}). Errors correspond to the standard deviation of two to four independent experiments.

^b $\text{SI} = \text{IC}_{50}$ (non-cancerous MCF12A cell line)/ IC_{50} (cancer cell line).

ruthenium complex and the enzyme using a docking simulation model we previously developed [26], based on the crystal structure of human placental aromatase cytochrome P450 (CYP19A1) (Fig. 3). These types of interactions between transition metal complexes and proteins (or DNA) were previously studied by other groups [82–84]. Molecular docking results suggest that bonding between the heme iron of CYP19 and triazole nitrogen atom is unlikely to occur. These results also reveal that significant conformational rearrangements of the protein would be required to accommodate compound **2** inside the active-site cavity of aromatase. Our simulations show that the interaction between **2** and the enzyme is energetically unfavorable because of significant steric clashes between compound **2** atoms and amino acids within the active-site cavity (Fig. 3C).

In the absence of conformational rearrangements of aromatase, the bulkiness of **2** (bearing two sterically hindered triphenylphosphine ligands) would prevent this complex from passing through the solvent-accessible access channel, preventing it to reach the active site of aromatase. This was further supported by results obtained from a tritiated water-release experiment we performed to assess the *in vitro* aromatase inhibitory effect of **2**. This method was previously reported as a sensitive and reproducible technique for aromatase activity assessment [85,86]. The H295R cell line was selected for this study as it expresses high levels of the aromatase enzyme [70,87]. As we previously reported for the investigation of the aromatase activity of H295R cells exposed to ruthenium species [26], H295R cells were co-incubated with 1β - ^3H - androstenedione and compound **2** (or anastrozole) for 1.5 h. The radioactivity of the tritium oxide produced from the conversion of the labeled androgen to its corresponding estrogen, catalyzed by the aromatase enzyme, was quantified and reported as an indication of aromatase activity (Fig. 4). Because of the high cytotoxicity of **2** in H295R cells ($\text{IC}_{50} = 0.63 \pm 0.05 \mu\text{M}$), its potential aromatase inhibitory activity was assessed at concentrations no greater than 100 nM (compound **2** becomes slightly cytotoxic at 1 μM when incubated for 1.5 h). As predicted from the docking simulation, a significantly lower aromatase inhibitory activity was observed in cells exposed to **2** compared to those treated with free anastrozole. No significant inhibition of aromatase activity was observed for complex **2** up to 10 nM, whereas about 50% inhibition of enzyme activity was observed for anastrozole alone at 10 nM (Fig. 4). It is likely that the slight aromatase inhibitory activity observed for **2** at higher concentrations was a consequence of free anastrozole released from the complex (4%, Table S2) under the conditions of the assay, making it difficult to draw a clear conclusion about the aromatase inhibitory activity of the complex itself.

The *in vivo* toxicity of **2** was determined in a zebrafish embryo

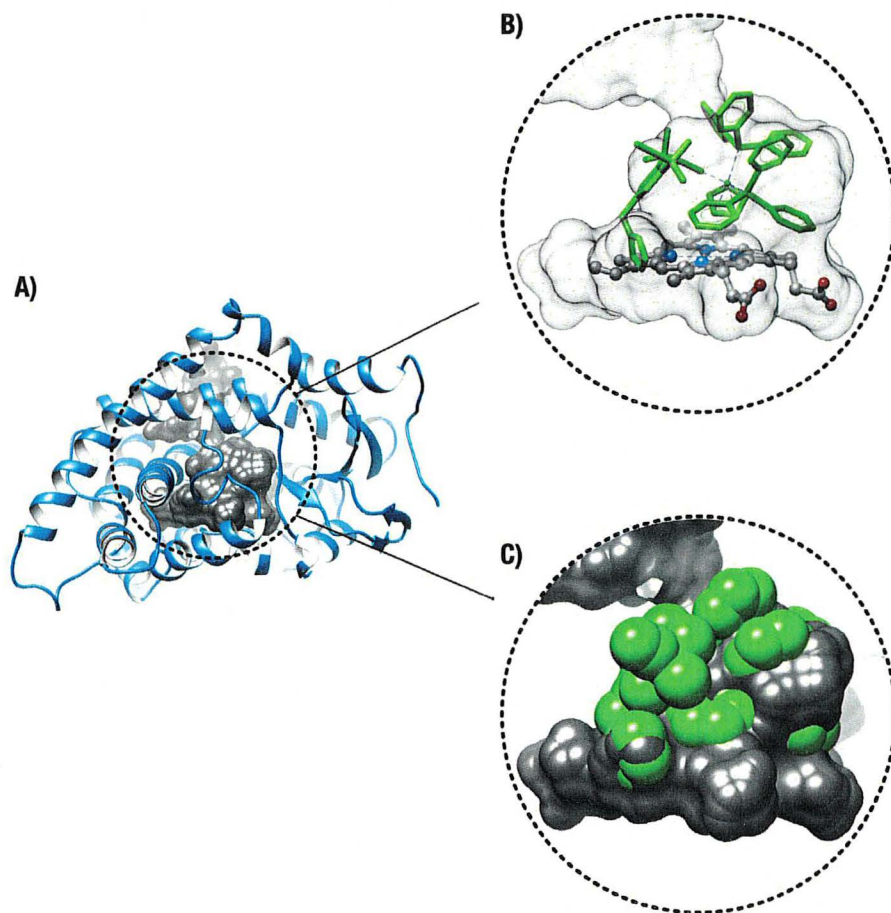


Fig. 3. Molecular docking of compound **2** inside the active-site cavity of aromatase. A) The active-site cavity of aromatase is shown in gray and the protein model is displayed as a blue ribbon. The illustrated surface represents the solvent-accessible area of the active site. B) Preferred conformer extracted for the ternary complex between the enzyme, cofactor group (heme), and compound **2**. The cofactor and compound **2** are respectively depicted as ball-and-stick and green stick models. C) Disruption of the internal cavity of the enzyme by compound **2**, illustrated as full atomic volume representation of van der Waals radii. Compound **2** atoms are shown as green spheres calculated according to the Corey-Pauling-Koltun model for van der Waals radii. Compound **2** atoms directly clash with amino acids within the active site of the enzyme, suggesting that such ternary complex formation is energetically unfavorable and nonspontaneous. (For interpretation of the references to colour in this figure legend, the reader is referred to the Web version of this article.)

model. Several publications support the use of this assay as a suitable model for the investigation of the *in vivo* toxicity of ruthenium species [26,27,88]. The zebrafish has become a prominent *in vivo* model in toxicology and drug discovery due to several advantages such as high fecundity (200–300 embryos per mating pair per week), ease of manipulation, embryo transparency, high degree of genetic conservation with humans and low cost [88–90]. Importantly, results arising from zebrafish toxicity screenings have been used as prediction tools prior to undertaking preclinical and clinical studies [91]. Accordingly, mortality rates, hatching rates and phenotype changes of zebrafish embryos exposed to **2** at concentrations around its IC_{50} value (0.1 μ M, 0.5 μ M and 1 μ M) for *in vitro* cytotoxicity in human cancer cells were determined at 24, 48, 72 and 96 h post fertilization (hpf) (Fig. 5). Compared to untreated control embryos, no apparent mortality (data not shown), hatching delay or phenotype changes were observed in zebrafish embryos treated with **2** at the tested concentrations. It is noteworthy that we have previously reported a significant inhibition of the hatching rate for zebrafish embryos exposed to cisplatin at concentrations far less than its IC_{50} value in human cancer cells [26,27]. There are also a few studies reported for which Ru(II)Cp complexes have been investigated for their overall toxicity in a zebrafish model [78,92,93]. Although different conditions have been used for these

studies preventing us from making direct comparisons, signs of toxicity such as delayed hatching, mortality and abnormalities such as pericardial edema, yolk sac edema, curved tail and head malfunction have been observed for some of the reported Ru(II)Cp complexes at the tested concentrations. Thus, compound **2** could be considered a promising candidate for further *in vivo* investigations.

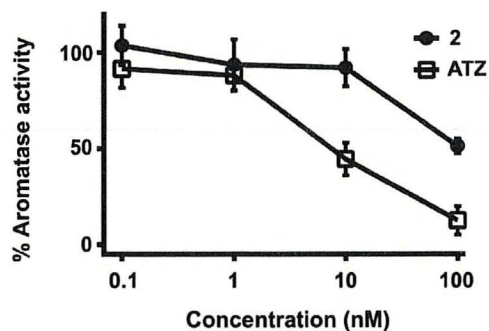


Fig. 4. Effects of the exposure of H295R cells to anastrozole (ATZ) and **2** on the aromatase activity. Cells were treated for 1.5 h with the indicated concentrations of the compounds. Values represent the mean \pm SD.

3. Conclusion

From this study of a series of ruthenium complexes bearing anastrozole or letrozole (1–6), we observed that the solubility and the stability of the complexes can be highly affected by their type of backbone, the nature of their ligands or counterions and the type of coordination of their ligands. Our study clearly shows that Ru(II)Cp complex **2**, the only species in this series for which anastrozole is coordinated ruthenium through the nitrile moiety (and not via the nitrogen of the triazole ring), was the only complex found to be stable in DMSO and in cell culture medium. Whereas Ru(II)Cp complexes have been overlooked for their anticancer properties compared to their Ru(II) arene counterparts, *in vitro* and *in vivo* investigations of **2** confirm the high potential for this type of complexes for cancer therapy. Furthermore, results from the aromatase inhibition assay and the molecular docking simulation suggest that the bulkiness of a ruthenium complex such as **2** can be a factor preventing its interaction with the targeted enzyme, and that bulky moieties such as PPh₃ may not be ligands of choice for that purpose. Moreover, this study opens the door to the development of a novel class of Ru(II)Cp complexes for breast cancer therapy, particularly against TNBCs which respond poorly to existing chemotherapeutic agents.

4. Experimental section

General comments. All reagents were purchased from commercial sources and used without further purification. Experiments were performed under a nitrogen atmosphere using standard Schlenk techniques, and solvents were dried using a solvent purification system (Pure Process Technology). Anastrozole and letrozole were purchased from Triplebond and AK scientific, respectively. RuCl₃.xH₂O, 5-cyclooctadiene, dicyclopentadiene, triphenylphosphine, and silver tetrafluoroborate were purchased from Sigma Aldrich. [Ru(COD)Cl₂]_n [94], RuCp(PPh₃)₂Cl [95], and Na [trans-RuCl₄(DMSO)₂] [96] were prepared according to previously reported procedures. Tecan Infinite M1000 PRO microplate reader was used to read the absorbance of multiwell plates (at 510 nm) for SRB assay. NMR spectra (¹H, ¹³C{¹H}), COSY, HSQC, and ROESY were recorded on a 400 MHz Varian or 600 MHz Bruker Avance III NMR spectrometers. Chemical shifts (δ) and coupling constants are expressed in ppm and Hz, respectively. ¹H and ¹³C{¹H} spectra were referenced to solvent resonances, and spectral assignments were confirmed by 2D experiments. The purity of all ruthenium complexes (>95%) was assessed by elemental analyses (Laboratoire d'Analyse Élémentaire, Department of Chemistry, Université de

Montréal). High-resolution and high accuracy mass spectra (HR-ESI-MS) were obtained using an Exactive Orbitrap spectrometer from ThermoFisher Scientific (Department of Chemistry, McGill University). Diffraction measurements were performed on a SMART APEX II diffractometer equipped with a CCD detector, an Incoatec IMuS source (Cu) and a Quazar MX mirror (1 and 2) or a Bruker Venture diffractometer (a liquid Ga Metal Jet source) equipped with a Photon 100 CMOS detector, a Helios MX optics and a Kappa goniometer (4–6) (Department of Chemistry, Université de Montréal). All statistical analyses were done using the GraphPad Prism 6.01 software. ANOVA analysis was used for testing the significance of the difference between the means and a p-value <0.05 was considered statistically significant.

4.1. Complex synthesis and characterization

RuCOD(ATZ)₂Cl₂ (1). Acetonitrile (18 mL) was added to anastrozole (0.208 g, 0.71 mmol), and [Ru(COD)Cl₂]_n (0.100 g, 0.35 mmol). The mixture was heated under reflux for 48 h and then cooled to room temperature and filtered. The filtrate was evaporated to dryness and the crude yellow compound was purified by flash chromatography (silica gel) with ethyl acetate:hexane (4:1) as the mobile phase. Compound **1** (0.020 g, 13%) was obtained as a light-yellow precipitate. **Microwave-assisted synthesis.** A mixture of [Ru(COD)Cl₂]_n (0.05 g, 0.18 mmol) and anastrozole (0.104 g, 0.36 mmol) in acetonitrile (10 mL) was heated in a microwave reactor at 80 °C for 25 min (set points: pressure 15 psi, power 200 W). The solvent was removed under vacuum and a light-yellow color product (0.034 g, 22%) was obtained after purification by column chromatography as mentioned above. ¹H NMR (CDCl₃, 600 MHz): δ 1.71 (s, CH₃, 24H), 2.06 (m, C₈H₁₂, 4H), 2.66 (br, C₈H₁₂, 4H), 4.09 (br, C₈H₁₂, 4H), 5.34 (s, CH₂, 4H), 7.26 (d, J = 1.9 Hz, ArH, 4H), 7.49 (t, J = 1.7 Hz, ArH, 2H), 8.53 (s, H_{triazole}, 2H), 8.93 (s, H_{triazole}, 2H). ¹³C{¹H} NMR (CDCl₃, 100 MHz): δ 29.04 (s), 30.05 (s), 37.30 (s), 53.82 (s), 89.53 (s), 122.02 (s), 123.76 (s), 124.25 (s), 135.87 (s), 143.4 (s), 145.15 (s), 151.92 (s). Found (%): C, 57.94; H, 5.83; N, 15.92. C₄₂H₅₀Cl₂N₁₀Ru₁ requires C, 58.17; H, 5.82; N, 16.16. HR-ESI-MS m/z (+): found 889.25 [M + Na]⁺ (calc. 889.25).

RuCp(PPh₃)₂(ATZ)BF₄ (2). To a suspension of RuCp(PPh₃)₂Cl (0.200 g, 0.276 mmol) in acetone (20 mL) were added anastrozole (0.164 g, 0.558 mmol) and AgBF₄ (0.060 g, 0.308 mmol). The solution was refluxed for 2 h until the colour changed from orange to pale yellow. The solution was centrifuged and the supernatant was evaporated under vacuum. The residue was dissolved in 2 mL of dichloromethane and was passed through a Celite pad. Diethyl ether was added to the filtrate and the resulting precipitate was

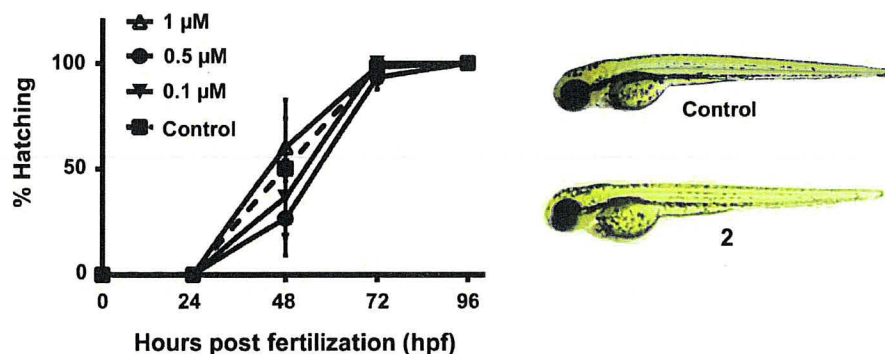


Fig. 5. (A) Effect of **2** on the hatching rate of developing zebrafish embryos. Hatching rates were assessed at 0.1, 0.5 and 1 μM over 4 days post fertilization (96 hpf). Control hatching rates are shown as a dashed line. (B) Gross morphological phenotypes of zebrafish embryos: untreated (control) and treated with 1 μM of **2** (96 hpf). Results are expressed as means ± standard deviation of three independent experiments (a total of 60 embryos).

washed with ethyl acetate (3 × 10 mL) and diethyl ether (3 × 10 mL). Compound **2** (0.107 g, 36%) was obtained as a pale-yellow precipitate. ¹H NMR (CDCl₃, 600 MHz): δ 1.42 (s, CH₃, 6H), 1.70 (s, CH₃, 6H), 4.51 (s, C₅H₅, 5H), 5.51 (s, CH₂, 2H), 7.00 (m, H_{PPH3}, 12H), 7.17 (t, J = 7.16 Hz, H_{PPH3}, 12H), 7.33 (t, J = 7.17 Hz, H_{PPH3}, 6H), 7.39 (t, J = 1.76, ArH, 1H), 7.47 (s, ArH, 1H), 7.73 (s, ArH, 1H), 7.97 (s, H_{triazole}, 1H), 8.60 (s, H_{triazole}, 1H). ¹³C{¹H} NMR (CDCl₃, 100 MHz): δ 27.65 (s), 29.13 (s), 37.50 (s), 39.39 (s), 52.47 (s), 83.80 (s), 121.66 (s), 124.34 (s), 124.91 (s), 126.26 (s), 128.39 (t), 130.13 (s), 133.06 (t), 135.75 (t), 136.21 (s), 138.28 (s), 141.38(s), 142.95(s), 144.38 (s), 152.10 (s). ³¹P{¹H} NMR (CDCl₃, 200 MHz): δ 41.50. Found (%): C, 62.40; H, 5.23; N, 6.21. C₅₈H₅₄BF₄N₅P₂Ru₅/2H₂O requires C, 62.42, H 5.33, N 6.28. HR-ESI-MS *m/z* (+): found 984.29 M⁺ (calc. 984.29), 691.13 [M⁺-ATZ]⁺ (calc. 691.13).

Na[trans-RuCl₄(DMSO)] (L = ATZ, **3; L = LTZ, **4**).** Na [trans-RuCl₄(DMSO)₂] (0.36 mmol, 0.150 g) and L (1.08 mmol, L = ATZ: 0.315 g; L = LTZ: 0.303 g) were dissolved in acetone (10 mL) and the reaction was carried out overnight. The solution was evaporated to dryness and the crude compound was purified by flash chromatography (silica gel) with dichloromethane:methanol (20:1) as the mobile phase. **3** and **4** were obtained as light-yellow precipitates (**3**: 0.128 g, 56%; **4**: 0.149 g, 66%). **3**: Found (%): C, 35.02; H, 4.22; N, 10.65; S, 5.38. C₁₉H₂₅Cl₄N₅NaORuS_{1/2}H₂O requires C, 35.29; H, 4.06; N, 10.84; S, 4.95. HR-ESI-MS *m/z* (-): found 614.96 M⁻ (calc. 614.96); **4**: Found (%): C, 35.50; H, 3.15; N, 10.55, S, 4.85. C₁₉H₁₇Cl₄N₅NaORuS_{1/2}H₂O requires C, 35.25; H, 2.96; N, 10.82; S, 4.95. HR-ESI-MS *m/z* (-): found 606.89 M⁻ (calc. 606.89).

PPh₄[trans-RuCl₄(DMSO)] (L = ATZ, **5; L = LTZ, **6**).** PPh₄Cl (1.25 mmol, 470 mg) was added to a solution of **3** (0.125 mmol, 80 mg) or **4** (0.125 mmol, 79 mg) in methanol (8 mL) and the reaction was stirred at ambient temperature for 4 h. The solution was filtered, and the filtrate was dried under vacuum. The residue was washed by distilled water (4 × 20 mL) and diethyl ether (2 × 10 mL). Compounds **5** and **6** were obtained as yellow powders (**5**: 0.083 g, 69.6%; **6**: 0.045 g, 38.6%). **5**: Found (%): C, 53.66; H, 4.83; N, 7.24; S, 3.96. C₄₃H₄₅Cl₄N₅OPRuS_{1/2}H₂O requires C, 53.63; H, 4.82; N, 7.28; S, 3.32. HR-ESI-MS *m/z* (-): found 614.96 M⁻ (calc. 614.96), *m/z* (+): found 339.13 X⁺ (calc. 339.13); **6**: Found (%): C, 54.24; H, 3.97; N, 7.35, S, 3.36. C₄₃H₃₇Cl₄N₅OPRuS_{1/2}H₂O requires C, 54.60; H, 3.95; N, 7.41; S, 3.38. HR-ESI-MS *m/z* (-): found 606.89 M⁻ (calc. 606.89), *m/z* (+): found 339.13 X⁺ (calc. 339.13).

Solubility in DMSO, media/DMSO, water/DMSO. UV–vis spectroscopy was used to evaluate the solubility of **1–6** in DMSO. Accordingly, solutions of **1–6** at different concentrations (5, 10, 15, 20 mM) were prepared in DMSO. The solutions were filtered using a short Celite pad and were then diluted 10 times in DMSO prior to UV–Vis measurements. The solubility of **2** was also investigated in phenol red free DMEM-F12 (DMSO 0.1%) at 0.01, 0.1, 1, 5, 10, 20 μM and in water (max DMSO 0.5%) at 1, 5, 10, 15 μM. All solutions were filtered (using a 0.2 μm syringe filter) prior to the UV–Vis measurements and the absorbance (350 nm–370 nm) was recorded using a microplate reader. The linearity between concentration and absorbance was considered as an indication of the solubility of the compounds at the desired concentrations. It is important to note that no supplementary technique was used here to evaluate if nanoaggregates were formed under these conditions.

Stability in cell culture media/DMSO. A previously developed HPLC-UV method [26] was used to measure the anastrozole (or letrozole) release in cell culture media supplemented with 0.1% DMSO. Stock solutions (10⁴ μM) of **2–5** were prepared in DMSO. 10 μM solutions of the compounds were prepared by adding 20 μL of a stock solution to 20 mL of DMEM/F12. Solutions were incubated at 37 °C for 1.5 h, and further steps were achieved as described previously [26]. Briefly, after incubation, anastrozole or letrozole was retrieved from the media solution by liquid/liquid

extraction using diethyl ether. After evaporation of the diethyl ether and after dissolving the residue in 2 mL of acetone, the solution was passed through a thin layer of silica (using 20 mL of acetone) to completely recover anastrozole (or letrozole) while minimizing the amount of undesired media residue in the final HPLC samples. Acetone was evaporated to dryness and the residue was dissolved in 1 mL of HPLC grade acetone containing 100 μM hydrocortisone as an external standard. The HPLC sample was injected into an Agilent UHPLC system (1260 Infinity GPC/SEC) using an Agilent Poroshell 120 EC-C18 column (4.6 × 100 mm, 2.7 μm) through a 13 min gradient of a mixture of acetonitrile and water at a flow rate of 2 mL/min: (a) 0–1 min, water, 100%; (b) 1–4 min, acetonitrile, 0–30%; (c) 4–10 min, acetonitrile, 30%; (d) 10–11 min, acetonitrile, 30%–100%; 11–13 min, acetonitrile, 100%. UV absorbance was acquired at 215 and standard curves of anastrozole and letrozole as the ones reported before [26] were used to quantify the amount of the aromatase inhibitors. All the experiments were carried out in three replicates.

X-ray diffraction analysis. Single crystals suitable for X-ray analysis were obtained by the room temperature slow evaporation of solutions of **1** (in ethyl acetate), **4** (in methanol), **5** (in dichloromethane), and **6** (in dichloromethane/diethyl ether). Single crystals of **2** were obtained from an ethyl acetate solution kept at 4 °C for two weeks. Cell refinement and data reduction were done using APEX2. Absorption corrections were applied using SADABS. Structures were solved by direct methods using SHELXS-97 and refined on F² by full-matrix least squares using SHELXL-97 or SHELXL-2014. All non-hydrogen atoms were refined anisotropically, whereas hydrogen atoms were refined isotropic on calculated positions using a riding model [97–99].

Cell culture. All the protocols reported for biological studies were approved by the Institutional Research Ethics Committee of INRS – Centre Armand-Frappier Santé Biotechnologie. All cell culture products were obtained from commercial sources such as Gibco, Sigma Aldrich, Corning, and Invitrogen. RPMI 1640 supplemented with fetal bovine serum (10%) was used to culture human breast cancer MCF7 and MDA-MB-231 cell lines. Human breast cancer T47D cells were grown in RPMI 1640 supplemented with HEPES (2.38 g/L), sodium pyruvate (0.11 g/L), glucose (2.5 g/L), insulin bovine (10 μg/mL), and fetal bovine serum (10%). Adrenocortical carcinoma H295R cells were grown in DMEM/F-12 supplemented with Nu Serum (2.5%) and ITS (1%). MCF12A cells were maintained in phenol Dulbecco's modified Eagle's medium Ham's F12 (DMEM/F12) culture medium supplemented with 5% (v/v) horse serum, hEGF recombinant (20 ng/mL), hydrocortisone (500 ng/mL), and insulin (10 μg/mL). All growth media were supplemented with penicillin/streptomycin. Cells were propagated according to ATCC guidelines.

Sulforhodamine B (SRB) Assay. The cytotoxicity of **2**, anastrozole and cisplatin in MCF7, T47D, MDA-MB-231 and MCF12A cells were evaluated using the SRB assay. Cells were cultured in 96-well plates (10⁴ cells/well) and incubated in 5% CO₂ at 37 °C overnight. Cells were treated with different concentrations of each compound, carrier (media containing maximum 0.5% DMSO) and positive control (media containing 25% DMSO). The plates were incubated for 48 h and further steps were done as previously reported [26]. IC₅₀ values were determined by the plots of viability versus concentration. Error bars were calculated as the standard error of three independent experiments.

Aromatase activity measurement. Aromatase activity was measured using a tritiated water-release assay. H295R cells that can express high level of aromatase enzyme *in vitro* [70] were cultured in 24-well plates (100,000 cells/well) containing 1 mL of DMEM/F-12 supplemented with Nu Serum and ITS and were incubated for 24 h. After removing the medium and washing cells with 500 μL

PBS, a volume of 250 μ L of phenol red free DMEM/F-12 containing 54 nM 1β - 3 H-androstenedione and different concentrations of anastrozole and **2** (0.1, 1, 10 and 100 nM) were added to each well, and cells were incubated for 1.5 h at 37 °C (5% CO₂). Further steps were performed as described previously [71]. Tritiated water in a liquid scintillation cocktail was counted using a Microbeta Trilux (PerkinElmer, Waltham, Massachusetts). Incubations in the absence of cells (blanks) and in the presence of DMSO 0.1% (which was the concentration used to dissolve the complexes in the growth media for this study) were included as controls.

Zebrafish embryo assay. Wild-type zebrafish (*Danio rerio*) embryos were raised at 28.5 °C and staged as previously described [100]. Embryos at the 2-cell or 4-cell stage were seeded in 6-well plates and exposed to 5 mL fish medium containing **2** at different concentrations (0.1, 0.5, 1 μ M). Final concentration of DMSO in which the stock solutions were prepared was 0.5%. The mortality, gross morphology, and hatching rates of the zebrafish embryos without and with the desired compounds were observed every 24 h for a period of 96 h under a stereo microscope (Leika S6E). The medium (containing the compound to be tested) was refreshed after 48 h for each experiment. A no-treatment control was also included. Experiments were performed in triplicates, and a total of 60 embryos from the pooling of three different crosses have been used per each treatment. Zebrafish experiments were performed following a protocol approved by the Canadian Council for Animal Care (CCAC) and our local animal care committee.

Virtual docking of compound 2 to human aromatase. Human aromatase (PDB entry 5JL6) was previously solvated with water molecules using the YASARA minimization system and standard protocols [101]. Complex **2** was used as ligand and its structure was generated with the XT structure solution program and refined using a least squares minimization protocol [26]. Compound **2** was then used in combination with the heme group as cofactor and the energetically minimized aromatase structure, as previously described [26]. We used the cavity detection standard protocol incorporated in the Molegro Virtual Docker 6.0 suite as first step to identify and establish the active-site cavity of the enzyme. The best ternary complex solution for this compound was obtained after a 20-run simulation of 3,500 iteration cycles with an initial population of 100 conformers per iteration. The preferred conformer arose from a protocol that explored up to 7,000,000 combinations. The MolDock scoring function was used to score the best conformer solution without the incorporation of solvent molecules [102]. USCF Chimera 1.1 was used for molecular structure visualization [45].

Accession Codes

CCDC 1962264–1962268 contain the supplementary crystallographic data for this paper. These data can be obtained free of charge via www.ccdc.cam.ac.uk/data_request/cif, or by emailing data_request@ccdc.cam.ac.uk, or by contacting The Cambridge Crystallographic Data Centre, 12 Union Road, Cambridge CB2 1EZ, UK; fax: +44 1223 336033.

Declaration of competing interest

The authors declare that they have no known competing financial interests or personal relationships that could have appeared to influence the work reported in this paper.

Acknowledgements

This work was supported by the Institut national de la recherche scientifique (INRS), the Natural Sciences and Engineering Research

Council of Canada (NSERC) (A.C., J.T.S. and N.D.), the Fonds de Recherche du Québec Santé (FRQS) (A.C., S.A.P., N.D.), the Canadian Institutes of Health Research (CIHR) (S.A.P.), the Canada Foundation for Innovation (CFI) (A.C., S.A.P., and N.D.), the National Institutes of Health (NIH) (N.D.) and the Armand-Frappier Foundation (scholarship to G.G.). We would like to thank Prof. David Chatenet and Prof. Isabelle Plante for providing the human cancer cell lines used in this study, as well as Prof. Charles Ramassamy for providing access to his laboratory instrumentation.

Appendix A. Supplementary data

Supplementary data to this article can be found online at <https://doi.org/10.1016/j.ejmech.2019.112030>.

References

- [1] C.S. Allardyce, P.J. Dyson, Metal-based drugs that break the rules, *Dalton Trans.* 45 (2016) 3201–3209.
- [2] R.H. Berndsen, A. Weiss, U.K. Abdul, T.J. Wong, P. Meraldi, A.W. Griffioen, P.J. Dyson, P. Nowak-Sliwinska, Combination of ruthenium(II)-arene complex [Ru(η^6 -p-cymene)Cl₂(pta)] (RAPTA-C) and the epidermal growth factor receptor inhibitor erlotinib results in efficient angiostatic and antitumor activity, *Sci. Rep.* 7 (2017) 43005.
- [3] T.C. Johnstone, G.Y. Park, S.J. Lippard, Understanding and improving platinum anticancer drugs—phenanthriplatin, *Anticancer Res.* 34 (2014) 471–476.
- [4] J. Li, L. Guo, Z. Tian, S. Zhang, Z. Xu, Y. Han, R. Li, Y. Li, Z. Liu, Half-sandwich iridium and ruthenium complexes: effective tracking in cells and anticancer studies, *Inorg. Chem.* 57 (2018) 13552–13563.
- [5] D.S. Williams, G.E. Atilla, H. Bregman, A. Arzoumanian, P.S. Klein, E. Meggers, Switching on a signaling pathway with an organoruthenium complex, *Angew. Chem. Int. Ed.* 44 (2005) 1984–1987.
- [6] K.S.M. Smalley, R. Contractor, N.K. Haass, A.N. Kulp, G.E. Atilla-Gokcemen, D.S. Williams, H. Bregman, K.T. Flaherty, M.S. Soengas, E. Meggers, M. Herlyn, An organometallic protein kinase inhibitor pharmacologically activates p53 and induces apoptosis in human melanoma cells, *Cancer Res.* 67 (2007) 209–217.
- [7] E. Alessio, Thirty years of the drug candidate NAMI-A and the myths in the field of ruthenium anticancer compounds: a personal perspective, *Eur. J. Inorg. Chem.* 2017 (2017) 1549–1560.
- [8] S. Leijen, S.A. Burgers, P. Baas, D. Plum, M. Tibben, E. van Werkhoven, E. Alessio, G. Sava, J.H. Beijnen, J.H.M. Schellens, Phase I/II study with ruthenium compound NAMI-A and gemcitabine in patients with non-small cell lung cancer after first line therapy, *Investig. New Drugs* 33 (2015) 201–214.
- [9] A.A. Holder, L. Lilje, W.R. Browne, M.A.W. Lawrence, J.L. Bullock, *Ruthenium Complexes: Photochemical and Biomedical Applications*, first ed., Wiley-VCH, 2017.
- [10] H.A. Burris, S. Bakewell, J.C. Bendell, J. Infante, S.F. Jones, D.R. Spigel, G.J. Weiss, R.K. Ramanathan, A. Ogden, D. Von Hoff, Safety and activity of IT-139, a ruthenium-based compound, in patients with advanced solid tumours: a first-in-human, open-label, dose-escalation phase I study with expansion cohort, *ESMO Open* 1 (2016), e000154.
- [11] S. Monro, K.L. Colón, H. Yin, J. Roque, P. Konda, S. Gujar, R.P. Thummel, L. Lilje, C.G. Cameron, S.A. McFarland, Transition metal complexes and photodynamic therapy from a tumor-centered approach: challenges, opportunities, and highlights from the development of TLD1433, *Chem. Rev.* 119 (2019) 797–828.
- [12] A. Bergamo, C. Gaidon, J.H.M. Schellens, J.H. Beijnen, G. Sava, Approaching tumour therapy beyond platinum drugs: status of the art and perspectives of ruthenium drug candidates, *J. Inorg. Biochem.* 106 (2012) 90–99.
- [13] S. Thota, D.A. Rodrigues, D.C. Crans, E.J. Barreiro, Ru(II) compounds: next-generation anticancer metallodrugs? *J. Med. Chem.* 61 (2018) 5805–5821.
- [14] S. Bonnet, Why develop photoactivated chemotherapy? *Dalton Trans.* 47 (2018) 10330–10343.
- [15] D. Wernitznig, K. Kiakos, G. Del Favero, N. Harrer, H. Machat, A. Osswald, M.A. Jakupec, A. Wernitznig, W. Sommergruber, B.K. Keppler, First-in-class ruthenium anticancer drug (KP1339/IT-139) induces an immunogenic cell death signature in colorectal spheroids in vitro, *Metalomics* 11 (2019) 1044–1048.
- [16] A. Castonguay, C. Doucet, M. Juhas, D. Maysinger, New ruthenium(II)-Letrozole complexes as anticancer therapeutics, *J. Med. Chem.* 55 (2012) 8799–8806.
- [17] K.J. Kilpin, P.J. Dyson, Enzyme inhibition by metal complexes: concepts, strategies and applications, *Chem. Sci.* 4 (2013) 1410–1419.
- [18] C. Mu, K.E. Prosser, S. Harrypersad, G.A. MacNeil, R. Panchmatia, J.R. Thompson, S. Sinha, J.J. Warren, C.J. Walsby, Activation by oxidation: ferrocene-functionalized Ru(II)-arene complexes with anticancer, antibacterial, and antioxidant properties, *Inorg. Chem.* 57 (2018) 15247–15261.

- [19] W.H. Ang, L.J. Parker, A. De Luca, L. Juillerat-Jeanneret, C.J. Morton, M. Lo Bello, M.W. Parker, P.J. Dyson, Rational design of an organometallic glutathione transferase inhibitor, *Angew. Chem. Int. Ed.* 48 (2009) 3854–3857.
- [20] R.W. Brueggemeier, J.C. Hackett, E.S. Diaz-Cruz, Aromatase inhibitors in the treatment of breast cancer, *Endocr. Rev.* 26 (2005) 331–345.
- [21] P.E. Goss, K. Strasser, Aromatase inhibitors in the treatment and prevention of breast cancer, *J. Clin. Oncol.* 19 (2001) 881–894.
- [22] R. Jeselsohn, J.S. Bergholz, M. Pun, M. Cornwell, W. Liu, A. Nardone, T. Xiao, W. Li, X. Qiu, G. Buchwalter, A. Feiglin, K. Abell-Hart, T. Fei, P. Rao, H. Long, N. Kwiatkowski, T. Zhang, N. Gray, D. Melchers, R. Houtman, X.S. Liu, O. Cohen, N. Wagle, E.P. Winer, J. Zhao, M. Brown, Allele-specific chromatin recruitment and therapeutic vulnerabilities of ESR1 activating mutations, *Cancer Cell* 33 (2018) 173–186, e175.
- [23] I.E. Krop, I.A. Mayer, V. Ganju, M. Dickler, S. Johnston, S. Morales, D.A. Yardley, B. Melichar, A. Forero-Torres, S.C. Lee, R. de Boer, K. Petrakova, S. Vallentin, E.A. Perez, M. Piccart, M. Ellis, E. Winer, S. Gendreau, M. Derynck, M. Lackner, G. Levy, J. Qiu, J. He, P. Schmid, Pictilisib for oestrogen receptor-positive, aromatase inhibitor-resistant, advanced or metastatic breast cancer (FERGI): a randomised, double-blind, placebo-controlled, phase 2 trial, *Lancet Oncol.* 17 (2016) 811–821.
- [24] M. O'Neill, F.E.M. Paulin, J. Vendrell, C.W. Ali, A.M. Thompson, The aromatase inhibitor letrozole enhances the effect of doxorubicin and docetaxel in an MCF7 cell line model, *BioDiscovery* 6 (2012), e8940.
- [25] A.A. Miranda, J. Limon, F.L. Medina, C. Arce, J.W. Zinser, E.B. Rocha, C.M. Villarreal-Garza, Combination treatment with aromatase inhibitor and capecitabine as first- or second-line treatment in metastatic breast cancer, *J. Clin. Oncol.* 30 (2012), e11016.
- [26] G. Golbaghi, M.M. Haghdoust, D. Yancu, Y. López de los Santos, N. Doucet, S.A. Patten, J.T. Sanderson, A. Castonguay, Organoruthenium(II) complexes bearing an aromatase inhibitor: synthesis, characterization, in vitro biological activity and in vivo toxicity in zebrafish embryos, *Organometallics* 38 (2019) 702–711.
- [27] M.M. Haghdoust, G. Golbaghi, M. Letourneau, S.A. Patten, A. Castonguay, Lipophilicity-antiproliferative activity relationship study leads to the preparation of a ruthenium(II) arene complex with considerable in vitro cytotoxicity against cancer cells and a lower in vivo toxicity in zebrafish embryos than clinically approved cis-platin, *Eur. J. Med. Chem.* 132 (2017) 282–293.
- [28] M.M. Haghdoust, J. Guard, G. Golbaghi, A. Castonguay, Anticancer activity and catalytic potential of ruthenium(II)–Arene complexes with N,O-donor ligands, *Inorg. Chem.* 57 (2018) 7558–7567.
- [29] J.P.C. Coverdale, I. Romero-Canelón, C. Sanchez-Cano, G.J. Clarkson, A. Habtemariam, M. Wills, P.J. Sadler, Asymmetric transfer hydrogenation by synthetic catalysts in cancer cells, *Nat. Chem.* 10 (2018) 347–354.
- [30] V. Moreno, J. Lorenzo, F.X. Aviles, M.H. Garcia, J.P. Ribeiro, T.S. Morais, P. Florindo, M.P. Robalo, Studies of the antiproliferative activity of ruthenium(II) cyclopentadienyl-derived complexes with nitrogen coordinated ligands, *Bioinorg. Chem. Appl.* 2010 (2010) 11.
- [31] L. Côte-Real, F. Mendes, J. Coimbra, T.S. Morais, A.I. Tomaz, A. Valente, M.H. Garcia, I. Santos, M. Bicho, F. Marques, Anticancer activity of structurally related ruthenium(II) cyclopentadienyl complexes, *J. Biol. Inorg. Chem.* 19 (2014) 853–867.
- [32] B.T. Loughrey, P.C. Healy, P.G. Parsons, M.L. Williams, Selective cytotoxic Ru(II) arene cp* complex salts [R-PhRuCp*]⁺X⁻ for X = BF₄⁻, PF₆⁻, and BPh₄⁻, *Inorg. Chem.* 47 (2008) 8589–8591.
- [33] S. Thangavel, R. Rajamanikandan, H.B. Friedrich, M. Ilanchelian, B. Omondi, Binding interaction, conformational change, and molecular docking study of N-(pyridin-2-ylmethylene)aniline derivatives and carbazole Ru(II) complexes with human serum albumins, *Polyhedron* 107 (2016) 124–135.
- [34] P.R. Florindo, D.M. Pereira, P.M. Borralho, C.M.P. Rodrigues, M.F.M. Piedade, A.C. Fernandes, Cyclopentadienyl–Ruthenium(II) and iron(II) organometallic compounds with carbohydrate derivative ligands as good colorectal anticancer agents, *J. Med. Chem.* 58 (2015) 4339–4347.
- [35] V. Moreno, M. Font-Bardia, T. Calvet, J. Lorenzo, F.X. Avilés, M.H. Garcia, T.S. Morais, A. Valente, M.P. Robalo, DNA interaction and cytotoxicity studies of new ruthenium(II) cyclopentadienyl derivative complexes containing heteroaromatic ligands, *J. Inorg. Biochem.* 105 (2011) 241–249.
- [36] L. Côte-Real, M.P. Robalo, F. Marques, G. Nogueira, F. Aveccilla, T.J.L. Silva, F.C. Santos, A.I. Tomaz, M.H. Garcia, A. Valente, The key role of coligands in novel ruthenium(II)–cyclopentadienyl bipyridine derivatives: ranging from non-cytotoxic to highly cytotoxic compounds, *J. Inorg. Biochem.* 150 (2015) 148–159.
- [37] P. Florindo, I.J. Marques, C.D. Nunes, A.C. Fernandes, Synthesis, characterization and cytotoxicity of cyclopentadienyl ruthenium(II) complexes containing carbohydrate-derived ligands, *J. Organomet. Chem.* 760 (2014) 240–247.
- [38] T.S. Morais, A. Valente, A.I. Tomaz, F. Marques, M.H. Garcia, Tracking anti-tumor metallodrugs: promising agents with the Ru(II)- and Fe(II)-cyclopentadienyl scaffolds, *Future Med. Chem.* 8 (2016) 527–544.
- [39] D. Mavrynsky, J. Rahkila, D. Bandarra, S. Martins, M. Meireles, M.J. Calhorda, I.J. Kovács, I. Zupkó, M.M. Hänninen, R. Leino, Cytotoxicities of poly-substituted chlorodicarbonyl(cyclopentadienyl) and (indenyl)ruthenium complexes, *Organometallics* 32 (2013) 3012–3017.
- [40] L. Côte-Real, R.G. Teixeira, P. Girio, E. Comsa, A. Moreno, R. Nasr, H. Baubichon-Cortay, F. Aveccilla, F. Marques, M.P. Robalo, P. Mendes, J.P.P. Ramalho, M.H. Garcia, P. Falson, A. Valente, Methyl-cyclopentadienyl ruthenium compounds with 2,2'-bipyridine derivatives display strong anticancer activity and multidrug resistance potential, *Inorg. Chem.* 57 (2018) 4629–4639.
- [41] C. Kasper, H. Alborzina, S. Can, I. Kitanovic, A. Meyer, Y. Geldmacher, M. Oleszak, I. Ott, S. Wölfl, W.S. Sheldrick, Synthesis and cellular impact of diene–ruthenium(II) complexes: a new class of organoruthenium anticancer agents, *J. Inorg. Biochem.* 106 (2012) 126–133.
- [42] N. Mendes, F. Tortosa, A. Valente, F. Marques, A. Matos, T.S. Morais, A.I. Tomaz, F. Gärtner, M.H. Garcia, In vivo performance of a ruthenium-cyclopentadienyl compound in an orthotopic triple negative breast cancer model, *Anti Cancer Agents Med. Chem.* 17 (2017) 126–136.
- [43] B. Dutta, C. Sclaro, R. Scopelliti, P.J. Dyson, K. Severin, Importance of the π -ligand: remarkable effect of the cyclopentadienyl ring on the cytotoxicity of ruthenium PTA compounds, *Organometallics* 27 (2008) 1355–1357.
- [44] G. Süß-Fink, Arene ruthenium complexes as anticancer agents, *Dalton Trans.* 39 (2010) 1673–1688.
- [45] A.I. Tomaz, T. Jakusch, T.S. Morais, F. Marques, R.F.M. de Almeida, F. Mendes, É.A. Enyedy, I. Santos, J.C. Pessoa, T. Kiss, M.H. Garcia, [Ru(II)(η^5 -C₅H₅)(bipy)(PPh₃)]⁺, a promising large spectrum antitumor agent: cytotoxic activity and interaction with human serum albumin, *J. Inorg. Biochem.* 117 (2012) 261–269.
- [46] T. Moreira, R. Francisco, E. Comsa, S. Duban-Deweer, V. Labas, A.-P. Teixeira-Gomes, L. Combes-Soia, F. Marques, A. Matos, A. Favrelle, C. Rousseau, P. Zinck, P. Falson, M.H. Garcia, A. Preto, A. Valente, Polymer “ruthenium-cyclopentadienyl” conjugates – new emerging anti-cancer drugs, *Eur. J. Med. Chem.* 168 (2019) 373–384.
- [47] T.S. Morais, T.J.L. Silva, F. Marques, M.P. Robalo, F. Aveccilla, P.J.A. Madeira, P.J.G. Mendes, I. Santos, M.H. Garcia, Synthesis of organometallic ruthenium(II) complexes with strong activity against several human cancer cell lines, *J. Inorg. Biochem.* 114 (2012) 65–74.
- [48] S. Al-Mahmood, J. Sapiezynski, O.B. Garbuzenko, T. Minko, Metastatic and triple-negative breast cancer: challenges and treatment options, *Drug Deliv. Transl. Res.* 8 (2018) 1483–1507.
- [49] G. Bianchini, J.M. Balko, I.A. Mayer, M.E. Sanders, L. Gianni, Triple-negative breast cancer: challenges and opportunities of a heterogeneous disease, *Nat. Rev. Clin. Oncol.* 13 (2016) 674–690.
- [50] R. Trondl, P. Heffeter, C.R. Kowol, M.A. Jakupc, W. Berger, B.K. Keppler, NKP-1339, the first ruthenium-based anticancer drug on the edge to clinical application, *Chem. Sci.* 5 (2014) 2925–2932.
- [51] J. Cao, Q. Wu, W. Zheng, L. Li, W. Mei, Microwave-assisted synthesis of polypyridyl ruthenium(II) complexes as potential tumor-targeting inhibitors against the migration and invasion of HeLa cells through G2/M phase arrest, *RSC Adv.* 7 (2017) 26625–26632.
- [52] F.A. Beckford, J.M. Shalowski, G. Leblanc, J. Thessing, L.C. Lewis-Alleyne, A.A. Holder, L. Li, N.P. Seeram, Microwave synthesis of mixed ligand diimine–thiosemicarbazone complexes of ruthenium(II): biophysical reactivity and cytotoxicity, *Dalton Trans.* (2009) 10757–10764.
- [53] T.J. Anderson, J.R. Scott, F. Millett, B. Durham, Decarboxylation of 2,2'-Bipyridinyl-4,4'-dicarboxylic acid diethyl ester during microwave synthesis of the corresponding trichelated ruthenium complex, *Inorg. Chem.* 45 (2006) 3843–3845.
- [54] M.M. Haghdoust, G. Golbaghi, J. Guard, S. Sielanczyk, S.A. Patten, A. Castonguay, Synthesis, characterization and biological evaluation of cationic organoruthenium(II) fluorene complexes: influence of the nature of the counteranion, *Dalton Trans.* 48 (2019) 13396–13405.
- [55] J. Geisler, Differences between the non-steroidal aromatase inhibitors anastrozole and letrozole – of clinical importance? *Br. J. Canc.* 104 (2011) 1059–1066.
- [56] J. Geisler, B. Haynes, G. Anker, M. Dowsett, P.E. Lønning, Influence of letrozole and anastrozole on total body aromatization and plasma estrogen levels in postmenopausal breast cancer patients evaluated in a randomized, crossover study, *J. Clin. Oncol.* 20 (2002) 751–757.
- [57] N. Bharti, M.R. Maurya, F. Naqvi, A. Azam, Synthesis and antiaromatic activity of new cyclooctadiene ruthenium(II) complexes with 2-acetylpyridine and benzimidazole derivatives, *Bioorg. Med. Chem. Lett.* 10 (2000) 2243–2245.
- [58] J.A. Widegren, H. Weiner, S.M. Miller, R.G. Finke, Improved synthesis and crystal structure of tetrakis(acetonitrile)(η^4 -1,5-cyclooctadiene)ruthenium(II) bis[tetrafluoroborate(1-)], *J. Organomet. Chem.* 610 (2000) 112–117.
- [59] J.J. Adams, A.S. Del Negro, N. Arulsamy, B.P. Sullivan, Unexpected formation of ruthenium(II) hydrides from a reactive dianiline precursor and 1,2-(ph₂P)₂-1,2-closo-C₂B₁₀H₁₀, *Inorg. Chem.* 47 (2008) 1871–1873.
- [60] E.A. Nyawade, H.B. Friedrich, B. Omondi, H.Y. Chenia, M. Singh, S. Gorle, Synthesis and characterization of new α,α' -diaminoalkane-bridged dicarbonyl(η^5 -cyclopentadienyl)ruthenium(II) complex salts: antibacterial activity tests of η^5 -cyclopentadienyl dicarbonyl ruthenium(II) amine complexes, *J. Organomet. Chem.* 799–800 (2015) 138–146.
- [61] E. Růba, W. Simanko, K. Mauthner, K.M. Soldouzi, C. Slugovc, K. Mereiter, R. Schmid, K. Kirchner, [RuCp(PR₃)(CH₃CN)₂]PF₆ (R = ph, me, cy). Convenient precursors for mixed ruthenium(II) and ruthenium(IV) half-sandwich complexes, *Organometallics* 18 (1999) 3843–3850.
- [62] J.-B. Sortais, N. Pannetier, A. Holuigue, L. Barloy, C. Sirlin, M. Pfeffer, N. Kyritsakis, Cyclometalation of primary benzyl amines by ruthenium(II), rhodium(III), and iridium(III) complexes, *Organometallics* 26 (2007) 1856–1867.

- [63] S. Jung, K. Ilg, C.D. Brandt, J. Wolf, H. Werner, A series of ruthenium(II) complexes containing the bulky, functionalized trialkylphosphines $^t\text{Bu}_2\text{PCH}_2\text{XC}_6\text{H}_5$ as ligands, *J. Chem. Soc., Dalton Trans.* (2002) 318–327.
- [64] E. Alessio, G. Balducci, A. Lutman, G. Mestroni, M. Calligaris, W.M. Attia, Synthesis and characterization of two new classes of ruthenium(III)-sulfoxide complexes with nitrogen donor ligands (L): $\text{Na}[\text{trans-RuCl}_4(\text{R}_2\text{SO})(\text{L})]$ and mer, cis- $\text{RuCl}_3(\text{R}_2\text{SO})(\text{R}_2\text{SO})(\text{L})$. The crystal structure of $\text{Na}[\text{trans-RuCl}_4(\text{DMSO})(\text{NH}_3)] \cdot 2\text{DMSO}$, $\text{Na}[\text{trans-RuCl}_4(\text{DMSO})(\text{Im})] \cdot \text{H}_2\text{O}$, Me_2CO (Im = imidazole) and mer, cis- $\text{RuCl}_3(\text{DMSO})(\text{DMSO})(\text{NH}_3)$, *Inorg. Chim. Acta* 203 (1993) 205–217.
- [65] A.H. Velders, A. Bergamo, E. Alessio, E. Zangrando, J.G. Haasnoot, C. Casarsa, M. Cocchietto, S. Zorzet, G. Sava, Synthesis and Chemical–Pharmacological Characterization of the Antimetastatic NAMI-A-Type Ru(III) Complexes (Hdmp)[$\text{trans-RuCl}_4(\text{dmsO-S})(\text{dmp})$], ($\text{Na}[\text{trans-RuCl}_4(\text{dmsO-S})(\text{dmp})]$), and [mer- $\text{RuCl}_3(\text{H}_2\text{O})(\text{dmsO-S})(\text{dmp})$] (dmp = 5,7-Dimethyl[1,2,4]triazolo [1,5-a]pyrimidine), *J. Med. Chem.* 47 (2004) 1110–1121.
- [66] M. Delferro, L. Marchiò, M. Tegoni, S. Tardito, R. Franchi-Gazzola, M. Lanfranchi, Synthesis, structural characterisation and solution chemistry of ruthenium(III) triazole-thiadiazine complexes, *Dalton Trans.* (2009) 3766–3773.
- [67] M. Groessl, E. Reisner, C.G. Hartinger, R. Eichinger, O. Semenova, A.R. Timerbaev, M.A. Jakupcic, V.B. Arion, B.K. Keppler, Structure–Activity relationships for NAMI-A-type complexes (HL)[$\text{trans-RuCl}_4(\text{S-dmsO})\text{ruthenate(III)}$] (L = imidazole, indazole, 1,2,4-triazole, 4-Amino-1,2,4-triazole, and 1-Methyl-1,2,4-triazole): aqution, redox properties, protein binding, and antiproliferative activity, *J. Med. Chem.* 50 (2007) 2185–2193.
- [68] I. Turel, M. Pečanac, A. Golobič, E. Alessio, B. Serli, A. Bergamo, G. Sava, Solution, solid state and biological characterization of ruthenium(III)-DMSO complexes with purine base derivatives, *J. Inorg. Biochem.* 98 (2004) 393–401.
- [69] V. Vichai, K. Kirtikara, Sulforhodamine B colorimetric assay for cytotoxicity screening, *Nat. Protoc.* 1 (2006) 1112–1116.
- [70] É. Caron-Beaudoin, J.T. Sanderson, M.S. Denison, Effects of neonicotinoids on promoter-specific expression and activity of aromatase (CYP19) in human adrenocortical carcinoma (H295R) and primary umbilical vein endothelial (HUVEC) cells, *Toxicol. Sci.* 149 (2015) 134–144.
- [71] J.T. Sanderson, W. Seinen, J.P. Giesy, M. van den Berg, 2-Chloro-s-Triazine herbicides induce aromatase (CYP19) activity in H295R human adrenocortical carcinoma cells: a novel mechanism for estrogenicity? *Toxicol. Sci.* 54 (2000) 121–127.
- [72] M. Di Nunzio, V. Valli, L. Tomás-Cobos, T. Tomás-Chisbert, L. Murgui-Bosch, F. Danesi, A. Bordonì, Is cytotoxicity a determinant of the different in vitro and in vivo effects of bioactives? *BMC Complement Altern. Med.* 17 (2017), 453–453.
- [73] M.J. Garle, J.H. Fentem, J.R. Fry, In vitro cytotoxicity tests for the prediction of acute toxicity in vivo, *Toxicol. In Vitro* 8 (1994) 1303–1312.
- [74] F. Joris, B.B. Manshian, K. Peynshaert, S.C. De Smedt, K. Braeckmans, S.J. Soenen, Assessing nanoparticle toxicity in cell-based assays: influence of cell culture parameters and optimized models for bridging the in vitro–in vivo gap, *Chem. Soc. Rev.* 42 (2013) 8339–8359.
- [75] M. Ni, Y. Chen, E. Lim, H. Wimberly, Shannon T. Bailey, Y. Imai, David L. Rimm, X. Shirley Liu, M. Brown, Targeting androgen receptor in estrogen receptor-negative breast cancer, *Cancer Cell* 20 (2011) 119–131.
- [76] A. Valente, M.H. Garcia, F. Marques, Y. Miao, C. Rousseau, P. Zinck, First polymer “ruthenium-cyclopentadienyl” complex as potential anticancer agent, *J. Inorg. Biochem.* 127 (2013) 79–81.
- [77] L. Côte-Real, A.P. Matos, I. Alho, T.S. Morais, A.I. Tomaz, M.H. Garcia, I. Santos, M.P. Bicho, F. Marques, Cellular uptake mechanisms of an anti-tumor ruthenium compound: the endosomal/lysosomal system as a target for anticancer metal-based drugs, *Microsc. Microanal.* 19 (2013) 1122–1130.
- [78] L. Côte-Real, B. Karas, A.R. Brás, A. Pilon, F. Avecilla, F. Marques, A. Preto, B.T. Buckley, K.R. Cooper, C. Doherty, M.H. Garcia, A. Valente, Ruthenium–cyclopentadienyl bipyridine–biotin based compounds: synthesis and biological effect, *Inorg. Chem.* 58 (2019) 9135–9149.
- [79] C. Scolaro, A. Bergamo, L. Brescacin, R. Delfino, M. Cocchietto, G. Laurency, T.J. Geldbach, G. Sava, P.J. Dyson, In vitro and in vivo evaluation of ruthenium(II)–Arene PTA complexes, *J. Med. Chem.* 48 (2005) 4161–4171.
- [80] A.K. Renfrew, A.D. Phillips, A.E. Egger, C.G. Hartinger, S.S. Bosquain, A.A. Nazarov, B.K. Keppler, L. Gonsalvi, M. Peruzzini, P.J. Dyson, Influence of structural variation on the anticancer activity of RAPTA-type complexes: ptn versus pta, *Organometallics* 28 (2009) 1165–1172.
- [81] S. Maurelli, M. Chiesa, E. Giamello, G. Di Nardo, V.E.V. Ferrero, G. Gilardi, S. Van Doorslaer, Direct spectroscopic evidence for binding of anastrozole to the iron heme of human aromatase. Peering into the mechanism of aromatase inhibition, *Chem. Commun. (J. Chem. Soc. Sect. D)* 47 (2011) 10737–10739.
- [82] J. Zhao, D. Zhang, W. Hua, W. Li, G. Xu, S. Gou, Anticancer activity of bifunctional organometallic Ru(II) arene complexes containing a 7-hydroxycoumarin group, *Organometallics* 37 (2018) 441–447.
- [83] Y. Liu, N.J. Agrawal, R. Radhakrishnan, A flexible-protein molecular docking study of the binding of ruthenium complex compounds to PIM1, GSK-3 β , and CDK2/Cyclin A protein kinases, *J. Mol. Model.* 19 (2013) 371–382.
- [84] P. Mandal, B.K. Kundu, K. Vyas, V. Sabu, A. Helen, S.S. Dhankhar, C.M. Nagaraja, D. Bhattacherjee, K.P. Bhabak, S. Mukhopadhyay, Ruthenium(II) arene NSAID complexes: inhibition of cyclooxygenase and anti-proliferative activity against cancer cell lines, *Dalton Trans.* 47 (2018) 517–527.
- [85] J. Weisz, In vitro assays of aromatase and their role in studies of estrogen formation in target tissues, *Cancer Res.* 42 (1982) 3295–3298.
- [86] E.D. Lephart, E.R. Simpson, [45] Assay of aromatase activity, in: *Methods in Enzymology*, Academic Press, 1991, pp. 477–483.
- [87] J.T. Sanderson, J. Boerma, G.W.A. Lansbergen, M. van den Berg, Induction and inhibition of aromatase (CYP19) activity by various classes of pesticides in H295R human adrenocortical carcinoma cells, *Toxicol. Appl. Pharm.* 182 (2002) 44–54.
- [88] O.A. Lenis-Rojas, A.R. Fernandes, C. Roma-Rodrigues, P.V. Baptista, F. Marques, D. Pérez-Fernández, J. Guerra-Varela, L. Sánchez, D. Vázquez-García, M.L. Torres, A. Fernández, J.J. Fernández, Heteroleptic mononuclear compounds of ruthenium(II): synthesis, structural analyses, in vitro anti-tumor activity and in vivo toxicity on zebrafish embryos, *Dalton Trans.* 45 (2016) 19127–19140.
- [89] N. Mandrekar, N.L. Thakur, Significance of the zebrafish model in the discovery of bioactive molecules from nature, *Biotechnol. Lett.* 31 (2008) 171–179.
- [90] C.A. MacRae, R.T. Peterson, Zebrafish as tools for drug discovery, *Nat. Rev. Drug Discov.* 14 (2015) 721–731.
- [91] S. Berghmans, P. Butler, P. Goldsmith, G. Waldron, I. Gardner, Z. Golder, F.M. Richards, G. Kimber, A. Roach, W. Alderton, A. Fleming, Zebrafish based assays for the assessment of cardiac, visual and gut function — potential safety screens for early drug discovery, *J. Pharmacol. Toxicol. Methods* 58 (2008) 59–68.
- [92] L. Côte-Real, B. Karas, P. Gírio, A. Moreno, F. Avecilla, F. Marques, B.T. Buckley, K.R. Cooper, C. Doherty, P. Falson, M.H. Garcia, A. Valente, Unprecedented inhibition of P-gp activity by a novel ruthenium-cyclopentadienyl compound bearing a bipyridine-biotin ligand, *Eur. J. Med. Chem.* 163 (2019) 853–863.
- [93] B.F. Karas, L. Côte-Real, C.L. Doherty, A. Valente, K.R. Cooper, B.T. Buckley, A novel screening method for transition metal-based anticancer compounds using zebrafish embryo-larval assay and inductively coupled plasma-mass spectrometry analysis, *J. Appl. Toxicol.* 39 (2019) 1173–1180.
- [94] M.O. Albers, E. Singleton, J.E. Yates, F.B. McCormick, Dinuclear ruthenium(II) carboxylate complexes, in: *Inorganic Syntheses*, John Wiley and Sons, Inc., 1989.
- [95] M. Bruce, N. Windsor, Cyclopentadienyl-ruthenium and -osmium chemistry. IV. Convenient high-yield synthesis of some cyclopentadienyl ruthenium or osmium tertiary phosphine halide complexes, *Aust. J. Chem.* 30 (1977) 1601–1604.
- [96] E. Alessio, G. Balducci, M. Calligaris, G. Costa, W.M. Attia, G. Mestroni, Synthesis, molecular structure, and chemical behavior of hydrogen trans-bis(dimethyl sulfoxide)tetrachlororuthenate(III) and mer-trichlorotris(dimethyl sulfoxide)ruthenium(III): the first fully characterized chloride-dimethyl sulfoxide-ruthenium(III) complexes, *Inorg. Chem.* 30 (1991) 609–618.
- [97] O.V. Dolomanov, L.J. Bourhis, R.J. Gildea, J.A.K. Howard, H. Puschmann, OLEX2: a complete structure solution, refinement and analysis program, *J. Appl. Crystallogr.* 42 (2009) 339–341.
- [98] G. Sheldrick, A short history of SHELX, *Acta Crystallogr. A* 64 (2008) 112–122.
- [99] G. Sheldrick, Crystal structure refinement with SHELXL, *Acta Crystallogr. C* 71 (2015) 3–8.
- [100] C.B. Kimmel, W.W. Ballard, S.R. Kimmel, B. Ullmann, T.F. Schilling, Stages of embryonic development of the zebrafish, *Dev. Dynam.* 203 (1995) 253–310.
- [101] E. Krieger, K. Joo, J. Lee, J. Lee, S. Raman, J. Thompson, M. Tyka, D. Baker, K. Karplus, Improving physical realism, stereochemistry, and side-chain accuracy in homology modeling: four approaches that performed well in CASP8, *Proteins: Struct., Funct., Bioinf.* 77 (2009) 114–122.
- [102] R. Thomsen, M.H. Christensen, MolDock: A new technique for high-accuracy molecular docking, *J. Med. Chem.* 49 (2006) 3315–3321.

Cationic Ru(II) cyclopentadienyl complexes with antifungal activity against several *Candida* species

Complexes de Ru (II) cyclopentadiényles cationiques ayant une activité antifongique contre plusieurs espèces de *Candida*

Authors: Golara Golbaghi, Marie-Christine Groleau, Yossef López de los Santos, Nicolas Doucet, Eric Deziel, and Annie Castonguay*

INRS - Institut Armand-Frappier, Université du Québec, 531 boul. des Prairies, Laval, Québec, H7V 1B7, Canada

This article was accepted for publication in ChemBioChem – Special issue Metals in Medicine (June 2020)

Contribution of authors:

Golara Golbaghi designed and performed the biology and chemistry experiments, the statistical analyses and wrote the original draft of the manuscript.

Marie-Christine Groleau trained me to perform *in vitro* antifungal experiments.

Dr. Yossef López de los Santos performed the Docking simulations.

Professors Eric Deziel and Nicolas Doucet were our collaborators who provided us with their knowledge, materials and facilities to perform antifungal experiments and theoretical studies, respectively.

Prof. Annie Castonguay obtained the research funding, supervised the project and participated in conceptualization, writing and revising the manuscript.

Cationic Ru(II) cyclopentadienyl complexes with antifungal activity against several *Candida* species

Golara Golbaghi,^[a] Marie-Christine Groleau,^[b] Yossef López de los Santos,^[b] Nicolas Doucet,^[b] Eric Déziel,^[b] and Annie Castonguay*^[a]

Special issue Metals in Medicine (academic editor: Gilles Gasser)

[a] *Organometallic Chemistry Laboratory for the Design of Catalysts and Therapeutics*
INRS-Centre Armand-Frappier Santé Biotechnologie, Laval, Canada
E-mail: annie.castonguay@inrs.ca

[b] INRS-Centre Armand-Frappier Santé Biotechnologie, Laval, Canada

Supporting information for this article is given via a link at the end of the document.

Abstract: Fungal infections, including those caused by antifungal-resistant *Candida*, are a very challenging health problem worldwide. Whereas different ruthenium complexes were previously studied for their anti-*Candida* potential, Ru-cyclopentadienyl complexes were overlooked. Here, we report an antifungal activity assessment of three Ru-cyclopentadienyl complexes with some insights into their potential mode of action. Among these complexes, only cationic species [Ru-ACN]⁺ and [Ru-ATZ]⁺ displayed a significant antifungal activity against different *Candida* strains, notably against the ones that did not respond to one of the most currently used antifungal drugs fluconazole (FCZ). However, no apparent activity was observed for the neutral species, Ru-Cl, indicating the important role of the cationic backbone of these complexes on their biological activity. We suggest that reactive oxygen species (ROS) generation might be involved in the mechanism of action of these complexes as unlike neutral Ru-Cl, [Ru-ACN]⁺ and [Ru-ATZ]⁺ could generate intracellular concentration-dependent ROS. We also observed a correlation between the ruthenium cellular uptake, ROS generation and fungal growth inhibitory activity of the compounds. Furthermore, docking simulations showed that the CYP51 enzyme can form more energetically favorable complexes with [Ru-ATZ]⁺ than fluconazole (FCZ), suggesting that CYP51 inhibition could also be considered as a potential mode of action.

Introduction

Infectious diseases are a common cause of serious health problems worldwide. Despite notable recent advances in the field of antifungal therapy, considerable efforts are devoted to the treatment of fungal infections.^[1-3] Notably, the treatment of candidiasis still remains challenging, as antifungal resistance emergence can limit the clinical use of currently used antifungal drugs.^[4] Moreover, *Candida* infections are often reported as a common cause of bloodstream infections.^[5] Although *Candida albicans* is the predominant cause of *Candida* infections, an alteration in the epidemiology of this type of infection has been observed in recent years.^[6-9] Due to the selection of less sensitive *Candida* strains, the widespread use of azole-containing drugs

such as FCZ resulted in a considerable rise of infections caused by other species of *Candida*.^[7, 9] Although current treatment guidelines include FCZ as one of the most common options for the treatment of candidiasis, the azole resistance of multiple strains limits its clinical use.^[8, 10-12] For some *Candida* species, notably *C. glabrata*, *C. krusei* and *C. auris*, the increasing rate of azole resistance is prevalent,^[7-8, 11, 13-14] emphasizing the importance of finding alternatives for the treatment of these infections. The mode of action of azole-containing antifungal agents involves the inhibition of 14 α -lanosterol demethylase (CYP51), a key enzyme in the biosynthesis of ergosterol (resulting in its depletion).^[15-16] Ergosterol is the major component of the fungal cell membrane, and plays an essential role as a bioregulator of membrane fluidity and integrity.^[17-18] Azole-containing antifungal drugs can block the catalytic activity of the CYP51 enzyme by the interaction of one of their azole ring nitrogen atoms with the iron cofactor.^[19-20] Although the main mechanisms of fluconazole-resistance were found to involve an increased drug efflux, an alteration or overexpression of the drug target, and the development of compensatory pathways for producing ergosterol, resistance mechanisms remain unidentified for some of the strains.^[10]

To identify alternatives to currently used drugs, some efforts were devoted to the design of metal-based antifungal agents. Indeed, metal complexes display reactivities that differ from simple organic molecules, and could potentially lead to the discovery of therapeutics with unique properties and/or modes of action.^[21] Although numerous compounds based on various other metals (Cu, Ni, Zn, Co, Ag, Pd, etc) were previously reported for their activity against a wide range of fungal species including *Candida*,^[22-30] our long-standing interest in the biological activity of ruthenium complexes prompted us to investigate the promising antifungal potential of compounds based on this particular metal.^[31-50] It is noteworthy that ruthenium complexes are currently extensively studied for their anticancer properties and are even now considered as potential alternatives to cisplatin, a chemotherapeutic agent currently widely used in clinical settings.^[51-55]

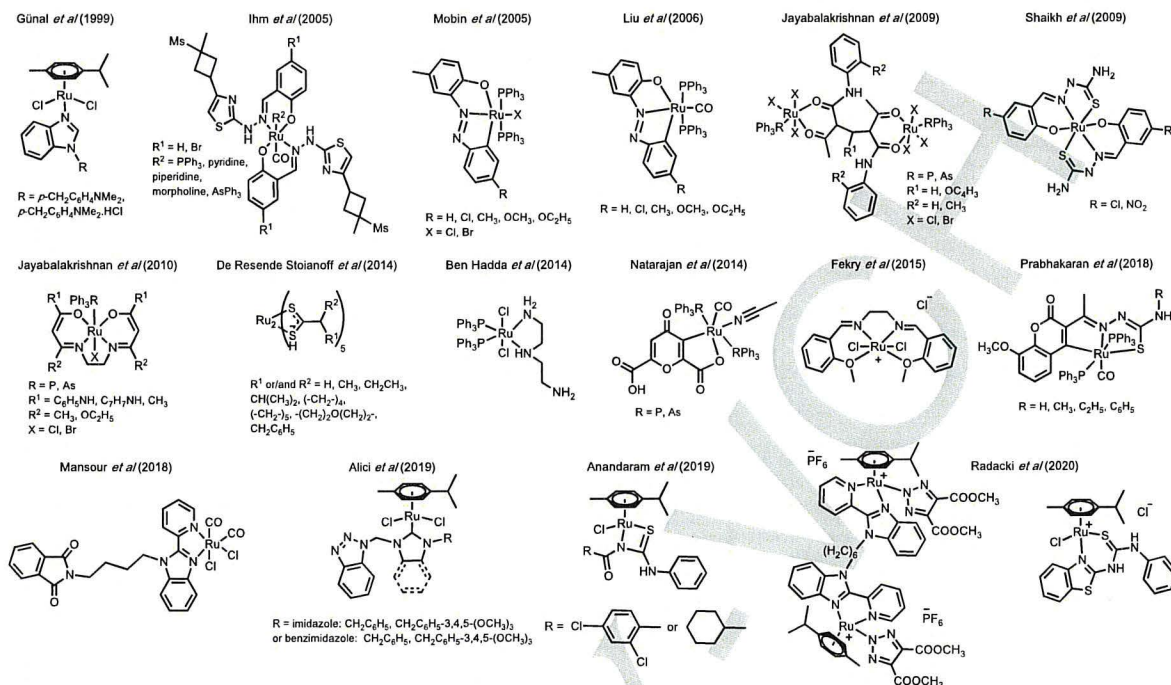


Figure 1. Chemical structures of ruthenium complexes previously tested for their anti-*Candida* properties.

For instance, Turel *et al* reported Ru(II) complexes bearing antifungalazole-containing drugs clotrimazole, miconazole, and tioconazole that could inhibit the growth of *Curvularia lunata*.^[31] In another study, Sivagamasundari *et al* noted the antifungal activity of Ru(II) complexes against *Aspergillus flavus*.^[33] Notably, several ruthenium species were also previously studied for their potential anti-*Candida* properties (Figure 1).^[34–50] Some of the first examples were reported by Günal *et al* (1999) and consisted in a series of Ru(II)-cymene complexes with promising activities against different fungal species including *C. albicans* and *C. tropicalis*.^[44] Since then, most reports of ruthenium species with an anti-*Candida* activity (Figure 1) showed a superior antifungal activity for the complexes compared to their corresponding ligands, suggesting an important role of the ruthenium moiety in the observed antifungal activity.^[35–41] Although lipophilicity and steric factors have been reported to affect the antifungal activity of the ruthenium complexes,^[37, 41] the anti-*Candida* modes of action of these compounds remain elusive. The notable differences in the *in vitro* experimental parameters reported in these studies (such as time of incubation, type of assay, temperature, etc), prevent a direct comparison of their activities. Nevertheless, to provide a complete overview, a summary of the antifungal activity of ruthenium complexes tested against *Candida* species is provided in Table S1.

The study presented here was motivated *i*) by the fact that, although several organoruthenium complexes were previously studied for this purpose,^[34, 40–41, 44–48] the antifungal activity of Ru(II)-cyclopentadienyl complexes has so far scarcely been examined, but also *ii*) by the unique features of a cationic Ru(II)-

cyclopentadienyl complex of anastrozole (ATZ) we recently reported ([Ru-ATZ]⁺, Figure 2), which showed promising stability in biologically relevant conditions, *in vitro* anticancer activity against different human breast cancer cell lines and low systemic *in vivo* toxicity on the development of zebrafish embryos.^[56] ATZ is a triazole-containing aromatase inhibitor that inhibits the activity of the human P450 enzyme CYP19, aromatase, by blocking the production of estrogen in postmenopausal women diagnosed with estrogen receptor-positive breast cancer.^[56] Given the similarity between the anti-aromatase (CYP19) mode of action of ATZ and the anti-CYP51 mode of action of theazole-containing antifungal drugs such as FCZ,^[19] both involving an interaction between a triazole nitrogen^[57] and the iron of a P450 enzyme cofactor, we reasoned that the presence of a metal-uncoordinated triazole moiety in [Ru-ATZ]⁺ could be a factor enhancing its antifungal activity. It is interesting to note that Turel *et al* previously reported a similar approach with Ru-cymene complexes bearingazole-containing antifungal agents for the treatment of a non-*Candida* fungal species, *Curvularia lunata*. However, the interaction between the ruthenium complexes and the CYP51 enzyme was found unlikely to occur in this system because of the involvement of theazole ring in the coordination sphere of the metal.^[31]

Herein, we report an *in vitro* evaluation of the antifungal activity of [Ru-ATZ] and a few related Ru(II)-cyclopentadienyl complexes (Figure 2) against a range of *Candida* species and their relative ability to generate reactive oxygen species (ROS) in *C. glabrata*.

Results and Discussion

Ru-Cl, [Ru-ACN]⁺ and [Ru-ATZ]⁺ (Figure 2) were synthesized and purified according to previously reported procedures.^[56, 58-59] Due to the generally poor water-solubility of metal-based drug candidates, the preparation of stock solutions of these compounds in an organic solvent (usually DMSO), followed by their dilution in cell growth media, is routinely achieved prior to testing their biological activity.^[60-61] Although DMSO is commonly used for this purpose, the solubility^[61] and stability assessment of drug candidates in this solvent are often overlooked. Indeed, due to the coordinative nature of DMSO, ruthenium complexes are prone to undergo DMSO-mediated ligand dissociation, which may alter the nature and consequently the biological properties of the species being tested.^[56, 60] UV-Vis spectra of DMSO solutions of complexes Ru-Cl, [Ru-ACN]⁺ and [Ru-ATZ]⁺ (after filtration) recorded at various concentrations suggested their solubility to be considerable up to 10, 15 and 20 mM,^[56] respectively (Figure S1). The three complexes were also found to be highly stable in DMSO, as no spectral alteration was observed by UV-Vis (at 0.8 mM) up to at least 30 minutes (Figure S2).^[56]

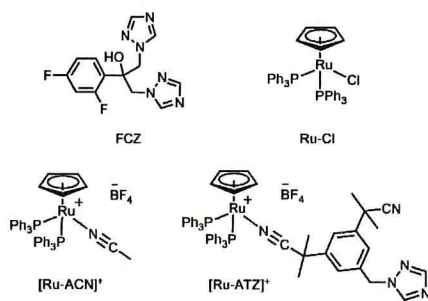


Figure 2. Chemical structures of the species investigated in this study.

The *in vitro* antifungal activity of the three complexes was evaluated against five different *Candida* species (*albicans*, *glabrata*, *tropicalis*, *krusei* and *lusitanae*). Their activity was also assessed against a *Cryptococcus neoformans* strain, an emerging pathogen, including as a cause of a meningitis with a high death rate partly due to its emerging resistance to antifungal drugs such as FCZ.^[56] For comparison purposes, the activity of FCZ, ATZ and sodium tetrafluoroborate was also tested. A time-kill kinetic analysis (at 1 h intervals over 24 h) was initially performed to screen the growth inhibitory activity of all compounds at a single concentration (20 μM) on all six strains by performing optical density measurements at 600 nm (OD₆₀₀, representative of cell concentration) (Figure S3). Importantly, no antifungal activity was observed for neutral complex Ru-Cl, ATZ nor sodium tetrafluoroborate at 20 μM (data not shown), whereas complexes [Ru-ACN]⁺ and [Ru-ATZ]⁺ could significantly inhibit the growth of all tested strains, suggesting an important role for the cationic ruthenium complex backbone on the antifungal properties of the species, and a negligible contribution of the BF₄ counterion of these complexes. In addition, the lack of activity of ATZ on all strains suggests that the presence of a triazole ring in the structure of a given compound is not warrant of its antifungal

activity (most likely resulting from an interaction with CYP51). Minimal inhibitory concentrations (MIC) values were then determined for both cationic complexes and FCZ after 24 h using the broth microdilution method (Table 1).

Table 1. *In vitro* antifungal susceptibility (minimum inhibitory concentration, MIC) (μM) of Ru-Cl, [Ru-ACN]⁺, [Ru-ATZ]⁺ and FCZ (24 h).

| Species | Ru-Cl | [Ru-ACN] ⁺ | [Ru-ATZ] ⁺ | FCZ |
|----------------------|-------|-----------------------|-----------------------|------------|
| <i>C. albicans</i> | >20 | 3.5 ± 0.9 | 3.6 ± 0.9 | 4.7 ± 2.2 |
| <i>C. glabrata</i> | >20 | 5.6 ± 2.1 | 3.5 ± 1.2 | >20 |
| <i>C. tropicalis</i> | >20 | 4.5 ± 1.5 | 3.2 ± 1.3 | 19.4 ± 0.5 |
| <i>C. krusei</i> | >20 | 5.4 ± 1.9 | 2.5 ± 0.0 | >20 |
| <i>C. lusitanae</i> | >20 | 7.9 ± 2.5 | 9.3 ± 3.7 | 2.5 ± 0.0 |
| <i>C. neoformans</i> | >20 | 2.4 ± 0.7 | 2.5 ± 0.0 | 14.2 ± 5.0 |

Importantly, for all the *Candida* strains tested, a more significant antifungal behavior of the two cationic ruthenium complexes was observed from the time-kill kinetics experiment compared to the clinically-relevant drug FCZ (Figure S3), which was further reflected by their MIC values (ranging from 2.4 - 5.6 μM) found in most cases lower than that of FCZ (except for *C. lusitanae*) (Table 1). Moreover, both cationic species induced significant growth inhibition even at a very early stage of incubation (1 - 2 h) (Figure S3). Of high importance is the significant antifungal activity of the cationic ruthenium complexes against the *Candida* strains that did not respond at all to the FCZ treatment; these species have been previously reported to develop resistance towards this drug.^[7-8, 11] For instance, MIC values for *C. glabrata* and *C. krusei* were respectively found to be 5.6 ± 2.1 μM and 5.4 ± 1.9 μM for [Ru-ACN]⁺ and 3.5 ± 1.2 μM and 2.5 ± 0.0 μM for [Ru-ATZ]⁺, whereas FCZ did not inhibit the growth of these strains at concentrations up to 20 μM. It is worth mentioning that De Resende Stoianoff *et al* also reported antifungal activity of some ruthenium complexes (Figure 1) against *C. glabrata* and *C. krusei* for which the lowest MIC values reported were 40 μM and 17 μM, respectively (Table S1).^[37] The high MIC value of FCZ compared to the considerable activity of both cationic ruthenium complexes on our *C. tropicalis* strain is also in line with recent reports on the emerging FCZ resistance of this strain.^[62-64] Prabhakaran *et al* (Figure 1) also reported some organoruthenium complexes with MIC values of 15-20 μM against *C. tropicalis* (Table S1).^[45] Interestingly, we observed lower MIC values of [Ru-ACN]⁺ (2.5 ± 0.7 μM) and [Ru-ATZ]⁺ (2.5 ± 0.0 μM) compared to that of FCZ (MIC = 14.2 ± 5.0 μM) on *C. neoformans*. It is noteworthy that a few other studies have previously showed the antifungal activity of ruthenium complexes against *C. neoformans*^[65-66] highlighting the potential of the ruthenium-based agents, in addition to candidiasis, for the treatment of cryptococcosis. For instance, Fu *et al* reported a polypyridyl ruthenium complex for which a lower MIC value (1.6 μg/mL) was obtained compared to that of FCZ (4.1 μg/mL) against *C. neoformans* after 48 h.^[66] Importantly, regardless of the nature of the nitrile-coordinated ligand in the structure of [Ru-ACN]⁺ and [Ru-ATZ]⁺ (anastrozole vs CH₃CN), comparable MIC values were

observed for these complexes. These results prompted us to collect more information on the potential mode of action of these species.

Given that the antifungal properties of several metal-based compounds have been linked to their ROS generation ability,^[67-69] we were intrigued to learn whether the ruthenium complexes reported in this study could induce the formation of ROS. Although ROS are known to be continuously formed in yeast as a by-product of the cellular metabolism of oxygen,^[70] increased levels of ROS can act as a primary trigger for apoptosis.^[71] For instance, Vannier-Santos *et al* reported a Ru(III) species that could induce a significant amount of intracellular ROS in *C. tropicalis* (IC₅₀ = 20.3 μM).^[67] Moreover, Lubart *et al* and Dong Gun *et al* also suggested the respective cytotoxicity of zinc oxide and silver nanoparticles on *C. albicans* to be mediated through ROS generation.^[68-69] Considering the importance of finding new treatments against *C. glabrata*, given some reports about its azole-drug resistance,^[72-73] this strain was selected for further studies. The production of intracellular ROS was evaluated using 2',7'-dichlorofluorescein diacetate (DCFDA), an oxidant-sensitive dye which converts to a fluorescent species 2',7'-dichlorofluorescein (DCF) upon exposure to ROS.^[74] Briefly, *C. glabrata* cells were exposed to the dye (20 μM) for 1 h following a 4 h incubation with 10 μM solutions of the three ruthenium-based complexes. Since both cationic species were previously found to induce significant cell growth inhibition at the very early stage of incubation (Figure S3), optical density (OD₆₀₀) measurements were also achieved for all complexes to monitor cell concentration during the experiment. Significant amounts of intracellular ROS were measured for cells exposed to 10 μM solutions of both cationic species, whereas ROS levels induced by neutral complex Ru-Cl were comparable to the carrier (non-treated) (Figure 3A). These results are in line with the growth inhibitory activity observed for the three complexes against *C. glabrata* (Table 1), indicating once again the importance of the cationic ruthenium backbone for the activity of the metal complex. To verify if the formation of ROS could be responsible for the antifungal activity of the cationic backbone, cells were also treated with solutions of complex [Ru-ATZ]⁺ at concentrations below and above the MIC value, notably 2 and 5 μM. Interestingly, a relationship was observed between the concentration of [Ru-ATZ]⁺ used for the treatment, the growth inhibitory activity and the intracellular ROS levels (Figure 3B). Accordingly, increasing the concentration of [Ru-ATZ]⁺ from 2 μM to 10 μM resulted in a considerable drop in cell concentration (OD₆₀₀) and a dramatic increase in intracellular ROS levels (fluorescence intensity), suggesting that ROS formation might mediate cell death in this system. Importantly, despite the similar antifungal activity of [Ru-ACN]⁺ and [Ru-ATZ]⁺ (Table 1), significantly higher ROS levels were observed in cells exposed to [Ru-ATZ]⁺ compared to those treated with [Ru-ACN]⁺, suggesting that ROS generation might not be the only antifungal mode of action for these species.

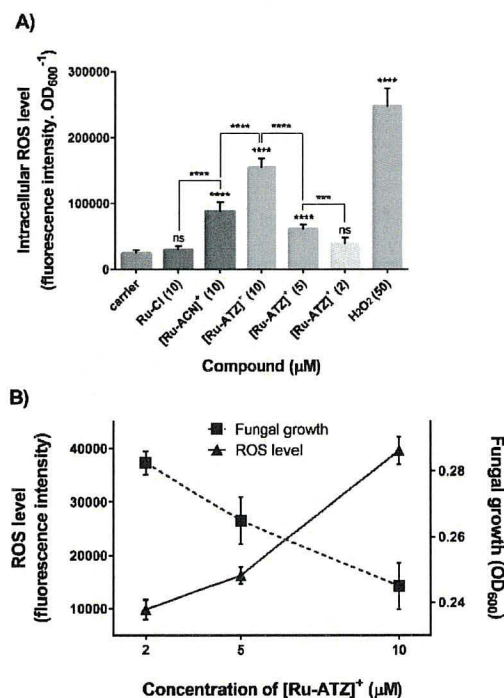


Figure 3. A) Intracellular ROS level expressed as the fluorescence intensity of DCF measured after 1h exposure of *C. glabrata* cells to DCFDA (20 μM) upon 4h treatment with Ru-Cl (10 μM), [Ru-ACN]⁺ (10 μM) and [Ru-ATZ]⁺ (2, 5, and 10 μM) (excitation at 485 nm and emission at 528 nm). H₂O₂ (50 μM) was used as a positive control. Fluorescence intensity values were normalized by cell density (OD₆₀₀). B) Relationship between concentration, ROS levels and fungal growth in *C. glabrata* cells exposed to 2, 5 and 10 μM solutions of [Ru-ATZ]⁺ for 4h. Error bars shown in the graph represent the standard deviation. Significant differences: ****p* < 0.001; *****p* < 0.0001.

In order to gain more insight into the anti-*Candida* behavior of these metal-based species, ruthenium cellular levels in *C. glabrata* cells were measured by ICP-MS after treatment with the three complexes for 4 h at the concentrations previously used for the ROS generation experiment. Notably, a significant Ru cellular uptake was observed for all treated samples (Figure 4A) compared to the carrier (0.5% DMSO). Interestingly, Ru cellular levels in *C. glabrata* cells treated with neutral complex Ru-Cl (10 μM) were significantly lower than the ones found after treatment with both cationic complexes [Ru-ACN]⁺ and [Ru-ATZ]⁺ (at the same concentration), suggesting that the lower cellular uptake of Ru-Cl might be responsible for its lack of ROS generation and hence, its lack of fungal growth inhibitory activity (Figure 4B). Importantly, Ru uptake levels noted after treatment of *C. glabrata* cells with both cationic species (10 μM) were found to be comparable (Figure 4A), and a direct correlation with their fungal growth inhibitory activity could be observed (Figure 4B). It is also noteworthy that increasing concentrations of [Ru-ATZ]⁺ led to increasing Ru levels in *C. glabrata* cells, in agreement with the concentration-dependent intracellular generation of ROS previously observed for this complex (Figure 4C). Taken together, these results suggest that [Ru-ATZ]⁺ and [Ru-ACN]⁺ most likely display their antifungal activity intracellularly, consistent with the previously formulated hypothesis that ROS generation might be involved, to some extent, in their mode of action.

Previous theoretical simulations have provided a better evaluation of the possible interactions between transition metal complexes and proteins or DNA.^[55, 75-77] Using docking simulations, we investigated plausible interactions between triazole-containing complex [Ru-ATZ]⁺ and the fungal CYP51 enzyme, allowing us to assess whether inhibition of this enzyme could possibly be involved in the mechanism of action of this species. Several molecular docking studies have previously been reported to assess possible interactions between different antifungal drug candidates and CYP51 enzymes.^[78-83] For instance, Podust *et al* showed that fluconazole binds the active site of the CYP51 enzyme by coordination to the heme iron *via* the aromatic nitrogen atom of a triazole ring and by multiple van der Waals and access tunnels. Consequently, docking simulations were performed on the CYP51 crystal structures of *C. glabrata* (PDB 5JLC) and *C. albicans* (PDB 5TZ1). For comparison purposes, docking simulations were also performed with FCZ. Results showed that, for both strains, the interaction of [Ru-ATZ]⁺ with CYP51 is energetically more favorable than with FCZ (Figure 5). Unlike with FCZ or some other reported azole-containing antifungal drug candidates^[78, 80], the interaction between the triazole ring of the [Ru-ATZ]⁺ complex and the heme cofactor is unlikely to occur, especially in the case of *C. albicans* (Figure 5C). However, a long-distance interaction (5.5 Å) was observed between the nitrogen of the triazole ring in [Ru-ATZ]⁺ and the iron of the heme cofactor in *C. glabrata* CYP51 (Figure 5B). This contact is significantly weaker than the corresponding interaction between the enzyme and FCZ in both strains in our study (3.1 Å and 3.3 Å) and a previously reported azole-containing compound (2.04 Å).^[81] In the case of the *C. glabrata* enzyme, we also observed an interaction between the nitrogen of the nitrile moiety of anastrozole in [Ru-ATZ]⁺ and the heme iron (3.0 Å). In addition to these cofactor interactions, several active-site residues are involved in stabilizing enzyme complex interactions, yielding slightly more energetically favorable complexes between CYP51 and [Ru-ATZ]⁺ over FCZ. Unlike our MIC results showing FCZ sensitivity for *C. albicans* and FCZ resistance for *C. glabrata*, similar binding energies were observed between FCZ and the CYP51 enzyme in both strains, suggesting that other resistance mechanisms are likely responsible for the lack of antifungal activity of FCZ in *C. glabrata*. These include drug efflux, alteration or increase in the drug target, and/or development of compensatory pathways for producing ergosterol^[10].

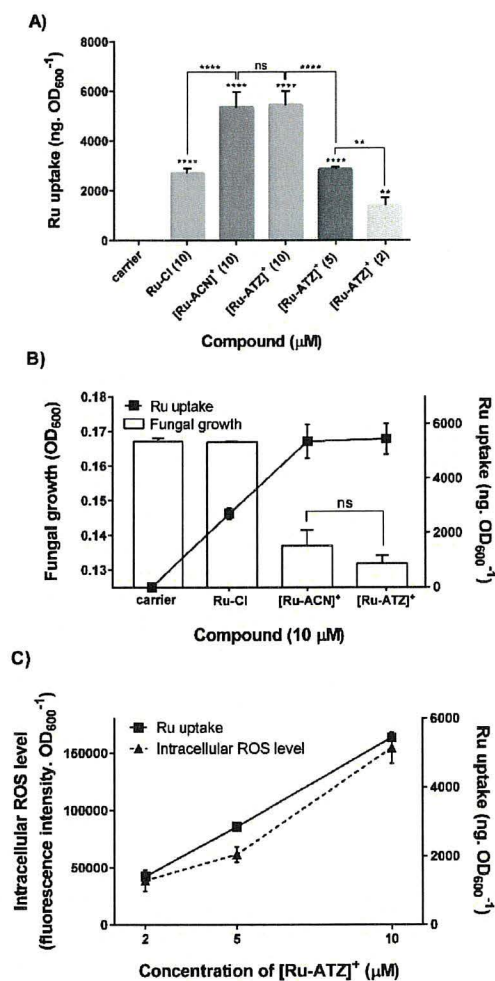


Figure 4. A) Ruthenium cellular uptake (determined by ICP-MS) after exposure of *C. glabrata* cells to Ru-Cl and [Ru-ACN]⁺ (10 μM) and [Ru-ATZ]⁺ (2, 5 and 10 μM) for 4 h. B) Correlation between Ru cellular uptake and fungal growth in *C. glabrata* cells treated with Ru-Cl, [Ru-ACN]⁺ and [Ru-ATZ]⁺ at 10 μM. Carrier (DMSO 0.5%) was used as a control. C) Correlation between Ru cellular uptake and intracellular ROS level in cells exposed to [Ru-ATZ]⁺ (2, 5 and 10 μM). Ru cellular levels (ng) and intracellular ROS levels (fluorescence intensity) represented in these graphs were normalized by cell density (OD₆₀₀) of each sample measured at the end of the incubation. Error bars in the graph represent the standard deviations. Significant differences: ****p* < 0.001, *****p* < 0.0001.

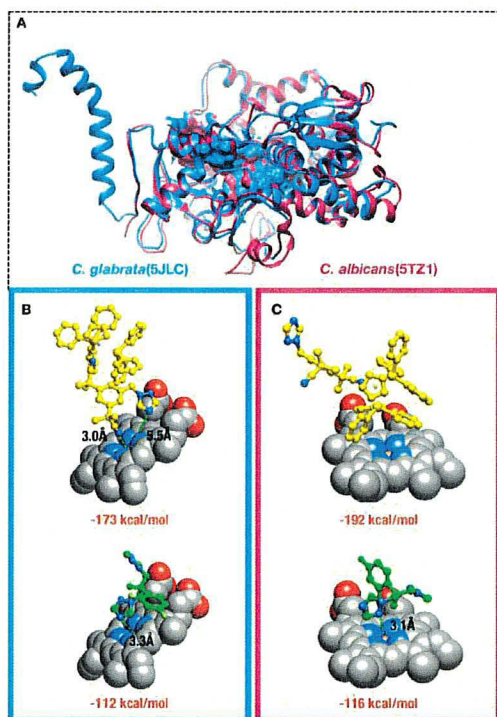


Figure 5. Predictive binding of [Ru-ATZ]⁺ and FCZ in the active-site pocket of two homologous CYP51 enzymes. A) Structural overlay of the *C. glabrata* (blue) and *C. albicans* (pink) CYP51 enzymes. Active-site pockets are shown in colored surface representation inside ribbon models. Protein folds and cavity surfaces are color coded for *C. glabrata* (blue) and *C. albicans* (pink). Molecular docking of compounds [Ru-ATZ]⁺ (yellow) and FCZ (green) relative to the heme co-factor are shown in the binary complex of B) *C. glabrata* and C) *C. albicans*. Green dash lines show distances between target positions and the iron atom of the heme cofactor. Binding energy values for each compound-enzyme binary complex are listed in red. Nitrogen atoms are shown in blue.

Conclusion

Ru(II)-cyclopentadienyl complexes were prepared and their antifungal activities investigated against five different *Candida* species and one *Cryptococcus* species. Among these complexes, only the cationic species [Ru-ACN]⁺ and [Ru-ATZ]⁺ were found to induce a significant fungal growth inhibition. This is especially interesting when considering that FCZ was not active against two of the strains we tested (*C. krusei* ED3908 and *C. glabrata* BG2) under the same conditions. Unlike the neutral complex Ru-Cl, both cationic species led to high levels of Ru cellular uptake as well as intracellular ROS generation potentially explaining their antifungal mode of action. A docking simulation suggests that interaction of [Ru-ATZ]⁺ with fungal CYP51 enzymes is energetically more favorable than that of the currently used antifungal drug FCZ, suggesting a second plausible mode of action for this compound. This study opens up the door to the development of a novel class of organometallic species, more specifically cationic ruthenium cyclopentadienyl complexes, for antifungal applications.

Experimental Section

General comments.

All chemicals were obtained from commercial sources and were used as received. Anastrozole (ATZ) was purchased from Triplebond. Fluconazole (FCZ), H₂O₂, NaBF₄ and 2',7'-Dichlorofluorescein diacetate (DCFDA) were purchased from Sigma-Aldrich. Ru-Cl, [Ru-ACN]⁺ and [Ru-ATZ]⁺ were prepared from previously reported procedures.^[56, 58-59] All syntheses were performed under a nitrogen atmosphere, and solvents were dried using a solvent purification system (Pure Process Technology). A PerkinElmer Nexion 300X ICP mass spectrometer was used for the determination of ruthenium in biological samples (Department of Chemistry, Université de Montreal). A Bioscreen C plate reader (Growth Curves USA, Piscataway, NJ, USA) and a Tecan Infinite M1000 PRO microplate reader were used to record OD₆₀₀ or/and fluorescence intensity.

Solubility and stability assessment of Ru-Cl and [Ru-ACN]⁺ in DMSO

UV-vis spectroscopy was used to evaluate the solubility of Ru-Cl and [Ru-ACN]⁺ in DMSO. Accordingly, solutions of Ru-Cl and [Ru-ACN]⁺ at different concentrations (1 - 15 mM) were prepared in DMSO. The solutions were filtered using a short celite pad and were then diluted 10 times in DMSO prior to UV-Vis measurements (at 350 nm). The linearity between concentration and absorbance was considered as an indication of the solubility of the compounds at the desired concentrations. No supplementary technique was used here to evaluate if nanoaggregates were formed under these conditions.^[61] For stability studies, a solution of Ru-Cl and [Ru-ACN]⁺ was prepared in DMSO (800 μM) and its absorption was recorded over 30 min (10 min intervals). A Tecan Infinite M1000 PRO microplate reader was used to record absorbance spectra for these experiments.

Fungal strains and growth conditions.

Six fungal strain, each one belonging to five different *Candida* species (*C. albicans* ATCC90028, *C. glabrata* BG2, *C. krusei* ED3908, *C. tropicalis* ED3910, *C. lusitanae* ED3909) and one *Cryptococcus* species (*C. neoformans* H99), were investigated. All strains were cultured at 37°C in Mueller-Hinton broth (Difco) with rotation in a TC-7 Roller Drum (New Brunswick).

Time-kill kinetic analysis.

Time-dependent killing of each fungal strain was studied by a time-kill kinetic analysis using a Bioscreen C plate reader. In brief, all the strains (at adjusted OD₆₀₀ = 0.05) in a 100-well plate were exposed to 200 μL of a 20 μM solution of each compound in triplicate wells. OD₆₀₀ was then measured over 24 h (time interval = 1h). Wells lacking compounds but containing 0.5% DMSO (carrier) and uninoculated wells (only containing growth medium, blank) were served as controls. This assay was carried out in two independent sets of experiments.

Minimum inhibitory concentration (MIC) determination.

MIC determination was achieved using the broth microdilution method.^[64] All six strains (at adjusted OD₆₀₀ = 0.05) were treated with solutions of FCZ, [Ru-ACN]⁺ or [Ru-ATZ]⁺ prepared by serial dilutions ranging from 0.15 μM to 20 μM in a 96-well plate. Stock solutions of the compounds were prepared in DMSO and were immediately diluted in fungal suspension in Mueller Hinton broth growth medium (maximum concentration of DMSO = 0.5%). MIC values were then determined visually, after 24 h of incubation at 37°C, as the lowest concentration of each compound that caused visual absence of fungal growth. Results are expressed as a mean of at least three independent sets of experiments with standard deviation.

Intracellular ROS generation.

Intracellular ROS generation was studied using a previously reported method with small modifications^[65]. Intracellular ROS levels in *C. glabrata* were measured by using an oxidant-sensitive fluorescent dye 2',7'-dichlorofluorescein diacetate (DCFDA). *C. glabrata* cells were grown in Muller-Hinton broth until reaching an OD₆₀₀ in the range of 1-1.2. Then, 1 mL of the fungal suspension was transferred to Microfuge tubes and cells were incubated with Ru-Cl and [Ru-ACN]⁺ at 10 μM and [Ru-ATZ]⁺ at 2, 5 and 10 μM for 4 h. The cells were then harvested by centrifugation (7,000 x g, 5 min) and washed two times with phosphate-buffered saline (PBS). Cells were resuspended in PBS and the fluorescent probe was added to each tube (final concentration 20 μM). After a 1 h incubation, cells were washed twice with PBS and resuspended in 1 mL PBS. 100 μL of each sample was transferred to a black 96-well plate with clear bottoms and the relative fluorescence intensity was measured using a microplate reader (excitation: 485 nm, emission: 528 nm). To evaluate the change in cell concentration for each sample, OD₆₀₀ was also measured at the end of the experiment. Carrier (cells treated only with DMSO 0.5%) and H₂O₂ (50 μM) were used as controls. This experiment was performed in three replicates per treatment.

Ruthenium cellular uptake.

Ruthenium cellular levels were measured following a procedure previously reported for metals uptake in yeast with some modifications.^[66] Briefly, a *C. glabrata* suspension at an OD₆₀₀ of 1-1.2 was prepared in growth medium. Cell solution was aliquoted to microfuge tubes (995 μL per tube). Stock solutions of Ru-Cl and [Ru-ACN]⁺ (2 mM) and [Ru-ATZ]⁺ (0.4, 1 and 2 mM) were prepared in DMSO and final concentrations of Ru-Cl and [Ru-ACN]⁺ (10 μM) and [Ru-ATZ]⁺ (2, 5 and 10 μM) were prepared by adding 5 μL of each stock solution to a corresponding tube (final DMSO concentration = 0.5%). Solutions were then incubated for 4 h after which cells were harvested by centrifugation (7,000 x g, 5 min) and washed three times with PBS. 100 μL of each sample was transferred to a clear 96-well plate and OD₆₀₀ was measured. The remaining solutions were centrifuged and digested in concentrated HNO₃ (70%, Sigma-Aldrich) for 3 days and the resulting solutions were diluted to 25 mL using Milli-Q water (final concentration of 2.8% nitric acid). To calculate Ru level per cell concentration, ng of Ru obtained from the ICP-MS measurements was divided by the OD₆₀₀ of the same sample recorded at the end of the experiment. Cells treated with DMSO (0.5%) was used as a control. Experiments were carried out in triplicates.

Virtual docking of [Ru-ATZ]⁺ and FCZ with the fungal CYP51 enzyme

Virtual docking simulations were performed using CYP51 enzyme targets from *C. glabrata* (PDB 5JLC) and *C. albicans* (PDB 5TZ1)^[67-68], in combination with ligands FCZ (PubChem CID 3365) and [Ru-ATZ]⁺ (for which single crystal X-ray diffraction data was previously reported).^[56] Ligands were generated with the XT structure solution software by applying a least square minimization refinement protocol included in the program.^[56] As first step, both CYP51 structures were solvated with water molecules and energetically minimized using the standard protocol of the YASARA software.^[69] The best conformers of both ligands arose from a docking process that simulated up to 2,000,000 ternary complexes between the CYP51 protein structure, the heme group as cofactor, and ligand molecule. During simulations, a cavity prediction algorithm was applied to delineate the active site and conformers were scored using the MolDock scoring function.^[90] The Molegro Virtual Docker 6.0 suite was used for all docking simulations and the molecular structure visualization presented here were made using UCSF Chimera 1.1.^[91]

Acknowledgements

This work was supported by the Institut national de la recherche scientifique (INRS), the Natural Sciences and Engineering Research Council of Canada (NSERC) (AC, ED, ND), the Fonds de Recherche du Québec Santé (FRQS) (AC, ND), the Canadian Institutes of Health Research (CIHR) (ED), the Canada Foundation for Innovation (CFI) (AC, ED, ND), the National Institutes of Health (NIH) (ND) and the Armand-Frappier Foundation (scholarship to GG).

Keywords: ruthenium complex • antifungal activity • *Candida* • fluconazole resistance • ROS generation

References

- [1] N. T. Grossman, C. D. Pham, A. A. Cleveland, S. R. Lockhart, *Antimicrobial Agents and Chemotherapy* **2015**, *59*, 1030-1037.
- [2] M. A. Pfaller, M. Castanheira, S. R. Lockhart, A. M. Ahlquist, S. A. Messer, R. N. Jones, *Journal of Clinical Microbiology* **2012**, *50*, 1199-1203.
- [3] R. Ben-Ami, *Journal of Fungi* **2018**, *4*, 97.
- [4] B. J. Kullberg, M. C. Arendrup, *New England Journal of Medicine* **2015**, *373*, 1445-1456.
- [5] H. Wisplinghoff, T. Bischoff, S. M. Tallent, H. Seifert, R. P. Wenzel, M. B. Edmond, *Clinical Infectious Diseases* **2004**, *39*, 309-317.
- [6] J. K. Chow, Y. Golan, R. Ruthazer, A. W. Karchmer, Y. Carmeli, D. Lichtenberg, V. Chawla, J. Young, S. Hadley, *Clinical Infectious Diseases* **2008**, *46*, 1206-1213.
- [7] M. Sanguinetti, B. Posteraro, C. Lass-Flörl, *Mycoses* **2015**, *58*, 2-13.
- [8] M. C. Arendrup, T. F. Patterson, *The Journal of Infectious Diseases* **2017**, *216*, S445-S451.
- [9] K. P. Ng, C. S. Kuan, H. Kaur, S. L. Na, N. Atiya, R. D. Velayuthan, *Tropical Medicine & International Health* **2015**, *20*, 1447-1453.
- [10] E. L. Berkow, S. R. Lockhart, *Infect Drug Resist* **2017**, *10*, 237-245.
- [11] B. Collin, C. J. Clancy, M. H. Nguyen, *Drug Resistance Updates* **1999**, *2*, 9-14.
- [12] A. Cortegiani, G. Misseri, A. Chowdhary, *Intensive Care Medicine* **2019**, *45*, 512-515.
- [13] K. Forsberg, K. Woodworth, M. Walters, E. L. Berkow, B. Jackson, T. Chiller, S. Vallabhaneni, *Medical Mycology* **2018**, *57*, 1-12.
- [14] S. R. Lockhart, *Fungal Genetics and Biology* **2019**, *131*, 103243.
- [15] G. I. Lepesheva, M. R. Waterman, *Biochim Biophys Acta* **2007**, *1770*, 467-477.
- [16] R. A. Akins, *Medical Mycology* **2005**, *43*, 285-318.
- [17] F. C. Odds, A. J. P. Brown, N. A. R. Gow, *Trends in Microbiology* **2003**, *11*, 272-279.
- [18] A. G. Sorgo, C. J. Heilmann, H. L. Dekker, M. Bekker, S. Brul, C. G. de Koster, L. J. de Koning, F. M. Klis, *Eukaryotic Cell* **2011**, *10*, 1071-1081.
- [19] A. A. Sagatova, M. V. Keniya, R. K. Wilson, B. C. Monk, J. D. A. Tyndall, *Antimicrobial agents and chemotherapy* **2015**, *59*, 4982-4989.
- [20] C.-K. Chen, S. S. F. Leung, C. Guilbert, M. P. Jacobson, J. H. McKerrow, L. M. Podust, *PLOS Neglected Tropical Diseases* **2010**, *4*, e651.
- [21] K. H. Thompson, C. Orvig, *Science* **2003**, *300*, 936-939.
- [22] Z. H. Chohan, M. Arif, M. Sarfraz, *Applied Organometallic Chemistry* **2007**, *21*, 294-302.
- [23] Z. H. Chohan, M. Arif, M. A. Akhtar, C. T. Supuran, *Bioinorganic Chemistry and Applications* **2006**, *2006*, 13.
- [24] S. H. Sumra, A. Suleman, Z. H. Chohan, M. N. Zafar, M. A. Raza, T. Iqbal, *Russian Journal of General Chemistry* **2017**, *87*, 1281-1287.
- [25] S. H. Sumra, M. Hanif, Z. H. Chohan, M. S. Akram, J. Akhtar, S. M. Al-Shehri, *Journal of Enzyme Inhibition and Medicinal Chemistry* **2016**, *31*, 590-598.
- [26] A. K. Mishra, N. K. Kaushik, *European Journal of Medicinal Chemistry* **2007**, *42*, 1239-1246.
- [27] F. Shaheen, A. Badshah, M. Gielen, G. Croce, U. Florke, D. d. Vos, S. Ali, *Journal of Organometallic Chemistry* **2010**, *695*, 315-322.
- [28] R. del Campo, J. J. Criado, E. García, M. a. R. Hermosa, A. Jiménez-Sánchez, J. L. Manzano, E. Monte, E. Rodríguez-Fernández, F. Sanz, *Journal of Inorganic Biochemistry* **2002**, *89*, 74-82.
- [29] V. Mantareva, V. Kussovski, I. Angelov, E. Borisova, L. Avramov, G. Schnurpfeil, D. Wöhrle, *Bioorganic & Medicinal Chemistry* **2007**, *15*, 4829-4835.
- [30] S. Shreaz, R. A. Sheikh, B. Rimple, A. A. Hashmi, M. Nikhat, L. A. Khan, *Microbial Pathogenesis* **2010**, *49*, 75-82.
- [31] J. Kljun, A. J. Scott, T. Lanišnik Rižner, J. Keiser, I. Turel, *Organometallics* **2014**, *33*, 1594-1601.
- [32] R. Ramesh, S. Maheswaran, *Journal of Inorganic Biochemistry* **2003**, *96*, 457-462.
- [33] R. Ramesh, M. Sivagamasundari, *Synthesis and Reactivity in Inorganic and Metal-Organic Chemistry* **2003**, *33*, 899-910.
- [34] A. M. Mansour, K. Radacki, *Polyhedron* **2020**, *175*, 114175.
- [35] R. G. de Lima, A. B. P. Lever, I. Y. Ito, R. Santana da Silva, *Transition Metal Chemistry* **2003**, *28*, 272-275.
- [36] N. P. Priya, S. V. Arunachalam, N. Sathya, V. Chinnusamy, C. Jayabalakrishnan, *Transition Metal Chemistry* **2009**, *34*, 437-445.
- [37] C. L. Donnici, L. J. Nogueira, M. H. Araujo, S. R. Oliveira, T. F. F. Magalhães, M. T. P. Lopes, A. C. A. e. Silva, A. M. d. C. Ferreira, C. V. B. Martins, M. A. De Resende Stoianoff, *Molecules* **2014**, *19*, 5402-5420.
- [38] N. Padma Priya, S. Arunachalam, N. Sathya, C. Jayabalakrishnan, *Journal of Coordination Chemistry* **2010**, *63*, 1440-1450.
- [39] T. D. Thangadurai, S.-K. Ihm, *Synthesis and Reactivity in Inorganic, Metal-Organic, and Nano-Metal Chemistry* **2005**, *35*, 499-507.
- [40] G. Venkatachalam, R. Ramesh, S. M. Mobin, *Journal of Organometallic Chemistry* **2005**, *690*, 3937-3945.
- [41] K. Naresh Kumar, R. Ramesh, Y. Liu, *Journal of Inorganic Biochemistry* **2006**, *100*, 18-26.
- [42] B. Mehta, J. Shaikh, *Special report series - Indian Council of Medical Research* **2009**, *26*, 1-6.
- [43] N. E. A. El-Gamel, A. M. Fekry, *Bioelectrochemistry* **2015**, *104*, 35-43.
- [44] B. Cetinkaya, I. Özdemir, B. Binbaştoğlu, S. Günal, *Arzneimittelforschung* **1999**, *49*, 538-540.
- [45] G. Kalaiarasi, S. R. Jeya Rajkumar, S. Dharani, F. R. Fronczek, R. Prabhakaran, *Journal of Organometallic Chemistry* **2018**, *866*, 223-242.
- [46] G. Kalaiarasi, S. R. J. Rajkumar, S. Dharani, F. R. Fronczek, M. M. Nadar, R. Prabhakaran, *New Journal of Chemistry* **2018**, *42*, 336-354.
- [47] R. Gandhaveeti, R. Konakanchi, P. Jyothi, N. S. P. Bhuvanesh, S. Anandaram, *Applied Organometallic Chemistry* **2019**, *33*, e4899.
- [48] G. Onar, C. Gürses, M. O. Karataş, S. Balcıoğlu, N. Akbay, N. Özdemir, B. Ateş, B. Alici, *Journal of Organometallic Chemistry* **2019**, *886*, 48-56.
- [49] A. M. Mansour, O. R. Shehab, K. Radacki, *European Journal of Inorganic Chemistry* **2020**, *2020*, 299-307.
- [50] M. Al-Noaimi, A. Nafady, I. Warad, R. Alshwafy, A. Husein, W. H. Talib, T. B. Hadda, *Spectrochimica Acta Part A: Molecular and Biomolecular Spectroscopy* **2014**, *122*, 273-282.
- [51] E. Alessio, L. Messori, *Molecules* **2019**, *24*, 1995.
- [52] L. Zeng, P. Gupta, Y. Chen, E. Wang, L. Ji, H. Chao, Z.-S. Chen, *Chemical Society Reviews* **2017**, *46*, 5771-5804.
- [53] F. Heinemann, J. Karges, G. Gasser, *Accounts of Chemical Research* **2017**, *50*, 2727-2736.
- [54] B. S. Murray, M. V. Babak, C. G. Hartinger, P. J. Dyson, *Coordination Chemistry Reviews* **2016**, *306*, 86-114.
- [55] G. Golbaghi, M. M. Haghdoost, D. Yancu, Y. López de los Santos, N. Doucet, S. A. Patten, J. T. Sanderson, A. Castonguay, *Organometallics* **2019**, *38*, 702-711.
- [56] G. Golbaghi, I. Pitard, M. Lucas, M. M. Haghdoost, Y. L. de los Santos, N. Doucet, S. A. Patten, J. T. Sanderson, A. Castonguay, *European Journal of Medicinal Chemistry* **2020**, *188*, 112030.
- [57] Y. Hong, H. Li, Y.-C. Yuan, S. Chen, *Annals of the New York Academy of Sciences* **2009**, *1155*, 112-120.
- [58] M. Bruce, N. Windsor, *Australian Journal of Chemistry* **1977**, *30*, 1601-1604.

FULL PAPER

- [59] H. Hebbache, T. Jerphagnon, Z. Hank, C. Bruneau, J.-L. Renaud, *Journal of Organometallic Chemistry* **2010**, *695*, 870-874.
- [60] M. Patra, T. Joshi, V. Pierroz, K. Ingram, M. Kaiser, S. Ferrari, B. Spingler, J. Keiser, G. Gasser, *Chemistry – A European Journal* **2013**, *19*, 14768-14772.
- [61] A. Notaro, G. Gasser, A. Castonguay, *ChemMedChem* **2020**, *15*, 345-348.
- [62] S. Paul, S. Singh, A. Chakrabarti, S. M. Rudramurthy, A. K. Ghosh, *Journal of Antimicrobial Chemotherapy* **2019**, *74*, 1269-1276.
- [63] J. Shao, G. Shi, T. Wang, D. Wu, C. Wang, *Frontiers in Microbiology* **2016**, *7*.
- [64] M. Castanheira, L. M. Deshpande, S. A. Messer, P. R. Rhomberg, M. A. Pfaller, *International Journal of Antimicrobial Agents* **2020**, *55*, 105799.
- [65] C. R. Madzivire, P. Caramés-Méndez, C. M. Pask, R. M. Phillips, R. M. Lord, P. C. McGowan, *Inorganica Chimica Acta* **2019**, *498*, 119025.
- [66] Q. Wang, C. Fu, Z. Zhao, A. Fu, *Molecular Pharmaceutics* **2020**, *17*, 145-154.
- [67] R. A. Gomes-Junior, R. S. da Silva, R. G. de Lima, M. A. Vannier-Santos, *FEMS Microbiology Letters* **2017**, *364*.
- [68] A. Lipovsky, Y. Nitzan, A. Gedanken, R. Lubart, *Nanotechnology* **2011**, *22*, 105101.
- [69] I.-s. Hwang, J. Lee, J. H. Hwang, K.-J. Kim, D. G. Lee, *The FEBS Journal* **2012**, *279*, 1327-1338.
- [70] N. N. Gessler, A. A. Aver'yanov, T. A. Belozerskaya, *Biochemistry (Moscow)* **2007**, *72*, 1091-1109.
- [71] F. Madeo, E. Fröhlich, M. Ligr, M. Grey, S. J. Sigrist, D. H. Wolf, K.-U. Fröhlich, *The Journal of Cell Biology* **1999**, *145*, 757-767.
- [72] J.-P. Vermitsky, T. D. Edlind, *Antimicrobial agents and chemotherapy* **2004**, *48*, 3773-3781.
- [73] M. Sanguinetti, B. Posteraro, B. Fiori, S. Ranno, R. Torelli, G. Fadda, *Antimicrobial Agents and Chemotherapy* **2005**, *49*, 668-679.
- [74] M. Degli Esposti, *Methods* **2002**, *26*, 335-340.
- [75] Y. Liu, N. J. Agrawal, R. Radhakrishnan, *Journal of Molecular Modeling* **2013**, *19*, 371-382.
- [76] H.-L. Huang, B. Tang, Q.-Y. Yi, D. Wan, L.-L. Yang, Y.-J. Liu, *Transition Metal Chemistry* **2019**, *44*, 11-24.
- [77] J. Zhao, D. Zhang, W. Hua, W. Li, G. Xu, S. Gou, *Organometallics* **2018**, *37*, 441-447.
- [78] A. Chowdhary, S. Kathuria, J. Xu, J. F. Meis, *PLoS Pathogens* **2013**, *9*, e1003633.
- [79] C.-K. Chen, S. S. F. Leung, C. Guilbert, M. P. Jacobson, J. H. McKerrow, L. M. Podust, *PLoS neglected tropical diseases* **2010**, *4*, e651-e651.
- [80] A. Macchiarulo, G. Costantino, D. Fringuelli, A. Vecchiarelli, F. Schiaffella, R. Fringuelli, *Bioorganic & Medicinal Chemistry* **2002**, *10*, 3415-3423.
- [81] F. Bohlooli, S. Sepehri, N. Razzaghi-Asl, *Computational Biology and Chemistry* **2017**, *67*, 158-173.
- [82] V. S. Pore, M. A. Jagtap, S. G. Agalave, A. K. Pandey, M. I. Siddiqi, V. Kumar, P. K. Shukla, *MedChemComm* **2012**, *3*, 484-488.
- [83] C. Sheng, W. Zhang, H. Ji, M. Zhang, Y. Song, H. Xu, J. Zhu, Z. Miao, Q. Jiang, J. Yao, Y. Zhou, J. Zhu, J. Lü, *Journal of Medicinal Chemistry* **2006**, *49*, 2512-2525.
- [84] I. Wiegand, K. Hilpert, R. E. W. Hancock, *Nature Protocols* **2008**, *3*, 163-175.
- [85] V. S. Radhakrishnan, S. P. Dwivedi, M. H. Siddiqui, T. Prasad, *Int J Nanomedicine* **2018**, *13*, 91-96.
- [86] P. Pedas, C. K. Ytting, A. T. Fuglsang, T. P. Jahn, J. K. Schjoerring, S. Husted, *Plant Physiol* **2008**, *148*, 455-466.
- [87] T. Y. Hargrove, L. Friggeri, Z. Wawrzak, A. Qi, W. J. Hoekstra, R. J. Schotzinger, J. D. York, F. P. Guengerich, G. I. Lepesheva, *J Biol Chem* **2017**, *292*, 6728-6743.
- [88] M. V. Keniya, M. Sabherwal, R. K. Wilson, M. A. Woods, A. A. Sagatova, J. D. A. Tyndall, B. C. Monk, *Antimicrobial agents and chemotherapy* **2018**, *62*, e01134-01118.
- [89] E. Krieger, K. Joo, J. Lee, J. Lee, S. Raman, J. Thompson, M. Tyka, D. Baker, K. Karplus, *Proteins* **2009**, *77 Suppl 9*, 114-122.
- [90] R. Thomsen, M. H. Christensen, *Journal of Medicinal Chemistry* **2006**, *49*, 3315-3321.
- [91] <http://www.rbvi.ucsf.edu/chimera>.

5 CONCLUSION

The focus of this Ph.D. project was on the design of novel ruthenium-based species for the treatment of breast cancer, the most common cause of cancer death among women worldwide. To this aim, a multitargeting approach was selected and several structurally different Ru(II) and Ru(III) complexes bearing aromatase inhibitors (anastrozole or letrozole) were synthesized using inert atmosphere techniques, purified and characterized using NMR spectroscopy, elemental analysis, mass spectrometry and single crystal X-ray diffraction analysis. Most of these syntheses resulted in reasonable reaction yields except the Ru(II)-COD synthesis for which a microwave-assisted reaction was then developed to improve the reaction yield and minimize the duration of the experiment. The stability and solubility of the complexes were studied by HPLC or/and UV-Vis techniques before assessing their biological activity, and this screening resulted in the exclusion of complexes that were showing stability or/and solubility issues under biologically-relevant conditions. For instance, Ru(II)-COD and Ru(III) species bearing anastrozole or letrozole could not be studied for their biological activity because of their lack of proper stability/solubility, making the Ru(II)-benzene and Ru(II)-Cp complexes the only species further examined. The *in vitro* cytotoxicity and aromatase inhibitory activity of the complexes, and their *in vivo* toxicity on the zebrafish embryonic development were then evaluated. Our results showed that some Ru(II) complexes bearing anastrozole were more cytotoxic than the currently used chemotherapeutic agent cisplatin or the aromatase inhibitor alone. Among the Ru(II) complexes, $[\text{Ru}(\eta^6\text{-C}_6\text{H}_6)(\text{PPh}_3)(\eta^1\text{-ATZ})\text{Cl}]\text{BPh}_4$ and $[\text{Ru}(\eta^5\text{-C}_5\text{H}_5)(\text{PPh}_3)_2(\text{ATZ})\text{Cl}]\text{BF}_4$, both bearing at least one lipophilic PPh_3 moiety, showed the most promising cytotoxicity on ER+ breast cancer cells. The later complex was also found to be highly cytotoxic on TNBC cells ($\text{IC}_{50} < 1\mu\text{M}$) which do not usually respond to the currently used therapeutic agents, demonstrating the potential of this type of complexes for the treatment of aggressive breast cancers. $[\text{Ru}(\eta^6\text{-C}_6\text{H}_6)(\text{PPh}_3)(\eta^1\text{-ATZ})\text{Cl}]\text{BPh}_4$ was found to slightly inhibit the aromatase activity which was evaluated experimentally and theoretically. On the other hand, despite the accessibility of the triazole ring in the structure of the $[\text{Ru}(\eta^5\text{-C}_5\text{H}_5)(\text{PPh}_3)_2(\text{ATZ})\text{Cl}]\text{BF}_4$ complex, this compound could not significantly inhibit the activity of the enzyme. We suggested that the bulkiness of the two PPh_3 moieties could be responsible for preventing the species to reach the active site of aromatase. Unlike cisplatin, the ruthenium complexes studied in the course of this project did not induce a severe toxicity on the development of zebrafish embryo at the tested concentrations, suggesting a low systematic toxicity for these species. It is noteworthy that we found a correlation between the lipophilicity, the ruthenium cellular uptake and the cytotoxicity of the complexes, more especially in the Ru(II)-benzene

series, for which the complexes bearing the lipophilic BPh₄ counterion could enter cells to a greater extent than analogous species bearing a BF₄ counterion, consequently inducing a more significant cytotoxicity. We noted that numerous properties of ruthenium complexes such as the solubility, stability, cytotoxicity and aromatase inhibitory activity can differ from one structure to the other. Our results showed that the biological activity of ruthenium complexes could benefit from lipophilic moieties such as PPh₃. We also confirmed that Ru(II)-Cp complexes are great candidates for further investigations as cancer therapeutics. It is interesting to note that, unlike Ru(II)-benzene species, Ru(II)-Cp complexes have been so far overlooked for this purpose.

Our study of the antifungal applications of Ru(II)-Cp complexes against Candidiasis infections revealed an interesting pharmaceutical potential for this type of compounds. Some of the tested complexes caused significant growth inhibitory activity in different *Candida* species, more specifically in species that did not show susceptibility to fluconazole. SAR studies showed that cationic species are more potent to induce an antifungal activity than a neutral complex. We also found that the antifungal potential of the complexes tested might be associated with their ability to generate intracellular ROS, since increasing their concentration resulted in a more important cellular uptake as well as higher intracellular ROS levels. Our theoretical studies also suggested that the Ru(II)-Cp complex bearing anastrozole ([Ru(η^5 -C₅H₅)(PPh₃)₂(ATZ)Cl]BF₄) might undergo an energetically favorable interaction with the fungal CYP51 enzyme, providing an additional mode of action for this complex. To the best of our knowledge, this is the first report of Ru(II)-Cp complexes for their anticandidal activity, making this type of compounds a new avenue for the development of novel anticandidal agents.

Finally, we conclude that some Ru(II)-benzene and Ru(II)-Cp complexes bearing an enzyme inhibitor can potentially be superior anticancer/antifungal drugs when compared to the enzyme inhibitor alone or/and a corresponding ruthenium complex that doesn't bear a biologically active ligand. Furthermore, most of the ruthenium complexes reported in our study showed a more significant therapeutic effect and a lower *in vivo* toxicity on the development of zebrafish embryos than the currently used anticancer (cisplatin) and antifungal (fluconazole) drugs, revealing that these species are promising candidates to be further investigated for a broad range of pharmaceutical applications.

6 PERSPECTIVES

Following the multitargeting approach that we investigated for the design of Ru-based therapeutic agents, we suggest developing a new series of ruthenium complexes bearing multidentate (bidentate or/and tridentate) synthetic ligands carrying an accessible bioactive moiety such as a triazole ring. This strategy can provide new pharmaceutical advantages such as: *i)* an enhancement of the stability of the complexes compared to the ones bearing monodentate ligands, which usually have a greater potential to undergo ligand exchange processes, *ii)* more structural modifications would be possible to bring on the synthetic ligands making the structure-activity tuning more facile *iii)* the accessibility of a triazole ring present in the structure of a ruthenium complex may provide a more potent multitargeting characteristics for a single molecule.

To this aim, a new project has been initiated for which a series of new bidentate ligands bearing a triazole ring have been synthesized, via Schiff base reactions between aldehydes and triazole-containing amines (Figure 5). Structurally different starting compounds were used to prepare Schiff base-type ligands with different electronic and steric properties, providing an elaborated platform for a SAR study. Ligands were purified and then characterized by NMR spectroscopy.

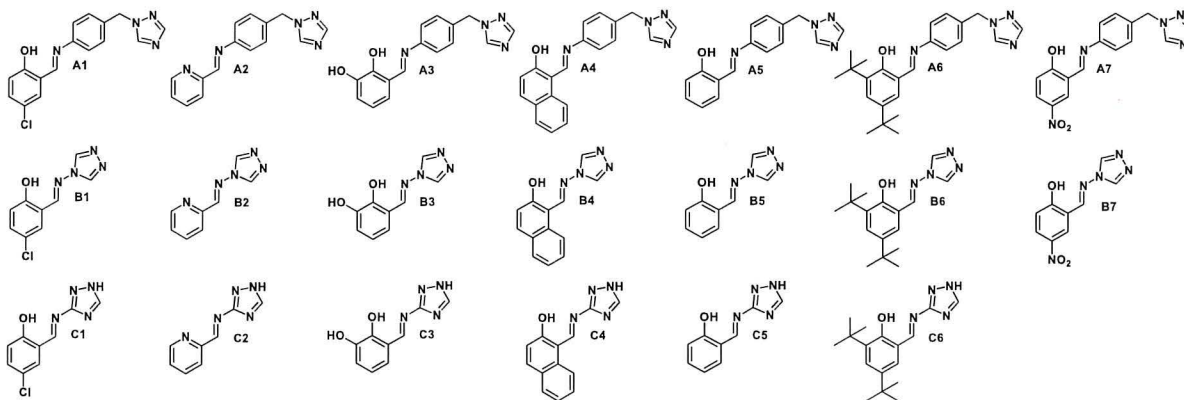


Figure 5. Schiff base-type ligands bearing a triazole ring.

Most of the ligands listed in figure 5 have been used to prepare corresponding Ru(II)-benzene complexes. However, this complexation was quite challenging mainly because of the multiple coordination sites of the ligands. Importantly, in some cases depending on the electrical and steric properties of the ligands, we could manage to selectively synthesize either a monodentate or a bidentate complex using two different synthetic routes. However, in most other cases, we could

either obtain a monodentate complex for which the triazole ring was involved in the coordination sphere (other than its N, O or N, N site) or a mixture of different ruthenium complexes which we were unable to isolate because of their very similar properties. Ligands A1 and A4 (figure 6) were the only species for which we could selectively obtain two distinct complexes (monodentate and bidentate). It is interesting to note that both these ligands have electron withdrawing or stabilizing characteristics (chloride substitution or naphthalene moiety) making the deprotonation of the hydroxyl moiety upon a pre-treatment with a strong base (potassium tert-butoxide) possible, thus facilitating and allowing the control of the coordination of the ligand through the N,O site. The four complexes were characterized by NMR spectroscopy and showed acceptable stability in DMSO, the solvent used to prepare their stock solution for biological screenings.

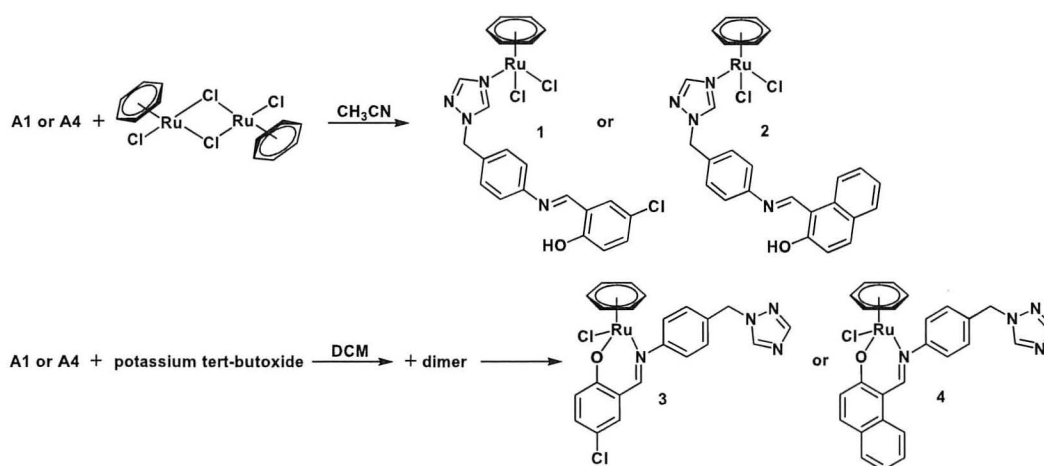


Figure 6. Synthetic routes to complexes 1-4.

Preliminary cytotoxicity results for the ligands and the complexes are presented in figure 7. Interestingly, a significant cell viability inhibition (at 50 μ M) was observed for the breast cancer cells exposed to most ligands, more specifically to A6, B6 and C6, which might be explained by their high lipophilicity due to the presence of tert-butyl moieties in their structures. The cytotoxicity of these three species was significantly higher than that of the clinically used anticancer drug cisplatin. We also observed a notable cytotoxicity for the ruthenium complexes. However, their activity was not significantly different than that of the corresponding free ligands or cisplatin on both tested cell lines.

To complete this SAR study and draw conclusions about the multitargeting ability of the complexes, their *in vitro* aromatase inhibitory activity should be determined and compared with

that of their corresponding free ligands. Moreover, other reaction pathways should also be closely examined to allow the synthesis of the ruthenium complexes that we did not so far succeed to prepare/purify.

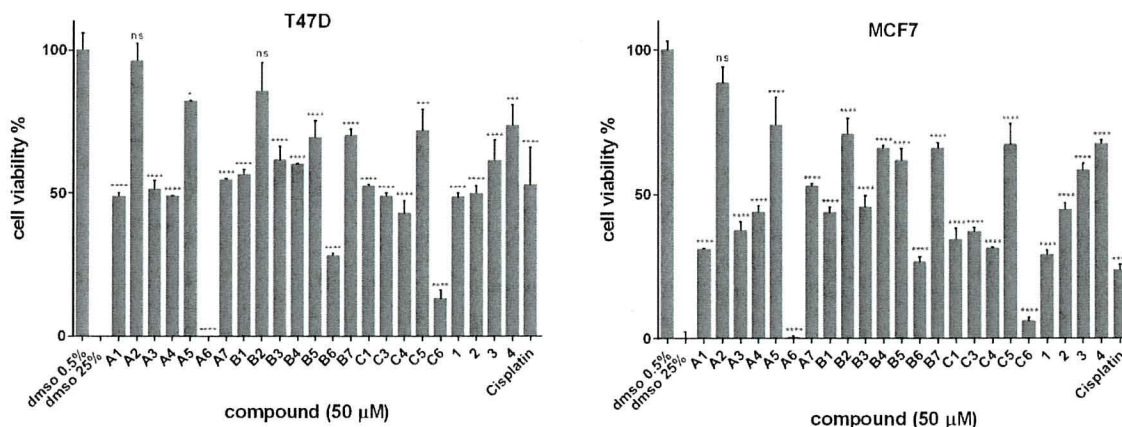


Figure 7. *In vitro* cytotoxicity of ligands and complexes at 50 μM on ER+ breast cancer cells MCF7 and T47D after 48 h incubation using SRB assay. Negative and positive controls were DMSO 0.5% (carrier) and DMSO 25%, respectively. Data are expressed as means \pm standard deviation (SD) from two or three independent experiments.

It is noteworthy that because of the unique structure of triazole, it can readily bind to a variety of enzymes and receptors in biological systems *via* different interactions, providing them with a broad spectrum of biological activities not limited to anticancer and antifungal applications [77-78]. Thus, we propose that a SAR study could also be conducted to screen the potential of these species for other applications such as antibacterial^[79], antiviral^[80], anti-inflammatory^[81], antiparasitic^[82], and etc. This could become the project of a graduate or trainee student in a near future.

7 REFERENCES

- [1] S. Antinori, L. Milazzo, S. Sollima, M. Galli, M. Corbellino, *European Journal of Internal Medicine* **2016**, *34*, 21-28.
- [2] S. M. Cohen, *Current Opinion in Chemical Biology* **2007**, *11*, 115-120.
- [3] K. H. Thompson, C. Orvig, *Science* **2003**, *300*, 936-939.
- [4] E. Severus, M. J. Taylor, C. Sauer, A. Pfennig, P. Ritter, M. Bauer, J. R. Geddes, *International Journal of Bipolar Disorders* **2014**, *2*, 15.
- [5] H. L. Dupont, *Drug Intelligence & Clinical Pharmacy* **1987**, *21*, 687-693.
- [6] P. Diós, K. Szigeti, F. Budán, M. Pócsik, D. S. Veres, D. Máthé, S. Pál, A. Dévay, S. Nagy, *European Journal of Pharmaceutical Sciences* **2016**, *95*, 46-53.
- [7] C. Roder, M. J. Thomson, *Drugs in R&D* **2015**, *15*, 13-20.
- [8] B. A. Wilky, D. M. Loeb, *Clin Exp Pharmacol* **2013**, *3*, 1000131.
- [9] S. Dasari, P. Bernard Tchounwou, *European Journal of Pharmacology* **2014**, *740*, 364-378.
- [10] S. M. Cohen, S. J. Lippard, in *Progress in Nucleic Acid Research and Molecular Biology*, Vol. 67, Academic Press, **2001**, pp. 93-130.
- [11] Z. Wang, G. Zhu, in *Reference Module in Chemistry, Molecular Sciences and Chemical Engineering*, Elsevier, **2018**.
- [12] A.-M. Florea, D. Büsselberg, *Cancers* **2011**, *3*, 1351-1371.
- [13] C. S. Allardyce, P. J. Dyson, Vol. 45, pp. 62-62.
- [14] M. Pongratz, P. Schluga, M. A. Jakupec, V. B. Arion, C. G. Hartinger, G. Allmaier, B. K. Keppler, *Journal of Analytical Atomic Spectrometry* **2004**, *19*, 46-51.
- [15] M. J. Clarke, *Coordination Chemistry Reviews* **2002**, *232*, 69-93.
- [16] E. S. Antonarakis, A. Emadi, *Cancer Chemother Pharmacol* **2010**, *66*, 1-9.
- [17] J. Reedijk, *Proceedings of the National Academy of Sciences* **2003**, *100*, 3611-3616.
- [18] A. Bergamo, G. Sava, *Dalton Transactions* **2011**, *40*, 7817-7823.
- [19] V. Brabec, O. Nováková, *Drug Resistance Updates* **2006**, *9*, 111-122.
- [20] S. Page, *Education in chemistry* **2012**, 26-29.
- [21] E. Alessio, *European Journal of Inorganic Chemistry* **2017**, *2017*, 1549-1560.
- [22] C. A. Vock, W. H. Ang, C. Scolaro, A. D. Phillips, L. Lagopoulos, L. Juillerat-Jeanneret, G. Sava, R. Scopelliti, P. J. Dyson, *Journal of Medicinal Chemistry* **2007**, *50*, 2166-2175.
- [23] S. Leijen, S. A. Burgers, P. Baas, D. Pluim, M. Tibben, E. van Werkhoven, E. Alessio, G. Sava, J. H. Beijnen, J. H. M. Schellens, *Investigational New Drugs* **2015**, *33*, 201-214.
- [24] C. G. Hartinger, M. A. Jakupec, S. Zorbass-Seifried, M. Groessler, A. Egger, W. Berger, H. Zorbass, P. J. Dyson, B. K. Keppler, *Chemistry & Biodiversity* **2008**, *5*, 2140-2155.
- [25] A. Weiss, R. H. Berndsen, M. Dubois, C. Müller, R. Schibli, A. W. Griffioen, P. J. Dyson, P. Nowak-Sliwiska, *Chemical Science* **2014**, *5*, 4742-4748.
- [26] S. A. McFarland, A. Mandel, R. Dumoulin-White, G. Gasser, *Current Opinion in Chemical Biology* **2020**, *56*, 23-27.
- [27] W. Zheng, Y. Zhao, Q. Luo, Y. Zhang, K. Wu, F. Wang, *Science China Chemistry* **2016**, *59*, 1240-1249.
- [28] Q. Hu, W. Sun, C. Wang, Z. Gu, *Advanced Drug Delivery Reviews* **2016**, *98*, 19-34.
- [29] R. Bayat Mokhtari, T. S. Homayouni, N. Baluch, E. Morgatskaya, S. Kumar, B. Das, H. Yeger, *Oncotarget* **2017**, *8*, 38022-38043.

- [30] A. Kurzwernhart, W. Kandioller, C. Bartel, S. Bächler, R. Trondl, G. Mühlgassner, M. A. Jakupec, V. B. Arion, D. Marko, B. K. Keppler, C. G. Hartinger, *Chemical Communications* **2012**, *48*, 4839-4841.
- [31] L. Ji, W. Zheng, Y. Lin, X. Wang, S. Lü, X. Hao, Q. Luo, X. Li, L. Yang, F. Wang, *European Journal of Medicinal Chemistry* **2014**, *77*, 110-120.
- [32] R. Pettinari, F. Marchetti, F. Condello, C. Pettinari, G. Lupidi, R. Scopelliti, S. Mukhopadhyay, T. Riedel, P. J. Dyson, *Organometallics* **2014**, *33*, 3709-3715.
- [33] J. E. Park, Z. Miller, Y. Jun, W. Lee, K. B. Kim, *Translational Research* **2018**, *198*, 1-16.
- [34] P.-C. Lv, A.-Q. Jiang, W.-M. Zhang, H.-L. Zhu, *Expert Opinion on Therapeutic Patents* **2018**, *28*, 139-145.
- [35] Y. Chen, H. Du, *Biomedicine & Pharmacotherapy* **2018**, *99*, 552-560.
- [36] R. M. Parks, M. G. M. Derks, E. Bastiaannet, K. L. Cheung, in *Breast Cancer Management for Surgeons: A European Multidisciplinary Textbook* (Eds.: L. Wyld, C. Markopoulos, M. Leidenius, E. Senkus-Konefka), Springer International Publishing, Cham, **2018**, pp. 19-29.
- [37] M. W. DeGregorio, V. J. Wiebe, *Tamoxifen and breast cancer*, Yale University Press, **1999**.
- [38] V. C. Jordan, *British Journal of Pharmacology* **1993**, *110*, 507-517.
- [39] I. E. Smith, M. Dowsett, *New England Journal of Medicine* **2003**, *348*, 2431-2442.
- [40] R. Carpenter, W. R. Miller, *British Journal of Cancer* **2005**, *93*, S1-S5.
- [41] S. M. Campos, *The oncologist* **2004**, *9*, 126-136.
- [42] P. Lønning, C. Pfister, A. Martoni, C. Zamagni, *Seminars in Oncology* **2003**, *30*, 23-32.
- [43] S. Maurelli, M. Chiesa, E. Giamello, G. Di Nardo, V. E. Ferrero, G. Gilardi, S. Van Doorslaer, *Chemical Communications* **2011**, *47*, 10737-10739.
- [44] W. R. Miller, *Maturitas* **2006**, *54*, 335-341.
- [45] J. A. Cortés, I. F. Corrales, in *Fungal Infection*, IntechOpen, **2018**.
- [46] P. G. Pappas, M. S. Lionakis, M. C. Arendrup, L. Ostrosky-Zeichner, B. J. Kullberg, *Nature Reviews Disease Primers* **2018**, *4*, 18026.
- [47] P. G. Pappas, J. H. Rex, J. Lee, R. J. Hamill, R. A. Larsen, W. Powderly, C. A. Kauffman, N. Hyslop, J. E. Mangino, S. Chapman, H. W. Horowitz, J. E. Edwards, W. E. Dismukes, N. M. S. Group, *Clinical Infectious Diseases* **2003**, *37*, 634-643.
- [48] B. J. Kullberg, M. C. Arendrup, *New England Journal of Medicine* **2015**, *373*, 1445-1456.
- [49] M. A. Pfaller, G. J. Moet, S. A. Messer, R. N. Jones, M. Castanheira, *Journal of Clinical Microbiology* **2011**, *49*, 396-399.
- [50] S. Vallabhaneni, A. A. Cleveland, M. M. Farley, L. H. Harrison, W. Schaffner, Z. G. Beldavs, G. Derado, C. D. Pham, S. R. Lockhart, R. M. Smith, *Open Forum Infect Dis* **2015**, *2*, ofv163-ofv163.
- [51] S. G. Whaley, E. L. Berkow, J. M. Rybak, A. T. Nishimoto, K. S. Barker, P. D. Rogers, *Frontiers in Microbiology* **2017**, *7*.
- [52] S. G. Whaley, P. D. Rogers, *Current Infectious Disease Reports* **2016**, *18*, 41.
- [53] A. Eshwika, B. Coyle, M. Devereux, M. McCann, K. Kavanagh, *Biometals* **2004**, *17*, 415-422.
- [54] A. Lateef, S. A. Ojo, S. M. Oladejo, *Process Biochemistry* **2016**, *51*, 1406-1412.
- [55] B. Coyle, K. Kavanagh, M. McCann, M. Devereux, M. Geraghty, *Biometals* **2003**, *16*, 321-329.
- [56] in *Ruthenium Complexes*, pp. 293-318.
- [57] V. K. Sharma, O. P. Pandey, S. K. Sengupta, *Transition Metal Chemistry* **1987**, *12*, 509-515.
- [58] T. D. Thangadurai, S.-K. Ihm, *Synthesis and Reactivity in Inorganic, Metal-Organic, and Nano-Metal Chemistry* **2005**, *35*, 499-507.

- [59] G. Venkatachalam, R. Ramesh, S. M. Mobin, *Journal of Organometallic Chemistry* **2005**, *690*, 3937-3945.
- [60] K. Naresh Kumar, R. Ramesh, Y. Liu, *J Inorg Biochem* **2006**, *100*, 18-26.
- [61] N. P. Priya, S. V. Arunachalam, N. Sathya, V. Chinnusamy, C. Jayabalakrishnan, *Transition Metal Chemistry* **2009**, *34*, 437-445.
- [62] N. Padma Priya, S. Arunachalam, N. Sathya, C. Jayabalakrishnan, *Journal of Coordination Chemistry* **2010**, *63*, 1440-1450.
- [63] C. L. Donnici, L. J. Nogueira, M. H. Araujo, S. R. Oliveira, T. F. F. Magalhães, M. T. P. Lopes, A. C. Araújo e Silva, A. M. d. C. Ferreira, C. V. B. Martins, M. A. de Resende Stoianoff, *Molecules* **2014**, *19*, 5402-5420.
- [64] N. E. A. El-Gamel, A. M. Fekry, *Bioelectrochemistry* **2015**, *104*, 35-43.
- [65] A. M. Mansour, K. Radacki, *Polyhedron* **2020**, *175*, 114175.
- [66] R. A. Gomes-Junior, R. S. da Silva, R. G. de Lima, M. A. Vannier-Santos, *FEMS Microbiology Letters* **2017**, *364*.
- [67] M. Al-Noaimi, A. Nafady, I. Warad, R. Alshwafy, A. Husein, W. H. Talib, T. B. Hadda, *Spectrochimica Acta Part A: Molecular and Biomolecular Spectroscopy* **2014**, *122*, 273-282.
- [68] B. Mehta, J. Shaikh, *Special report series - Indian Council of Medical Research* **2009**, *26*, 1-6.
- [69] R. Gandhaveeti, R. Konakanchi, P. Jyothi, N. S. P. Bhuvanesh, S. Anandaram, *Applied Organometallic Chemistry* **2019**, *33*, e4899.
- [70] C. L. Donnici, L. J. Nogueira, M. H. Araujo, S. R. Oliveira, T. F. F. Magalhães, M. T. P. Lopes, A. C. A. e. Silva, A. M. d. C. Ferreira, C. V. B. Martins, M. A. De Resende Stoianoff, *Molecules* **2014**, *19*, 5402-5420.
- [71] B. Cetinkaya, I. Özdemir, B. Binbaştoğlu, S. Günal, *Arzneimittelforschung* **1999**, *49*, 538-540.
- [72] A. M. Mansour, *European Journal of Inorganic Chemistry* **2018**, *2018*, 852-860.
- [73] A. M. Mansour, O. R. Shehab, K. Radacki, *European Journal of Inorganic Chemistry* **2020**, *2020*, 299-307.
- [74] G. Onar, C. Gürses, M. O. Karataş, S. Balcıoğlu, N. Akbay, N. Özdemir, B. Ateş, B. Alici, *Journal of Organometallic Chemistry* **2019**, *886*, 48-56.
- [75] T. S. Kamatchi, P. Kalaivani, P. Poornima, V. V. Padma, F. R. Fronczek, K. Natarajan, *RSC advances* **2014**, *4*, 2004-2022.
- [76] G. Kalaiarasi, S. R. Jeya Rajkumar, S. Dharani, F. R. Fronczek, R. Prabhakaran, *Journal of Organometallic Chemistry* **2018**, *866*, 223-242.
- [77] C. H Zhou, Y. Wang, *Current medicinal chemistry* **2012**, *19*, 239-280.
- [78] S. P. Mantoani, P. de Andrade, T. P. Chierrito, A. S. Figueredo, I. Carvalho, *Current medicinal chemistry* **2019**, *26*, 4403-4434.
- [79] Beena, N. Kumar, R. K. Rohilla, N. Roy, D. S. Rawat, *Bioorganic & Medicinal Chemistry Letters* **2009**, *19*, 1396-1398.
- [80] M. D. Grandi, M. Olson, A. S. Prashad, G. Bebernitz, A. Luckay, S. Mullen, Y. Hu, G. Krishnamurthy, K. Pitts, J. O'Connell, *Bioorganic & Medicinal Chemistry Letters* **2010**, *20*, 398-402.
- [81] H. Kumar, S. A. Javed, S. A. Khan, M. Amir, *European Journal of Medicinal Chemistry* **2008**, *43*, 2688-2698.
- [82] K. Brak, P. S. Doyle, J. H. McKerrow, J. A. Ellman, *Journal of the American Chemical Society* **2008**, *130*, 6404-6410.

8 APPENDIX (SUPPLEMENTARY INFORMATION OF PUBLICATIONS 1-4)

SUPPLEMENTARY INFORMATION

Rationally designed ruthenium complexes for breast cancer therapy

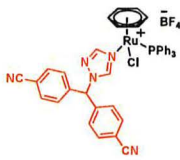
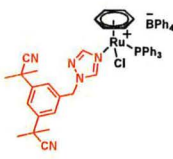
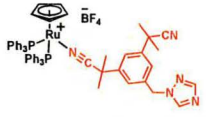
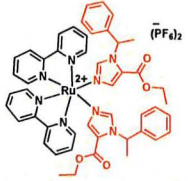
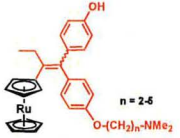
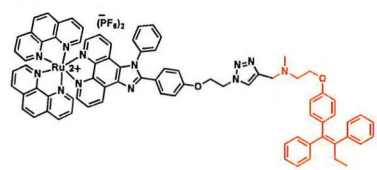
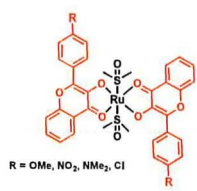
Golara Golbaghi, Annie Castonguay*

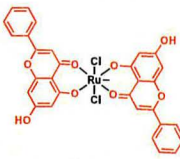
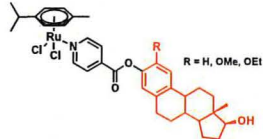
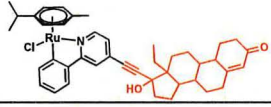
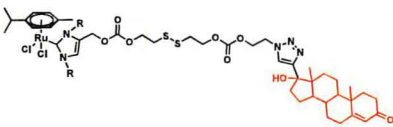
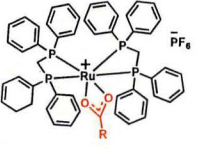
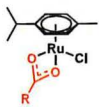
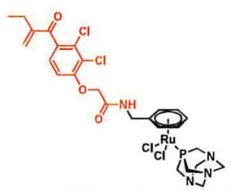
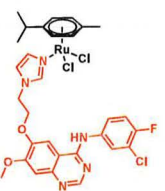
Organometallic Chemistry Laboratory for the Design of Catalysts and Therapeutics, INRS-Centre Armand-Frappier Santé Biotechnologie, Université du Québec, Laval, Canada

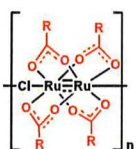
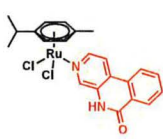
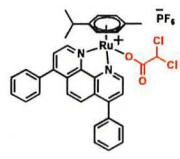
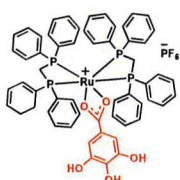
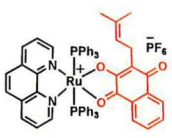
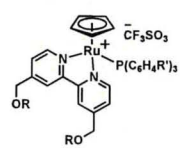

TABLE OF CONTENT

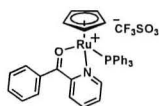
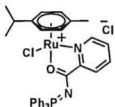
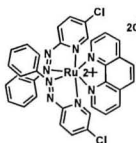
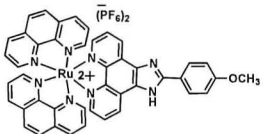
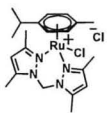
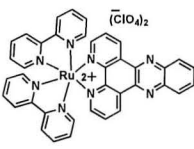
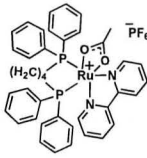
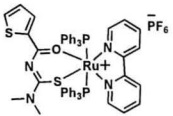
| | |
|---|-------|
| Table S1. Summary of the biological activity of the ruthenium complexes reviewed in this study | S2-S6 |
| References | S7-S9 |

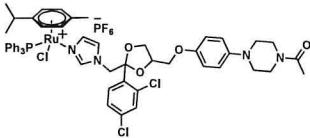
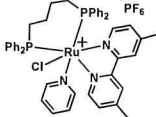
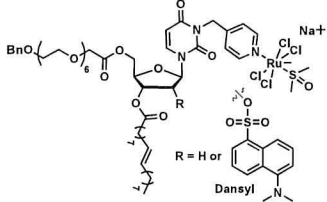
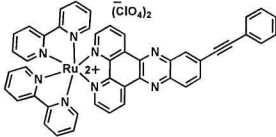
Table S1. Summary of the biological activity of the ruthenium complexes reviewed in this study.

| | Bioactive ligand | In vitro IC ₅₀ (μM) values in breast cancer cells | In vivo antitumoral activity and/or in vivo toxicity |
|---|---|--|---|
| 1 | Aromatase inhibitor (letrozole)  | >25 (MCF7) | N.A. [1] |
| 2 | Aromatase inhibitor (anastrozole)  | ≈ 4 (MCF7 and T47D) | No toxicity (12.5 μM) on the development of zebrafish embryos. [2] |
| 3 | Aromatase inhibitor (anastrozole)  | 0.50 ± 0.09 (MCF7) 0.32 ± 0.03 (T47D) 0.39 ± 0.09 (MDA-MB-231) | No toxicity (at concentrations around its IC ₅₀ values) on the development of zebrafish embryos. [3] |
| 4 | P450 enzyme inhibitor (etomidate)  | N.A. | N.A. [4] |
| 5 | Steroid hormone receptor targeting molecules (tamoxifen derivatives)  | >1 (MCF7) | N.A. [5] |
| 6 | Steroid hormone receptor targeting molecule (tamoxifen)  | <8 (light) (MCF7) >16 (dark) (MCF7) | N.A. [6] |
| 7 | Steroid hormone receptor targeting molecule (flavone)  | 16.0 (MCF7) when R = OMe | N.A. [7] |

| | | | | |
|----|---|--|--|---|
| 8 |  | Steroid hormone receptor targeting molecule (flavone) | > 100 (MCF7) | Mortality and body weight loss in rats (1000 mg/kg, at Day 20). [8] |
| 9 |  | Steroid hormone receptor targeting molecules (estradiol isonicotinates) | 0.08 ± 0.04 (MCF7) when R = OEt | N.A. [9] |
| 10 |  | Steroid hormone receptor targeting molecule (levonorgestrel) | 7.4 ± 0.1 (T47D) | N.A. [10] |
| 11 |  | Steroid hormone receptor targeting molecule (17α-ethynyl testosterone) | 4.48 ± 0.17 (MCF7) 20.71 ± 0.92 (MDA-MB-231) | Slight decrease in tumor volume (2 μmol/kg, every 4 days, 5 doses) in mice bearing MCF7 cells. [11] |
| 12 |  | Nonsteroidal anti-inflammatory drugs (NSAIDs) (diclofenac, ibuprofen) | Ru-Dicl: 47 ± 6 (MCF7) Ru-Ibp: 9 ± 3 (MCF7) | N.A. [12] |
| 13 |  | Nonsteroidal anti-inflammatory drugs (NSAIDs) (diclofenac, ibuprofen, naproxen, aspirin) | <0.1 (MCF7) except when RCOO ⁻ = aspirin which was inactive | N.A. [13] |
| 14 |  | Glutathione S-transferase (GST) inhibitor (ethacrynic acid) | >20 (MCF7) | N.A. [14] |
| 15 |  | Epidermal growth factor (EGFR) inhibitors (4-anilinoquinazoline derivatives) | 54 ± 4 (MCF7) | N.A. [15] |

| | | | | |
|----|---|---|--|--|
| 16 |  | Nonsteroidal anti-inflammatory drugs (NSAIDs) (ibuprofen, naproxen) | Ru-lbp-SPLNs: 70.3 ± 8.1 (MDA-MB-231) Ru-Npx-SPLNs: 101.8 ± 6.7 (MDA-MB-231) | N.A. [16] |
| 17 |  | Poly (ADP-ribose) polymerase (PARP) inhibitor | 93.3 ± 11.4 (Hcc1937) | N.A. [17] |
| 18 |  | Aerobic glycolysis inhibitor (dichloroacetato) | 0.86 ± 0.01 (MDA-MB-231) | N.A. [18] |
| 19 |  | Cell cycle arrest inducer (gallic acid) | 0.81 ± 0.08 (MDA-MB-231) 1.0 ± 0.1 (MDA-MB-468) | N.A. [19] |
| 20 |  | Topoisomerase-interacting and ROS-generating molecule (lapachol) | 0.20 ± 0.01 (MDA-MB-231) | N.A. [20] |
| 21 |  | Biotin | 11.6 ± 1.5 (MDA-MB-231) 31.5 ± 4.7 (MCF7) when R = biotin and R' = H | Zebrafish tolerance up to 1.17 mg/L. Morphologic lesions such as curved spine/tail malformation, yolk sac and pericardial sac edema, cranial malformation and underdeveloped eyes were observed at 2.18 mg/L. [21] |
| 22 |  | Biotin | 14.2 ± 0.7 when R' = F and R = biotin 7.7 ± 0.3 when R' = OCH3 and R = biotin (MDA-MB-231) 22.4 ± 1.6 when R' = F and R = biotin 18.7 ± 1.6 R' = OCH3 and R = biotin (MCF7) | LC50 values (lethality for 50% of the embryos/larvae) on zebrafish (120 hpf, 1.83-2.35 mg/L). Moderate to severe yolk sac edema and pericardial sac edema were observed. [22] |

| | | | | |
|----|---|------|--|--|
| 23 |  | N.A. | 0.03 ± 0.01 (MDA-MB-231) | Suppression of tumor growth (2.5 mg/kg/day, 10 days) in female athymic nude mice bearing MDA-MB-231 cells. No effect on the well-being of the animals. [23,24] |
| 24 |  | N.A. | 2.61 ± 1.2 (MDA-MB-231) | Significant decrease (56%) in tumor volume (5 mg/kg, every other day, 14 doses) in NOD.CB17-Prkdc SCID/J mice bearing MDA-MB-23 cells. Low systemic toxicity. [25] |
| 25 |  | N.A. | 1.8 ± 0.1 (HCC1937) 13.2 ± 0.3 (MDA-MB-231) 8.2 ± 0.1 (MCF7) | N.A. [26] |
| 26 |  | N.A. | 14.6 ± 3.1 (MDA-MB-231) 78.0 ± 19.8 (MDA-MB-468) 28.0 ± 4.9 (MCF7) | N.A. [27] |
| 27 |  | N.A. | 230.66 ± 0.02 (A17) 409.89 ± 0.04 (MDA-MB-231) | Suppression of tumor growth (52.5 mg/kg, every 3 days, 4 doses) in female FVB/NCrl mice bearing A17 cells. No apparent toxicity. [28] |
| 28 |  | N.A. | <4 (when complex is encapsulated) | Suppression of tumor growth (5 mg/kg/week, 4 doses) (encapsulated complex) in athymic nude mice bearing MDA-MB-231 cells. No apparent toxicity. [29] |
| 29 |  | N.A. | 31.16 ± 0.04 (MDA-MB-231) >200 (MCF7) | N.A. [30] |
| 30 |  | N.A. | 8.81 ± 0.81 (MDA-MB-231) | Low toxicity (up to 300 mg/kg, 14 days) in a Swiss mice model. [31] |

| | | | | |
|----|--|------|---|--|
| 31 |  | N.A. | 0.62 ± 0.02 (MDA-MB-231) | N.A. [32] |
| 32 |  | N.A. | 9.18 ± 0.30 (MDA-MB-231) | N.A. [33] |
| 33 |  | N.A. | 12.1 ± 3 (MDA-MB-231) 12.7 ± 4 (MCF7) (when R= H) Concentrations correspond to the effective metal concentration (15% mol/mol) carried by nanoaggregates | Suppression of tumor growth (15 mg/kg/week, 28 days) in athymic nude mice bearing MCF7 cells. No apparent toxicity. [34] |
| 34 |  | N.A. | 17.2 ± 0.9 (MDA-MB-231) 74.9 ± 3.5 (MCF7) | Inhibition of cancer cell proliferation and metastasis (5 μM, 72 h) in a xenograft model of human MDA-MB-231 cells in zebrafish. [35] |

References

1. Castonguay, A.; Doucet, C.; Juhas, M.; Maysinger, D. New Ruthenium(II)–Letrozole Complexes as Anticancer Therapeutics. *J. Med. Chem.* **2012**, *55*, 8799–8806, doi:10.1021/jm301103y.
2. Golbaghi, G.; Haghdoost, M.M.; Yancu, D.; López de los Santos, Y.; Doucet, N.; Patten, S.A.; Sanderson, J.T.; Castonguay, A. Organoruthenium(II) Complexes Bearing an Aromatase Inhibitor: Synthesis, Characterization, in Vitro Biological Activity and in Vivo Toxicity in Zebrafish Embryos. *Organometallics* **2019**, *38*, 702–711, doi:10.1021/acs.organomet.8b00897.
3. Golbaghi, G.; Pitard, I.; Lucas, M.; Haghdoost, M.M.; López de los Santos, Y.; Doucet, N.; Patten, S.A.; Sanderson, J.T.; Castonguay, A. Synthesis and biological assessment of a ruthenium(II) cyclopentadienyl complex in breast cancer cells and on the development of zebrafish embryos. *Eur. J. Med. Chem.* **2020**, doi: 10.1016/j.ejmech.2019.112030.
4. Zamora, A.; Denning, C.A.; Heidary, D.K.; Wachter, E.; Nease, L.A.; Ruiz, J.; Glazer, E.C. Ruthenium-containing P450 inhibitors for dual enzyme inhibition and DNA damage. *Dalton Trans.* **2017**, *46*, 2165–2173, doi:10.1039/C6DT04405K.
5. Pigeon, P.; Top, S.; Vessières, A.; Huché, M.; Hillard, E.A.; Salomon, E.; Jaouen, G. Selective Estrogen Receptor Modulators in the Ruthenocene Series. Synthesis and Biological Behavior. *J. Med. Chem.* **2005**, *48*, 2814–2821, doi:10.1021/jm049268h.
6. Zhao, X.; Li, M.; Sun, W.; Fan, J.; Du, J.; Peng, X. An estrogen receptor targeted ruthenium complex as a two-photon photodynamic therapy agent for breast cancer cells. *Chem. Commun.* **2018**, *54*, 7038–7041, doi:10.1039/C8CC03786H.
7. Singh, A.K.; Saxena, G.; Sahabjada; Arshad, M. Synthesis, characterization and biological evaluation of ruthenium flavanol complexes against breast cancer. *Spectrochim Acta A. Mol. Biomol. Spectrosc.* **2017**, *180*, 97–104, doi: 10.1016/j.saa.2017.02.056.
8. Roy, S.; Sil, A.; Chakraborty, T. Potentiating apoptosis and modulation of p53, Bcl2, and Bax by a novel chrysin ruthenium complex for effective chemotherapeutic efficacy against breast cancer. *J. Cell. Physiol.* **2019**, *234*, 4888–4909, doi: 10.1002/jcp.27287.
9. Schobert, R.; Seibt, S.; Effenberger-Neidnicht, K.; Underhill, C.; Biersack, B.; Hammond, G.L. (Arene)Cl₂Ru(II) complexes with N-coordinated estrogen and androgen isonicotinates: Interaction with sex hormone binding globulin and anticancer activity. *Steroids* **2011**, *76*, 393–399, doi: 10.1016/j.steroids.2010.12.009.
10. Ruiz, J.; Rodríguez, V.; Cutillas, N.; Espinosa, A.; Hannon, M.J. A Potent Ruthenium(II) Antitumor Complex Bearing a Lipophilic Levonorgestrel Group. *Inorg. Chem.* **2011**, *50*, 9164–9171, doi:10.1021/ic201388n.
11. Lv, G.; Qiu, L.; Li, K.; Liu, Q.; Li, X.; Peng, Y.; Wang, S.; Lin, J. Enhancement of therapeutic effect in breast cancer with a steroid-conjugated ruthenium complex. *New J. Chem.* **2019**, *43*, 3419–3427, doi: 10.1039/C8NJ04159H.
12. Lopes, J.C.S.; Damasceno, J.L.; Oliveira, P.F.; Guedes, A.P.M.; Tavares, D.C.; Defflon, V.M.; Lopes, N.P.; Pivatto, M.; Batista, A.A.; Maia, P.I.S., et al. Ruthenium(II) Complexes Containing Anti-Inflammatory Drugs as Ligands: Synthesis, Characterization and in vitro Cytotoxicity Activities on Cancer Cell Lines. *J. Braz. Chem. Soc.* **2015**, *26*, 1838–1847, doi: 10.5935/0103-5053.20150161.
13. Mandal, P.; Kundu, B.K.; Vyas, K.; Sabu, V.; Helen, A.; Dhankhar, S.S.; Nagaraja, C.M.; Bhattacharjee, D.; Bhabak, K.P.; Mukhopadhyay, S. Ruthenium(ii) arene NSAID complexes: inhibition of cyclooxygenase and antiproliferative activity against cancer cell lines. *Dalton Trans.* **2018**, *47*, 517–527, doi: 10.1039/C7DT03637J.
14. Chatterjee, S.; Biondi, I.; Dyson, P.J.; Bhattacharyya, A. A bifunctional organometallic ruthenium drug with multiple modes of inducing apoptosis. *J. Biol. Inorg. Chem.* **2011**, *16*, 715–724, doi: 10.1007/s00775-011-0772-0.
15. Du, J.; Zhang, E.; Zhao, Y.; Zheng, W.; Zhang, Y.; Lin, Y.; Wang, Z.; Luo, Q.; Wu, K.; Wang, F. Discovery of a dual-targeting organometallic ruthenium complex with high activity inducing early stage apoptosis of cancer cells. *Metalomics* **2015**, *7*, 1573–1583, doi: 10.1039/C5MT00122F.
16. Alves Rico, S.R.; Abbasi, A.Z.; Ribeiro, G.; Ahmed, T.; Wu, X.Y.; de Oliveira Silva, D. Diruthenium(ii,iii) metallodrugs of ibuprofen and naproxen encapsulated in intravenously injectable polymer–lipid nanoparticles exhibit enhanced activity against breast and prostate cancer cells. *Nanoscale* **2017**, *9*, 10701–10714, doi: 10.1039/C7NR01582H.
17. Wang, Z.; Qian, H.; Yiu, S.-M.; Sun, J.; Zhu, G. Multi-targeted organometallic ruthenium(II)–arene anticancer complexes bearing inhibitors of poly(ADP-ribose) polymerase-1: A strategy to improve cytotoxicity. *J. Inorg. Biochem.* **2014**, *131*, 47–55, doi: 10.1016/j.jinorgbio.2013.10.017.

18. Pracharova, J.; Novohradsky, V.; Kostrhunova, H.; Štarha, P.; Trávníček, Z.; Kasparkova, J.; Brabec, V. Half-sandwich Os(II) and Ru(II) bathophenanthroline complexes: anticancer drug candidates with unusual potency and a cellular activity profile in highly invasive triple-negative breast cancer cells. *Dalton Transactions* **2018**, *47*, 12197-12208, doi:10.1039/C8DT02236D.
19. Naves, M.A.; Graminha, A.E.; Vegas, L.C.; Luna-Dulcey, L.; Honorato, J.; Menezes, A.C.S.; Batista, A.A.; Cominetti, M.R. Transport of the Ruthenium Complex [Ru(GA)(dppe)₂]PF₆ into Triple-Negative Breast Cancer Cells Is Facilitated by Transferrin Receptors. *Mol. Pharm.* **2019**, *16*, 1167-1183, doi: 10.1021/acs.molpharmaceut.8b01154.
20. Oliveira, K.M.; Corrêa, R.S.; Barbosa, M.I.F.; Ellena, J.; Cominetti, M.R.; Batista, A.A. Ruthenium(II)/triphenylphosphine complexes: An effective way to improve the cytotoxicity of lapachol. *Polyhedron* **2017**, *130*, 108-114, doi: 10.1016/j.poly.2017.04.005.
21. Côrte-Real, L.; Karas, B.; Gírio, P.; Moreno, A.; Avecilla, F.; Marques, F.; Buckley, B.T.; Cooper, K.R.; Doherty, C.; Falson, P., et al. Unprecedented inhibition of P-gp activity by a novel ruthenium-cyclopentadienyl compound bearing a bipyridine-biotin ligand. *Eur. J. Med. Chem.* **2019**, *163*, 853-863, doi: 10.1016/j.ejmech.2018.12.022.
22. Côrte-Real, L.; Karas, B.; Brás, A.R.; Pilon, A.; Avecilla, F.; Marques, F.; Preto, A.; Buckley, B.T.; Cooper, K.R.; Doherty, C., et al. Ruthenium-Cyclopentadienyl Bipyridine-Biotin Based Compounds: Synthesis and Biological Effect. *Inorg. Chem.* **2019**, *58*, 9135-9149, doi: 10.1021/acs.inorgchem.9b00735.
23. Morais, T.S.; Silva, T.J.L.; Marques, F.; Robalo, M.P.; Avecilla, F.; Madeira, P.J.A.; Mendes, P.J.G.; Santos, I.; Garcia, M.H. Synthesis of organometallic ruthenium(II) complexes with strong activity against several human cancer cell lines. *J. Inorg. Biochem.* **2012**, *114*, 65-74, doi: 10.1016/j.jinorgbio.2012.04.014.
24. Mendes, N.; Tortosa, F.; Valente, A.; Marques, F.; Matos, A.; Morais, T.S.; Tomaz, A.I.; Gärtner, F.; Garcia, M.H. In Vivo Performance of a Ruthenium-cyclopentadienyl Compound in an Orthotopic Triple Negative Breast Cancer Model. *Anti-Cancer Agent Me.* **2017**, *17*, 126-136, doi: 10.2174/1871520616666160922165133.
25. Frik, M.; Martínez, A.; Elie, B.T.; Gonzalo, O.; Ramírez de Mingo, D.; Sanaú, M.; Sánchez-Delgado, R.; Sadhukha, T.; Prabha, S.; Ramos, J.W., et al. In Vitro and in Vivo Evaluation of Water-Soluble Iminophosphorane Ruthenium(II) Compounds. A Potential Chemotherapeutic Agent for Triple Negative Breast Cancer. *J. Med. Chem.* **2014**, *57*, 9995-10012, doi: 10.1021/jm5012337.
26. Nhukeaw, T.; Temboot, P.; Hansongnern, K.; Ratanaphan, A. Cellular responses of BRCA1-defective and triple-negative breast cancer cells and in vitro BRCA1 interactions induced by metallo-intercalator ruthenium(II) complexes containing chloro-substituted phenylazopyridine. *BMC Cancer* **2014**, *14*, 73-73, doi: 10.1186/1471-2407-14-73.
27. Cao, W.; Zheng, W.; Chen, T. Ruthenium polypyridyl complex inhibits growth and metastasis of breast cancer cells by suppressing FAK signaling with enhancement of TRAIL-induced apoptosis. *Sci. Rep.* **2015**, *5*, 9157-9157, doi: 10.1038/srep09157.
28. Montani, M.; Pazmay, G.V.B.; Hysi, A.; Lupidi, G.; Pettinari, R.; Gambini, V.; Tilio, M.; Marchetti, F.; Pettinari, C.; Ferraro, S., et al. The water soluble ruthenium(II) organometallic compound [Ru(p-cymene)(bis(3,5 dimethylpyrazol-1-yl)methane)Cl]Cl suppresses triple negative breast cancer growth by inhibiting tumor infiltration of regulatory T cells. *Pharmacol. Res.* **2016**, *107*, 282-290, doi: 10.1016/j.phrs.2016.03.032.
29. Shen, J.; Kim, H.-C.; Wolfram, J.; Mu, C.; Zhang, W.; Liu, H.; Xie, Y.; Mai, J.; Zhang, H.; Li, Z., et al. A Liposome Encapsulated Ruthenium Polypyridine Complex as a Theranostic Platform for Triple-Negative Breast Cancer. *Nano Lett.* **2017**, *17*, 2913-2920, doi: 10.1021/acs.nanolett.7b00132.
30. Popolin, C.P.; Reis, J.P.B.; Becceneri, A.B.; Graminha, A.E.; Almeida, M.A.P.; Corrêa, R.S.; Colina-Vegas, L.A.; Ellena, J.; Batista, A.A.; Cominetti, M.R. Cytotoxicity and anti-tumor effects of new ruthenium complexes on triple negative breast cancer cells. *PLoS One* **2017**, *12*, e0183275, doi: 10.1371/journal.pone.0183275.
31. Becceneri, A.B.; Popolin, C.P.; Plutin, A.M.; Maistro, E.L.; Castellano, E.E.; Batista, A.A.; Cominetti, M.R. The trans-[Ru(PPh₃)₂(N,N-dimethyl-N'-thiophenylthioureaato-k₂O,S)(bipy)]PF₆ complex has pro-apoptotic effects on triple negative breast cancer cells and presents low toxicity in vivo. *J. Inorg. Biochem.* **2018**, *186*, 70-84, doi: 10.1016/j.jinorgbio.2018.05.011.
32. Colina-Vegas, L.; Oliveira, K.M.; Cunha, B.N.; Cominetti, M.R.; Navarro, M.; Azevedo Batista, A. Anti-Proliferative and Anti-Migration Activity of Arene-Ruthenium(II) Complexes with Azole Therapeutic Agents. *Inorganics* **2018**, *6*, 132, doi: 10.3390/inorganics6040132.

33. Silva, H.V.R.; Dias, J.S.M.; Ferreira-Silva, G.Á.; Vegas, L.C.; Ionta, M.; Corrêa, C.C.; Batista, A.A.; Barbosa, M.I.F.; Doriguetto, A.C. Phosphine/diimine ruthenium complexes with Cl^- , CO, NO^+ , NO_2^- , NO_3^- and pyridine ligands: Pro-apoptotic activity on triple-negative breast cancer cells and DNA/HSA interactions. *Polyhedron* **2018**, *144*, 55-65, doi: 10.1016/j.poly.2018.01.005.
34. Piccolo, M.; Misso, G.; Ferraro, M.G.; Riccardi, C.; Capuozzo, A.; Zarone, M.R.; Maione, F.; Trifuoggi, M.; Stiuso, P.; D'Errico, G., et al. Exploring cellular uptake, accumulation and mechanism of action of a cationic Ru-based nanosystem in human preclinical models of breast cancer. *Sci. Rep.* **2019**, *9*, 7006, doi: 10.1038/s41598-019-43411-3.
35. Zhao, X.; Li, L.; Yu, G.; Zhang, S.; Li, Y.; Wu, Q.; Huang, X.; Mei, W. Nucleus-enriched Ruthenium Polypyridine Complex Acts as a Potent Inhibitor to Suppress Triple-negative Breast Cancer Metastasis In vivo. *Comput. Struct. Biotechnol. J.* **2019**, *17*, 21-30, doi: 10.1016/j.csbj.2018.11.010.

SUPPLEMENTARY INFORMATION

Organoruthenium(II) Complexes Bearing an Aromatase Inhibitor: Synthesis, Characterization, *in Vitro* Biological Activity and *in Vivo* Toxicity in Zebrafish Embryos

*Golara Golbaghi, Mohammad Mehdi Haghdooost, Debbie Yancu, Yossef López de los Santos, Nicolas Doucet, Shunmoogum A. Patten, J. Thomas Sanderson and Annie Castonguay**

INRS - Institut Armand-Frappier, Université du Québec, 531 boul. des Prairies, Laval, Quebec, H7V 1B7, Canada

TABLE OF CONTENT

| | |
|--|----|
| Table S1. Crystallographic data and structure refinement for complexes 2-5 . | S2 |
| Table S2. Selected bond lengths (Å) and angles (deg) of complexes 2-5 . | S3 |
| Table S3. Anastrozole release after incubation (48 h) of a 150 µM solution of complexes 1, 2, 3 , and 5 in water (DMSO 0.5%). | S4 |
| Table S4. Anastrozole (or letrozole) release after incubation (1.5 h) of a 10 µM solution of complexes 1, 2, 3, 5 and Ru-LTZ in DMEM/F-12 (DMSO 0.1%). | S4 |
| Figure S1. Calibration curves of the extracted anastrozole and letrozole from phenol red free DMEM/F-12. | S4 |
| Figure S2. Cell viability determined by the SRB assay in T47D cancer cells treated with a 25 µM solution of 2, 3 and NaBPh ₄ . | S5 |
| Figure S3. Migration inhibition assessment of MCF-7 cells after exposure to 10 µM solutions of 1, 2, 4, 5 , Ru-LTZ, anastrozole, and letrozole over 48 h. | S5 |
| Figure S4. Cell viability determined by the SRB assay in H295R cancer cells treated with 1 µM solutions of 1-5 , Ru-LTZ, anastrozole (ATZ) and letrozole (LTZ) (48 h). | S6 |
| Figure S5. Ruthenium cellular uptake determined by ICP-MS after exposure of H295R cells to a 10 µM solution of 3 for 1.5 h. | S6 |
| Figure S6. ¹ H NMR spectrum of 3 . | S7 |
| Figure S7. ¹³ C{ ¹ H} NMR spectrum of 3 . | S8 |
| Figure S8. ³¹ P{ ¹ H} NMR spectrum of 3 . | S9 |

Table S1. Crystallographic data and structure refinement for complexes **2-5**.

| | 2 | 3 | 4 | 5 |
|---|---|---|---|--|
| empirical formula | C ₆₄ H ₆₄ BCIN ₁₀ Ru | C ₆₅ H ₆₀ BCIN ₅ PRu | C ₈ H ₈ O ₅ Ru | C ₂₅ H ₂₅ N ₅ O ₄ Ru |
| formula weight | 1120.58 | 1089.48 | 285.21 | 560.57 |
| crystal size | 0.2 x 0.16 x 0.02 mm | 0.24 x 0.12 x 0.04 mm | 0.24 x 0.22 x 0.07 mm | 0.32 x 0.07 x 0.03 mm |
| crystal system, space group | triclinic, <i>P</i> -1 | monoclinic, <i>P</i> 2 ₁ / <i>c</i> | triclinic, <i>P</i> -1 | Monoclinic, <i>C</i> 2/ <i>c</i> |
| unit cell dimensions | a = 13.7319(6)Å | a = 38.2764(15) Å | a = 6.2877(2)Å | a = 32.8261(11)Å |
| | b = 14.5443(6)Å | b = 9.9847(4)Å | b = 7.8586(2)Å | b = 9.1294(2)Å |
| | c = 15.9097(7)Å | c = 31.5850(13) Å | c = 8.9078(2)Å | c = 16.3868(4)Å |
| | α = 113.327(2)° | α = 90° | α = 75.191(1)° | α = 90° |
| | β = 99.435(2)° | β = 114.361(2)° | β = 89.895(1)° | β = 95.992(1)° |
| | γ = 91.374(2)° | γ = 90° | γ = 78.879(1)° | γ = 90° |
| volume | 2864.4(2) Å ³ | 10996.3(8) Å ³ | 417.02(2) Å ³ | 4884.0(2) Å ³ |
| Z, Calculated density | 2, 1.299 Mg m ⁻³ | 8, 1.316 Mg m ⁻³ | 2, 2.271 Mg m ⁻³ | 8, 1.525 g/cm ³ |
| F(000) | 1168.0 | 4528.0 | 280.0 | 2288.0 |
| μ | 2.031 mm ⁻¹ | 2.235 mm ⁻¹ | 15.224 mm ⁻¹ | 5.554 mm ⁻¹ |
| temperature | 100 K | 150 K | 100 K | 100 K |
| wavelength | 1.34139Å (GaK _α) | 1.34139Å (GaK _α) | 1.54178 Å (CuK _α) | 1.54178 Å (CuK _α) |
| index ranges | -17 ≤ h ≤ 17 | -47 ≤ h ≤ 47 | -7 ≤ h ≤ 7 | -40 ≤ h ≤ 40 |
| | -18 ≤ k ≤ 18 | -12 ≤ k ≤ 12 | -9 ≤ k ≤ 9 | 0 ≤ k ≤ 10 |
| | -20 ≤ l ≤ 20 | -39 ≤ l ≤ 39 | -10 ≤ l ≤ 10 | 0 ≤ l ≤ 20 |
| 2θ range for data collection | 5.36 to 121.424° | 4.106 to 114.104° | 10.284 to 143.67° | 10.06 to 144.67° |
| reflections collected/unique | 76314/13153 | 80612/22364 | 21675/1584 | 4865/4865 |
| data/parameters/restraints | 13153/702/0 | 22364/1402/288 | 1584/135/6 | 4865/322/0 |
| Goodness-of-fit on F ² | 1.043 | 1.021 | 1.134 | 1.030 |
| Final R indices [<i>I</i> > 2σ(<i>I</i>)] ^{a,b} | R1 = 0.0280 | R1 = 0.0540 | R1 = 0.0383 | R1 = 0.0366 |
| | wR2 = 0.0741 | wR2 = 0.1321 | wR2 = 0.1012 | wR2 = 0.1076 |
| R indices (all data) | R1 = 0.0322 | R1 = 0.0540 | R1 = 0.0383 | R1 = 0.0370 |
| | wR2 = 0.0759 | wR2 = 0.1394 | wR2 = 0.1012 | wR2 = 0.1084 |
| Largest diff. peak and hole | 1.11 and -0.35 e Å ⁻³ | 1.12 and -0.85 e Å ⁻³ | 1.96 and -2.02 e Å ⁻³ | 1.35 and -1.07 Å ⁻³ |
| CCDC deposition no. | 1840870 | 1840871 | 1840872 | 1840873 |

$$^a R_1 = \sum ||F_o| - |F_c|| / \sum |F_o|. \quad ^b wR_2 = \{\sum [w(F_o^2 - F_c^2)^2] / \sum [w(F_o^2)^2]\}^{1/2}.$$

[S2]

Table S2. Selected bond lengths (Å) and angles (deg) of complexes **2-5**.

| 2 | | 3 | |
|------------------------------|-------------|------------------------------|-----------------------|
| bond length/angle | Å/deg | bond length/angle | Å/deg |
| Ru1-N1 | 2.1024 (12) | Ru1-N1 (Ru1'-N1') | 2.114 (4) (2.091 (5)) |
| Ru1-N2 | 2.1104 (12) | Ru1-P1 (Ru1'-P1') | 2.352 (1) (2.346 (3)) |
| Ru1-Cl1 | 2.3961 | Ru1-Cl1 (Ru1'-Cl1') | 2.401 (2) (2.380 (1)) |
| Ru-arene _{centroid} | 1.662 | Ru-arene _{centroid} | 1.699 (1.747) |
| N1-Ru1-N2 | 87.14 (5) | N1-Ru1-P1 (N1'-Ru1'-P1') | 90.5 (1) (89.6 (2)) |
| N1-Ru1-Cl1 | 86.15 (3) | N1-Ru1-Cl1 (N1'-Ru1'-Cl1') | 87.00 (1) (84.6 (3)) |
| N2-Ru1-Cl1 | 85.45 (3) | P1-Ru1-Cl1 (P1'-Ru1'-Cl1') | 88.27 (5) (84.0 (3)) |

| 4 | | 5 | |
|------------------------------|------------|------------------------------|-------------|
| bond length/angle | Å/deg | bond length/angle | Å/deg |
| Ru1-O1 | 2.086 (3) | Ru1-N1 | 2.1130 (15) |
| Ru1-O2 | 2.096 (3) | Ru1-O1 | 2.0847 (13) |
| Ru1-O3 | 2.143 (3) | Ru1-O2 | 2.0788 (13) |
| Ru-arene _{centroid} | 1.643 | Ru-arene _{centroid} | 1.653 |
| O1-Ru1-O2 | 78.31 (12) | O1-Ru1-O2 | 78.53 (6) |
| O1-Ru1-O3 | 82.78 (13) | O1-Ru1-N1 | 86.20 (6) |
| O2-Ru1-O3 | 85.97 (13) | O2-Ru1-N1 | 85.71 (6) |

Table S3. Anastrozole release after incubation (48 h) of a 150 μ M solution of complexes **1**, **2**, **3**, and **5** in water (DMSO 0.5%). Data are reported as mean \pm SD resulting from 3 independent experiments.

| Complex | 1 | 2 | 3 | 5 |
|-------------------------|---------------|----------------|---------------|----------------|
| Anastrozole release (%) | 7% (\pm 2) | 15% (\pm 2) | 3% (\pm 1) | 15% (\pm 3) |

Table S4. Anastrozole (or letrozole) release after incubation (1.5 h) of a 10 μ M solution of complexes **1**, **2**, **3**, **5** and Ru-LTZ in DMEM/F-12 (DMSO 0.1%). Data are reported as mean \pm SD resulting from 3 independent experiments.

| Complex | 1 | 2 | 3 | 5 | Ru-LTZ |
|---|-----------------|-----------------|-----------------|-----------------|-----------------|
| Equivalent(s) of released inhibitor | 1.54 (0.05) / 2 | 0.42 (0.03) / 2 | 0.04 (0.00) / 1 | 0.81 (0.05) / 1 | 2.00 (0.06) / 2 |

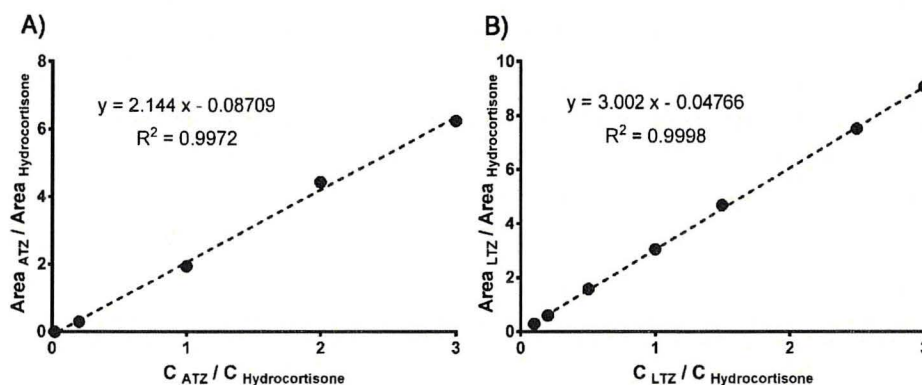


Figure S1. Calibration curves of extracted A) anastrozole (ATZ) and B) letrozole (LTZ) from phenol red free DMEM/F-12 (DMSO final concentration: 0.1%). Hydrocortisone was used as an external standard.

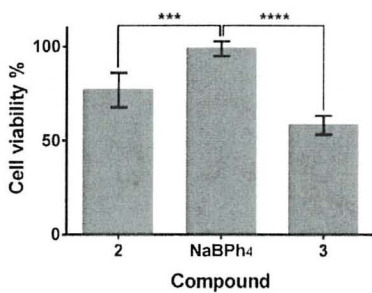


Figure S2. Cell viability determined by the SRB assay in T47D cancer cells treated with a 25 μ M solution of **2**, **3** and NaBPh₄ (48 h). All values are expressed as means (from three independent experiments) \pm SD relative to the carrier: media containing 0.25% DMSO and the negative control: growth media containing 25% DMSO (0%).

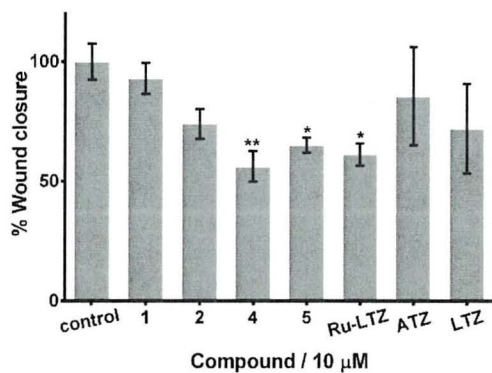


Figure S3. Migration inhibition assessment of MCF-7 cells after exposure to 10 μ M solutions of **1**, **2**, **4**, **5**, Ru-LTZ, anastrozole (ATZ) and letrozole (LTZ) over 48 h. Error bars shown in the graph represent the standard error of mean (n=8). Significant differences: *p < 0.05; **p < 0.01.

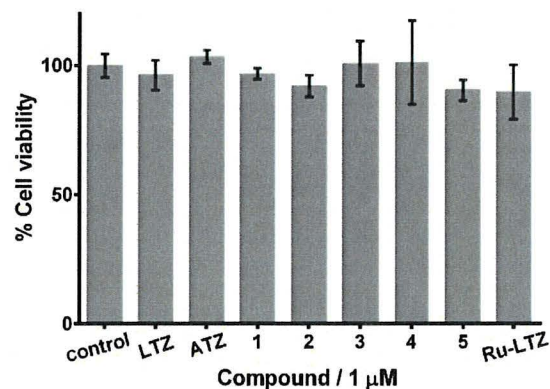


Figure S4. Cell viability determined by the SRB assay in H295R cancer cells treated with 1 μM **1-5**, Ru-LTZ, anastrozole (ATZ) and letrozole (LTZ) (48 h). All values are expressed as means (from three independent experiments) ± SD relative to the carrier: media containing 0.25% DMSO and the negative control: growth media containing 25% DMSO (0%).

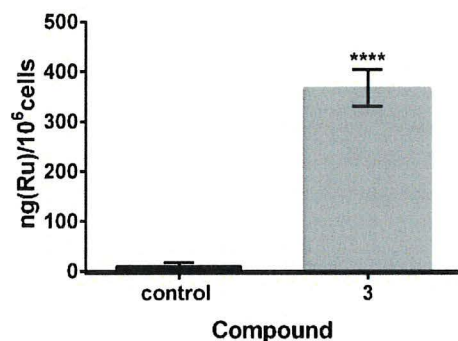


Figure S5. Ruthenium cellular uptake determined by ICP-MS after exposure of H295R cells to a 10 μM solution of **3** for 1.5 h. Error bar in the graph represent the standard deviation.

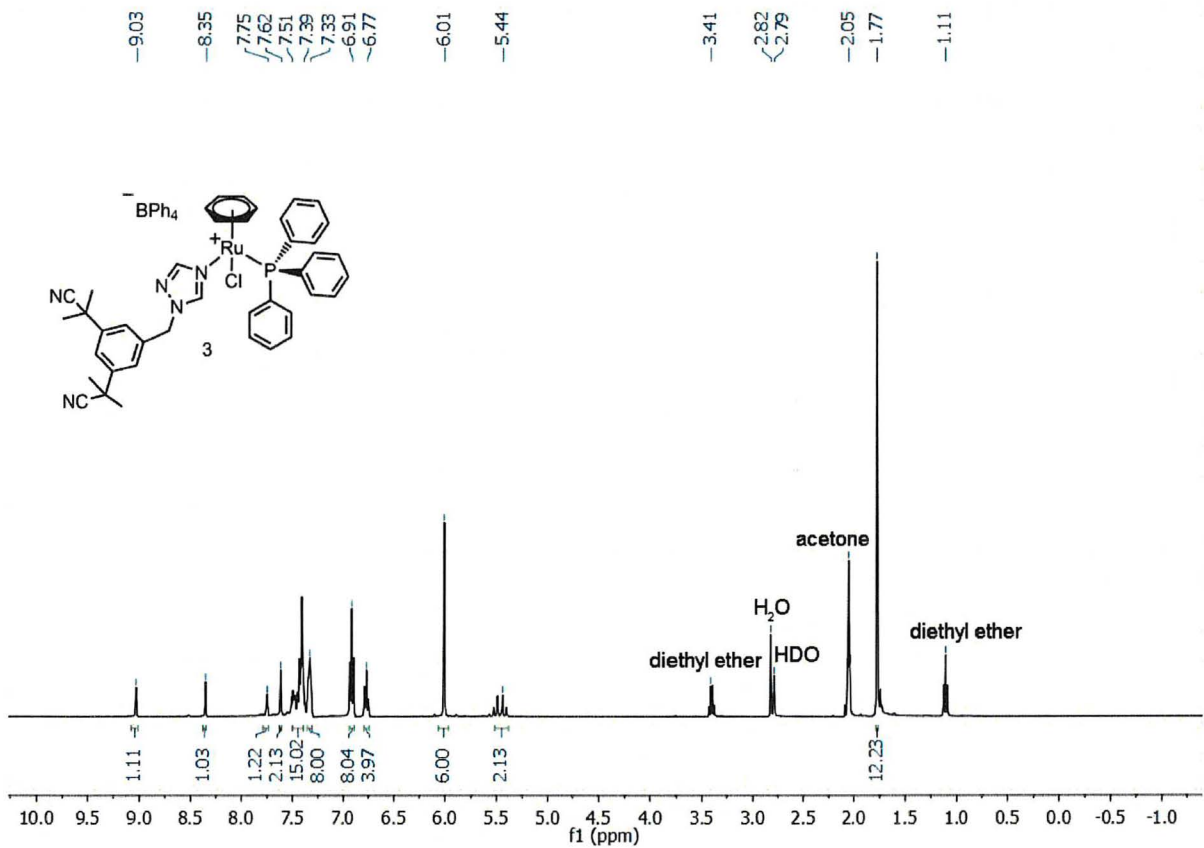


Figure S6. ¹H NMR ((CD₃)₂CO, 400 MHz) spectrum of 3.

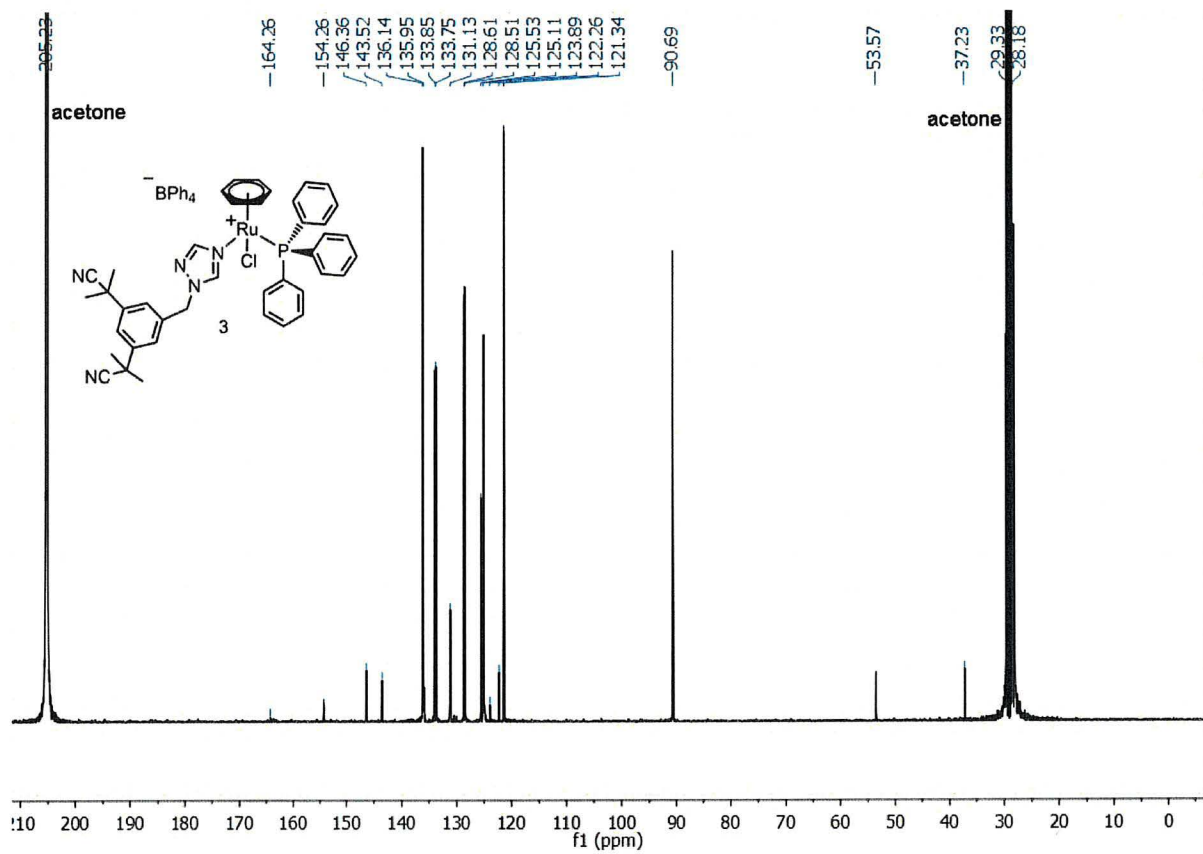


Figure S7. $^{13}\text{C}\{^1\text{H}\}$ NMR ($(\text{CD}_3)_2\text{CO}$, 100 MHz) of **3**.

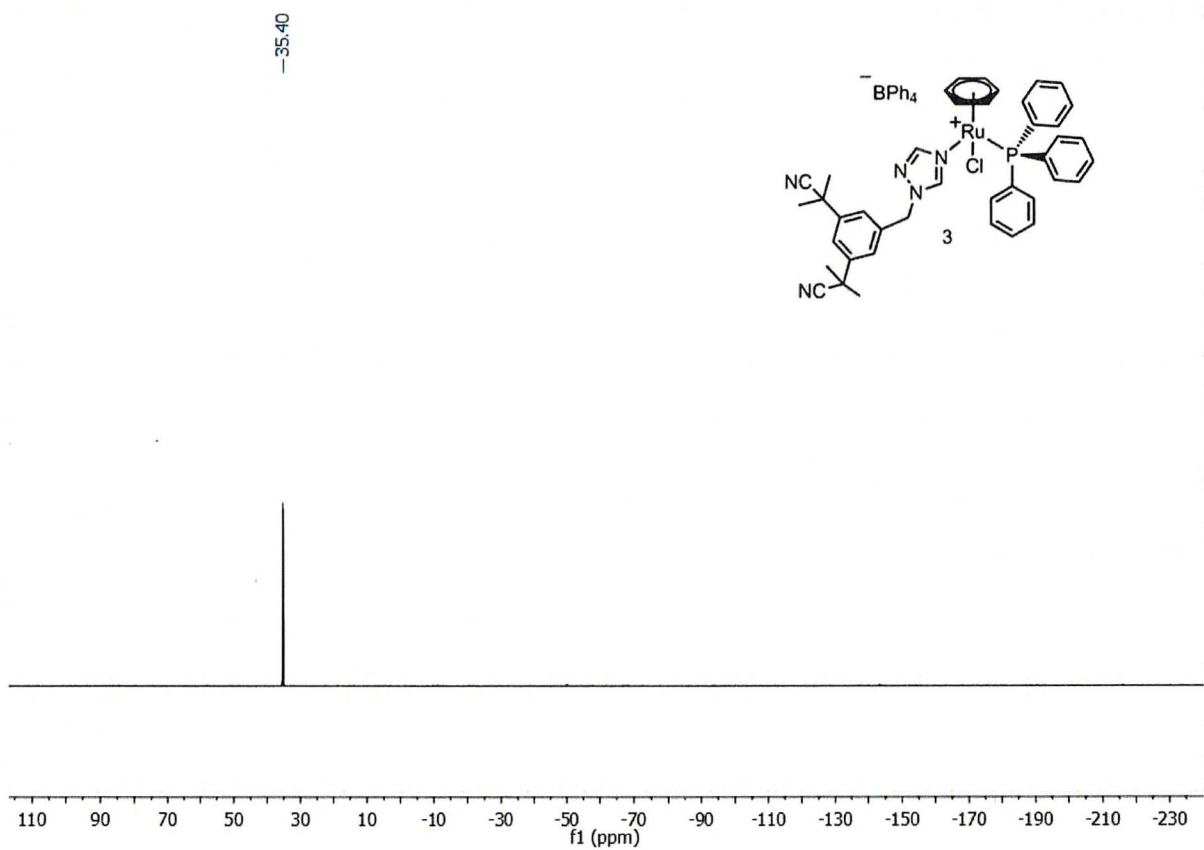


Figure S8. $^{31}\text{P}\{^1\text{H}\}$ NMR $(\text{CD}_3)_2\text{CO}$, 200 MHz) of **3**.

SUPPLEMENTARY INFORMATION

Synthesis and Biological Assessment of a Ruthenium(II) Cyclopentadienyl Complex in Breast Cancer Cells and on the Development of Zebrafish Embryos

Golara Golbaghi, Irène Pitard, Matthieu Lucas, Mohammad Mehdi Haghdooost, Yossef López de los Santos, Nicolas Doucet, Shunmoogum A. Patten, J. Thomas Sanderson, Annie Castonguay*

Organometallic Chemistry Laboratory for the Design of Catalysts and Therapeutics, and Endocrine Toxicology Laboratory, INRS-Centre Armand-Frappier Santé Biotechnologie, Université du Québec, Laval, Canada

TABLE OF CONTENT

| | |
|---|----|
| Table S1. Crystallographic data and structure refinement for complexes 1, 2, 4, 5, 6. | S2 |
| Table S2. Anastrozole (or letrozole) release after incubation (1.5 h) of a 10 μ M solution of complexes 2-5 in DMEM/F-12 (DMSO 0.1%). | S3 |
| Figure S1. ^1H NMR spectra of 1 (top) and 2 (bottom) in DMSO- d_6 recorded 15 min after sample preparation. | S3 |
| Figure S2. UV-Vis absorption spectrum of 2 (800 μ M) in DMSO over time (1 h, 5 min intervals) | S4 |
| Figure S3. Absorbance intensity measurement (at 350 nm) of complex 2 at various concentrations | S4 |

Table S1. Crystallographic data and structure refinement for complexes **1,2** and **4-6**.

| | 1 | 2 | 4 | 5 | 6 |
|--|--|---|--|---|--|
| empirical formula | C ₄₂ H ₅₀ Cl ₂ N ₁₀ Ru | C ₅₈ H ₅₈ BF ₄ N ₅ O ₂ P ₂ Ru | C ₂₀ H ₂₃ Cl ₄ NaO ₃ RuS | C ₄₃ H ₄₅ Cl ₄ N ₅ OPRuS | C ₄₃ H ₃₇ Cl ₄ N ₅ OPRuS |
| formula weight | 866.89 | 1106.91 | 679.35 | 953.74 | 945.67 |
| crystal size | 0.22 x 0.16 x 0.08 mm | 0.22 x 0.08 x 0.06 mm | 0.28 x 0.07 x 0.04 mm | 0.20 x 0.09 x 0.05 mm | 0.25 x 0.08 x 0.02 mm |
| crystal system, space group | monoclinic, <i>P2₁/n</i> | monoclinic, <i>P2₁/c</i> | orthorhombic, <i>Pbca</i> | triclinic, <i>P-1</i> | monoclinic, <i>P2₁/n</i> |
| unit cell dimensions | a = 15.6300(7)Å b = 14.4102(6)Å c = 20.2465(9)Å α = 90° β = 112.5566(14)° γ = 90° | a = 13.0418(6) Å b = 42.8922(17)Å c = 9.7505(4) Å α = 90° β = 98.248(3)° γ = 90° | a = 21.9838(6)Å b = 11.2879(3)Å c = 22.0725(6)Å α = 90° β = 90° γ = 90° | a = 11.8865(6)Å b = 13.3540(6)Å c = 16.1481(8)Å α = 67.997(2)° β = 71.229(2)° γ = 74.089(2)° | a = 15.7115(6)Å b = 16.3451(6)Å c = 17.8103(7)Å α = 90° β = 112.930(2)° γ = 90° |
| volume | 4211.3(3) Å ³ | 5397.9(4) Å ³ | 5477.3(3) Å ³ | 2215.42(19) Å ³ | 4212.4(3) Å ³ |
| Z, Calculated density | 4, 1.367 g/cm ³ | 4, 1.362 g/cm ³ | 8, 1.648 g/cm ³ | 2, 1.430 g/cm ³ | 4, 1.491 g/cm ³ |
| F(000) | 1800.0 | 2288.0 | 2728.0 | 978.0 | 1924.0 |
| μ | 4.513 mm ⁻¹ | 3.410 mm ⁻¹ | 6.187 mm ⁻¹ | 4.072 mm ⁻¹ | 4.283 mm ⁻¹ |
| temperature | 100 K | 100 K | 110 K | 150 K | 150 K |
| wavelength | 1.54178Å (CuK _α) | 1.54178Å (CuK _α) | 1.34139Å (GaK _α) | 1.34139Å (GaK _α) | 1.34139Å (GaK _α) |
| index ranges | -19 ≤ h ≤ 18 -17 ≤ k ≤ 17 -24 ≤ l ≤ 24 | -15 ≤ h ≤ 15 -50 ≤ k ≤ 51 -11 ≤ l ≤ 11 | -28 ≤ h ≤ 24 -14 ≤ k ≤ 14 -28 ≤ l ≤ 28 | -15 ≤ h ≤ 15 -15 ≤ k ≤ 17 -20 ≤ l ≤ 20 | -19 ≤ h ≤ 18 -20 ≤ k ≤ 20 -22 ≤ l ≤ 22 |
| 2θ range for data collection | 5.334 to 84.378° | 4.12 to 137.61° | 6.968 to 121.256° | 5.298 to 121.38° | 5.55 to 114.234° |
| reflections collected/unique | 155043/8255 | 72433/9950 | 83292/6287 | 63708/10119 | 60169/8598 |
| data/parameters/restraints | 8255/504/0 | 9950/668/0 | 6287/329/3 | 10119/512/0 | 8598/523/6 |
| Goodness-of-fit on F ² | 1.028 | 0.996 | 1.112 | 1.038 | 1.076 |
| Final R indices [I > 2σ(I)] ^{a,b} | R1 = 0.0263 wR2 = 0.0719 | R1 = 0.0488 wR2 = 0.1265 | R1 = 0.0371 wR2 = 0.0948 | R1 = 0.0316 wR2 = 0.0837 | R1 = 0.0458 wR2 = 0.1133 |
| R indices (all data) | R1 = 0.0264 wR2 = 0.0720 | R1 = 0.0644 wR2 = 0.1382 | R1 = 0.0383 wR2 = 0.0961 | R1 = 0.0358 wR2 = 0.0875 | R1 = 0.0563 wR2 = 0.1226 |
| Largest diff. peak and hole | 1.05 and -1.09 e Å ⁻³ | 0.93 and -0.60 e Å ⁻³ | 1.18 and -1.09 e Å ⁻³ | 0.82 and -0.86 Å ⁻³ | 0.93 and -0.64 Å ⁻³ |
| CCDC deposition no. | 1962264 | 1962265 | 1962266 | 1962267 | 1962268 |

$$^a R_1 = \sum ||F_o| - |F_c|| / \sum |F_o|, \quad ^b wR_2 = \{\sum [w(F_o^2 - F_c^2)] / \sum [w(F_o^2)]\}^{1/2}.$$

[S2]

Table S2. Anastrozole (or letrozole) release after incubation (1.5 h) of a 10 μM solution of complexes **2-5** in DMEM/F-12 (DMSO 0.1%). Data are reported as mean \pm SD resulting from 3 independent experiments.

| Complex | 2 | 3 | 4 | 5 |
|---|-----------------|-----------------|-----------------|-----------------|
| Equivalent(s) of released inhibitor | 0.04 (0.00) / 1 | 0.59 (0.07) / 1 | 0.55 (0.11) / 1 | 0.87 (0.08) / 1 |

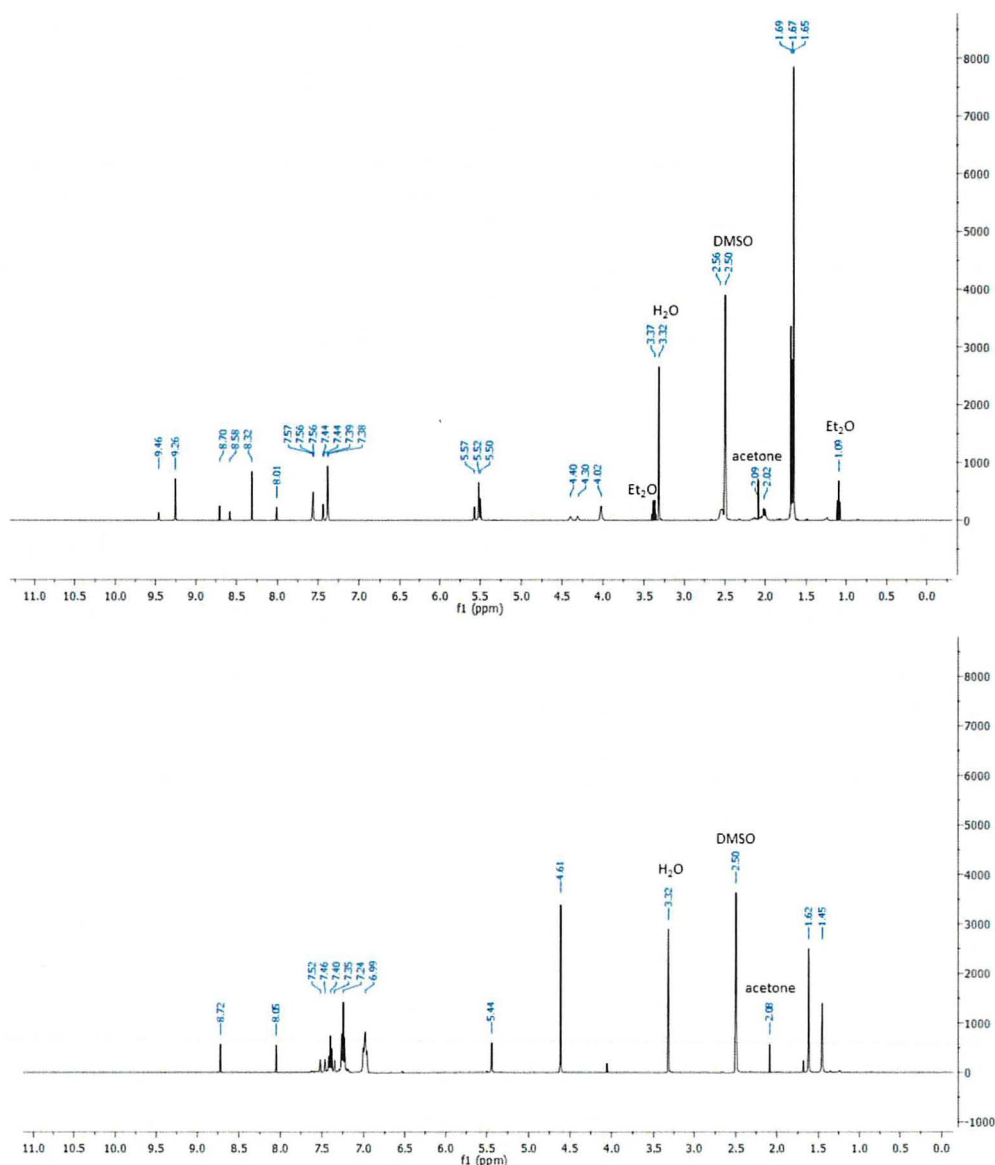


Figure S1. ^1H NMR spectra of **1** (top) and **2** (bottom) in DMSO-d_6 recorded 15 min after sample preparation.

[S3]

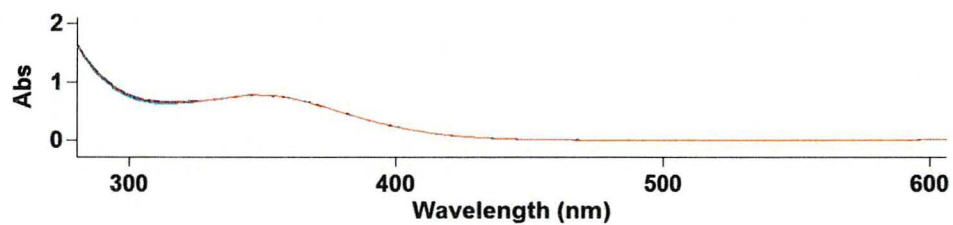


Figure S2. UV-Vis absorption spectrum of **2** (800 μM) in DMSO over time (1 h, 5 min intervals).

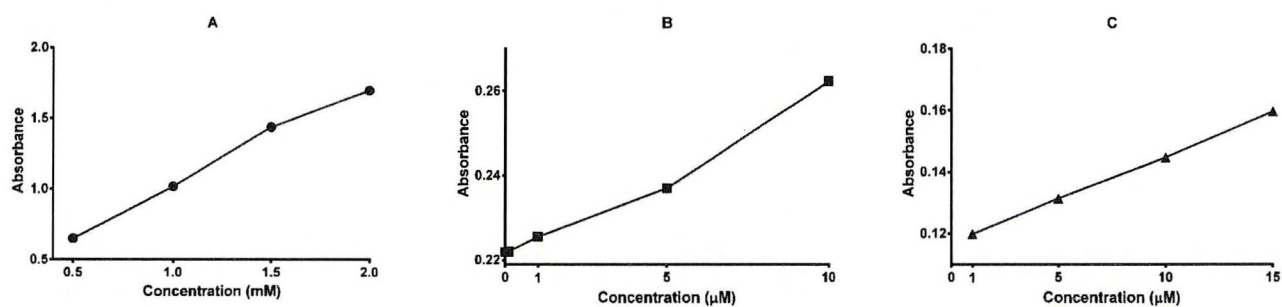


Figure S3. Absorbance intensity measurement (at 350 nm) of **2** at various concentrations in A) DMSO alone, B) DMEM/F12 growth medium supplemented with 0.1% DMSO and C) water supplemented with a maximum of 0.5% DMSO.

SUPPLEMENTARY INFORMATION

Cationic Ru(II) cyclopentadienyl complexes with antifungal activity against several *Candida* species

Golara Golbaghi^[a], Marie-Christine Groleau^[b], Yossef López de los Santos^[b], Nicolas Doucet^[b], Eric Deziel^[b], and Annie Castonguay^{*[a]}

[a] *Organometallic Chemistry Laboratory for the Design of Catalysts and Therapeutics*
INRS-Centre Armand-Frappier Santé Biotechnologie, Laval, Canada
E-mail: annie.castonguay@iaf.inrs.ca

[b] INRS-Centre Armand-Frappier Santé Biotechnologie, Laval, Canada

Table of content

| | |
|---|----|
| Table S1. Anticandidal activity of previously reported ruthenium complexes | S2 |
| Figure S1. Absorbance intensity measurement (at 350 nm) of Ru-Cl and [Ru-ACN] ⁺ at various concentrations in DMSO | S3 |
| Figure S2. UV-Vis absorption spectrum of Ru-Cl and [Ru-ACN] ⁺ (800 μM) in DMSO over time | S3 |
| Figure S3. Time-kill kinetic analysis of [Ru-ACN] ⁺ , [Ru-ATZ] ⁺ and fluconazole on different strains | S4 |
| References | S5 |

Table S1. Anticandidal activity of previously reported ruthenium complexes.

| | Type of assay | Species | Anticandidal activity ^[d] |
|---|--|--|--------------------------------------|
| Ihm <i>et al</i> ^[1] | Disk diffusion ^[a] | <i>C. albicans</i> | 9-13% (at 0.5%) |
| Mobin <i>et al</i> ^[2] | | | 9-13 mm (at 100 ppm) |
| Liu <i>et al</i> ^[3] | | | 6-7 mm (at 100 ppm) |
| Jayabalakrishnan <i>et al</i> ^[4] | | | 11-15 mm (at 2%) |
| Jayabalakrishnan <i>et al</i> ^[5] | | | 12-17 mm (at 2%) |
| Ben hadda <i>et al</i> ^[6] | | | 22.5 mm (at 0.2 mg/mL) |
| Fekry <i>et al</i> ^[7] | | | ≈ 17 mm (at 50 ppm) |
| Anandaram <i>et al</i> ^[8] | | | Disk diffusion ^[b] |
| Radacki <i>et al</i> ^[9] | Turbidity (broth microdilution) ^[b] | | 6.77 nM |
| De Resende Stoianoff <i>et al</i> ^[10] | | <i>C.albicans</i> | 0.4-13.6 × 10 ⁻⁵ M |
| | | <i>C.krusei</i> | 1.70-7.3 × 10 ⁻⁵ M |
| | | <i>C.parapsilosis</i> | 0.8-4.1 × 10 ⁻⁵ M |
| | | <i>C.tropicalis</i> | 0.8-7.3 × 10 ⁻⁵ M |
| | | <i>C.glabrata</i> | 4.0-29.3 × 10 ⁻⁵ M |
| Günel <i>et al</i> ^[11] | <i>C. albicans</i> <i>C. tropicalis</i> | 100 µg/mL 100 µg/mL | |
| Mansour ^[12] | <i>C. albicans</i> | 24 nM | |
| Radacki <i>et al</i> ^[13] | | 24 nM | |
| Alici <i>et al</i> ^[14] | | 200 µg/mL | |
| Vannier-Santos <i>et al</i> ^[15] | Cell counting ^[c] | <i>C. tropicalis</i> | 20.3 µM |
| Shaikh <i>et al</i> ^[16] | Well diffusion ^[a] | <i>C. albicans</i> | 12-15 mm (at 1 mg/mL) |
| Natarajan <i>et al</i> ^[17] | | | 50-100 µg/mL |
| Prabhakaran <i>et al</i> ^[18] | Well diffusion ^[b] | <i>C. albicans</i> <i>C. tropicalis</i> | 15-35 µM 15-20 µM |

Antifungal activity reported as: ^[a] inhibition zone diameter; ^[b] minimum inhibitory concentration (MIC); ^[c] IC₅₀.

^[d] Please note that the incubation time (24-72h) and the temperature (26-37 °C) varied from one study to another.

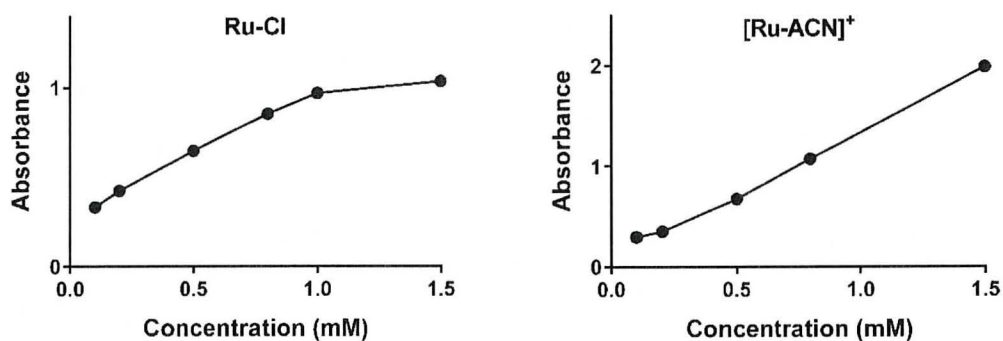


Figure S1. Absorbance intensity measurement (at 350 nm) of Ru-Cl and [Ru-ACN]⁺ at various concentrations (0.1 - 1.5 mM) in DMSO.

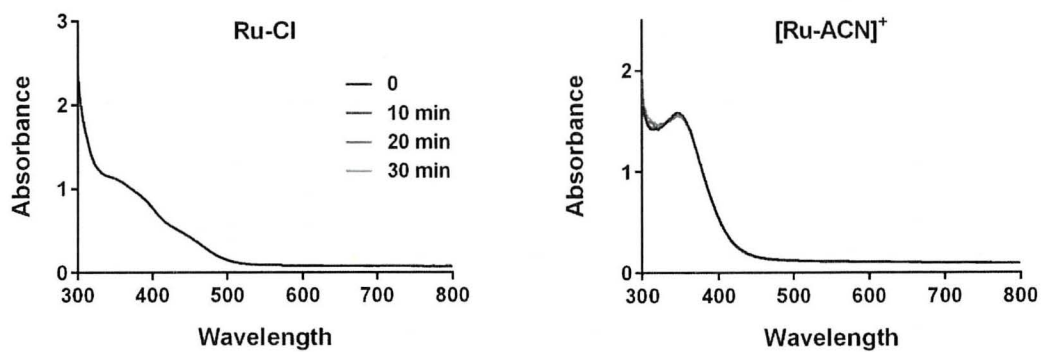


Figure S2. UV-Vis absorption spectra of Ru-Cl and [Ru-ACN]⁺ (800 μ M) in DMSO over time (30 min, 10 min intervals).

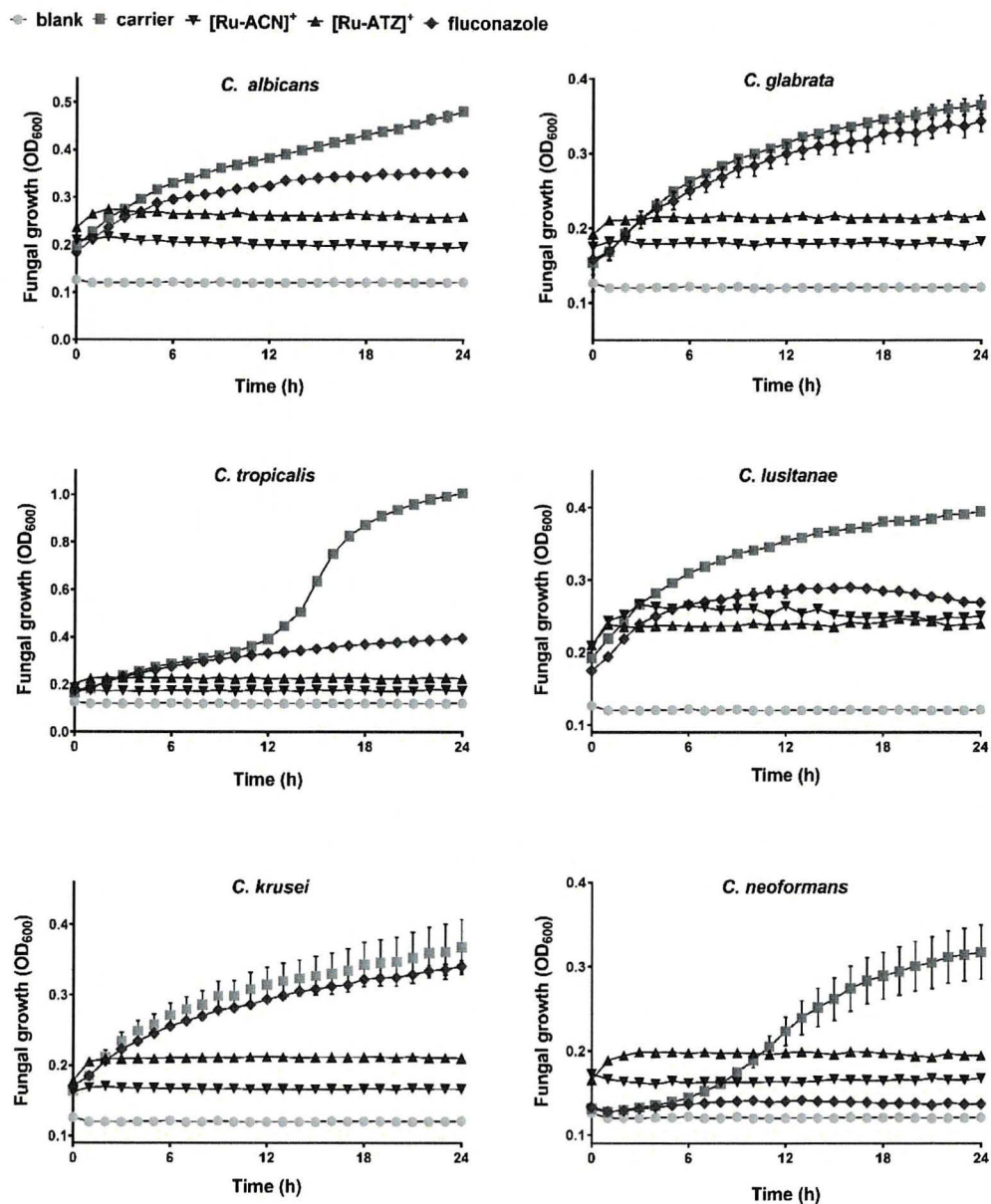


Figure S3. Time-kill kinetic analysis of [Ru-ACN]⁺, [Ru-ATZ]⁺ and fluconazole on different strains. Cells were treated with 20 μ M of each compound for 24 h and fungal growth (optical density, OD₆₀₀) was measured every 1 h. Error bars shown in the graph represent the standard deviation of the mean of three replicates.

References

- [1] T. D. Thangadurai, S.-K. Ihm, *Synthesis and Reactivity in Inorganic, Metal-Organic, and Nano-Metal Chemistry* **2005**, 35, 499-507.
- [2] G. Venkatachalam, R. Ramesh, S. M. Mobin, *Journal of Organometallic Chemistry* **2005**, 690, 3937-3945.
- [3] K. Naresh Kumar, R. Ramesh, Y. Liu, *Journal of Inorganic Biochemistry* **2006**, 100, 18-26.
- [4] N. P. Priya, S. V. Arunachalam, N. Sathya, V. Chinnusamy, C. Jayabalakrishnan, *Transition Metal Chemistry* **2009**, 34, 437-445.
- [5] N. Padma Priya, S. Arunachalam, N. Sathya, C. Jayabalakrishnan, *Journal of Coordination Chemistry* **2010**, 63, 1440-1450.
- [6] M. Al-Noaimi, A. Nafady, I. Warad, R. Alshwafy, A. Husein, W. H. Talib, T. B. Hadda, *Spectrochimica Acta Part A: Molecular and Biomolecular Spectroscopy* **2014**, 122, 273-282.
- [7] N. E. A. El-Gamel, A. M. Fekry, *Bioelectrochemistry* **2015**, 104, 35-43.
- [8] R. Gandhaveeti, R. Konakanchi, P. Jyothi, N. S. P. Bhuvanesh, S. Anandaram, *Applied Organometallic Chemistry* **2019**, 33, e4899.
- [9] A. M. Mansour, K. Radacki, *Polyhedron* **2020**, 175, 114175.
- [10] C. L. Donnici, L. J. Nogueira, M. H. Araujo, S. R. Oliveira, T. F. F. Magalhães, M. T. P. Lopes, A. C. A. e. Silva, A. M. d. C. Ferreira, C. V. B. Martins, M. A. De Resende Stoianoff, *Molecules* **2014**, 19, 5402-5420.
- [11] B. Cetinkaya, I. Özdemir, B. Binbaşoğlu, S. Günal, *Arzneimittelforschung* **1999**, 49, 538-540.
- [12] A. M. Mansour, *European Journal of Inorganic Chemistry* **2018**, 2018, 852-860.
- [13] A. M. Mansour, O. R. Shehab, K. Radacki, *European Journal of Inorganic Chemistry* **2020**, 2020, 299-307.
- [14] G. Onar, C. Gürses, M. O. Karataş, S. Balcıoğlu, N. Akbay, N. Özdemir, B. Ateş, B. Alici, *Journal of Organometallic Chemistry* **2019**, 886, 48-56.
- [15] R. A. Gomes-Junior, R. S. da Silva, R. G. de Lima, M. A. Vannier-Santos, *FEMS Microbiology Letters* **2017**, 364.
- [16] B. Mehta, J. Shaikh, *Special report series - Indian Council of Medical Research* **2009**, 26, 1-6.
- [17] T. S. Kamatchi, P. Kalaivani, P. Poornima, V. V. Padma, F. R. Fronczek, K. Natarajan, *RSC advances* **2014**, 4, 2004-2022.
- [18] G. Kalaiarasi, S. R. Jeya Rajkumar, S. Dharani, F. R. Fronczek, R. Prabhakaran, *Journal of Organometallic Chemistry* **2018**, 866, 223-242.